7-15-2016

Using Regression-Based Effect Size Meta-Analysis to Investigate Coral Responses to Climate Change

Niklas Alexander Kornder
Halmos College of Natural Sciences and Oceanography, niklaskornder@googlemail.com

Thesis of

NIKLAS KORNDER

Submitted in Partial Fulfillment of the Requirements for the Degree of

Masters of Science:

Marine Environmental Sciences

NIKLAS ALEXANDER KORNDER

Nova Southeastern University

Halmos College of Natural Sciences and Oceanography

July 2016

Approved:

Thesis Committee

Major Professor:_____
Joana Figueiredo, Ph.D

Committee Member:_____
Bernhard Riegl, Ph.D

Committee Member:_____
Christian Wild, Ph.D

HALMOS COLLEGE OF NATURAL SCIENCES AND OCEANOGRAPHY

USING REGRESSION-BASED EFFECT SIZE META-ANALYSIS TO INVESTIGATE CORAL RESPONSES TO CLIMATE CHNGE

By

Niklas Alexander Kornder

Submitted to the Faculty of
Halmos College of Natural Sciences and Oceanography
in partial fulfillment of the requirements for
the degree of Master of Science with a specialty in:

Marine Environmental Sciences

Nova Southeastern University

July, 2016

Table of content

List of figures

List of tables

List of equations

Abstract

Attempts to quantify the effects of ocean acidification and warming (OAW) on scleractinian corals provide a growing body of response measurements. However, placing empirical results into an ecological context is challenging, owing to variations that reflect both natural heterogeneity and scientific bias. This study addresses the heterogeneity of climate change induced changes in coral recruitment and calcification. To discern scientific bias and identify drivers of the remaining heterogeneity, 100 publications were analyzed using a combination of weighted *mixed effects* meta-regression and factorial effect size meta-analysis. A linear model was applied to quantify the variation caused by differing stress levels across studies. The least squares predictions were then used to standardize individual study outcomes and effect size meta-analysis was performed on original and standardized outcomes separately. On average, increased temperature significantly reduces larval survival, while ocean acidification impedes settlement and calcification. Coral resistance to OAW is likely governed by biological traits (genera and life cycle stage), environmental factors (abiotic variability) and experimental design (feeding regime, stressor magnitude, and exposure duration). Linear models suggest that calcification rates are driven by carbonate and bicarbonate concentrations, which interact additively with warming. Standardizing outcomes to linear model predictions proved useful in discerning strong sources of scientific bias. The approach used in this study can improve modelling projections and inform policy and management on changes in coral community structure associated with the expected future intensification of OAW.

Additional Keywords:
Multiple stressors, rising sea surface temperatures, elevated pCO_2, calcium carbonate, substrate-inhibitor ratio, proton-flux hypothesis, reproduction, taxonomic variability, fail-safe analysis, R computing

Introduction

Anthropogenic carbon dioxide (CO_2) emissions are changing the climate at a rate that is unprecedented in recent geological history (Hoegh-Guldberg et al., 2007) . Two globally present challenges mainly associated with climate change are elevated sea surface temperatures and ocean acidification (OA) (IPCC, 2014). This is based on the dynamics of ocean-atmosphere interactions coupled with geochemical properties of CO_2. As a greenhouse gas, CO_2 increases radiative heating of its environment. An increased abundance in the atmosphere traps excess solar heat and contributes to global warming (Mitchell, 1989). As ocean-atmosphere interactions are driven by equilibrium states, changes in atmospheric temperature and composition also translate to the marine environment. Consequently, large amounts of heat and about a quarter of all anthropogenic CO_2 are taken up by the surface ocean (Sabine & Feely, 2003; IPCC, 2014). In seawater, CO_2 reacts with water to form carbonic acid (H_2CO_3), which quickly breaks down and alters the carbonate chemistry of surface waters, leading to OA (Caldeira & Wickett, 2003; Feely et al., 2009).

Atmospheric pCO_2 is rising by about 0.5% annually (IPCC, 2014); however predictions can be challenging due to uncertainties about future emissions. The most widely accepted prognoses for the 21st century are conducted by the Intergovernmental Panel on Climate Change (IPCC, 2014). Different emission scenarios are described as Representative Concentration Pathways (RCP's). Estimates for pCO_2 levels in the atmosphere at the end of the century range from 490 ppm (RCP2.6) to as high as 1370 ppm (RCP8.5) (IPCC, 2014; Qin et al., 2014). The associated changes in temperature (increases of 1.8 – 4˚C) and seawater carbon chemistry pose a threat to the persistence of marine ecosystems across the globe (Orr et al., 2005; Cohen & Holcomb, 2009; IPCC, 2014).

Some of the ecosystems believed to be particularly threatened by ocean acidification and warming (OAW) are coral reefs (Donner et al., 2005; Kleypas & Yates, 2009). These communities support high diversity (Polidoro & Carpenter, 2013), provide major ecosystem goods and services (Moberg & Folke, 1999), and protect associated ecosystems such as seagrass beds and mangroves (Hoegh-Guldberg, 1999). Direct benefits for humans include large economic values through tourism (Yeo, 2004; Economics, 2007) and fisheries

(Gell & Roberts, 2003), as well as protection of shorelines from storm damage (Sheppard et al., 2005). Climate change threatens coral reefs by damaging the building blocks of the reef, scleractinian corals (Goreau, 1963; Hoegh-Guldberg et al., 2007).

Scleractinian corals may not be able to persist in the way they exist today. Potential negative impacts include effects of OA on skeleton formation (Chan & Connolly, 2013), stress from frequently exceeded thermal tolerance thresholds (Baker et al., 2004), and consequently, increasing risk of phase shifts from coral-dominated ecosystems to less desirable states (Bellwood et al., 2004; Norstrom et al., 2009; Bozec & Mumby, 2015). Some of the major reef crises in Earth's history have been linked to elevated atmospheric pCO_2 (Pandolfi et al., 2011). One example is the Paleocene–Eocene Thermal Maximum (PETM, 55.8 Ma), where many shallow water areas experienced extensive OAW conditions. The changes occurred over longer timescales than today (1,000 – 10,000 years) and caused major community shifts from coral-algal reefs to large benthic foraminifera (Scheibner & Speijer, 2008). Past atmospheric temperatures and CO_2 concentrations have reached levels much higher than today (Pearson & Palmer, 2000; Feely et al., 2009). However, the changes occurred over long time scales and corals developed a suite of adaptive mechanisms to cope with ocean warming (OW) (Grottoli et al., 2006; Baker et al., 2008). Also, the effects of reduced pH were likely buffered by geochemical processes such as dissolution of calcium carbonate and alkalinity input from weathering (Kump et al., 2009). Based on the accelerating increase of CO_2 concentrations due to ongoing fossil fuel extraction, it remains questionable whether the oceans can buffer and organisms can adapt in a similar fashion today. If not, humans are likely to induce a reef crisis far greater than those documented in geological records (Kump et al., 2009).

Coral responses to ocean warming

Organismal responses to elevated temperature typically involve initial metabolic benefits with upper thermal limits (Edmunds, 2005). Measurements of metabolic activity on coral reefs can yield positive relationships with temperature (Lough & Barnes, 2000; Cooper et al., 2012). Above the temperature limit, however, the functionality of important biochemical systems is compromised, leading to negative effects (Hoegh-Guldberg, 1999; Castillo et al., 2014). Some coral traits affected by OW include energy acquisition (Lesser,

2006), growth (Clarke & Fraser, 2004; Cantin et al., 2010; Castillo et al., 2014), reproductive output (Baird & Marshall, 2002; Negri et al., 2007), larval survival and development (Randall & Szmant, 2009b; Woolsey et al., 2013; Figueiredo et al., 2014), and settlement (Edmunds et al., 2001; Randall & Szmant, 2009a; Figueiredo et al., 2014).

Investigating the influence of elevated temperature on the energetic balance of corals is complicated by the complex coral-algal symbiosis. Most reef building corals fulfill their nutritional needs by hosting various associations of endosymbiotic dinoflagellates (*Symbiodinium* spp.) and other microbial communities (collectively referred to as coral holobiont). These symbionts fulfill the majority of the coral host's energy requirements via photosynthesis (Hoegh-Guldberg, 1999). The photosynthetic efficiency is estimated using the ratio between symbiont photosynthesis and host respiration (P/R). Both processes are stimulated by warmer environments (Edmunds et al., 2001; Reynaud et al., 2003) but host respiration increases more rapidly than photosythesis, causing photosynthetic efficiency to decrease (Jokiel & Coles, 1990; Edmunds et al., 2001). Overstimulation of photosynthesis may also lead to accumulations of reactive oxygen species (ROS) that can damage coral host tissue (Brown, 1997). Under prolonged and/or intensive thermal stress, the symbiosis breaks down and the endosymbionts are expelled (Lesser, 2006), depleting the coral of associated nutrients and energy benefits (Wall et al., 2014). The expulsion of *Symbiodinium* algae renders the coral pale or colorless and is commonly referred to as bleaching (Baker et al., 2008). The bleaching response may also be induced by high light irradiance (Lesser, 2006) and various local stressors including pollution, sedimentation and destructive fishing techniques (Polidoro & Carpenter, 2013). However, OW is currently the leading cause (Hoegh-Guldberg et al., 2007). Some biological traits affecting bleaching resistance are physiology of the coral host (Loya et al., 2001), dominant types of *Symbiodinium* (Berkelmans & Van Oppen, 2006; Takahashi et al., 2013), the symbiont's adaptive state (Howells et al., 2012) and interactions between host and symbionts (Abrego et al., 2008). All of these factors are subject to large spatial and species-specific variation and, consequently, so are the thresholds (Baskett et al., 2009). From an environmental perspective, the occurrence of bleaching is strongly linked to the magnitude and duration of maximum summer temperatures (Liu et al., 2003) and thermal history of the area (Castillo & Helmuth, 2005; Middlebrook et al., 2008).

The impact of OW on coral growth is highly variable and governed by individual temperature limits, potential adaptation or acclimatization, and energetic trade-offs. Corals grow in size by secreting calcium carbonate ($CaCO_3$) using a mechanism referred to as biomineralization (see *Coral responses to ocean acidification*). This mechanism is strongly coupled to metabolic activity and responds to OW in a similar manner. Lough and Barnes (2000) showed that annual average sea surface temperatures throughout the Great Barrier Reef (GBR) predicted more than 80% of the variation in calcification rates in massive *Porites*. This positive relationship has recently been corroborated for some taxa (Cooper et al., 2012; Lough & Cantin, 2014). However, the Northern section of the GBR is currently suffering from the largest mass bleaching event ever recorded, comprising 50 – 75% of bleached coral cover. This suggests that temperature now commonly exceeds thermal limits of tropical corals, temporarily diminishing growth benefits and leaving the coral in a vulnerable state. Further evidence for deleterious effects of temperature on coral calcification in other regions is provided by controlled *ex situ* experiments on *Siderastrea siderea* colonies from the Caribbean (Castillo et al., 2014) and *Diploastrea heliopora* from the Red Sea (Cantin et al., 2010). Under consideration of the IPCC RCP scenarios, the authors concluded that the investigated taxa will likely experience dramatic reductions in calcification within the current century. Their projections may be overestimated because laboratory experiments disregard the suite of adaptive mechanisms that corals can apply over short and long timescales. Examples of those mechanisms are increased heterotrophic feeding to meet higher energy demand (Grottoli et al., 2006), and observations of changing symbiotic communities in response to environmental perturbations. By monitoring symbiotic associations in corals following *in situ* transplantation to alternative thermal regimes, Berkelmans and Van Oppen (2006) demonstrated the potential of some corals to change dominance of their symbiotic community towards more suited *Symbiodinium* species. This temporary change increased thermal thresholds and reduced calcification rates, which implies an energetic trade-off between heat tolerance and growth (*i.e.* increased energy investment in thermal tolerance is accompanied by decreased energy investment in growth) (Jones & Berkelmans, 2010). However, more recent research indicates that this trade-off is ameliorated in warmer oceans (Cunning et al., 2015).

Another trade-off associated with coral responses to rising temperatures involves fertility and reproductive potential. Pronounced thermal stress can inhibit reproduction of corals directly or via latent effects. Direct effects have been demonstrated for *Acropora millepora* in the form of significant reductions in fertilization success and embryogenesis under exposure to elevated temperature (Negri et al., 2007). Latent effects on fecundity were sometimes evident in times of recovery following heat stress (Hoegh-Guldberg, 1999). The reduction or absence of egg production may be coupled with energy losses from sub-lethal bleaching effects (Baird & Marshall, 2002). The parent colony either ceases egg production or reabsorbs existing eggs in an attempt to save energy and ensure its own survival. A decreased or diminished reproductive output following bleaching was demonstrated in field assessments of *Acropora* spp. from the GBR (Baird & Marshall, 2002; Ward et al., 2002), and *Orbicella annularis* colonies from Florida, U.S.A. (Szmant & Gassman, 1990). Although OW causes negative effects, some corals have developed strategies to deal with energetic shortages so that reproduction is not affected. For instance, bleached *Montipora capitata* colonies in Hawaii produced similar numbers of gametes compared to unbleached colonies(Cox, 2007). Grottoli et al. (2006) demonstrated that *M. capitata* has the capacity to increase heterotrophic feeding which offsets the loss in energy from the symbionts. Understanding the effects of OW on reproduction is crucial for the persistence of coral reefs in this era of climate change.

Recruitment dynamics in corals are governed by life cycle stages, reproductive modes, and adaptive mechanisms. These differences lead to considerable variation in the effects of elevated temperatures. Most corals are broadcast spawners. They release gametes that fertilize in the water column and develop over longer time periods (Miller & Mundy, 2003; Tay et al., 2011). The remaining coral species brood larvae internally and release them in a competent state (*i.e.* ready to settle). *Pocillopora damicornis* and the Merulinid *Goniastrea aspera* represent two examples that can be found in both variants (Ward, 1992; Nozawa & Harrison, 2007). The free-swimming larvae are lecitotrophic (*i.e.* rely on yolk for nutrition) and metamorphose into primary polyps after settling on a suitable substrate (Fadlallah, 1983). Brooded larvae typically acquire *Symbiodinium* algae prior to release and therefore have a second source of energy. However, recent research challenged the beneficial aspects of endosymbionts during larval stages (Yakovleva et al., 2009; Nesa et

al., 2012). The thermal tolerance of larvae can deviate substantially from adults of the same species and is typically lower (Byrne, 2011). While lethal effects of elevated temperatures have been observed in several instances (Bassim & Sammarco, 2003; Randall & Szmant, 2009a; Woolsey et al., 2013; Figueiredo et al., 2014), other experiments yielded no effects on larval survival (Anlauf et al., 2011; Ross et al., 2013; Winkler et al., 2015). Species-specific differences account for parts of that variation. For instance, *Acropora* and *Pocillopora* larvae tend to suffer from increased mortality under OW conditions (Cumbo et al., 2013a; Cumbo et al., 2013b; Putnam et al., 2013), while *Porites* and *Fungia* larvae appear to be more resistant (Anlauf et al., 2011; Ross et al., 2013; Baria et al., 2015). However, this taxonomic distinction is not always supported (Schnitzler et al., 2012; Haryanti et al., 2015). Potential explanations for these contrasting results are provided with the concepts of phenotypic plasticity and adaptation.

Adults are able to imprint information regarding their abiotic environment into their gametes, providing larvae with molecular signals that up- or downregulate enzymatic co-factors and facilitate development under changing conditions (transgenerational acclimatization) (van Oppen et al., 2015). Corals obtained from separate locations are subjected to different local stressors. Depending on environmental history and remaining energy reserves, parental imprinting may be more or less profound. The occurrence of transgenerational acclimation therefore has the implication that a parent's direct environment can have profound impacts on the survival of larvae (Byrne, 2011). In addition, corals usually release larvae over several days, producing a pool of larvae that encompasses a range of thermal tolerances (Cumbo et al., 2013b). Thermal thresholds of coral larvae also relate positively with latitude, probably based on adaptation to fluctuating temperatures (Woolsey et al., 2015). An effect that seems to be present in most studies relates to the increased metabolic activity in warmer environments. This hastens the exhaustion of energy reserves and thus shortens larval durations (Edmunds et al., 2001; Brooke & Young, 2005; Figueiredo et al., 2014). Shorter competency periods reduce potential dispersal ranges and lead to increased local retention of larvae, while lowering spatial connectivity between meta-populations (Munday et al., 2009; Figueiredo et al., 2014). An important ramification on the ecosystem level is that OW may allow isolated

reefs to become more resilient to disturbances, while diminishing recovery potential of sink populations (Figueiredo et al., 2014).

Coral settlement and metamorphosis display mixed responses to OW, encompassing enhancements, reductions, and latent effects. Direct settlement responses to OW can vary substantially within the same coral family. For example, a rise in temperature between 2 - 4˚C reduced settlement in *Acropora palmata* (Randall & Szmant, 2009b), while larvae of three other members of *Acropora* settled similar to control treatments (Chua et al., 2013; Foster et al., 2015). Some of the factors driving these conflicting results may derive from experimental design. An example for this is given by two separate studies on *Porites astreoides* from Florida, United States. Ross et al. (2013) exposed larvae to + 3˚C and found no effect, while Edmunds et al. (2001) elevated experimental temperatures by + 5˚C, leading to significant reductions in settlement. Further, OW may compromise coral recruitment despite successful settlement by inducing latent effects. Larvae settling at their thermal tolerance limits have been shown to suffer from increased post-settlement mortality (Nozawa & Harrison, 2007; Ross et al., 2013). However, this is not always the case (Foster et al., 2015).

Coral responses to ocean acidification

Rising atmospheric concentrations of carbon dioxide (CO_2) change the carbonate chemistry of seawater. As CO_2 is taken up by the ocean, it reacts with water to form carbonic acid (H_2CO_3). In its simplest form, the chemical reaction is described with:

$$CO_2 + H_2O \leftrightarrow H_2CO_3 \quad . \qquad (1)$$

Carbonic acid is unstable and quickly splits into bicarbonate (HCO_3^-) and hydrogen ions (H^+):

$$H_2CO_3 \leftrightarrow HCO_3^- + H^+ \quad . \qquad (2)$$

The pH of water is calculated based on the concentration of active dissolved hydrogen ions. When H^+ concentration increases, pH declines (ocean acidification). Some of these protons combine with carbonate ions (CO_3^{2-}) to form more bicarbonate:

$$CO_3^{2-} + H^+ \leftrightarrow HCO_3^- \quad . \qquad (3)$$

By the year 2100, shifting chemical equilibria towards the right side of the equations above are expected to increase H^+ in seawater 2.5 fold in relation to preindustrial concentrations

(Feely et al., 2009). At the same time, CO_3^{2-} will decrease by about 50%, while HCO_3^- and dissolved CO_2 will increase by 15% and 200%, respectively (Roleda et al., 2012).

The associated changes of increasing CO_2 concentrations may introduce several physiological constraints on marine biota. However, the underlying biochemical and physical mechanisms of these constraints are still debated, despite more than a decade of research (Zeebe & Wolf-Gladrow, 2001; Kleypas & Langdon, 2006; Jokiel, 2016). Most of the current insights on the effects of OA on coral physiology come from laboratory comparisons and field observations. The most extensively studied response is calcification, typically showing reductions in response to OA (Chan & Connolly, 2013; Kroeker et al., 2013). Several relationships and drivers have been proposed that potentially regulate coral calcification in OA scenarios. These potential drivers center around two opposing ideas that are largely supported by either chemists or biologists.

Coral skeletons are primarily comprised of calcium carbonate ($CaCO_3$) or more specifically, a mineral phase of $CaCO_3$ referred to as aragonite. The solubility of aragonite in seawater is described by the aragonite saturation Ω_A that can be estimated using:

$$\Omega_A = \frac{Ca^{2+} + CO_3^{2-}}{K_{sp}} \quad , \tag{4}$$

where Ca^{2+} and CO_3^{2-} represent the concentrations of dissolved calcium and carbonate ions, respectively. K_{sp} is a constant describing the apparent solubility product of aragonite at the *in situ* conditions of pressure, salinity and temperature. If Ω_A is 1, then $Ca^{2+} + CO_3^2 = K_{sp}$ and the mineral phase is in chemical equilibrium with the surrounding seawater (*i.e.* saturated). Values of Ω_A larger than 1 occur when natural crystallization of aragonite is inhibited. This 'supersaturated' state is common in seawater (Feely et al., 2009) due to kinetic barriers, such as strong hydration energy of calcium ions (Lippmann, 1973) or the presence of other dissolved minerals (Usdowski, 1968). The current carbonate chemistry in the oceans is therefore favoring precipitation of $CaCO_3$. Molecular kinetic activity increases with temperature, causing latitudinal gradients of Ω_A = 2.41 – 3.94 (Feely et al., 2009) with highest mean values in the tropics and lowest saturation states around the poles (Jiang et al., 2015). When $\Omega_A < 1$, the environment is undersaturated with respect to aragonite and dissolution of CaCO3 is favored. Since Ca^{2+} is conservative and scales with salinity (Fassbender et al., 2016), the balance between precipitation and dissolution of aragonite in seawater is almost exclusively governed by CO_3^{2-}:

$$Ca^{2+}_{[aq]} + CO_3^{2-}{}_{[aq]} \leftrightarrow CaCO_{3\,[s]} \quad , \qquad (5)$$

with subscripts describing the mineral phase; [aq] = aqueous (dissolved) and [s] = solid (precipitated). From a purely chemical perspective, this provides a simple framework describing how CO_3^{2-} availability may dictate calcification rates in marine organisms (Kleypas & Yates, 2009; Bates et al., 2010). Aragonite is widely used in empirical studies and future model predictions as primary determinant of coral calcification (Kleypas et al., 1999; Doney et al., 2009; Evenhuis et al., 2015; Rosón et al., 2016) under the assumption that corals use CO_3^{2-} as a substrate to produce $CaCO_3$.

Although the relationship between coral calcification and Ω_A has been demonstrated *in situ* and in the field (Chan & Connolly, 2013; Kroeker et al., 2013), it does not always hold true (Rodolfo-Metalpa et al., 2010; Roleda et al., 2012; Shamberger et al., 2014). Several biological mechanisms have been proposed that would render CO_3^{2-} and Ω_A less relevant for calcification. Molecular transport mechanisms within the coral holobiont are one example. To supply endosymbiotic algae with inorganic carbon for photosynthesis, corals actively take up bicarbonate (HCO_3^-) and aqueous CO_2 using specific transport molecules (Bedwell-Ivers et al., 2016). The processes are coupled with a proton pump, as bicarbonate is dehydrated and hydrolyzed during import. Considering these and other involved molecular conversion processes, it is not surprising that corals have been shown to use both CO_3^{2-} and HCO_3^- for calcification (Cohen et al., 2009; Comeau et al., 2013a; Castillo et al., 2014). Wall and Edmunds (2013) found 81% elevations in calcification of *Porites* spp. exposed to increased HCO_3^- but no effect of low pH. In some instances, calcification correlated better with HCO_3^- than with CO_3^2 (Jury et al., 2010). Bicarbonate is also the largest contributor to alkalinity (*i.e.* the capacity of seawater to resist changes in pH), which has been proposed to buffer the adverse effects of OA on coral calcification (Jokiel, 2016).

Based on a wide distribution of calcification responses to OA, several biological and environmental traits have been proposed to drive contradicting results. Examples include morphological differences (Jokiel, 2011; Comeau et al., 2014c), taxonomic variability (Edmunds et al., 2012) (Fabricius et al., 2011) , life stage (Albright & Langdon, 2011; Drenkard et al., 2013), and nutritional status (Drenkard et al., 2013; Ohki et al., 2013). Varying rates and types of calcification are assumed to relate to different problematics of

OA. Fast-growing species have increased demand for dissolved minerals and are therefore considered more vulnerable to potential mineral limitation compared to slow-growing corals (Fabricius et al., 2011; Movilla et al., 2012). In contrast, increasing porosity of the skeleton facilitates proton efflux and may render perforate (*i.e.* porous) species more resilient against increasing H^+ concentrations (Edmunds, 2011; Jokiel, 2011). Comeau et al. (2014c) tested both assumptions subjecting eight coral species to similar treatments and found only growth rate to be inversely associated with OA resistance.

Different coral taxa show considerable variation of calcification resistance to high-CO_2 environments. Edmunds et al. (2012) compiled data from 12 studies and found differences between calcification of *Acropora*, *Favia*, and *Madracis* colonies following modifications of pH, CO_3^{2-}, and HCO_3^-. Branching *Acropora* and massive *Favia* were shown to be strongly affected by OA (Movilla et al., 2012; Ohki et al., 2013). As long as $\Omega_A > 1$, calcification was maintained in massive *Porites* (Comeau et al., 2013a; Crook et al., 2013) and branching *Pocillopora damicornis* (Comeau et al., 2013c; Comeau et al., 2014a), while *Stylophora pistillata* (Pocilloporidae) reduced calcification only at very low pH (Venn et al., 2013). *Siderastrea siderea* showed a consistent parabolic response to OA (Castillo et al., 2014).

Under sufficient nutrition, juvenile corals may tolerate OA. Coral resistance to OA is thought to vary among life stages (Albright & Langdon, 2011) and the above described pattern of adult taxa appears to translate to juveniles. Evidence for this comes from compromised calcification in *Acropora* spp. (Suwa et al., 2010; Ohki et al., 2013; Foster et al., 2015) and *Favia* spp. (Cohen et al., 2009; Drenkard et al., 2013), while *Porites* recruits continued to accrete $CaCO_3$ at similar rates (Anlauf et al., 2011; Edmunds, 2011). Juvenile *P. damicornis* calcification decreased by 34% under elevated pCO_2 (Jiang et al., 2015) but lower light intensities ameliorated this effect (Dufault et al., 2013).

Increased energy reserves generally benefit coral growth (Edmunds et al., 2005) and are particularly important during the onset of calcification (Pandolfi et al., 2011). This has been demonstrated for many taxa as well as symbiotic and non-symbiotic nutritional pathways. The presence of endosymbiotic algae allowed *Acropora digitifera* recruits to maintain calcification under elevated pCO_2 (Ohki et al., 2013). This benefit was augmented in *P. damicornis* juveniles by increasing light conditions up to 200 µmol photons m^{-2} s^{-1}

(Dufault et al., 2013). Provision of particulate food to support heterotrophic feeding leads to similar results in primary polyps of *Porites* spp. (Edmunds, 2011) and *F. fragum* (Drenkard et al., 2013). These experiments underline the role of nutritional status in regulating calcification responses of juvenile corals to OA.

Earlier recruitment processes can also be affected by OA. Findings in a previous meta-analysis suggest that OA will drastically compromise recruitment success in many calcifying marine animals (Dupont et al., 2010). However, this view has been challenged in another meta-analysis (Hendriks et al., 2010). Whether coral recruitment will suffer from elevated pCO_2 with repercussions on the population level remains questionable. OA could impact several early steps of the recruitment process including fertilization, survival of larvae, and metamorphosis. However, coral larvae of some species have been shown to develop and survive well despite OA. Gametes of two *Acropora* species fertilized equally in ambient and low pH environments (Chua et al., 2013) but the amount of sperm needed to reach 50% fertilization increased 5-fold (Albright et al., 2010). Larval survival in high pCO_2 treatments was unaffected in *Acropora* and *Fungia* spp. (Suwa et al., 2010; Baria et al., 2015) but mortality in *Pocillopora* larvae doubled (Cumbo et al., 2013c).

Ocean acidification can affect coral settlement in two ways; direct impairment of the ability to metamorphose (Viyakarn et al., 2015) and concurrent changes in the substratum indirectly compromising settlement (Doropoulos & Diaz-Pulido, 2013). Initial studies demonstrated intolerance of *Acropora* larvae to settle under acidified seawater conditions (Albright et al., 2010; Nakamura et al., 2011) and this has been corroborated for larvae of *Porites* and *Pocillopora* spp. (Albright & Langdon, 2011; Viyakarn et al., 2015). Suggested mechanisms for these findings include disruption of the settlement process (Albright et al., 2010) or a lowering of the adhesion between substrate and recruits (Edmunds et al., 2013b). Opposing results showing unaffected settlement in similar species (Anlauf et al., 2011; Chua et al., 2013; Foster et al., 2015) have fostered more thorough investigation. Albright et al. (2010) suggested indirect effects of OA via alterations of the substrate community. They conditioned settlement tiles in experimental conditions and noted an increase in filamentous algae and concomitant reductions in crustose coralline algae (CCA) under elevated pCO_2. CCA produce chemical cues that attract coral larvae and initiate settlement (Yadav et al., 2016). If corals continue to rely on these chemicals to find suitable substrates,

a population decline of CCA may compromise coral settlement (Albright et al., 2010; Webster et al., 2013). Changes in carbonate chemistry of seawater are also suggested to rapidly alter chemical cues emitted by CCA, making them inaccessible to coral larvae (Doropoulos & Diaz-Pulido, 2013).

OA potentially affects additional physiological responses, especially those involving *pH* gradients across cell membranes (e.g. photosynthesis or nutrient transport) (Doney et al., 2009). We are beginning to understand how these processes interact with each other and respond to changing carbon chemistry. However, the amount of empirical data is still insufficient to warrant meaningful results from quantitative analyses.

Combined effects of ocean acidification and warming on coral physiology

The assessment of interactive effects of OAW on the physiology of marine organisms is becoming a research priority. Recent empirical studies and subsequent meta-analyses have provided insights on the responses of several life stages of corals to OAW. Larval survival is sometimes unaffected if temperature and CO_2 act together (Chua et al., 2013), particularly in Fungids and brooding corals (Putnam et al., 2013; Baria et al., 2015). A recent meta-analysis supports this finding (Przeslawski et al., 2015), although under prolonged exposure (5 days) the effect can be negative and similar to the effect of stressors independently (Cumbo et al., 2013c). In contrast, OAW in combination has neutral or positive effects on settlement and metamorphosis (Anlauf et al., 2011; Chua et al., 2013; Foster et al., 2015).

The combined effect of OAW is thought to act synergistically on the growth of marine calcifying organisms, generally reducing calcification rates when temperature thresholds are approached or exceeded (Harvey et al., 2013). The synergistic interaction of elevated temperature and pCO_2 is evident for some taxa such as echinoderms or bivalves but not for corals (Hendriks et al., 2010; Harvey et al., 2013). Kroeker et al. (2013) also found that the effects of OA on coral calcification were unaffected by warmer temperatures. Further, the calcification response of corals to interacting effects of OAW can be subject to large variation (Harvey et al., 2013). Additional empirical studies and quantitative analyses are needed to elucidate how interacting OAW relate to the biomineralization process and thermal thresholds of individual coral taxa.

Objectives

Despite providing useful insights, the conflicting findings describing the impact of OAW on coral physiology limit the potential to identify general factors that drive coral resistance to changing environments. Empirical testing and field observations add to the portfolio of hypotheses attempting to explain the variation in coral responses to climate change. Standard meta-analytical tools can be used to assess these hypotheses but do not account for the bias caused by differing stress levels across studies. The objectives in this study were to:

i.) estimate the overall effects of OAW on coral responses (larval survival, settlement, and calcification)

ii.) quantify the influence of varying stress levels across studies, and

iii.) test if certain proposed traits or conditions can drive coral responses to individual and combined effects of OAW.

A sensitivity analysis was conducted to identify additional sources of scientific bias (e.g. publication bias or type I errors). The specific hypotheses addressed in this study (Table 1) describe characteristic traits, conditions, or mechanisms that potentially regulate coral sensitivities to OAW. These drivers range from biological traits such as reproductive strategies (brooders vs. broadcast spawners), growth rates (slow vs. fast), growth forms (e.g. branching vs. massive), and life stages (larvae vs. juveniles vs. adults) to environmental factors such as type of habitat (e.g. back reef vs. fringing reef) and native climate (tropical vs. subtropical). Differences in experimental design may also impact study outcomes. Some of the methodological components included in the factorial analysis were stressor magnitude (medium vs. high), duration of the experiment (short-term vs. long-term), and filter size (< 50 µm vs. > 50 µm). A description of all 27 potential drivers tested in this study is provided in the *supplementary material* (Table S1).

Table 1: Study-specific hypotheses relating to drivers of coral resistance to climate change. Mathematical operator '>' refers to sensitivity. Attributes on the left side ('Losers') are hypothesized to cause increased sensitivity to ocean warming (hypotheses 1 – 7) or ocean acidification (hypotheses 8 – 18).

ID	Effect size related hypothesis			Sources
	'Losers'		'Winners'	
Ocean warming and calcification				
1	Branching corals	>	Massive corals	Gates and Edmunds (1999) Mydlarz et al. (2010) van Woesik et al. (2011)
2	Adults	>	Juveniles	Loya et al. (2001)
3	Corals from thermally stable environments	>	Corals from thermally variable environments	McClanahan and Maina (2003) Palumbi et al. (2014)
4	Tropical corals	>	Subtropical corals	Hoegh-Guldberg (1999)
Ocean warming and larval survival				
5	Larval survival rates	>	Settlement & growth rates	Byrne (2011) Putnam et al. (2010)
6	Symbiotic larvae of brooding corals	>	Aposymbiotic larvae of broadcast spawning corals	Baird et al. (2006) Yakovleva et al. (2009)
7	Larvae in filtered treatments	>	Larvae in unfiltered treatments	This study
Ocean acidification and calcification				
8	Juveniles	>	Adults	Albright and Langdon (2011) Edmunds et al. (2012) Ohki et al. (2013)
9	Branching corals	>	Massive corals	Fabricius et al. (2011) Comeau et al. (2013b) Edmunds et al. (2012)
10	Fast-growing corals	>	Slow-growing corals	Rodolfo-Metalpa et al. (2010) Fabricius et al. (2011) Comeau et al. (2014b)
11	Imperforate corals	>	Perforate corals	Jokiel (2011)
12	Subtropical corals	>	Tropical corals	This study
13	Corals experiencing stable CO2 conditions	>	Corals experiencing CO2 fluctuations	This study
14	Starved corals	>	Well-fed corals	Cohen et al. (2009) Holcomb et al. (2010) Pandolfi et al. (2011)
15	Corals in short-term exposures	>	Corals in long-term exposures	Pandolfi et al. (2011)
Ocean acidification and settlement				
16	Growth rates	>	Settlement rates	Byrne (2011)

Methods

Data selection

Peer-reviewed articles on manipulative laboratory experiments were assembled from the Web of Science database, using the keyword "coral" in all possible combinations with a second keyword describing the stressor (climate change, ocean warming, and ocean acidification) and a third keyword referring to life stage and physiological responses (larvae, survival, reproduction, metamorphosis, settlement, and calcification). A detailed list including all keyword combinations and the number of articles returned for each search is provided in the *supplementary material* (Table S2). All pCO_2 and temperature levels were accepted for initial sorting. However, studies involving temperature increases above +4°C or pCO_2 manipulations above the projected ranges of the 'Representative Concentration Pathways' (RCP's, 490 – 1370 ppm by 2100) (IPCC, 2014) were analyzed in a preliminary effect size comparison. If the effects were stronger compared to moderate stress treatments, they were excluded from the original dataset and added to a secondary dataset (see *Sensitivity analysis*). If the opposite was true or effect sizes were equal, all data were maintained in the original dataset. This was done to ensure that the original data include only realistic future estimates of changes in surface water temperature and acidity.

When multiple responses, species or treatment levels were assessed in one study, all suitable measurements were included in the analysis. Suitable measurements reported mean responses, sample sizes and some form of variance (standard errors, standard deviations or confidence intervals) following experimental and controlled stress treatments. Stressors were either reduced aragonite saturation or elevated temperature under ambient levels of any additional stress (e.g. irradiance or oxygen saturation). Measurements were on larval survival, settlement or calcification of shallow water corals. Data was further limited to single response measurements per treatment that fall under the same category. For instance, if calcification was measured and the results were reported in buoyant weight and surface area, only the more accurate and/or common measurement (here buoyant weight) was included in the dataset.

Data extraction

Three types of data were extracted from every publication, describing its outcome, stress level and specific independent variables potentially driving variation between outcomes. Outcome data was extracted from graphical elements (usually bar charts) using the software application Datathief (http://www.datathief.org). The results of the experimental and control treatments were combined and log transformed to compute the log response ratio (L) of each particular comparison according to Hedges et al. (1999):

$$L = \ln\left(\overline{X}_E \Big/ \overline{X}_C + C\right) , \quad (6)$$

where $\overline{X}_E$ and $\overline{X}_C$ represent the mean response of the experimental and control treatments, respectively. The constant C ensured values for L ranging from 0 to 1 and was calculated as:

$$C = 1 - \min\left(\overline{X}_E \Big/ \overline{X}_C\right) . \quad (7)$$

In most cases, $\overline{X}_E$ and $\overline{X}_C$ were extracted from the last exposure time point but sometimes this was limited. When larval survival studies showed 100% mortality in experimental treatments, the log response ratio was computed from the last exposure time point that still contained live larvae in experimental treatments. Standard deviations (SD) were extracted from each treatment as variance component. If standard errors (SE) or 95 % confidence intervals (CI) were reported, transformation was applied using:

$$SD = SE\sqrt{n} = \frac{CI}{1.96}\sqrt{n} , \quad (8)$$

with n representing the sample size.

Treatment temperature was extracted from OW experiments, while OA treatments involve multiple carbonate chemistry parameters including pCO_2, pH, CO_3^{2-}, HCO_3^-, dissolved inorganic carbon (DIC), alkalinity (a_T) and aragonite saturation state (Ω_A). For these parameters, the difference between experimental and control setting was computed according to the following example using Ω_A:

$$\Delta\Omega_{\mathbf{A}} = \Omega_{\mathbf{A_{exp}}} - \Omega_{A_{con}} , \quad (9)$$

where $\Omega_{A_{exp}}$ and $\Omega_{A_{con}}$ represent the aragonite saturation state of the experimental and control treatments, respectively. Salinity and temperature data were also extracted from ocean acidification experiments and entered into the statistical software R (R Development

Core Team, 2010). Using the package *seacarb*, input of salinity, temperature alkalinity and pCO_2 enabled calculation of additional carbonate chemistry parameters. The calculated estimates were entered into the dataset whenever they were not reported in the study.

Finally, independent variables potentially driving variation across study results were identified and extracted from each study. Potential drivers were classified as biological traits, environmental factors or differences in experimental design. Categorical variables were noted whenever they were reported and continuous variables were transformed into ordinal type by setting interval limits.

Data analysis

Factorial effect size comparison

Six separate effect size meta-analyses were conducted according to the methods described below. One for each response (larval survival, settlement or calcification) and stressor (elevated temperature or pCO_2). Analyses were carried out in R using the packages *devtools*, *broom*, *ggplot2*, *R.basic*, *doBy*, *lme4*, *lattice*, *lmtest*, *lsmeans*, *bear* and *xlsx*. The R codes to compute the statistical model (Fig. 1) are provided in the *supplementary material*.

Parametric computations were taken from Hedges et al. (1999). Initially, the random variance of the whole dataset was tested by comparing the heterogeneity statistics Q against a chi square distribution with n-1 degrees of freedom. The heterogeneity statistics was calculated as:

$$Q = \sum_{i=1}^{n} \lambda_i (L_i)^2 - \frac{\sum_{i=1}^{n} (\lambda_i L_i)^2}{\sum_{i=1}^{n} \lambda_i} \quad , \tag{10}$$

where i (subscript) represents each individual sample and λ is the reciprocal of the given within-study variance v_w computed as:

$$\lambda = 1/v_w \quad . \tag{11}$$

The null hypothesis stated that observations share a common effect size. If the null hypothesis could not be rejected, random variation was assumed to be insignificant and the sample was analyzed using a *fixed effects* model. In a fixed model, λ is used to describe the relative contribution of each sample point (*i.e.* it's statistical weight). If, however, random variation was significant, a *mixed effects* model was applied. Here, the statistical

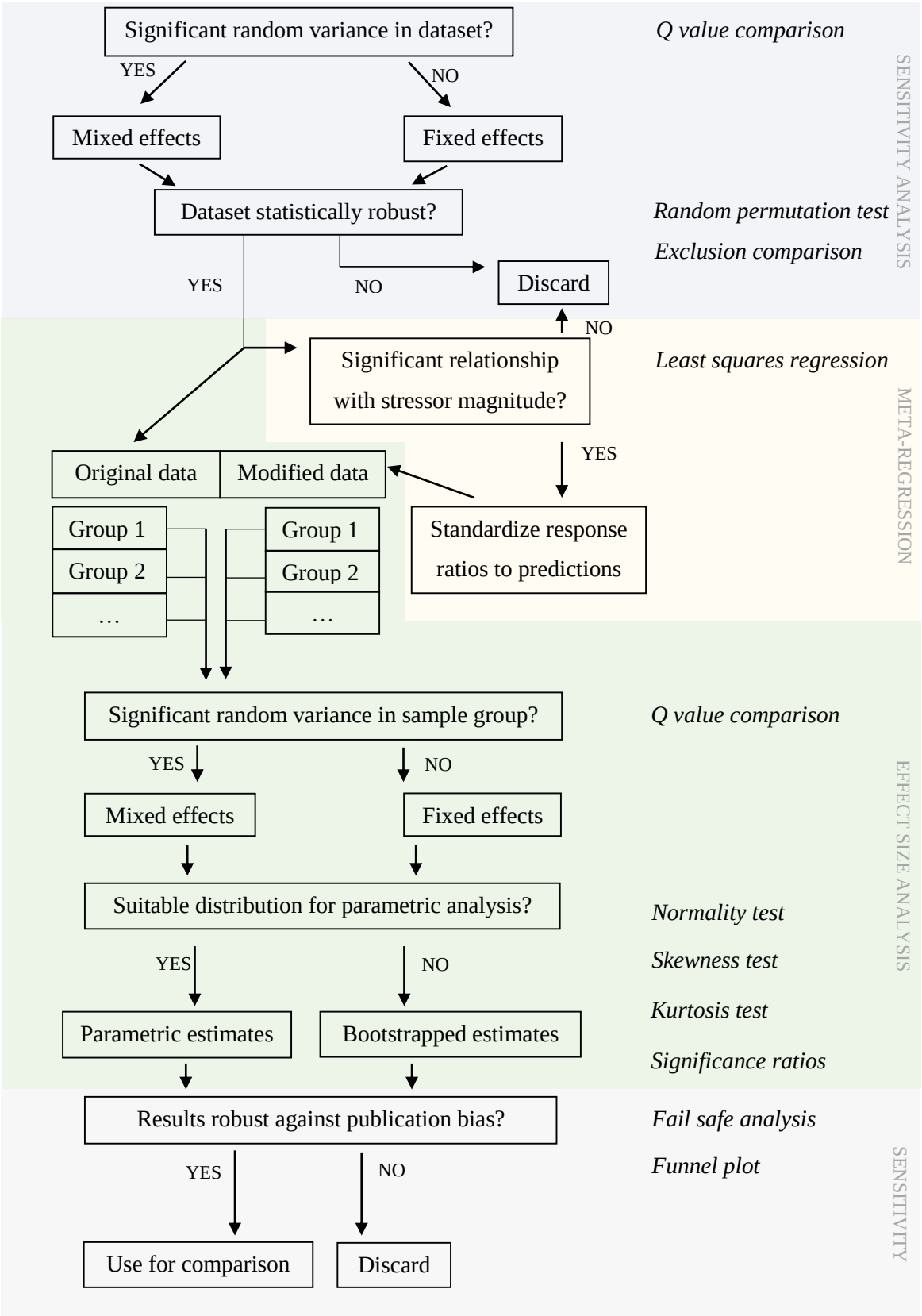

Figure 1: Schematic diagram showing individual steps of the statistical model and relevant computations.

weight of each sample incorporates the additional between-study variation v_b resulting from:

$$v_b = \frac{Q-(n-1)}{\sum_{i=1}^{n}\lambda_i - \frac{\sum_{i=1}^{n}\lambda_i^{\,2}}{\sum_{i=1}^{n}\lambda_i}} \quad . \tag{12}$$

The statistical weight for each sample point in the *mixed effects* model (λ^*) was then computed as:

$$\lambda^* = 1/(v_b + v_w) \quad . \tag{13}$$

In the next step, distribution and precision of log response ratios L_i were investigated. This was done graphically by creating histogram plots, QQ-plots, and funnel plots using the R package *ggplot2*. Additional numerical procedures included a Shapiro-Wilk normality test and quantitative estimates of kurtosis, skew, and suitability ratios. Suitability ratios offer a good way to investigate sample bias and skew (Hedges et al., 1999). The ratios s_{iC} and s_{iE} were calculated for the control and experimental treatments of each study outcome:

$$s_{iC} = \sqrt{n_C}\frac{\bar{X}_C}{SD_C} \quad , \quad s_{iE} = \sqrt{n_E}\frac{\bar{X}_E}{SD_E} \quad , \tag{14}$$

where SD_C and SD_E are the standard deviations of the control and experimental treatment, respectively. If the smaller value of s_{iC} and s_{iE} is less than 3 in greater than one third of the studies within the analyzed group, approximations based on parametric statistics may be misleading (Hedges et al., 1999). If the data were approximately normally distributed and the suitability ratios were large enough, parametric mean estimates as described in Hedges et al. (1999) were used to obtain mean effect sizes. Using the individual log response ratios L_i and their respective weights λ_i or λ^*_i (depending on the significance of the random variance), the mean effect size was calculated as:

$$\bar{L}_{fix} = \frac{\sum_{i=1}^{n}\lambda_i L_i}{\sum_{i=1}^{n}\lambda_i} \quad , \quad \bar{L}_{mix} = \frac{\sum_{i=1}^{n}\lambda_i^* L_i}{\sum_{i=1}^{n}\lambda_i^*} \quad , \tag{15}$$

with the subscripts fix and mix denoting the model type (*fixed effects* and *mixed effects*, respectively). The standard error estimate (SE) was obtained from:

$$SE_{fix} = \sqrt{\frac{1}{\sum_{i=1}^{n}\lambda_i}} \quad , \quad SE_{mix} = \sqrt{\frac{1}{\sum_{i=1}^{n}\lambda_i^*}} \quad . \tag{16}$$

In mixed models, a small sample size may lead to inaccurate estimates using the equation above (Hedges et al., 1999). Standard errors of smaller samples (n < 50) were thus computed from:

$$SE = \sqrt{\frac{1}{\sum_{i=1}^{n}\lambda_i^*}\left(1 + 4\sum_{i=1}^{n}\frac{1}{df_i}\left(\frac{\lambda_i^*}{\lambda_i}\right)^2 \frac{\lambda_i^*[(\sum_{i=1}^{n}\lambda_i^*)-\lambda_i^*]}{(\sum_{i=1}^{n}\lambda_i^*)^2}\right)} \quad , \tag{17}$$

with df_i denoting the degrees of freedom in the ith study, which was calculated using the sample sizes of the experimental and control treatment (n_{iE} and n_{iC}, respectively):

$$df_i = n_{iE} + n_{iC} - 2 \quad . \tag{18}$$

Significance of effect sizes were tested by computing 95% upper and lower confidence intervals (CI_U and CI_L, respectively) according to:

$$CI_L = \bar{L} - \tau\, SE(\bar{L}) \leq \bar{L} \leq \bar{L} + \tau\, SE(\bar{L}) = CI_U \quad , \tag{19}$$

with τ being the 97.5 % point of the standard normal distribution (1.96). If, however, normality and/ or suitability assumptions were not met, the mean effect size was computed as weighted percentile bootstrapped interval (Adams et al., 1997). The weights were transformed into probabilities p_i using:

$$p_{i_{fix}} = \frac{\lambda_i}{\sum_{i=1}^{n}\lambda_i} \quad , \quad p_{i_{mix}} = \frac{\lambda_i^*}{\sum_{i=1}^{n}\lambda_i^*} \quad . \tag{20}$$

The probabilities were fed into a subsampling command (with replacement, 9999 iterations) and the arithmetic mean response was computed each time. The resulting distribution was used to extract the 2.5% and 97.5% points and build 95% confidence intervals. Effects were considered significant, when the confidence interval did not include zero.

In the subsequent intent to identify drivers of the variation between studies, the dataset was split into subsamples according to factorial variables (Table S1). Identical to the procedure described above, normality and the significance of the random variance were tested for each subsample and the confidence intervals were calculated with the appropriate model variation (*fixed effects* vs. *mixed effects*, parametric vs. bootstrapped). Subsample means L_m (subscript m refers to the subsample) were considered significantly different, when the confidence intervals did not overlap. Finally, partitioned heterogeneity statistics were calculated to estimate the amount of heterogeneity explained by each categorical

comparison. Total heterogeneity of the sample Q_T and the heterogeneity described by the single factorial model Q_M were estimated using:

$$Q_T = \sum_{i=1}^{n} \lambda_i (L_i - \bar{L})^2 \quad , \quad Q_M = \sum_{m=1}^{M} W_m (L_m - \bar{L})^2 \quad , \qquad (21)$$

where M is the number of subsamples and W is the sum of the weights (λ_i or λ^*_i) in subsample m. The residual heterogeneity Q_E was then simply computed as the difference between total and model heterogeneity ($Q_E = Q_T - Q_M$).

Meta-regression

Weighted meta-regression was performed to account for a type of research bias (researchers applying varying degrees of stress across studies) that has complicated interpretations in previous ecological effect size meta-analyses (Chan & Connolly, 2013). Originally excluded data using unrealistically high in situ stress levels (see *Data selection*) were reintroduced to the dataset. First and second order linear models were fitted to the log response ratios using magnitude of the stressor as continuous independent variable. This required a preliminary comparison of different metrics describing the stressor. For temperature data, the stressor magnitude could be described by experimental temperature (T_E) or the difference between experimental and control temperatures (ΔT). Meta-regression was therefore performed two times using either T_E or ΔT as independent variable (unit in ℃). For acidification data, the relevant carbon chemistry parameters are currently debated (Jokiel, 2011, 2016). Therefore, meta-regression on response ratios was conducted 14 separate times, each time using a different parameter as independent variable (Table 2).

Different models for the same relationship were compared by investigating p-values, R^2, and the model heterogeneity Q_M. Model heterogeneity was obtained from:

$$Q_M = \frac{\beta^2}{SE_\beta{}^2} \quad , \qquad (22)$$

with β as the estimated slope of the relationship and SE_β as its standard error. Total heterogeneity Q_T was derived from equation (22) and residual heterogeneity computed as the difference of the two ($Q_E = Q_T - Q_M$). In addition, a random permutation test was performed to test the significance of Q_M, using 4999 iterations with replacement. Each time, a linear model was fit and Q_M was calculated to test whether random subsampling

can produce more significant heterogeneity statistics. The respective p-value was obtained from:

$$p = \frac{Q_0+1}{5000} \ , \tag{23}$$

where Q_0 represents the number of permutations resulting in larger values for Q_M.

The best fit was selected based on significance of the relationship (p-value) and amount of variation explained (R^2 and model heterogeneity Q_M). If a significant relationship ($p < 0.05$) was detected for a large dataset ($n > 50$), the best least squares predictions LS_i were used to standardize all log response ratios (*i.e.* effect sizes from individual studies) according to their accompanying stress levels:

$$L_i^* = {L_i}/{LS_i} \ . \tag{24}$$

Table 2: Computations of independent variables from carbon chemistry parameters for use in stressor-effect meta-regression. n/u = no unit.

Parameter	***Symbols***	***Δ Calculation***	***Unit***
pH	$pH_E,\ \Delta pH$	$\Delta pH = pH_E - pH_C$	n/u
pCO_2	$pCO_{2_E},\ \Delta pCO_2$	$\Delta pCO_2 = pCO_{2_E} - pCO_{2_C}$	µatm
Aragonite saturation	$\Omega_{A_E},\ \Delta\Omega_A$	$\Delta\Omega_A = \Omega_{A_E} - \Omega_{A_C}$	n/u
Carbonate ion concentration	$CO_3^{2-}{}_E,\ \Delta CO_3^{2-}$	$\Delta CO_3^{2-} = CO_3^{2-}{}_E - CO_3^{2-}{}_C$	µmol kg^{-1}
Bicarbonate ion concentration	$HCO_3^-{}_E,\ \Delta HCO_3^-$	$\Delta HCO_3^- = HCO_3^-{}_E - HCO_3^-{}_C$	µmol kg^{-1}
Bicarbonate-hydrogen ratio	$\frac{HCO_3^-{}_E}{H^+{}_E},\ \Delta\left(\frac{HCO_3^-}{H^+}\right)$	$\Delta\left(\frac{HCO_3^-}{H^+}\right) = \frac{HCO_3^-{}_E}{H^+{}_E} - \frac{HCO_3^-{}_C}{H^+{}_C}$	n/u
Carbon-hydrogen ratio	$\frac{DIC_E}{H^+{}_E},\ \Delta\left(\frac{DIC}{H^+}\right)$	$\Delta\left(\frac{DIC}{H^+}\right) = \frac{DIC_E}{H^+{}_E} - \frac{DIC_C}{H^+{}_C}$	n/u

Using standardized log response ratios L^*_i, the complete analysis was rerun according to the methods described above. Mean effect sizes resulting from this approach do not display relative increases or decreases of the physiological response. Instead, they depict whether certain subsamples perform better or worse compared to what is expected under consideration of the inherent stress levels in each subsample. In other words, if a significant

difference between two groups for L_i becomes insignificant for L^*_i, it means that the original difference likely resulted from lower stress levels in the apparently better performing group (*i.e.* research bias). Alternatively, an insignificant difference for L_i that becomes significant for L^*_i would indicate a type II error. In this case, an actual statistical difference was shadowed because the better performing group has been subjected to higher stress levels, which lowers the resulting effect size and gives the impression that the two groups perform equally. For these reasons, categorical comparisons from L^*_i were used as a quality assessment to find or rule out significant differences that were affected by varying stress levels between studies.

Sensitivity analyses

Synthesizing results of different studies to reach a global understanding requires careful evaluation of different sources of bias. Sensitivity of the data was analyzed using five separate investigations. First, an exclusion comparison was conducted as described by Kroeker et al. (2013) to assess individual contributions of the most significant studies. Second, a random permutation test was designed to estimate the likelihood of committing type I errors. Third, funnel plots were investigated to assess distribution properties of the dataset and potential for publication bias. Fourth, a fail-safe analysis (Rosenthal, 1979) was performed to address robustness against publication bias of individual subsamples. Lastly, alternative effect sizes were computed using only the largest two datasets (calcification response to OAW). The different metrics were then compared to evaluate the importance of the choice of effect size.

The contribution of the most significant studies was estimated by selectively excluding the five most significant studies, one at a time, and re-computing the overall mean effect size as described above. If the procedure changed the significance of the overall result for any of the excluded studies, that particular study remained absent from the dataset. To obtain a final quality assessment of the dataset, a random permutation test with 2999 iterations was used. Each time, two random subsamples were created without replacement. The sample size of the first subsample n_1 was determined randomly and limited to any number between 3 and n – 3. The sample size for the second subsample n_2 was computed from n_1 ($n_2 = n - n_1$). The mean effect sizes and confidence intervals of

both groups were estimated using weighted bootstrapping as described above except that only 2999 iterations were used due to constraints arising from computations involving double-iterations. Subsequently, the distances d_{S1} and d_{S2} were computed from the upper and lower confidence intervals CI_U and CI_L as:

$$d_{S1} = \sqrt{CI_{U1}^2 + CI_{L2}^2} \quad , \quad d_{S2} = \sqrt{CI_{U2}^2 + CI_{L1}^2} \ , \tag{25}$$

where subscripts refer to the subsamples 1 and 2. The smaller of d_{S1} and d_{S2} reveals the shorter distance between upper confidence limits of one subsample and lower confidence limits of the other subsample. The respective confidence limits of the smaller of d_{S1} and d_{S2} are then used to obtain a measure of significance D_S between the groups:

$$D_S = CI_{Um} - CI_{Lj} \ , \tag{26}$$

where subscripts m and j refer to the subsamples. If D_S becomes negative, the confidence intervals of the two randomly allocated subsamples do not overlap each other (*i.e.* type I error). Finally, the distribution of D_S is investigated and a p-value for the likelihood to commit a type I error can be derived from:

$$p = \frac{D_0+1}{3000} \ , \tag{27}$$

where D_0 equals the number of permutations with $D_S < 0$ (Adams et al., 1997). An arbitrary threshold was set at $p = 0.06$ and any datasets displaying more than 6% likelihood for type I errors to occur were discarded from the analysis.

Publication bias results from unequal effect size distribution among published and unpublished data. In ecological response measurements, results are more likely to be published if they show significant effects. Therefore, publication bias may lead to an overestimation of the mean effect. Funnel plots were obtained by plotting response ratios over sample sizes or standard errors. They can be used to estimate two sources of bias; unequal source populations and potential for publication bias. If the dataset describes a common mean response, the response ratios should 'funnel' in towards that response as sample sizes increase or standard errors decrease. Alternatively, an equal spread of response ratios with varying sample size or standard error is an indication of two or more true mean effect sizes within the dataset. Assuming the estimated response ratios derive from an approximate standard distribution, the two sides of the funnel should be equally occupied by empirical data. Publication bias may be pronounced if the response ratios tend to aggregate in one side of the funnel.

For every significant comparison, Rosenthal's fail safe analysis (Rosenthal, 1979) was conducted to estimate the number of insignificant results that would change the mean effect of each subsample into an insignificant result (*i.e.* raise the *p*-value of any significant difference between two subsamples above 0.05). By comparing this number to an arbitrary threshold ($I_{min} = 5n + 10$), the robustness of any significant comparison against potential publication bias could be estimated. The fail-safe statistics I was calculated as:

$$I = \frac{n}{2.706}[n(\bar{Z}_n)^2 - 2.706] \quad , \tag{28}$$

where $\bar{Z}_n$ is the Z score obtained by comparing the mean effect size of the subsample with 1 (*i.e.* no effect). Rosenthal provides a conservative estimate of the minimum value for I ($I_{min} = 5n + 10$) that would render the effect size of the subsample robust against publication bias. The fail-safe statistics were compared to their respective thresholds and results were limited to those identified as robust against publication bias. However, fail-safe analysis only assesses publication bias towards significance. Therefore, a high sensitivity against publication bias may increase the certainty of significant differences in some instances. For instance, when two groups of corals are negatively affected but one group is less affected than the other, a low I-value in the less affected group would add certainty to the result. The interpretation would be that unpublished insignificant results may drive the less affected group into a neutral effect, which would increase the statistical difference. If, however, the more affected group is sensitive towards publication bias, it shows that some unpublished results would easily lessen the effect observed in that group and make it more similar to the less affected subsample. As a result of this, significant differences between groups were disregarded only when the stronger mean effect size was considered sensitive against publication bias (*i.e.* $I < I_{min}$).

Based on an alternative effect size calculation, the interactive effects of OAW on coral calcification were quantified using a suitable subset of the data. Data were limited to studies reporting four treatment responses; one for the individual effects of OA and OW, one for their combined effect and one control response. Data were analyzed using the methodology described above but with different calculations for individual response ratios. In this model, effect sizes L^* were generated as described in Gurevitch et al. (2000). The individual effects of OA and OW in each study were computed as:

$$L^*_T = \frac{\bar{X}_T - \bar{X}_C}{s_p} \quad , \quad L^*_{pH} = \frac{\bar{X}_{pH} - \bar{X}_C}{s_p} \ , \tag{29}$$

where the subscripts T and pH denote the stressor (temperature increase or pH decrease) and s_p is the pooled standard deviation. The interactive strength L^*_{int} was estimated from:

$$L^*_{int} = \frac{(\bar{X}_{both} - \bar{X}_T) - (\bar{X}_{pH} - \bar{X}_C)}{s_p} \ , \tag{30}$$

where $\bar{X}_{both}$ is the mean response of the combined stress treatment. The sampling variance of L^*_{int} is:

$$s^2_N = \frac{1}{n_{both}} + \frac{1}{n_T} + \frac{1}{n_{pH}} + \frac{1}{n_C} + \frac{{L^*_{int}}^2}{2(n_{both} + n_T + n_{pH} + n_C)} \ . \tag{31}$$

If the effect was neutral, L^* was close to 0 (as opposed to 1 for estimates of L). If L^* and its 95% confidence interval were greater than 0, the effect was positive, while a negative effect was considered in the opposite case. The interpretation of the interactive strength depended on the outcome of individual stressors. For synergism to occur, the overall effects of warming, acidification and their interaction had to point in the same direction. Antagonistic effects were considered in all other cases where the interaction plus 95% confidence interval does not include zero. Resulting values for L^* were compared to their respective counterparts from this study (L) as well as to results obtained in a previous meta-analysis (Harvey et al., 2013) that also used estimations of L^*.

Results

Available data

Calcification was the most studied response to assess the consequences of OA for coral physiology (Fig. 2). More than half of the data addressed this particular response (63 publications, 212 samples). In contrast, recent studies investigating the effects of OW are equally focused on adult and larval performances. However, larval survival and settlement responses are often analyzed using survival curves and other Kaplan-Meier estimates without reporting variance estimates. These data are unfeasible for inclusion in parametric meta-analyses. Over the last few years, interactive effects of OAW have been established as a research priority. However, only calcification responses to combined stressors provided enough data for a separate meta-analysis (13 publications, 40 samples).

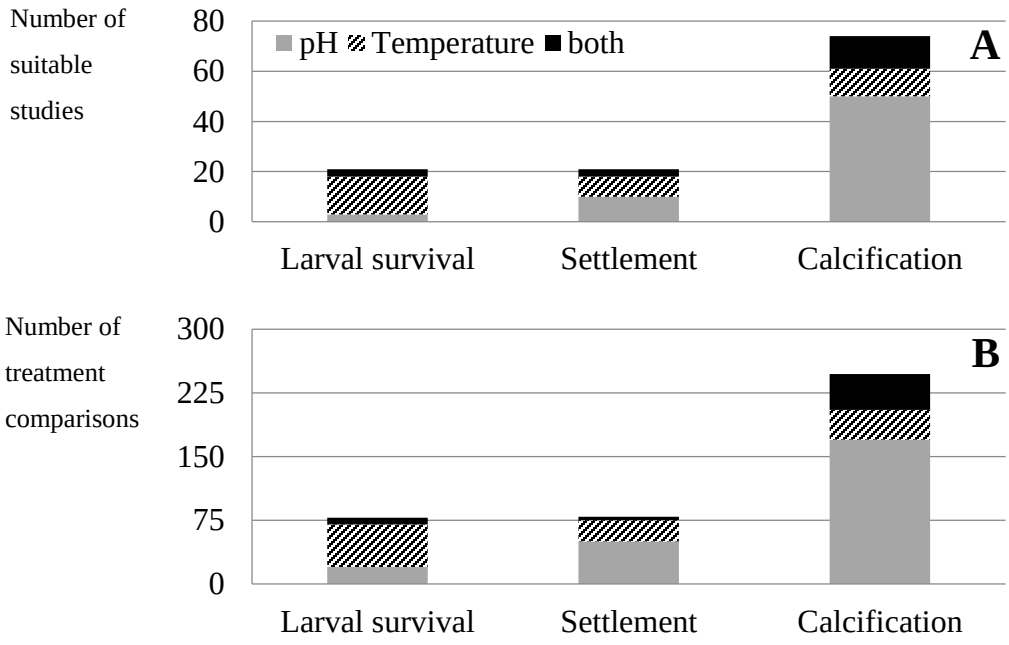

Figure 2: Number of suitable studies (A) and treatment comparisons (B) for each response to pH stress (grey bars), temperature stress (striped bars) and combined stresses (black bars) after the selection criteria were applied.

Individual effects of ocean acidification and warming on coral physiology

Pooled analyses for each response show that OAW negatively affects coral physiology. Ocean acidification projected for the end of the century causes average

reductions of 11.7% in coral settlement and 16.7% in coral calcification (Fig. 3A). A marginally significant negative effect on larval survival was dismissed due to uncertainty arising from potential publication bias (see *Sensitivity assessment*). In contrast, OW causes a 13.5% reduction in the survival of coral larvae. This is significantly different from calcification, which is unaffected by OW. Although settlement responses to elevated temperatures are predominantly negative, the mean effect was neutral (Fig. 3B). Effects sizes of OA and OW varied among taxa and life stages, as well as other environmental and methodological factors. However, factorial analysis was sometimes confounded by existing relationships between study outcomes and the varying stress levels applied in different experiments.

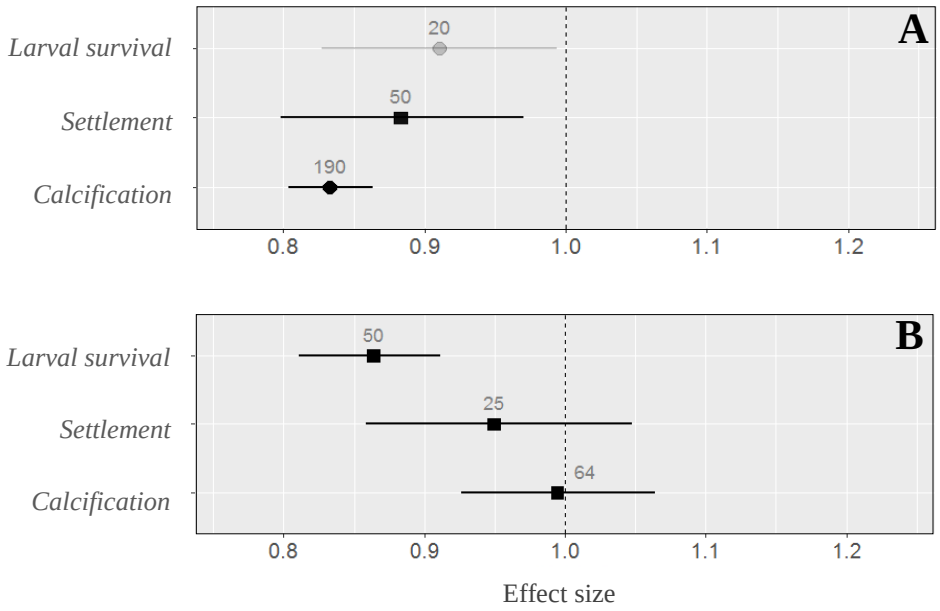

Figure 3: Pooled effect sizes (mean ± 95% CI) for different physiological responses of corals to ocean acidification (A) and ocean warming (B). Numbers are sample sizes and transparency of effect sizes and CI's represents sensitivity to publication bias (more transparent = more sensitive).

Influence of varying stress levels

Least squares regression revealed significant negative relationships between calcification responses and stress levels for both OA ($R^2 = 0.21$, $p = 5.61 \times 10^{-12}$, $Q_M = 56.22$, Fig. 4A) and OW ($R^2 = 0.15$, $p = 2.96 \times 10^{-4}$, $Q_M = 14.41$, Fig. 4B). The stressor metrics bearing the most significant relationships with study outcomes were ΔT (*i.e.* temperature difference between ambient and elevated treatments) for temperature data and Ω_{AE} (*i.e.* experimental aragonite saturation state) for acidification data (Table 3).

However, appropriate comparison of carbon chemistry parameters was compromised by virtue of experimental design. Specifically, researchers tended to maintain constant alkalinity levels among experimental and control treatments, obscuring potential cause-and-effect relationships. The comparison was therefore repeated under omission of studies keeping alkalinity constant over all treatments (*i.e.* $\Delta a_T < 40$ µmol kg^{-1}). Meta-regression of the remaining 56 treatment comparisons revealed that the strongest driver of calcification responses to OA was the difference in bicarbonate concentrations between ambient and elevated treatments ($\Delta(HCO_3^-)$) ($R^2 = 0.34$, $p = 4.55 \times 10^{-6}$, $Q_M = 26.56$, Table 4). In the original comparison, this parameter was the least significant driver (Table 5). Incorporating stress levels (Ω_{AE} or ΔT) into effect sizes obtained from each study resulted in secondary datasets for calcification responses that were analyzed parallel to the original datasets (see *Data analysis*).

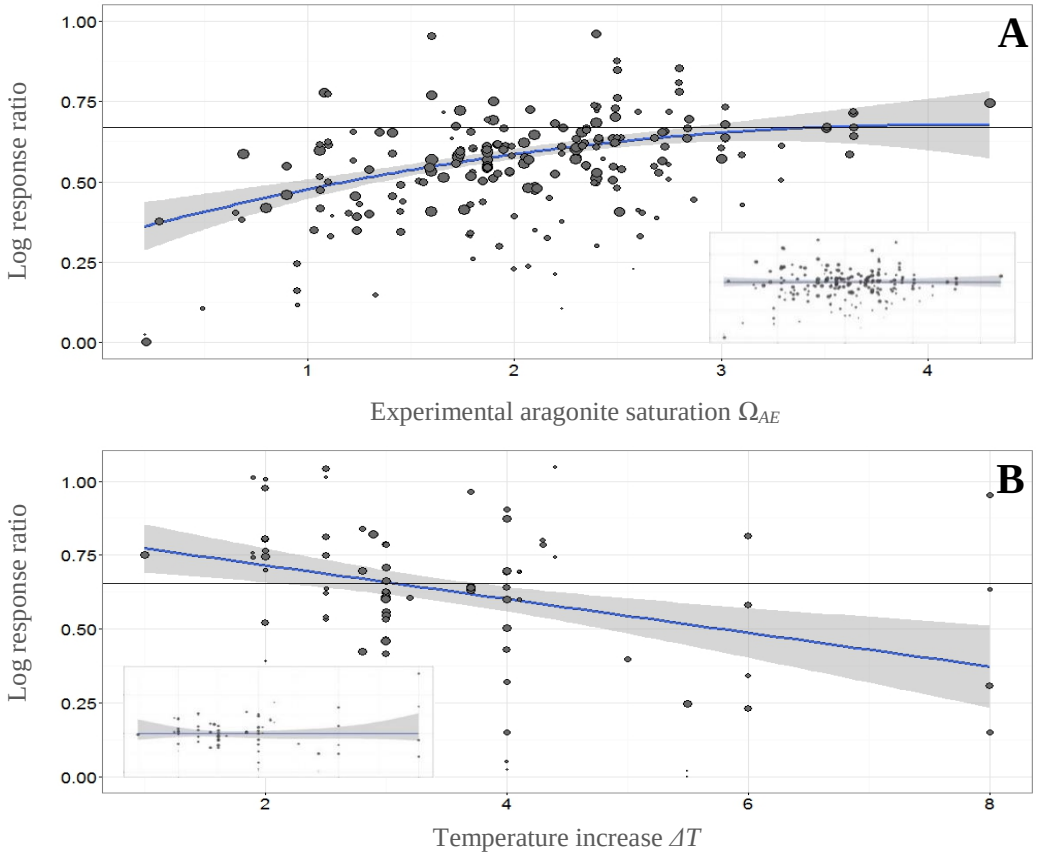

Figure 4: Best fit linear models describing stressor-effect relationships for calcification responses to ocean acidification (A) and ocean warming (B). Points are log transformed response ratios of individual treatment comparisons. Point size illustrates precision of each estimate. Secondary datasets to account for varying stress levels (small boxes) were produced by standardizing log response ratios to least square means from the linear model (blue lines).

Table 3: Model outputs of least squares meta-regressions for temperature metrics (rows 1 and 2) and acidification metrics (remaining rows), sorted by statistical significance of the model fit.

Independent variable	***p-value***	R^2	Q_M	Q_T	***n***
ΔT	2.96 x 10^{-4}	0.15	14.41	70.12	77
T_E	6.34 x 10^{-3}	0.00	1.24	70.12	77
Ω_{A_E}	5.61 x 10^{-12}	0.21	56.22	207.98	212
$CO_3^{2-}{}_E$	6.42 x 10^{-12}	0.22	55.66	198.59	203
$\Delta\Omega_A$	4.15 x 10^{-8}	0.13	32.52	197.98	204
$\Delta\left(\frac{HCO_3^-}{H^+}\right)$	1.39 x 10^{-7}	0.13	29.91	184.46	195
$\frac{HCO_3^-{}_E}{H^+{}_E}$	2.12 x 10^{-6}	0.11	23.91	184.46	195
$\frac{DIC_E}{H^+{}_E}$	4.05 x 10^{-6}	0.11	22.68	164.77	174
ΔCO_3^{2-}	7.03 x 10^{-7}	0.11	26.25	198.59	201
ΔpH	3.07 x 10^{-6}	0.10	23.01	206.65	210
pH_E	1.67 x 10^{-4}	0.06	14.70	206.65	210
pCO_{2_E}	2.99 x 10^{-3}	0.04	9.03	191.38	198
ΔpCO_2	5.40 x 10^{-3}	0.03	7.91	197.43	208
ΔHCO_3^-	8.71 x 10^{-3}	0.03	7.03	184.46	195
$HCO_3^-{}_E$	1.38 x 10^{-1}	0.01	2.22	184.46	195

Table 4: Model outputs of least squares meta-regressions for acidification metrics under omission of studies employing constant alkalinity levels (*i.e.* Δa_T < 40 µmol kg^{-1}). Outcomes are sorted by statistical significance of the model fit.

Independent variable	*p-value*	R^2	Q_M	Q_T	*n*
ΔHCO_3^-	4.55 x 10^{-6}	0.34	26.56	55.18	51
Ω_{A_E}	1.66 x 10^{-5}	0.28	22.36	58.85	56
$CO_3^{2-}{}_E$	4.03 x 10^{-5}	0.26	19.99	58.85	56
$HCO_3^-{}_E$	1.04 x 10^{-3}	0.18	12.17	55.18	51
$\Delta\left(\frac{HCO_3^-}{H^+}\right)$	1.71 x 10^{-3}	0.17	11.02	55.18	51
$\Delta\left(\frac{DIC}{H^+}\right)$	3.27 x 10^{-3}	0.19	7.31	56.08	49
ΔpCO_2	4.53 x 10^{-3}	0.16	1.88	57.26	53
ΔCO_3^{2-}	6.96 x 10^{-3}	0.11	7.87	58.85	56
pCO_{2_E}	8.93 x 10^{-3}	0.16	0.73	57.26	53
$\Delta\Omega_A$	8.78 x 10^{-3}	0.10	7.40	58.85	56
$\frac{HCO_3^-{}_E}{H^+{}_E}$	3.67 x 10^{-2}	0.07	4.61	55.18	51
ΔpH	1.35 x 10^{-1}	0.04	1.87	56.98	56
pH_E	4.89 x 10^{-1}	0.01	0.49	58.85	56

Variation in effects of ocean acidification

The factorial investigation of OA was limited to calcification and settlement treatments because data on larval survival was insufficient to produce strong and meaningful results (see *Sensitivity assessment*). Insignificant results as well as outcomes failing the sensitivity assessment are provided in Fig. S1 of the *supplementary material*.

Calcification

Data from 212 experiments were assembled to investigate the variation of coral calcification responses to OA. Experimental pCO_2 concentrations exceeded the projected IPCC ranges in 22 cases, which were removed from the original data but included in the standardized dataset. Significant parts of the variation in response ratios were based on biological, environmental and methodological factors.

The strongest biological driver producing significantly different effect sizes was coral taxa, followed by life stage (Table. 5, Fig. 5). Siderastreids and Pocilloporid corals appeared to be less sensitive to OA than Acroporids and members of the Porites family. Data were scarce for the remaining genera and the subsamples produced results displaying high sensitivity for publication bias. When all taxa were pooled together, calcification of juveniles was more affected by OA than calcification of adult corals. A trend in the original dataset showing increasing sensitivity to OA with decreasing fragment size was likely based on scientific bias because all size classes perform equally when response ratios were standardized to stress levels (Fig. 5, bottom right). Slow-growing and fast-growing corals equally responded to OA (Fig. 6) and there was also no significant difference between corals with porous (perforate) and dense (imperforate) corals (Fig. 7). The same was true for different growth forms but inspection of effect sizes from the standardized dataset displayed higher sensitivity to OA for massive corals (Fig. S1).

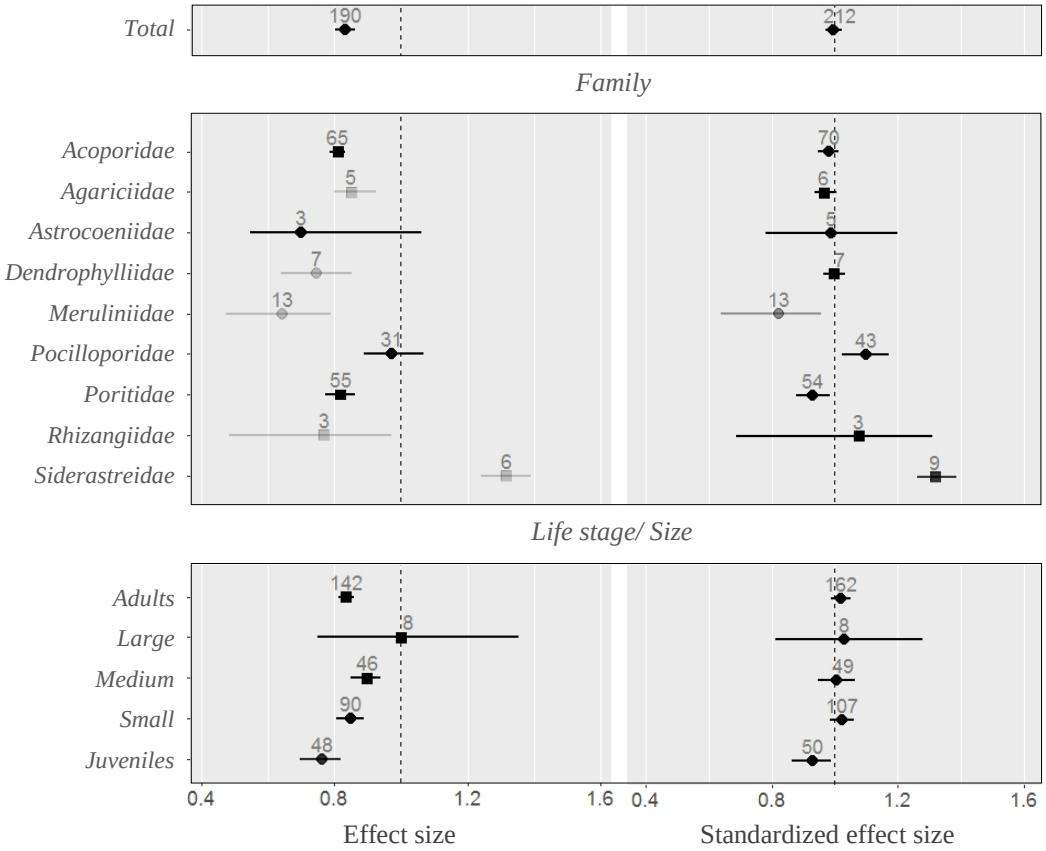

Figure 5: Effect sizes showing mean coral calcification response to ocean acidification for individual coral taxa and life/ size stages. Pooled response is shown at the top. Data are weighted means ± 95% CI. Means were calculated using either *mixed effects* (circles) or *fixed effects* (squares) models. Shown are percentage values using original data (left) and deviation from expected mean responses using standardized data (right). Numbers are sample sizes and intensity transparency represents sensitivity to publication bias.

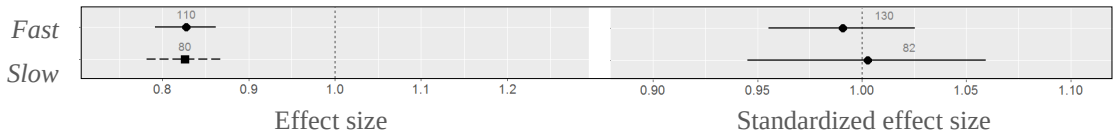

Figure 6: Effect sizes showing coral calcification response to ocean acidification for corals with different growth rates. Data are weighted means ± 95% CI. Means were calculated using either *mixed effects* (circles) or *fixed effects* (squares) models. Confidence intervals were calculated using parametric methods (dashed lines) or bootstrapping (solid lines). Shown are percentage values using original data (left) and deviation from expected mean responses using standardized data (right). Numbers are sample sizes.

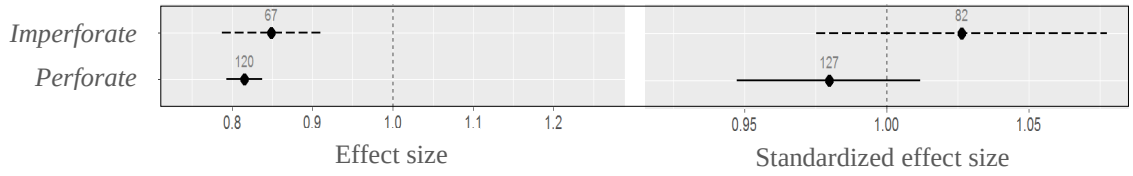

Figure 7: Effect sizes showing coral calcification response to ocean acidification for corals with different skeleton architectures. Data are weighted means ± 95% CI. Confidence intervals were calculated using parametric methods (dashed lines) or bootstrapping (solid lines). Shown are percentage values using original data (left) and deviation from expected mean responses using standardized data (right). Numbers are sample sizes.

Environmental aspects that were identified as significant drivers of variation in calcification responses to OA were climate, stress variability and reef type (Fig. 9). Corals from tropical, subtropical and temperate areas were all negatively affected by OA, but tropical corals performed significantly better than subtropical corals. In addition, corals taken from collection sites with rather stable carbon chemistry performed worse than corals from sites with larger abiotic fluctuations. The strongest environmental driver, type of reef, was in line with this finding (Table 5). Corals inhabiting lagoons and back reefs are typically subject to higher daily fluctuations of abiotic stressors and showed smaller reductions in growth capacity compared to corals inhabiting shoreward fringing reefs.

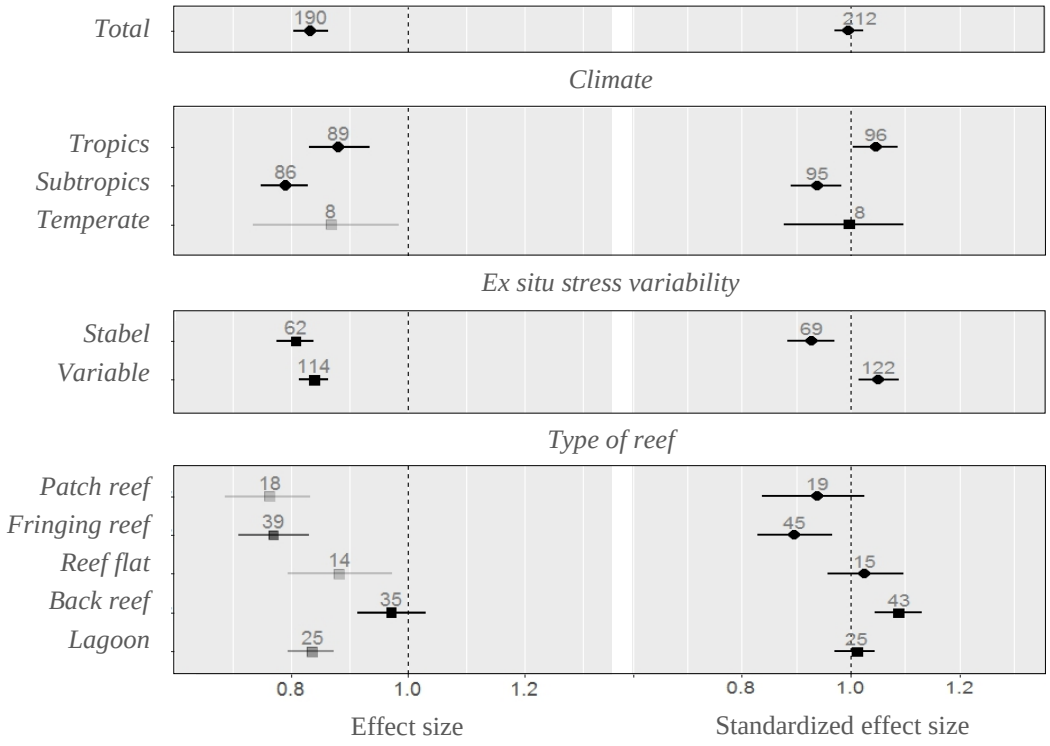

Figure 8: Effect sizes showing mean coral calcification response to ocean acidification for corals from different climates, abiotic fluctuation regimes (*i.e.* stress variability), and reef types. Pooled response is shown at the top. Data are weighted means ± 95% CI. Means were calculated using either *mixed effects* (circles) or *fixed effects* (squares) models. Shown are percentage values using original data (left) and deviation from expected mean responses using standardized data (right). Numbers are sample sizes and intensity of transparency represents sensitivity to publication bias.

Differences in experimental design driving the variation in response ratios were nutritional status, duration of the experiment and magnitude of the stress level (Fig. 9). As expected from the regression analysis, the stressor magnitude of experimental treatments explained most of the heterogeneity among methodological factors (Table 5). Corals

subjected to pCO_2 > 900 ppm had stronger decreases in calcification than corals in milder stress treatments. Under similar stress, longer exposure durations increased the strength of the effect. Short term experiments (≤ 1 day) resulted in less dramatic effects than long-term experiments (≥ 1 month). Lastly, the energetic status also affected outcomes, leading to higher calcification reductions in starved corals compared to treatments where particulate food was provided. There was no significant difference between effect sizes of different measurements such as buoyant weight or the alkalinity anomaly technique. However, estimates using surface area to measure growth showed greater than average reductions, but this result was prone to publication bias (Fig. S1).

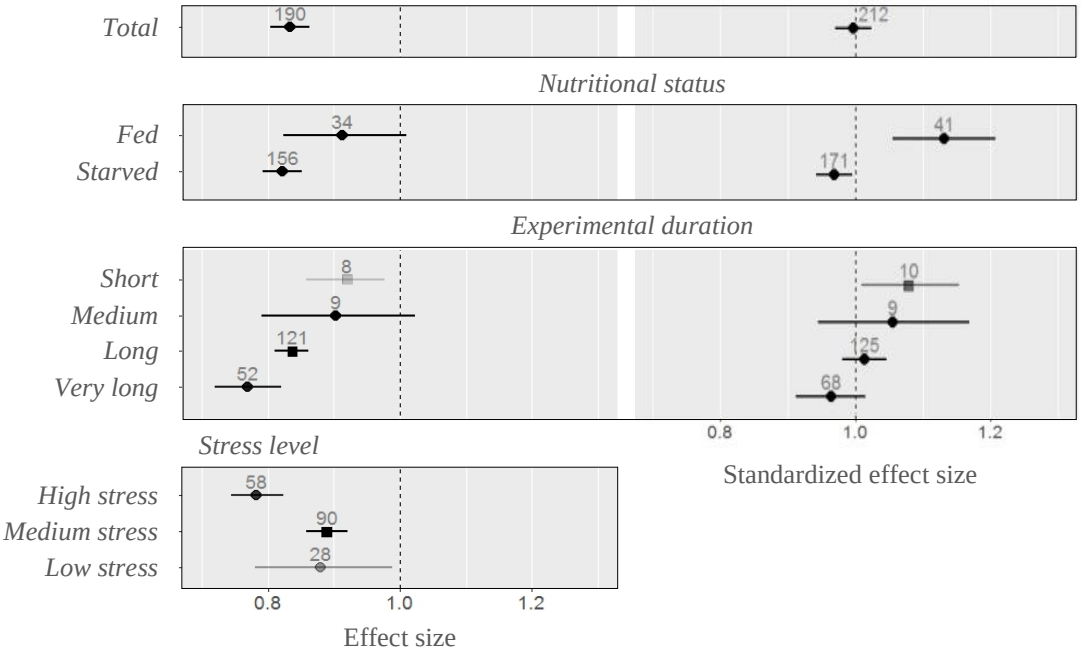

Figure 9: Effect sizes showing mean coral calcification response to ocean acidification for corals under different feeding regimes, exposure durations, and stress levels. Pooled response is shown at the top. Data are weighted means ± 95% *CI*. Means were calculated using either *mixed effects* (circles) or *fixed effects* (squares) models. Shown are percentage values using original data (left) and deviation from expected mean responses using standardized data (right). Numbers are sample sizes and intensity of transparency represents sensitivity to publication bias.

Table 5: Heterogeneity statistics of factorial analyses on coral calcification responses to ocean acidification. Listed are total heterogeneity Q_T, model heterogeneity Q_M, and residual heterogeneity Q_E.

Comparison	Q_T	Q_M	Q_E	Comparison	Q_T	Q_M	Q_E
Coral taxa	182.22	36.75	145.48	*Reef type*	121.88	21.42	100.47
Life stage	182.22	9.311	172.91	*Nutrition status*	182.22	3.11	179.11
Climate	174.16	7.38	166.78	*Duration*	182.22	6.48	175.74
Stress variability	189.01	2.13	186.88	*Stress level*	163.55	16.62	146.93

Settlement

The dataset on the effects of OA on settlement was highly sensitive to publication bias. Statistical differences existed for different oceans, *ex situ* stress variabilities, water depths, experimental durations, filter pore sizes, and substrate types (Fig. S1). However, they were not considered significant because of the high uncertainty related to publication bias. A few studies that find no significant effect may potentially neglect those findings, rendering them inappropriate to be discussed in detail. Reliable outcomes presented differences in settlement responses to OA based on skeleton porosity (Fig. 10, Table 6). The overall negative effect of OA translated to species with perforate skeletons (*i.e.* Acroporids, Porites, and Siderastreids) and to larvae that contain endosymbiotic algae upon settlement. Contrastingly, settlement success was maintained by imperforate coral species as well as corals that have not acquired symbiotic algae.

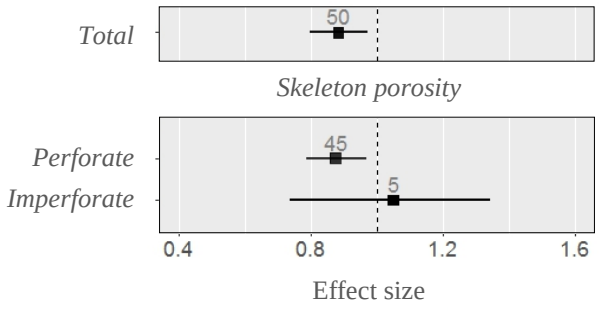

Figure 10: Effect sizes showing mean coral settlement response (percentage values) to ocean acidification for corals with different skeleton architectures. Pooled response is shown at the top. Data are weighted means ± 95% CI and calculation was based on *fixed effects* models. Numbers are sample sizes.

Table 6: Heterogeneity statistics of factorial analyses on coral settlement responses to ocean acidification. Listed are total heterogeneity Q_T, model heterogeneity Q_M, and residual heterogeneity Q_E.

Comparison	Q_T	Q_M	Q_E
Skeleton porosity	45.76	0.58	45.18

Variation in effects of ocean warming

Closer investigation of the underlying drivers of variation in responses to OW was focused on calcification and larval survival treatments. Suitable study outcomes regarding

the effects of elevated temperatures on settlement were rare and sensitive to publication bias (see *Sensitivity assessment*).

Calcification

In 13 out of 77 measurements quantifying the effect of OW on coral calcification, temperature was increased by 4°C or more. This resulted in 64 suitable comparative measurements, while the additional 13 samples were included and analyzed in the standardized dataset. The factors driving the variation of calcification responses to OW were of biological and environmental nature (Figures 12 & 14). No differences were detected for any of the methodological comparisons (e.g. study duration or type of measurement).

Similar to acidification, the effects of thermal stress on calcification were different for various taxa and life stages (Fig. 11). Pocilloporids performed better in temperature experiments than all other taxa. In contrast, Oculinids and Siderastreids performed worse but this result is sensitive to publication bias. Comparing life stages also led to significant differences, albeit describing less heterogeneity (Table 7). Juvenile corals are less sensitive to OW than adults and even benefited from increased temperature. No differences were detected in the calcification response of corals employing different growth forms (Fig. 12).

Environmental factors driving the variation in calcification responses to thermal stress were associated with the collection site. While the overall effect was neutral, corals from more stable environments (*i.e.* fringing reefs and deeper waters) showed positive responses to increased temperature (Fig. 13). Within this comparison, the type of reef was a stronger driver of variation than abiotic variability (Table 7). No significant differences were detected for corals from different climatic regions (Fig. 14).

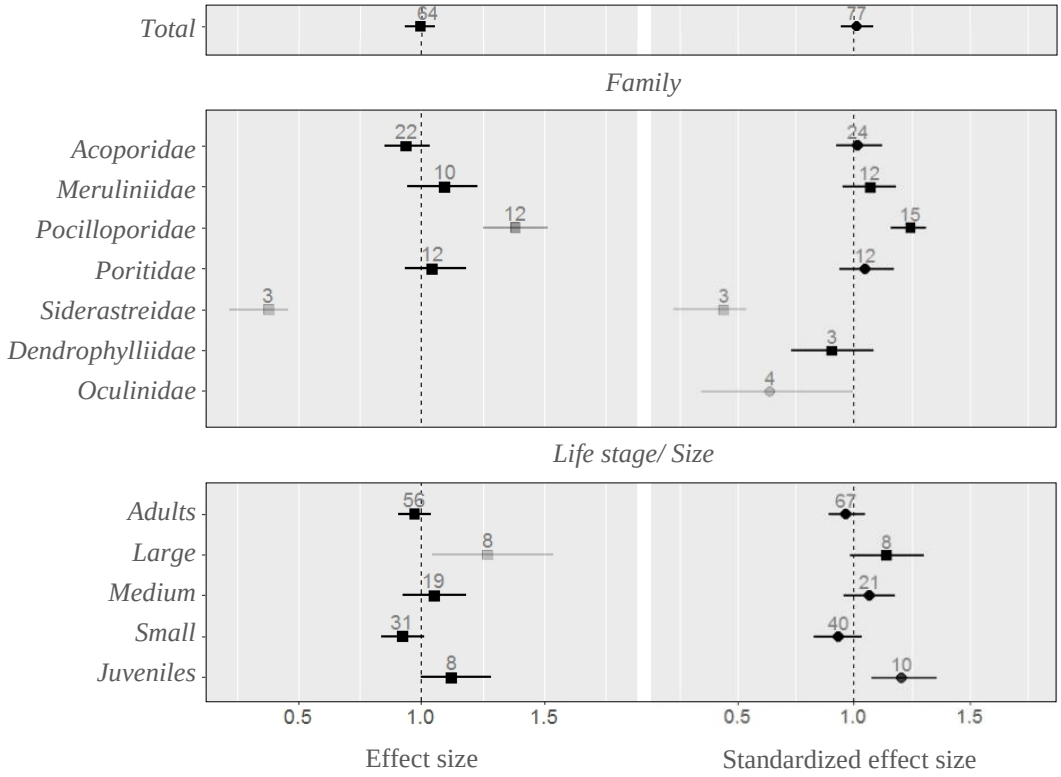

Figure 11: Effect sizes showing mean coral calcification response to ocean warming for individual coral taxa and life/ size stages. Pooled response is shown at the top. Data are weighted means ± 95% CI. Means were calculated using either *mixed effects* (circles) or *fixed effects* (squares) models. Shown are percentage values using original data (left) and deviation from expected mean responses using standardized data (right). Numbers are sample sizes and intensity of transparency represents sensitivity to publication bias.

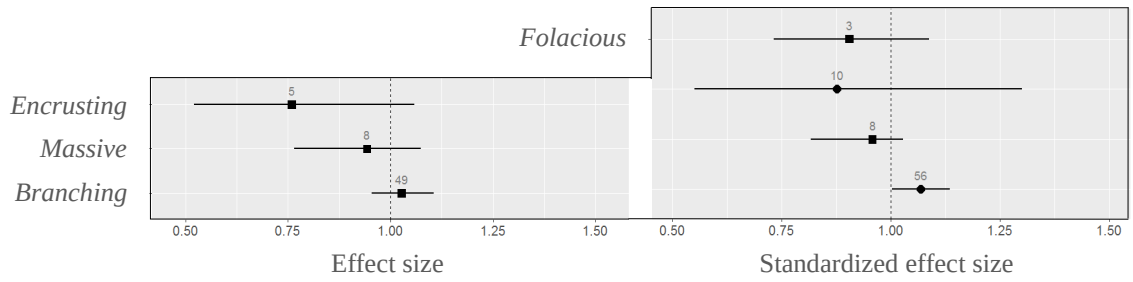

Figure 12: Effect sizes showing calcification response to ocean warming for corals with different growth forms. Data are weighted means ± 95% CI. Means were calculated using either *mixed effects* (circles) or *fixed effects* (squares) models. Shown are percentage values for all responses using original data and deviation from expected mean responses for calcification data (bottom right). Numbers are sample sizes and transparency represents sensitivity to publication bias.

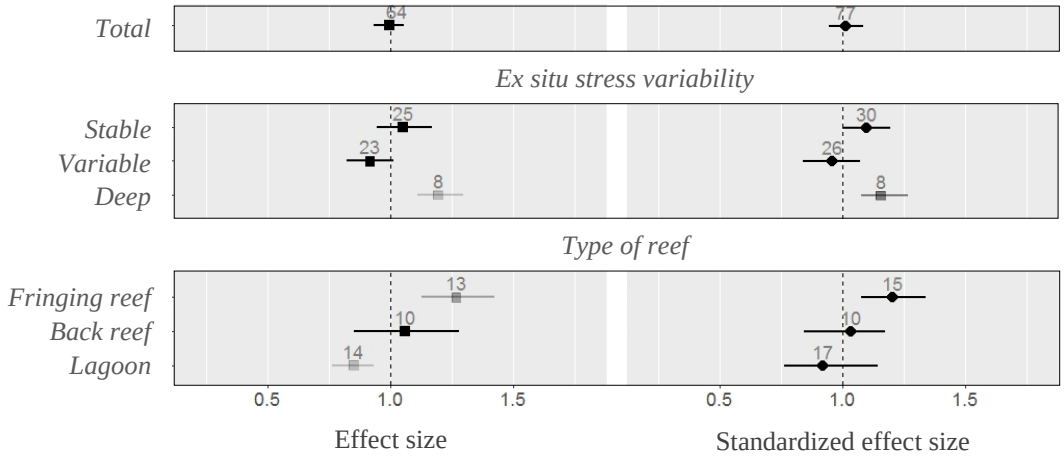

Figure 13: Effect sizes showing mean coral calcification response to ocean warming for corals from different abiotic fluctuation regimes (*i.e.* stress variability), and reef types. Pooled response is shown at the top. Data are weighted means ± 95% CI. Means were calculated using either *mixed effects* (circles) or *fixed effects* (squares) models. Shown are percentage values using original data (left) and deviation from expected mean responses using standardized data (right). Numbers are sample sizes and intensity of transparency represents sensitivity to publication bias.

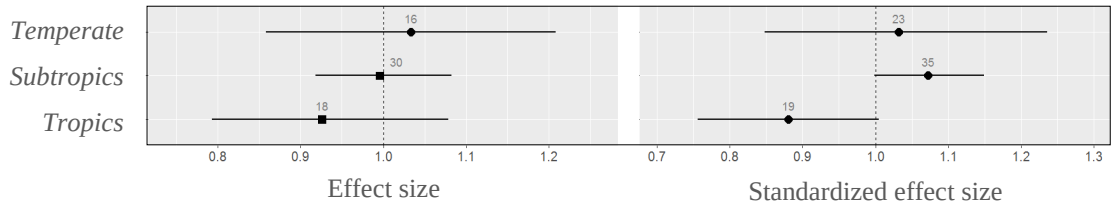

Figure 14: Effect sizes showing coral calcification response to ocean warming for corals from different climates. Data are weighted means ± 95% CI. Means were calculated using either *mixed effects* (circles) or *fixed effects* (squares) models. Shown are percentage values using original data (left) and deviation from expected mean responses using standardized data (right). Numbers are sample sizes.

Table 7: Heterogeneity statistics of factorial analyses on coral calcification responses to ocean warming. Listed are total heterogeneity Q_T, model heterogeneity Q_M, and residual heterogeneity Q_E.

Comparison	Q_T	Q_M	Q_E	Comparison	Q_T	Q_M	Q_E
Family	64.49	18.20	46.29	*Reef type*	68.74	18.94	49.80
Life stage	78.23	3.04	75.18	*Ex situ stress variability*	61.75	7.00	54.75

Larval survival

The dataset for larval survival responses to OW was limited to 50 samples. As a result, some significant differences had to be discarded due to statistical weakness (Fig. S2). However, moderately robust results were obtained for biological, environmental and methodological factors. Interestingly, filtration appeared to have the strongest effect

on the outcome (Table 8). In unfiltered seawater or water filtered through larger pores (> 50 µm), the average effect of increased temperature was neutral. This was significantly different from the strong negative responses obtained in treatments using smaller filters (Fig. 15). The second strongest determinant was growth form. Survival of larvae from branching corals were more sensitive to OW than larvae of solitary corals, where the effect was neutral. Massive species also displayed a negative effect of OW, but this effect was only marginally negative. There was no difference between larvae of brooding and broadcasting corals. However, the effect was weaker in brooding corals and the low fail-safe number indicates a possible neutral effect for this subgroup. In contrast, the negative effect on larval survival of broadcast spawning corals is strong and robust against publication bias. Lastly, the native region of the species played a significant role in moderating larval survival responses. The respective comparison produced an overall negative effect for Indo-Pacific species, while Caribbean corals are neutrally affected by OW.

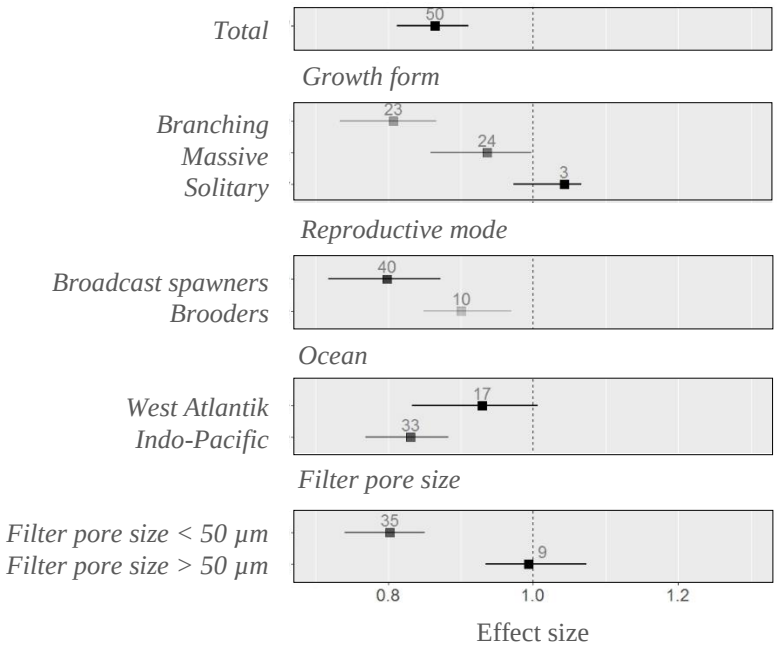

Figure 15: Effect sizes showing mean coral larval survival response (percentage values) to ocean acidification for corals with different growth forms and reproductive modes, as well as corals in different regions and filter regimes. Pooled response is shown at the top. Data are weighted means ± 95% CI and calculation was based on *fixed effects* models. Numbers are sample sizes and intensity of transparency represents sensitivity to publication bias.

Table 8: Heterogeneity statistics of factorial analyses on coral calcification responses to ocean warming. Listed are total heterogeneity Q_T, model heterogeneity Q_M, and residual heterogeneity Q_E.

Comparison	Q_T	Q_M	Q_E
Growth form	51.14	7.97	43.18
Reproductive mode	51.14	3.86	47.29
Ocean	51.14	3.37	47.78
Filter pore size	47.94	10.85	37.08

Combined effect of ocean acidification and warming on coral calcification

Coral calcification responses to interactive effects of elevated temperature and pCO_2 have been investigated sufficiently to produce quantitative estimates for some families. The collection of 13 publications resulted in 40 separate samples (*i.e.* effect sizes). When all studies were pooled together, warming had no effect on calcification responses to OA. The growth reductions induced by OA matched the effect of combined stressors (-16.7% and -15.7%, respectively). The combined effect of elevated temperature and reduced pH on coral calcification appeared to be additive. The division into most studied taxa showed inconsistencies in the direction of the interaction across different families (Fig. 16). Acroporids responded with stronger reductions in growth following exposure to combined stressors compared to the effects of single stressors. All other main taxa experienced mitigating effects in combined treatments. In Merulinids and *Porites* spp., OW offset negative effects of OA while in Pocilloporids the image was reversed (OA offset positive effects of OW).

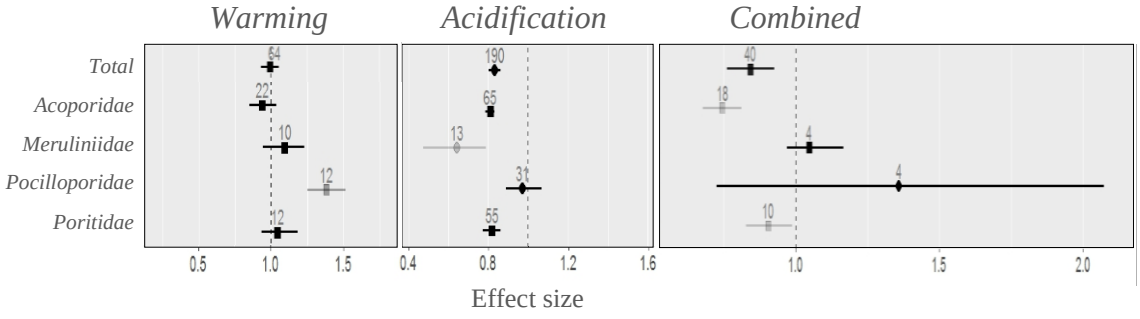

Figure 16: Effect sizes showing mean coral calcification response (percentage values) to ocean warming, ocean acidification, and combined stressors for individual coral taxa. Data are weighted means ± 95% CI. Means were calculated using either *mixed effects* (circles) or *fixed effects* (squares) models. Numbers are sample sizes and intensity of transparency represents sensitivity to publication bias.

Sensitivity assessment

Data quality

Some datasets and many subsample sets were found to be either non-normally distributed (Table 9) or heavily skewed and therefore analyzed using resampling procedures (*i.e.* weighted percentile bootstrapped confidence intervals). The distribution of each dataset is provided in the supplement (Fig. S3). The number of suitable studies ($\sqrt{n}\,\bar{X}/SD > 3$) was above 70% in every subsample and did not confine application of parametric analysis. Exclusion comparisons showed no disproportional contributions of individual studies. None of the exclusions in any of the datasets changed the significance of the overall effect size. However, in one dataset (dataset 2, Table 9) the effect size was insignificant when the lowest two response ratios were excluded. Permutation tests with random allocation of individual studies into one of two groups showed that most datasets were not prone to committing type I errors. The likelihoods to produce false differences fell below 6 % for all datasets except dataset 2 ($p_{\text{type I error}}$ = 14.9, Table 9).

Table 9: Statistical properties of the datasets. 1, 2, and 3 = calcification, larval survival, and settlement response (respectively) to ocean acidification. 4, 5, 6 = calcification, larval survival, and settlement response to ocean warming. Listed are sample size *n*, overall effect, outcome of random variance test, percentage of low suitability ratios (see *Sensitivity analysis*), fail-safe number I, and p-values for normality and probability to commit type I errors. I-values for neutral effects are not available (n/a). Bold values did not pass the sensitivity analysis.

ID	*n*	Effect	Random variance	% unsuitable	*I*	*p*-values	
						Normality	Type I error
1	190	*reduced*	*True*	6.84	4300 (4.49)	0.000002	0.036333
2	20	*reduced*	*True*	10	**3 (0.02)**	**0.061492**	**0.148667**
3	50	*reduced*	*False*	28	243 (0.93)	**0.714073**	0.042667
4	64	*neutral*	*False*	12.5	n/a	0.009932	0.053
5	50	*reduced*	*False*	12	292 (1.12)	0.007981	0.051
6	25	*neutral*	*False*	16	n/a	**0.669385**	0.059667

Publication bias

Funnel plots (Figures S4 - S6) were investigated to identify the underlying distributions of each dataset. This is important as each dataset is essentially a small subsample of all existing empirical research in the specific field, which is again a small

subsample of the true natural responses. If the response ratio funnels towards a common mean as the precision of the study increases (decreasing SE, increasing n), the data are likely associated with the same underlying distribution. An equal or increasing spread of response ratios with increasing precision would imply the opposite case that multiple distributions (*i.e.* populations of response ratios) are forming the sample dataset. Additionally, the two sides of the funnel (left: more negative responses, right: more positive responses) could be compared to evaluate the potential for publication bias towards either more negative or more positive responses. The generated funnel plots show that datasets 2, 3 and 4 display a rather chaotic spread of response ratios unrelated to the precision of the study. They are therefore assumed to derive from multiple natural populations (*i.e.* reflecting multiple factorial groups with separate intrinsic mean responses). In contrast, datasets 1, 5 and 6 funnel in towards the calculated mean response displaying only few outliners and are therefore assumed to derive from fewer populations with more similar means. The funnel plots also revealed that dataset 4 (OW - calcification) was prone to positive publication bias (publications biased towards significantly positive responses) as the response ratios

were more aggregated on the right side of the funnel. The opposite was true for datasets 1, 3 and 5, where more negative responses are observed, especially among studies with low precision.

Fail-safe analysis showed that the overall effect size of dataset 2 (OA - larval survival) was prone to publication bias and therefore not discussed in the context of the present work. Factorial analysis for this dataset was omitted from the discussion based on statistical weakness (Table 9). Among factorial comparisons, 41 out of 58 significant results were discarded based on sensitivity to publication bias. These results are displayed in the supplements (Figures S1 & S2) but were excluded from the discussion. In some instances, moderately robust results against publication bias were discussed. This was done only if the fail-safe number did not fall below half of the recommended threshold I_{min} and if the respective funnel plot of the dataset displayed low potential for publication bias.

Choice of effect size

The differences of effect sizes using alternative computations was larger than expected. Mean responses of coral calcification to OAW obtained in this study (Fig. 17,

black triangles) were in line with results from Harvey et al. (2013) (white squares), albeit effect sizes were computed differently. However, adopting effect size calculations from Harvey et al. (2013) to the dataset of this study (black circles) yielded significantly different responses for the effects of OA, as well as the interaction between OA and OW. Comparing individual stressors revealed an important distinction between the two effect size choices; L^* generated more dramatic effects with more conservative confidence intervals. This was particularly evident for calcification responses to OA. The effect was stronger than estimates of Harvey et al. (2013) using the same effect size computations. Larger confidence intervals of L^* reflect inflation of standard errors based on the inclusion of variance estimates in the denominator of L^*. Combined stressors of OAW produced a negative effect on coral calcification, when using effect size calculations of L as described in Hedges et al. (1999). The same effect was neutral when effect sizes of L^* were computed as in Harvey et al. (2013) and according to Gurevitch et al. (2000). It is important to note that L (black triangles) and L^* (black circles and white squares, Fig. 17) compute two different aspects of synergistic potential. Values of L represent the response of the combined treatment related to the control response and therefore give an estimate on the average effect when stressors are acting together. Values for L^* incorporate all treatments (control, single and combined stressors) and essentially represent the strength of the interaction rather than their combined effect. Therefore, OAW in combination led to significant reductions in calcification but the average strength of the interaction was zero.

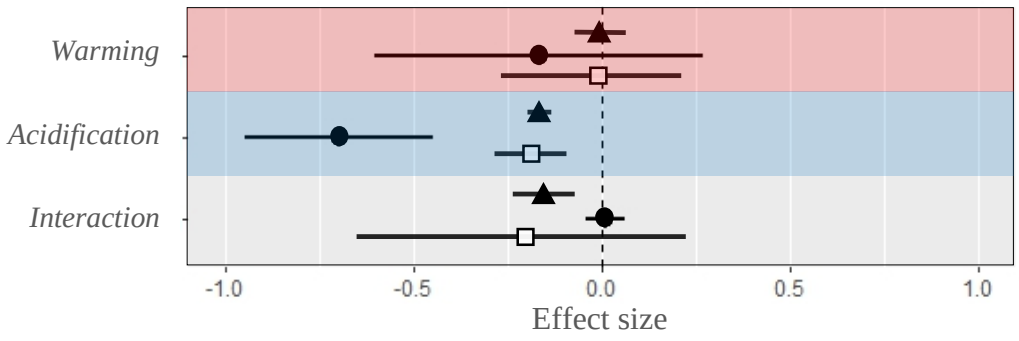

Figure 17: Effect sizes showing mean coral calcification response to ocean warming, ocean acidification, and combined stressors. Data are weighted means ± 95% CI. Black symbols are data from this study with means computed according to Hedges et al. (1999) (triangles) or Gurevitch et al. (2000) (circles). Means shown by triangles were modified (1 was subtracted) to allow direct comparison. White squares are data from Harvey et al. (2013) and were computed according to Gurevitch et al. (2000).

Discussion

Climate change affects coral recruitment and growth with repercussions on demographic and spatial community structure. Most of these effects are negative and may compromise recovery potential and resilience of coral reef ecosystems throughout this century. Coral tolerance levels for elevated temperature and/ or pCO_2 vary dramatically between coral families and life stages. Additional drivers of variation were associated with environmental circumstances and experimental design, which may govern coral responses to OAW by controlling energetic status and adaptive potential. Some suggested drivers of variation could not be supported by this analysis, which highlights our current limits of understanding of coral resistance to climate change. These unsupported hypotheses (see *Potential drivers of coral resistance to climate change*) are predominantly based on direct empirical observations or field evidence. They hold true in isolated instances but may not be generalizable in the context of global climate change effects on coral communities.

Effects of climate change on coral physiology

Meta-analysis of empirical estimates of coral responses to clime change revealed that OW significantly reduces larval survival, while OA lowers settlement and calcification rates. Limited thermal tolerance in coral larvae has been demonstrated in many studies (Byrne, 2011) but appears to be less pronounced compared to larvae of other marine calcifiers such as mollusks or echinoderms (Przeslawski et al., 2015). Increased mortality rates in larvae under OW conditions have the potential to reduce the number of recruits, which lowers community resilience and slows coral recovery after disturbances (Fabricius et al., 2011). However, elevated temperatures also shorten larval durations and reduce the number of larvae that get flushed away from natal reefs (i.e. suitable settlement sites) (Figueiredo et al., 2014). This may partially offset the adverse effects on larval survival, particularly in self-seeding populations.

Hampered larval settlement of corals under OA conditions may contribute to lower recruitment. Result from this study are in agreement with the finding that elevated pCO_2 reduces coral settlement rates (Albright et al., 2010). It is unclear whether these effects act primarily over direct pathways (e.g. physical disruption of the settlement process) or indirectly (e.g. changing substrate community and associated chemical cues). To combat

indirect effects of OA on the substrate biota, coral larvae may have to fine-tune or adapt their sensory capacities to detect altered chemical cues in acidified environments (Doropoulos & Diaz-Pulido, 2013). However, elevated carbon dioxide levels appear to shift substrate communities from primarily crustose coralline algae (CCA) towards dominance of turf algae (Albright & Langdon, 2011). The shift is likely to create unfavorable conditions for larval settlement and exacerbate the negative effects of OA on coral recruitment.

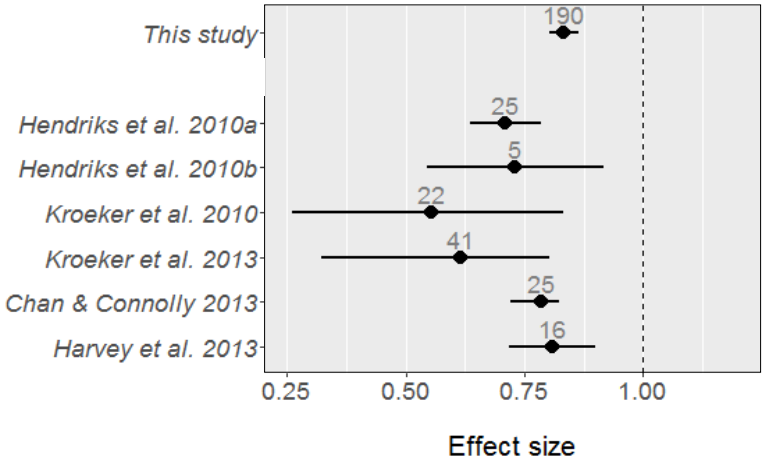

Figure 18: Effect sizes showing mean coral calcification response to ocean acidification from several meta-analyses. Data are weighted means ± 95% CI. Numbers are sample sizes. Effect sizes that were computed around 0 were converted by adding 1.

Reduced biomineralization of calcium carbonate skeletons under OA will likely change demographic distributions of corals towards smaller sizes. Impeded coral skeleton growth in increasingly acidic environments has been suggested in many reviews and meta-analyses (Fig. 18). Estimates of effect sizes in other studies are based on smaller samples and usually show more dramatic reductions in coral calcification responses to OA. This suggests that the negative effects of elevated pCO_2 on skeleton production in reef building corals are currently overestimated. Nevertheless, the ramifications concerning general reef accretion in the 21st century are not clear yet. In this context, two important aspects to consider are differences between life stages (juveniles vs. adults) and effects of OA on the internal structure of coral skeletons. $CaCO_3$ deposition of juvenile corals appears to be particularly impeded by OA (Fig. 5). Similar to the effects of climate change on larval survival and settlement, elongation of juvenile stages due to slowed growth may reduce fecundity and community resilience (Albright & Langdon, 2011). Together, the overall

effects on coral physiology show that all later stages of coral recruitment (larval survival, settlement, and juvenile growth) can be affected by climate change in different ways. The combined effects of OAW on coral recruitment and community resilience to disturbances may therefore be more severe than current estimates suggest. Another possible ramification addresses the structural stability of future reefs under climate change. Specifically, increasing acidity has been shown to shorten the crystal aspect ratio of aragonite crystals, rendering the coral skeleton less structurally stable (Cohen et al., 2009). This is commonly referred to as stretch modulation effect (Carricart-Ganivet, 2004). A serious implication of these observations is the fact that changes in coral skeletons associated with OA may be undetected in studies measuring only the rate of calcification. If OA decreases the structural integrity of coral skeletons, reefs may become more prone to bioerosion and physical damage from storms (Cohen & Holcomb, 2009; Crook et al., 2013).

The interactive effect of elevated temperature and pCO_2 on calcification is additive for individual coral genera (Fig. 16). This can result in mitigation or intensification of single stressor effects, depending on the coral's thermal threshold. For instance, calcification rates are more dramatically suppressed by OA in Merulinids compared to Acroporids. However, Merulinids seem to have higher thermal thresholds than Acroporids. Consequently, Merulinids may experience increased metabolic turnover under elevated temperatures, which can offset adverse effects of OA. In contrast, thermal thresholds of Acroporids are more frequently exceeded (Hoegh-Guldberg, 1999), leading to metabolic compromises that add to the negative effects of OA. When coral families are pooled together, calcification responses to OA alone do not differ from those under combined stressors, which is in agreement with results from previous meta-analyses (Kroeker et al., 2013). Synergism between OA and OW was not identified, although this interaction is common among other phyla and physiological responses (Przeslawski et al., 2015). A possible reason for the additive interaction in calcification responses is the effect of warming on coral energy reserves. Maintaining calcification rates becomes more energetically costly under acidification conditions (Cohen & Holcomb, 2009). As mentioned above, elevated temperatures can increase or decrease energy reserves and therefore facilitate or hinder maintenance of calcification. Warming may also benefit coral calcification in OA scenarios indirectly by changing calcium carbonate precipitation

kinetics. Higher kinetic energy increases Ω_A, favoring chemical equilibria towards precipitation of $CaCO_3$ (McCulloch et al., 2012).

Stressor-effect relationships

Effects of warming on calcification

The relationship between temperature elevation and coral calcification describes a parabolic response of calcification to warming, which is commonly observed in empirical studies (Castillo et al., 2014). Among temperature treatments, ambient temperatures varied between 13.3˚C (Rodolfo-Metalpa et al., 2010) and 28.9˚C (Anlauf et al., 2011), reflecting the wide range of temperature regimes assessed in this study. It is therefore not surprising that experimental temperatures alone did not explain any variation in calcification responses ($R^2 = 0.00$). A more accurate quantification of temperature stress was obtained using ΔT (*i.e.* the difference between ambient and elevated temperatures), which explained a significant amount of variation in effects of OA on coral calcification ($R^2 = 0.15$). The linear model suggests that corals benefit from temperature elevations up to + 3˚C in laboratory settings. Further warming exceeds thermal thresholds of most corals, with every additional degree leading to a 10% decline in expected calcification rates.

Effects of acidification on calcification

Calcification responses to OA correlated with experimental aragonite saturations but may be driven by multiple carbon chemistry parameters. Aragonite saturation of experimental treatments explained up to 28% of the variation (Table 4), but it is not clear whether aragonite is driving or responding to calcification rates. On some natural reefs, aragonite has been shown to lag behind calcification rates during diel fluctuations (Shamberger et al., 2014; Jokiel, 2016). The relationship found in this study may therefore derive from a correlation of aragonite with other carbon chemistry parameters (Jokiel, 2016). The roles of the individual components of OA in driving calcification in marine organisms may be elucidated by combining results from this study with recently suggested hypothetical models.

A possible relationship between coral calcification responses and changes in the ratio of HCO_3^- and H^+ (Table 3) may have been masked in this study by virtue of experimental design. Bach (2015) suggests that bicarbonate is described as the substrate

mineral and protons are regarded as inhibitors of calcification. The ratio is therefore referred to as substrate-inhibitor ratio (SIR). The assumptions are in line with a theoretical model proposed by Jokiel (2011), describing how increased H^+ concentration alone may inhibit $CaCO_3$ production. Corals induce crystallization of aragonite by drastically increasing Ω_A ($\approx$ 20) within a designated calcification compartment (Feely et al., 2009; Kleypas & Yates, 2009)). This compartment is isolated from the surrounding bulk water and therefore not directly affected by its pH. Jokiel (2011) suggested that corals use proton pumps to rid themselves of access protons that would build up when using bicarbonate for calcification (see equation 3, reversed). According to this 'proton flux hypothesis', calcification is limited by suppressed efflux of H^+ due to rising H^+ concentrations rather than substrate limitation based on CO_3^{2-}. In laboratory comparisons, hydrogen becomes more abundant under elevated pCO_2, while bicarbonate is often kept constant. Consequently, substrate-inhibitor ratios are commonly lower in experimental OA treatments. The proton flux model and substrate-inhibitor ratio therefore provide an explanation for the observed reductions in calcification without depending on Ω_A as the primary driver. However, constant bicarbonate concentrations in the majority of experiments may have led to minimal impact of SIR, potentially increasing the relative importance of confounding factors. Under omission of these experiments, the variation in coral calcification responses to OA described by differences in bicarbonate concentration increased from 3% to 34%, while that of Bach's ratio increased from 11% to 17%. These findings support the assumption that bicarbonate concentrations can drive coral calcification rates (Pandolfi et al., 2011) and suggest that this relationship is undetected in many empirical studies.

The ratio of total dissolved inorganic carbon (DIC) and H^+ has also been proposed to drive coral calcification (Comeau et al., 2013a). Using this ratio as independent variable improved the predictability of the model (Table 4). The hypothesis is based on observations of corals using both carbonate and bicarbonate as substrate mineral for calcification (Pandolfi et al., 2011). In addition, increased aqueous carbon dioxide can stimulate photosynthesis (Bedwell-Ivers et al., 2016). Enhanced photosynthesis provides more energy and the associated liberation of hydroxide (OH^-) from HCO_3^- prior to Symbiodinium fixation may serve to neutralize protons generated by calcification

(Holcomb et al., 2010). Based on these assumptions, it would make sense to include carbonate and aqueous CO_2 on the beneficial side (*i.e.* the numerator) of a metric that describes calcification responses. However, increases in H^+ concentrations will outpace increases in dissolved inorganic carbon. If the hypothesis holds true, global calcification rates will decline towards the end of this century, albeit at a much slower rate than currently assumed (Bach, 2015).

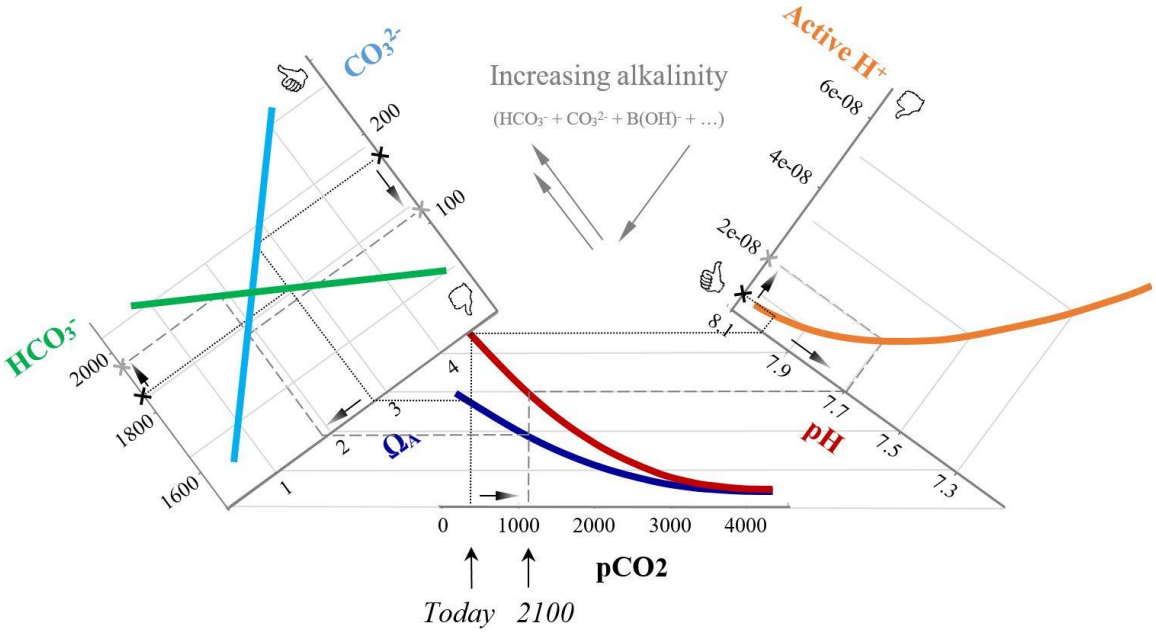

Figure 19: Graphical illustration of the relationships between different carbon chemistry parameters, using data from this study. Dotted lines show current levels and dashed lines show levels for 2100 (RCP 8.5) (IPCC 2014). Black arrows show expected trajectories of individual parameters towards the end of this century. Gray arrows show influence of increasing alkalinity. Thumbs illustrate hypothesized effects on coral calcification, which are beneficial (thumbs up) or detrimental (thumbs down).

The beneficial effects of increasing carbon mineral concentration on coral calcification are illustrated in a recent case study by Shamberger et al. (2014), who investigated a flourishing semi-enclosed reef in the Rock Islands, Palau. Both pH and aragonite are subject to considerable daily fluctuations and can reach levels as low as 7.8 and 2.4, respectively. Nevertheless, the reef system supports high coral cover and biodiversity. While calcification rates at this site do not agree with traditional correlations based on aragonite, consideration of the proton flux hypothesis and the buffering effect of DIC provides a reasonable explanation for the apparent resistance to OA. On the Rock Islands reef, biological $CaCO_3$ deposition depletes the surface seawater of carbonate, while enriching it with carbon dioxide. The resulting low-pH stress becomes chronic due to little

mixing between bay water and fresh open ocean water (Shamberger et al., 2014). In contrast to pH, local DIC levels within the bay are raised by various inputs. HCO_3^- is high due to extensive OA conditions, while some CO_3^{2-} is reintroduced by dissolution of the local carbonate platforms. Together, these biogeochemical influences produce frequently low pH waters under high DIC levels, illustrating how DIC may buffer the effects of reduced pH on coral calcification (Comeau et al., 2013a). The scenario agrees with the outcomes of this study and suggests that currenty established relationship between aragonite (i.e. carbonate) and coral calcification may be incomplete. Based on the beneficial influence of bicarbonate, the ability of corals to build reef structures could be less compromised by future OA than currently estimated (Fig. 18). In addition, regional differences in calcification responses to OA would follow spatial patterns of DIC, alkalinity, and CO_2 uptake rates rather than aragonite saturation. Alkalinity levels of global surface waters are relatively constant, both temporally (Sabine et al., 2004) and spatially (Bach, 2015; Fassbender et al., 2016). However, local heterogeneity occurs in areas of upwelling and river outflow (Lee et al., 2006). DIC and CO_2 fluxes depend on a suite of biological and meteorological factors, with coastal regions showing large spatial and seasonal variations (Borges, 2005). Therefore, if the scenario above holds true, overall coral calcification responses to OA will be less severe but more spatially variable compared to suggestions from previous estimates.

Potential drivers of coral resistance to climate change

Ocean warming and coral calcification

Hypothesis 1: Branching corals are more sensitive to ocean warming than massive corals

This hypothesis was not supported by the analysis, which showed no differences between branching and massive corals for any of the assessed responses (Fig. 12). In fact, incorporation of the stress levels in each study revealed that calcification responses of branching corals were significantly better than average. The assumption that branching corals are particularly sensitive to thermal stress derives from multiple field observations showing greater losses (Gleason, 1993; Loya et al., 2001) and low recovery (van Woesik et al., 2011) in branched corals following thermal stress events. In contrast, massive and

encrusting colonies in the field appear to possess higher thermal resistance and recover well after temperature anomalies (Hoegh-Guldberg, 1999). Loya et al. (2001) suggested that tissue thickness affects coral sensitivity to OW. Thicker tissues in massive corals may act as self-shading layer and protect endosymbiotic algae from high irradiance levels. High light can become problematic in warm waters and can harm the coral holobiont by reducing photosynthetic efficiency (Evenhuis et al., 2015). While this hypothesis provides reasonable explanation for increased bleaching resistance in massive species, their thicker tissue may render them more susceptible to moderate temperature stress. To maintain a healthy status, corals have to rid themselves of harmful metabolites such as reactive oxygen species (Brown, 1997). These are commonly produced as a by-product of photosynthesis and become more abundant under elevated temperatures. Efflux of harmful metabolites may be facilitated in corals possessing thinner tissues, which may explain why thick-tissued massive corals maintain calcification rates less efficiently in warmer *ex situ* environments (Fig. 12). However, Yost et al. (2013) found lower levels of superoxides within the thicker tissue of Porites lobata compared to branching corals. A possible explanation for the apparent resistance of massive corals in field observations relates to acclimatization. Due to lower growth rates and higher metabolic rates, massive corals are thought to acclimatize more efficiently than branching corals (Gates & Edmunds, 1999). However, taxonomic categorization of the data in this study suggests that the branching coral *Pocillopora damicornis* has adapted to elevated temperatures in recent years. Despite showing worldwide losses and being described as one of the 'losers' of climate change (Hoegh-Guldberg, 1999; Loya et al., 2001; van Woesik et al., 2011), this species has demonstrated much higher resistance to thermal stress compared to all other taxa (Fig. 11). These results challenge the current paradigm that Pocilloporids and other branching corals are more sensitive to thermal stress than corals with massive growth forms (Yost et al., 2013). The global decline in predominantly branching corals after thermal stress events may not be directly related to thermal stress resistance. Instead, these declines may be due to increased vulnerability to multiple interacting stressors and subsequent disease outbreaks.

Hypothesis 2: Adult corals are more sensitive to ocean warming than juvenile corals

The data support this hypothesis and show that elevated temperatures projected for the end of this century tend to increase calcification rates of coral spat (Fig. 11). This is likely the result of the 2-dimensional morphology in juvenile corals. Patterson (1992) showed that mass transfer is higher in flat invertebrates, leading to more efficient outward transport of harmful metabolites associated with warming (Loya et al., 2001). Since maturity in corals is size dependent (Harvell et al., 2002), OW has the potential to increase fertility in coral populations by enhancing growth and reducing the time that corals spend in juvenile stages.

Hypothesis 3: Tropical corals are more sensitive to ocean warming than subtropical corals

The difference between calcification rates under OW for tropical and subtropical corals was masked by unequal distribution of stress levels. Nevertheless, maintaining calcification rates in elevated temperatures appears to be facilitated in subtropical corals (Fig. 14), which is likely a result of adaptation in subtropical corals to more fluctuating abiotic conditions in higher latitude regions. The stresses applied in experimental treatments are often abrupt and change more quickly compared to progressive *in situ* changes resulting from climate change. Smaller daily temperature fluctuations at low latitudes may render tropical corals less adapted to abrupt thermal changes. Consequently, the same temperature elevation in laboratory treatments would induce greater stress to tropical corals compared to subtropical corals. Field observations on the Great Barrier Reef contrast this finding and display an inverse relationship between latitude and bleaching threshold (*i.e.* higher thresholds at low latitudes) (Hoegh-Guldberg, 1999). Thermal thresholds of tropical corals may be higher, but are exceeded more easily because they live closer to their temperature limit (Berkelmans & Willis, 1999). Longer exposure to seasonal heat stress may produce environmental pressures selecting for tolerance of high and stable temperatures. This suggests that the tolerances of tropical and subtropical corals derived from this study may not necessarily translate to global community changes. While climate change acts progressively over multiple decades, the slowest temperature increases in empirical studies are still at a much faster rate, which may explain the low sensitivity of tropical corals in this study. Another ramification of this scenario is that corals will likely not be able to escape rising temperatures via dispersal into higher latitudes, since new

recruits from stable environments experience additional challenges when settling in high-variability environments.

Hypothesis 4: Corals from thermally stable environments are more sensitive to ocean warming than corals from variable environments

The analysis in this study did not provide quantitative evidence for this hypothesis. Although increased thermal tolerance thresholds in corals living under highly fluctuating thermal regimes has been demonstrated in the field (McClanahan & Maina, 2003; Palumbi et al., 2014), the assumption could not be validated (Fig. 13). To divide the dataset into subsamples, several geographical factors were considered such as climatic region and habitat type. The result seemed to be driven by positive effect sizes for many corals taken from fringing reefs. Fringing reefs generally face the open ocean and are subject to relatively stable abiotic conditions. There is no comprehensive explanation for the increased resistance to OA in this group of corals. It is possible, that other factors accounted for the lower performance in corals taken from more fluctuating habitats such as back reefs or lagoons (Fig. 13). Putnam and Edmunds (2011) investigated calcification of *Pocillopora* and *Porites* colonies from back reef areas with large diel temperature fluctuations. Corals were subjected to elevated or fluctuating temperatures and significantly reduced calcification rates in both stress treatments. However, a second trial conducted two weeks later displayed no significant differences between any of the treatments. The authors concluded that the different outcomes may be attributed to recent thermal history. If seasonal variation in calcification responses to thermal stress differs between regions, results obtained in this study may have been biased by inconsistent timing of coral collection.

Ocean warming and coral larval survival

Hypothesis 5: Survival of coral larvae is more affected by ocean warming than settlement rates or coral growth

This hypothesis was clearly supported by the overall effects in this study, showing reductions in larval survival but not in settlement or growth rates (Fig. 3B). These results illustrate how complex life cycles of invertebrates can complicate population responses to OW. Increased larval mortality may reduce the number of settling larvae and limit successful recruitment. Larval development is also hastened in warmer environments,

rendering coral planulae more likely to be retained and find suitable substrates (Figueiredo et al., 2014). In addition, coral larvae may offset negative effects of increased temperature through phenotypic plasticity (Munday, 2015). Since juvenile growth is supported by mild heat stress (Fig. 11), larvae that manage to settle will reach maturity faster and are more likely to contribute to the reproductive output of the population. However, settlement under elevated temperatures can reduce post-settlement survival rates (Ross et al., 2013). Consequently, OW has the potential to limit recruitment success by reducing survival rates of larvae and juveniles, while simultaneously increasing their retention and production rates. Estimating the relative effect sizes on each life stage will advance predictions on changes in coral community resilience associated with OW.

Hypothesis 6: Symbiotic larvae of brooded corals are more sensitive to ocean warming than aposymbiotic larvae of broadcast spawning corals

The hypothesis could not be supported by this study but there are potential sources of scientific bias. Comparison of symbiont-bearing and symbiont-deplete (also aposymbiotic) coral larvae was restricted because the symbiotic status was not always reported. However, brooded coral larvae typically inherit endosymbiotic algae from their parents, while larvae of broadcast spawning corals more commonly obtain them after settlement (Baird et al., 2009). The hypothesis that larvae containing symbionts are more sensitive to OW than aposymbiotic larvae can therefore be tested by comparing the reproductive modes of parental colonies. Contrary to current beliefs, brooded (symbiotic) coral larvae showed lower mortality rates under thermal stress than (aposymbiotic) larvae of broadcast spawners (Fig. 15). Survival may have been facilitated in laboratory treatments by the additional energy from endosymbiotic algae. However, Yakovleva et al. (2009) argue that *in situ* larvae are exposed to high surface irradiance levels, leading to oxidative tissue damage from overstimulated photosynthesis. This additional stress is absent in many temperature tolerance treatments, which may obscure potential inferences regarding larval survival rates in the field. The comparison between brooding and broadcast spawning corals may also be biased by experimental design. Larvae of broadcast spawners are commonly subjected to temperature stress at early developmental stages, while brooded larvae are always at the planuala stage when exposed to heat. In addition, the average

temperature increase was + 0.7˚C higher in stress treatments using spawned larvae compared to brooded larvae, potentially exceeding thermal thresholds more commonly. Thermal thresholds are characteristically low in coral larvae (Byrne, 2011) and the combined results from qualitative and quantitative analyses suggest that endosymbiotic algae can be both beneficial and detrimental to coral larvae, depending on individual temperature thresholds and timing of developmental stages and stress exposure.

Hypothesis 7: Coral larvae survive better in unfiltered treatments under elevated temperature

A rather unexpected result was the finding that larval survival rates were unaffected in unfiltered temperature treatments (Fig. 15). Frequent water changes and cleanups are commonly executed and are thought to prevent build-up of algae or waste products that could be harmful to coral larvae. However, intense filtration might remove other organisms or sensory cues that help larvae survive in thermally stressful environments. The involved processes would probably act at the boundary between larvae and the surrounding seawater, which is a poorly studied research area. Based on the small sample size of the group of unfiltered treatments (n = 9), it cannot be ruled out that the difference was produced by chance or based on a hidden confounding factor.

Ocean acidification and coral calcification

Hypothesis 8: Juvenile corals are more sensitive to ocean acidification than adult corals

The results from this analysis support the statement that young coral recruits will suffer more from OA than adults (Fig. 5). A lower capacity of juvenile corals to calcify in acidified seawater has been suggested in other studies (Albright & Langdon, 2011) and may be related to limited energy availability. Older corals can allocate energy reserves in response to environmental perturbations (Anthony et al., 2008). This is not the case for juvenile corals that need to grow rapidly to accumulate biomass. The additional energetic cost of calcification associated with OA may therefore hamper juvenile growth in particular (Cohen et al., 2009; Edmunds et al., 2012). In adult corals, McCulloch et al. (2012) quantified the required energy to combat an external pH reduction from 8.1 to 7.8 and estimated that less than 1% of the energy provided by autotrophic endosymbionts would be needed to maintain calcification. A recent meta-analysis failed to detect the difference

between juvenile and adult sensitivity (Kroeker et al., 2013). However, the difference may have been masked by varying stress levels between studies as was the case in this study. Juvenile corals were found to be more vulnerable to OA after the data were standardized to stress levels (see *Data analysis*). This procedure has not been incorporated in Kroeker et al. (2013) and addresses an important source of variation. Different stress levels among laboratory experiments may have biased other ecological meta-analyses that quantify empirical tolerance estimates.

Hypothesis 9: Branching corals are more sensitive to ocean acidification than massive corals

No evidence was found in this analysis to support the statement above. The general belief that massive corals are more resistant to OA than branching corals originates from field observations. Fabricius et al. (2011) investigated coral reefs in Papua New Guinea (PNG) situated within shallow volcanic CO_2 seeps. Spatially heterogeneous bubbling of CO_2 creates acidified conditions (pH = 7.8) on some parts of the reef framework. This setting provides the opportunity to assess coral communities that live in OA conditions projected to be the norm towards the end of this century. The authors noted that communities located at the seeps consisted mainly of structurally simple massive *Porites*. In contrast, coral diversity was higher on unaffected reefs nearby, leading to the conclusion that OA is likely to shift reef communities towards mounding corals. The ramification of this on an ecosystem level would be severe reductions in structural complexity and habitat quality of reefs worldwide (Fabricius et al., 2011). However, analyses from this study challenge the generality of observations from PNG, showing no statistical difference in calcification responses of branching and massive corals. In fact, effect sizes were greater in massive corals. These results are in alignment with Comeau et al. (2014c), who found larger reductions in calcification of mounding corals under elevated pCO_2. Regarding the volcanic reefs in PNG, Fabricius et al. (2011) highlight the occurrence of larval exchange between acidified and neutral reef patches. The underlying driver of high survival in *Porites* and other mounding corals are possibly linked to demographic traits such as larval retention rates and the ability to acclimatize.

One way for corals to cope with new conditions is transgenerational acclimatization (see *Coral responses to ocean warming*). If larvae end up in abiotic conditions that differ

from their parent's environment, phenotypic changes resulting from transgenerational acclimatization can compromise fitness (*i.e.* phenotype-environment mismatch) (Marshall et al., 2010). The spatial heterogeneity of CO_2 levels in the PNG reef complex can therefore limit recruitment success. To be equipped with adequate phenotypic regulations, larvae from corals on acidified patches would also have to settle on acidified patches. However, strong winds and currents around the reef area are more likely to transport these larvae to other patches, creating phenotype-environment mismatches. The dominance of mounding corals at the CO_2 seeps in PNG may be attributed to larval characteristics such as swimming speed, pelagic larval durations, the ability to delay metamorphosis, and sensory capacities. All of these traits can affect larval retention rates and regulate acclimatization potential. Support for this hypothesis is provided by Shamberger et al. (2014), who report highly diverse coral reef communities under chronically acidified conditions in Palau. The reef is semi-enclosed with reduced mixing and a mean water residence time of 71 days (Golbuu et al., 2016). The stable conditions and restricted water movement could potentially favor local retention and therefore enable local acclimatization and/ or genetic adaptation for larvae from all inhabiting corals, regardless of pelagic larval durations or growth form.

Hypothesis 10: Fast-growing corals are more sensitive to ocean acidification than slow-growing corals

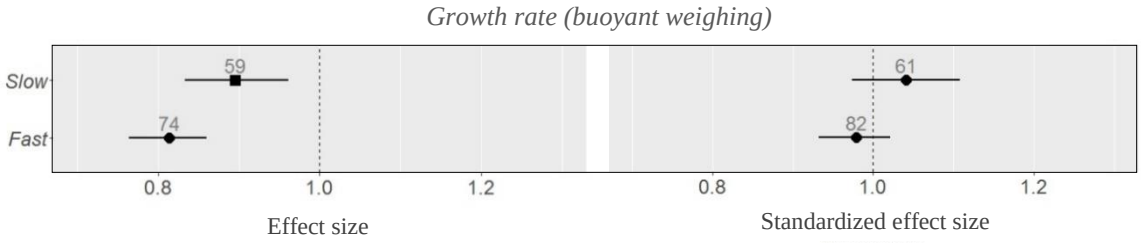

Figure 20: Effect sizes showing coral calcification response to ocean acidification for corals with different growth rates using a data subset containing only estimates that use buoyant weighing to quantify calcification. Data are weighted means ± 95% CI. Means were calculated using either *mixed effects* (circles) or *fixed effects* (squares) models. Confidence intervals were calculated using parametric methods (dashed lines) or bootstrapping (solid lines). Shown are percentage values using original data (left) and deviation from expected mean responses using standardized data (right). Numbers are sample sizes.

Addressing the hypothesis above can potentially help elucidate the mechanisms that drive calcification reductions in response to OA. Fast-growing corals require more substrate minerals than slow-growing corals. This substrate mineral is commonly believed to be carbonate (Kleypas & Yates, 2009; Bates et al., 2010), which becomes less abundant

with increasing pCO_2 (Cohen et al., 2009). Consequently, if carbonate concentrations drive coral calcification, fast-growing coral taxa will suffer more from OA compared to slow-growing corals (Rodolfo-Metalpa et al., 2010; Comeau et al., 2013a). In this study calcification responses were equal across the two groups (Fig. 6), suggesting that carbonate concentration is not a sole driver of coral calcification. A recent meta-analysis also found no evidence of increased vulnerability to OA in fast-growing coral taxa (Chan & Connolly, 2013). These results have been challenged by Comeau et al. (2014c), who compared calcification responses of four fast-growing and four slow-growing coral species to increasing pCO_2. The authors found larger reductions in fast-growing coral taxa and pointed out that results from Chan and Connolly (2013) were based solely on linear extension rates as a measure of calcification. Confining the analysis in this study to treatments measuring buoyant weights also revealed no difference between fast-growing and slow-growing taxa (Fig. 20). The discrepancy between empirical estimates and meta-analytical inferences may result from inconsistent classification. The branching coral *Porites rus* and other massive *Porites* spp. were classified as fast growers according to Comeau et al. (2014c). In this study, these corals were identified as slow-growing taxa (Gates & Edmunds, 1999; Lough & Barnes, 2000). Coral growth rates can vary between regions within a species (Lough & Barnes, 2000), which complicates uniform characterization of this trait. In some areas, massive *Porites* spp. extend no more than 10 – 15 mm per year (Lough & Cantin, 2014) but keep up with faster growing *Acropora* spp. in other areas (Brown & Edmunds, 2016). In addition, calcification in *Porites* corals is significantly more affected by OA compared to other taxa (Fig. 5) and may have already declined during the last two decades (Fabricius et al., 2011). Classification of these corals as fast-growers in Comeau et al. (2014c) may have driven the effect relationship of this subsample and could explain why similar differences were not observed in this study.

Hypothesis 11: Imperforate corals are more sensitive to ocean acidification than perforate corals

The skeleton structure of corals did not affect their ability to maintain calcification rates under elevated pCO_2 (Fig. 7). Corals need to invest energy to ensure sufficient efflux of hydrogen ions from the calcification compartment. This process becomes more energetically costly under increasing hydrogen concentrations (Cohen & Holcomb, 2009).

Because hydrogen efflux is facilitated in the porous skeletons of perforate corals, imperforate corals have been suggested to be more sensitive to OA (Jokiel, 2011). The similarity of responses among perforate and imperforate corals in this study suggests that hydrogen ions alone do not regulate coral calcification. Recent empirical comparisons between perforate and imperforate corals resulted in additional evidence for similar resistance to OA (Comeau et al., 2014c). Further, some imperforate corals have demonstrated exceptional resistance to OA. *Favia fragum* managed to calcify in highly undersaturated waters (Ω_A = 0.22) (Cohen et al., 2009). However, $CaCO_3$ deposition was delayed and the resulting skeleton showed structural weakness (*i.e.* stretch modulation effect). Although OA affects the rate of perforate and imperforate skeleton deposition equally, the structural integrity of the resulting skeleton may be affected differently. More specifically, perforate corals may be able to maintain calcification rate and stability of the resulting skeleton under OA, whereas imperforate corals experience a trade-off between the two.

Hypothesis 10 & 11: Imperforate fast-growing corals are more sensitive to ocean acidification than perforate slow-growing corals

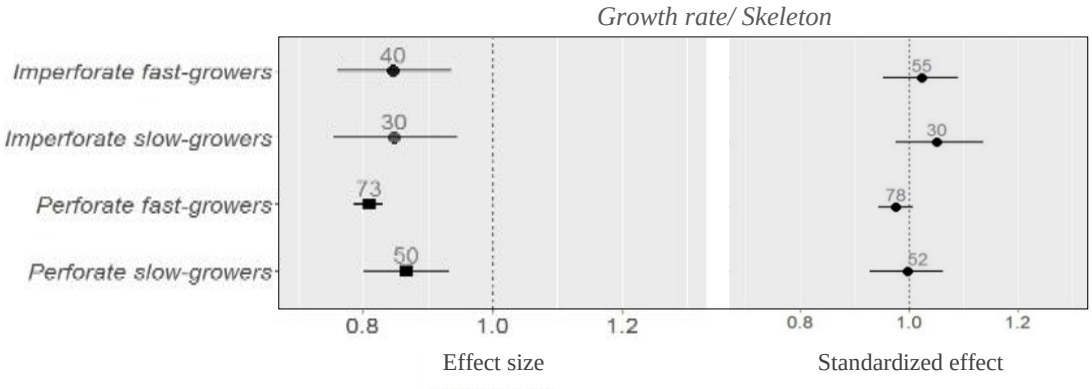

Figure 21: Effect sizes showing coral calcification response to ocean acidification for corals with different shapes (perforate vs. imperforate) and rates (fast-growing vs. slow-growing) of $CaCO_3$ deposition. Data are weighted means ± 95% CI. Means were calculated using either *mixed effects* (circles) or *fixed effects* (squares) models. Shown are percentage values using original data (left) and deviation from expected mean responses using standardized data (right). Numbers are sample sizes and intensity of transparency represents sensitivity to publication bias.

The limitation of substrate minerals is thought to render fast-growing corals more vulnerable to OA (Comeau et al., 2014c), while increasing hydrogen concentrations may render imperforate corals more susceptible (Jokiel, 2011). However, many fast-growing coral taxa are perforate and some imperforate corals grow slowly. This mixture of traits

describing the rate and shape of $CaCO_3$ deposition among coral taxa may have masked potential differences in OA resistance related to the hypotheses 10 and 11. If both of these hypotheses hold true, perforate slow-growing coral taxa would be expected to outperform imperforate fast-growers. However, the data do not support this expectation, showing no difference between the two (Fig. 21). Calcification responses of the opposite crosses of growth rate and skeleton structure (*i.e*. imperforate slow-growers and perforate fast-growers) fall in the same effect size range. Therefore, neither one of the hypotheses 10 and 11 could be supported by this analysis, suggesting that carbon chemistry parameters act together and that other biochemical mechanisms are involved in the regulation of calcification responses to OA. As the source of energy for calcification, photosynthesis likely plays an important role in coral sensitivity to elevated pCO_2 (Langdon & Atkinson, 2005; Bedwell-Ivers et al., 2016). However, some mechanisms involving transport and conversion of minerals and nutrients (especially bicarbonate) within the coral holobiont are still in question (Jokiel, 2011). Unraveling the involved molecular processes will help elucidate the role of photosynthesis and nutrient transport in coral calcification under changing seawater carbon chemistry.

Hypothesis 12: Subtropical corals are more sensitive to ocean acidification than tropical corals

The hypothesis above is supported by this analysis, showing how tropical corals maintain calcification rates more efficiently under OA than subtropical corals (Fig. 8). A possible reason could be the indirect mitigating effect of warmer temperatures on calcification reductions associated with OA (see *Combined effects of ocean acidification and warming on coral calcification*). Simulation models and other meta-analysis suggest that increased temperature can favor $CaCO_3$ precipitation kinetics and aid corals in maintaining high internal aragonite saturations (McCulloch et al., 2012; Kroeker et al., 2013). In addition, warming increases the rate of metabolic energy acquisition, as long as thermal limits are not exceeded and nutrients are not limiting. This could potentially offset increased energy demand for calcification in acidified seawater (Pandolfi et al., 2011). Another reason why tropical corals cope better with OA may be a dependency on the fluctuation regime of alkalinity and other carbon chemistry parameters, which is discussed as individual hypothesis below.

Hypothesis 13: Corals living in stable CO_2 and/or alkalinity regimes are more sensitive to ocean acidification than corals experiencing fluctuations in CO_2 and/ or alkalinity

This hypothesis derives partly from the conclusion above and relates to selective pressures induced by abiotic fluctuations. Larger amplitudes in the variability of seawater carbon chemistry or alkalinity could induce genetic adaptation or phenotypic acclimatization that renders the local inhabitants more resistant to OA. This is essentially a reversed image of latitudinal variation in thermal thresholds (Hypotheses 3 and 4). Tropical corals may be more adapted to OA based on increased variability of surface alkalinity and pCO_2 in tropical costal regions. Alkalinity is more variable due to tropical upwelling and increased river input from heavy rainfall along the Intertropical Convergence Zone (Lee et al., 2006). Since coral reef metabolism acts to elevate seawater pCO_2 (Bates et al., 2010), increased metabolic turnover in warmer waters may contribute to local variation in seawater carbon chemistry. Especially within tropical semi-enclosed reefs, the additional variability may have induced adaptation and/ or acclimatization to tolerate a larger range of carbon chemistry settings. This would explain why corals from back reef areas maintain calcification under OA in laboratory treatments (Fig. 8).

Hypothesis 14: Nutritionally depleted corals are more sensitive to ocean acidification than nutritionally replete corals

This hypothesis was supported based on results showing increased vulnerability to OA under low nutrient conditions (Fig. 9). The results of traditional effect size meta-analysis suggest that nutrients have no effect on calcification responses of corals to OA. However, the difference was masked by virtue of varying stress levels across studies. Specifically, the effect size for the group of fed corals was driven down by exposure to higher pCO_2 compared to the group comprising starved corals. Evidence for this is given by standardized effect sizes that incorporate stress level variation (Fig. 9, right side). Previous studies have also shown that heterotrophic feeding can partially offset negative effects of OA (Cohen et al., 2009; Edmunds, 2011). Increasing heterotrophy is a good way for corals to combat energy shortages (Grottoli et al., 2006) and may fulfil a similar function to support enhanced biomineralization in high-CO_2 environments.

Hypothesis 15: Coral resistance to elevated pCO_2 increases with exposure time

This hypothesis may not be generalizable in the context of coral calcification responses to OA. Factorial analyses of exposure duration displayed a negative relationship between experimental duration and coral calcification resistance under elevated pCO_2 (Fig. 9). Effect sizes were negative, regardless of duration, and differed between short treatments (≤ 1 day, 8% average reduction) and very long treatments (> 1 month, 23% average reduction). This result contradicts previous suggestions that resistance of corals to OA is elevated with increasing exposure duration due to acclimation (Pandolfi et al., 2011; Form & Riebesell, 2012). However, the analysis in this study is assumed to be more accurate because a large part of the inherent data was not available at the time when previous conclusions were drawn. Results from this study suggests that juvenile or adult corals may not be able to acclimate to OA conditions in laboratory settings.

Ocean acidification and coral settlement

Hypothesis 16: Ocean acidification impedes coral growth more than settlement and metamorphosis

The effects of OA are generally believed to affect post-settlement and adult growth rates of corals more than prior larval development and settlement (Byrne, 2011). However, many studies emphasize the adverse effects of OA on coral settlement, which could represent a stronger bottleneck for population growth (Albright et al., 2010). Neither one of these hypotheses could be supported in this study as there was no statistical difference between settlement and calcification responses to OA (Fig. 3A). The analysis suggests that OA will hamper coral growth and community resilience by affecting settlement and calcification rates equally. However, settlement responses to elevated pCO_2 may be underestimated in some studies based on potential indirect *in situ* effects, which are not captured by current experimental designs. Albright and Langdon (2011) noted that OA shifted the dominant substrate community from crustose coralline algae (CCA) to filamentous algae. They compared settlement rates of coral larvae under varying conditioning regimes and found that settlement was more compromised on surfaces that were conditioned at high pCO_2. Absence of the chemical cues from CCA may lower the

chances for larvae to detect suitable settlement substrates without direct impacts on larval physiology (Doropoulos et al., 2012; Webster et al., 2013).

Certainty and limitations

Most data were non-normally distributed (Fig. S3) and analyzed using a combination of resampling procedures (i.e. bootstrapping) and parametric weighting. Resampling procedures generate their own distributions and are therefore not based on normality assumptions of parametric tests. They can be equally powerful in determining accurate confidence intervals (Adams et al., 1997). The incorporation of statistical weights in non-parametric bootstraps by converting them to probabilities further enhanced the precision of results. In fixed models, parametric weights are solely based on the within-study variance (see *Data analysis*, equation 12). Mixed models also incorporate the between-study variance (equations 11 and 13) and were applied only if the variation between studies was significant (*i.e.* greater than expected by chance). Although parametric weights are coupled with distribution assumptions, they were used in resampling procedures to represent the mere precision of each individual effect size. As a result, larger studies contributed more heavily to the overall means, which is desirable in empirical research (Hedges et al., 1999). Together, bootstrapping and parametric weighting are among the most powerful statistical procedures for quantitative, hypothesis-driven meta-analyses (Gurevitch & Hedges, 1999).

The drivers of variation presented above are statistically robust and likely represent general patterns of coral sensitivity to climate change. The number of studies with low precision did not exceed 30% in any of the datasets (Table 9), which is below the recommended threshold for quantitative analyses (Hedges et al., 1999). Consequently, most overall effect estimates (Fig. 3) are statistically robust. However, the pooled effect of OA on larval survival was subject to other sources of bias. Two individual treatment comparisons (10% of the data) resulted in large effects that were driving the overall negative effect. Omission of these two effect sizes resulted in an overall neutral effect. This is in agreement with results from the fail-safe analysis (Rosenthal, 1979), which showed that only 3 insignificant studies would be needed to change the direction of the effect (*i.e.* I = 3, Table 9). The dataset on coral larval survival responses to OA also failed the

random permutation test. Every significant difference between subsamples had a 15% likelihood to be based on chance, rendering the dataset unsuitable for factorial analysis. This probability remained below 6% for all other datasets and fail-safe numbers were typically large. However, publication bias may still occur in some datasets that showed skewed funnel plots and multiple underlying populations of individual effect sizes (Figures S4 - S6). Incorporation of fail-safe analysis into factorial comparisons resulted in omitting more than 70% of the statistical differences between subsamples (Figures S1 & S2), including all differences obtained for dataset 6 (*i.e.* coral settlement responses to OW). The extensive sensitivity analysis allowed for repeated testing of the same dataset using different explanatory variables without the inherent problem of committing type I errors.

Differences between stress levels of individual studies represented another source of variation that was addressed using standardization procedures. Chan and Connolly (2013) noted that interpretations of differences between subsamples are complicated by study-specific variation in the magnitude of the stressor. The problem can occur in two ways: separate subsamples can be statistically different because corals were subjected to more pronounced stresses in one of the subsamples, or real differences between subsamples can be masked because the group with more sensitive corals experienced lower stress levels. In larger datasets (*i.e.* calcification responses to OA and OW), this variation could be incorporated by standardizing individual outcomes based on the level of stress in their respective studies (Fig. 4). However, results obtained from standardized data do not represent the size of the effect, but rather its deviation from the expected effect based on stressor magnitudes. These 'standardized effect sizes' should only be used to identify if apparent similarities or differences in organismal tolerance are based on stress levels and, as shown in this study, do so with high precision. This form of bias has likely influenced results from previous meta-analyses that summarize stress responses in organisms. The use of standardized effect sizes offers a simple solution to the problem and may warrant enhanced precision in future analyses.

The choice of effect size can dramatically influence meta-analytical results (Koricheva et al., 2013). For single stressors, analysis of the calcification data using alternative metrics produced effect sizes that differed from original ones in magnitude, but not in direction (Fig. 17). This was especially pronounced in calcification responses to OA.

Despite using identical data, the original metric produced the most conservative effect size among recent meta-analytical results, whereas the alternative metric produced the most dramatic estimate (Figures 18 & 19). For multiple stressors acting together, effect sized based on different metrics varied in direction, but not in magnitude. This comparison illustrates how different metrics are more or less desirable depending on the specific research question. In this case, the original metric (see Hedges et al., 1999) was more appropriate to estimate the overall effect of combined stressors and showed a negative effect on coral calcification. However, the alternative metric (see Gurevitch et al., 2000) summarized the strength of the interaction between elevated temperature and pCO_2, which is additive and therefore statistically neutral. Despite using different effect size computations, the overall coral calcification responses to OAW in this study were almost identical to estimates from Harvey et al. (2013), indicating that the choice of effect size was appropriate in both studies.

The findings in this study do not directly translate to expected changes in coral community compositions with OAW. Stress tolerances of corals to elevated temperature and pCO_2 levels are just one piece of the puzzle that shows how coral distributions will change in the 21st century. Other important aspects include the potential of corals to adapt or acclimate (Baker et al., 2004; Palumbi et al., 2014), their ability to recover from disturbances (Fabricius et al., 2011; Polidoro & Carpenter, 2013), species interactions (Barry, 2011; Wernberg et al., 2012), and the presence of local stressors possibly creating synergies with elevated temperature or pCO_2 (Hughes et al., 2007; Negri & Hoogenboom, 2011). Meta-analytical results on all of these aspects can be incorporated into climatic projection models to create powerful tools that can help determine how coral communities will change with the expected intensification of OAW.

Summary of main findings

This study represents one of the most comprehensive reviews on coral resistance to ocean acidification and warming to date. Factorial comparisons between tolerances of different groups of corals has been conducted for a few potential drivers in empirical studies (Edmunds et al., 2013a; Comeau et al., 2014c) and meta-analyses (Chan & Connolly, 2013; Kroeker et al., 2013). However, the number of potential drivers tested in this study is much

higher compared to previous efforts. Factorial analysis was possible due to the strong increase of available data in recent years (50% of the data were published during the last three years, that is, 2013 – 2015) and led to a number of general inferences regarding coral resistance to climate change.

1. The global stressors associated with climate change will likely impair recruitment and growth of reef-building corals worldwide. Ocean warming reduces survival rates of coral larvae, while ocean acidification hampers the settlement process. Growth rates and/ or structural integrity of the skeletons are also compromised in more acidic environments. This effect can be mitigated through an additive interaction with OW as long as temperature thresholds are not exceeded.
2. The biochemical mechanisms and relationships leading to declining coral calcification under high-CO_2 exposure need to be reevaluated. The widely accepted relationship between aragonite saturation (*i.e.* carbonate concentration) and coral calcification does not always hold true (Jokiel, 2016). Additionally, coral calcification reacts to changes in bicarbonate under constant aragonite (Pandolfi et al., 2011). Results from this study support the hypotheses that calcification is hampered by increasing hydrogen concentrations (Jokiel, 2011; Bach, 2015), while benefitting from increasing alkalinity (Jokiel, 2016) and DIC (Comeau et al., 2013a). Further testing is necessary to evaluate this assumption, which could be achieved by testing the effect of alkalinity and different components of DIC on coral calcification rates under constant aragonite and pCO_2.
3. Knowledge gaps in our current understanding of potential drivers of coral resistance to climate change are evident and highlighted by the fact that 50% of the relevant hypotheses could not be supported by this analysis (see *Potential drivers of coral resistance to climate change*).
4. Physiological responses of reef-building corals to OAW are generally driven by biological traits (taxonomy and life stage), environmental factors (*in situ* variability of the stressor), and differences in experimental design (stress level, exposure duration and feeding regime). These drivers ultimately affect the ability of corals to maintain growth and recruitment under changing temperature and pCO_2 by enabling or impeding genetic and non-genetic adaptive mechanisms.

References

Abrego, D., Ulstrup, K. E., Willis, B. L., & van Oppen, M. J. (2008). Species–specific interactions between algal endosymbionts and coral hosts define their bleaching response to heat and light stress. *Proceedings of the Royal Society B: Biological Sciences, 275*(1648), 2273-2282.

Adams, D. C., Gurevitch, J., & Rosenberg, M. S. (1997). Resampling tests for meta-analysis of ecological data. *Ecology, 78*(4), 1277-1283.

Albright, R., & Langdon, C. (2011). Ocean acidification impacts multiple early life history processes of the Caribbean coral Porites astreoides. *Global Change Biology, 17*(7), 2478-2487.

Albright, R., Mason, B., Miller, M., & Langdon, C. (2010). Ocean acidification compromises recruitment success of the threatened Caribbean coral Acropora palmata. *Proceedings of the National Academy of Sciences, 107*(47), 20400-20404.

Anlauf, H., D'Croz, L., & O'Dea, A. (2011). A corrosive concoction: the combined effects of ocean warming and acidification on the early growth of a stony coral are multiplicative. *Journal of Experimental Marine Biology and Ecology, 397*(1), 13-20.

Anthony, K. R. N., Kline, D. I., Diaz-Pulido, G., Dove, S., & Hoegh-Guldberg, O. (2008). Ocean acidification causes bleaching and productivity loss in coral reef builders. *Proceedings of the National Academy of Sciences of the United States of America, 105*(45), 17442-17446. doi:10.1073/pnas.0804478105

Bach, L. T. (2015). Reconsidering the role of carbonate ion concentration in calcification by marine organisms. *Biogeosciences, 12*(16), 4939-4951. doi:10.5194/bg-12-4939-2015

Baird, A. H., Gilmour, J. P., Kamiki, T. M., Nonaka, M., Pratchett, M. S., Yamamoto, H. H., & Yamasaki, H. (2006). Temperature tolerance of symbiotic and non-symbiotic coral larvae. *Proc 10th Int Coral Reef Symp, Okinawa Convention Center, Okinawa, Japan. Japanese Coral Reef Society 1, 38–42 (2006).* 38-42.

Baird, A. H., Guest, J. R., & Willis, B. L. (2009). Systematic and Biogeographical Patterns in the Reproductive Biology of Scleractinian Corals. *Annual Review of Ecology, Evolution, and Systematics, 40*(1), 551-571. doi:doi:10.1146/annurev.ecolsys.110308.120220

Baird, A. H., & Marshall, P. A. (2002). Mortality, growth and reproduction in scleractinian corals following bleaching on the Great Barrier Reef. *Marine Ecology Progress Series, 237*, 133-141. doi:10.3354/meps237133

Baker, A. C., Glynn, P. W., & Riegl, B. (2008). Climate change and coral reef bleaching: An ecological assessment of long-term impacts, recovery trends and future outlook. *Estuarine, Coastal and Shelf Science, 80*(4), 435-471.

Baker, A. C., Starger, C. J., McClanahan, T. R., & Glynn, P. W. (2004). Corals' adaptive response to climate change. *Nature, 430*(7001), 741-741. doi:10.1038/430741a

Baria, M. V. B., Kurihara, H., & Harii, S. (2015). Tolerance to Elevated Temperature and Ocean Acidification of the Larvae of the Solitary Corals Fungia fungites (Linnaues, 1758) and Lithophyllon repanda (Dana, 1846). *Zoological Science, 32*(5), 447-454. doi:10.2108/zs150036

Barry, J. P., Widdicombe, S. and Hall-Spencer, J.M. (2011). Effects of ocean acidification on marine biodiversity and ecosystem function. *Ocean acidification*, pp.192-209.

Baskett, M. L., Gaines, S. D., & Nisbet, R. M. (2009). Symbiont diversity may help coral reefs survive moderate climate change. *Ecological Applications, 19*(1), 3-17. doi:10.1890/08-0139.1

Bassim, K. M., & Sammarco, P. W. (2003). Effects of temperature and ammonium on larval development and survivorship in a scleractinian coral (Diploria strigosa). *Marine Biology, 142*(2), 241-252. doi:10.1007/S00227-002-0953-z

Bates, N. R., Amat, A., & Andersson, A. J. (2010). Feedbacks and responses of coral calcification on the Bermuda reef system to seasonal changes in biological processes and ocean acidification. *Biogeosciences, 7*(8), 2509-2530. doi:10.5194/bg-7-2509-2010

Bedwell-Ivers, H. E., Koch, M. S., Peach, K. E., Joles, L., Dutra, E., & Manfrino, C. (2016). The role of in hospite zooxanthellae photophysiology and reef chemistry on elevated pCO2 effects in two branching Caribbean corals: Acropora cervicornis and Porites divaricata. *ICES Journal of Marine Science: Journal du Conseil*. doi:10.1093/icesjms/fsw026

Bellwood, D., Hughes, T., Folke, C., & Nyström, M. (2004). Confronting the coral reef crisis. *Nature, 429*(6994), 827-833.

Berkelmans, R., & Van Oppen, M. J. (2006). The role of zooxanthellae in the thermal tolerance of corals: a 'nugget of hope'for coral reefs in an era of climate change. *Proceedings of the Royal Society B: Biological Sciences, 273*(1599), 2305-2312.

Berkelmans, R., & Willis, L. B. (1999). Seasonal and local spatial patterns in the upper thermal limits of corals on the inshore Central Great Barrier Reef. *Coral reefs, 18*(3), 219-228. doi:10.1007/s003380050186

Borges, A. V. (2005). Do we have enough pieces of the jigsaw to integrate CO2 fluxes in the coastal ocean? *Estuaries, 28*(1), 3-27. doi:10.1007/bf02732750

Bozec, Y.-M., & Mumby, P. J. (2015). Synergistic impacts of global warming on the resilience of coral reefs. *Philosophical Transactions of the Royal Society B: Biological Sciences, 370*(1659), 20130267.

Brooke, S., & Young, C. M. (2005). Embryogenesis and larval biology of the ahermatypic scleractinian Oculina varicosa. *Marine Biology, 146*(4), 665-675. doi:10.1007/s00227-004-1481-9

Brown, B. E. (1997). Coral bleaching: causes and consequences. *Coral reefs, 16*, S129-S138. doi:10.1007/s003380050249

Brown, D., & Edmunds, P. J. (2016). Differences in the responses of three scleractinians and the hydrocoral Millepora platyphylla to ocean acidification. *Marine Biology, 163*(3), 1-10. doi:10.1007/s00227-016-2837-7

Byrne, M. (2011). IMPACT OF OCEAN WARMING AND OCEAN ACIDIFICATION ON MARINE INVERTEBRATE LIFE HISTORY STAGES: VULNERABILITIES AND POTENTIAL FOR PERSISTENCE IN A CHANGING OCEAN. In R. N. Gibson, R. J. A. Atkinson, & J. D. M. Gordon (Eds.), *Oceanography and Marine Biology: An Annual Review, Vol 49* (Vol. 49, pp. 1-42).

Caldeira, K., & Wickett, M. E. (2003). Oceanography: anthropogenic carbon and ocean pH. *Nature, 425*(6956), 365-365.

Cantin, N. E., Cohen, A. L., Karnauskas, K. B., Tarrant, A. M., & McCorkle, D. C. (2010). Ocean warming slows coral growth in the central Red Sea. *Science, 329*(5989), 322-325.

Carricart-Ganivet, J. P. (2004). Sea surface temperature and the growth of the West Atlantic reef-building coral Montastraea annularis. *Journal of Experimental Marine Biology and Ecology, 302*(2), 249-260.

Castillo, K., & Helmuth, B. (2005). Influence of thermal history on the response of Montastraea annularis to short-term temperature exposure. *Marine Biology, 148*(2), 261-270.

Castillo, K. D., Ries, J. B., Bruno, J. F., & Westfield, I. T. (2014). The reef-building coral Siderastrea siderea exhibits parabolic responses to ocean acidification and warming. *Proceedings of the Royal Society B: Biological Sciences, 281*(1797), 20141856.

Chan, N., & Connolly, S. R. (2013). Sensitivity of coral calcification to ocean acidification: a meta-analysis. *Global Change Biology, 19*(1), 282-290.

Chua, C. M., Leggat, W., Moya, A., & Baird, A. H. (2013). Temperature affects the early life history stages of corals more than near future ocean acidification. *Marine Ecology Progress Series, 475*, 85-92. doi:10.3354/meps10077

Clarke, A., & Fraser, K. (2004). Why does metabolism scale with temperature? *Functional Ecology, 18*(2), 243-251.

Cohen, A. L., & Holcomb, M. (2009). Why corals care about ocean acidification: uncovering the mechanism.

Cohen, A. L., McCorkle, D. C., de Putron, S., Gaetani, G. A., & Rose, K. A. (2009). Morphological and compositional changes in the skeletons of new coral recruits reared in acidified seawater: Insights into the biomineralization response to ocean acidification. *Geochemistry Geophysics Geosystems, 10*. doi:10.1029/2009gc002411

Comeau, S., Carpenter, R., & Edmunds, P. (2013a). Coral reef calcifiers buffer their response to ocean acidification using both bicarbonate and carbonate. *Proceedings of the Royal Society B: Biological Sciences, 280*(1753), 20122374.

Comeau, S., Carpenter, R. C., & Edmunds, P. J. (2013b). Effects of feeding and light intensity on the response of the coral Porites rus to ocean acidification. *Marine Biology, 160*(5), 1127-1134. doi:10.1007/s00227-012-2165-5

Comeau, S., Carpenter, R. C., Nojiri, Y., Putnam, H. M., Sakai, K., & Edmunds, P. J. (2014a). Pacific-wide contrast highlights resistance of reef calcifiers to ocean acidification. *Proceedings of the Royal Society B-Biological Sciences, 281*(1790). doi:10.1098/rspb.2014.1339

Comeau, S., Edmunds, P. J., Lantz, C. A., & Carpenter, R. C. (2014b). Water flow modulates the response of coral reef communities to ocean acidification. *Scientific Reports, 4*. doi:10.1038/srep06681

Comeau, S., Edmunds, P. J., Spindel, N. B., & Carpenter, R. C. (2013c). The responses of eight coral reef calcifiers to increasing partial pressure of CO2 do not exhibit a tipping point. *Limnology and Oceanography, 58*(1), 388-398. doi:10.4319/lo.2013.58.1.0388

Comeau, S., Edmunds, P. J., Spindel, N. B., & Carpenter, R. C. (2014c). Fast coral reef calcifiers are more sensitive to ocean acidification in short-term laboratory

incubations. *Limnology and Oceanography, 59*(3), 1081-1091. doi:10.4319/lo.2014.59.3.1081

Cooper, T. F., O'Leary, R. A., & Lough, J. M. (2012). Growth of Western Australian corals in the Anthropocene. *Science, 335*(6068), 593-596.

Cox, E. F. (2007). Continuation of sexual reproduction in Montipora capitata following bleaching. *Coral reefs, 26*(3), 721-724. doi:10.1007/s00338-007-0251-9

Crook, E. D., Cohen, A. L., Rebolledo-Vieyra, M., Hernandez, L., & Paytan, A. (2013). Reduced calcification and lack of acclimatization by coral colonies growing in areas of persistent natural acidification. *Proceedings of the National Academy of Sciences, 110*(27), 11044-11049.

Cumbo, V., Fan, T., & Edmunds, P. (2013a). Effects of exposure duration on the response of Pocillopora damicornis larvae to elevated temperature and high pCO 2. *Journal of Experimental Marine Biology and Ecology, 439*, 100-107.

Cumbo, V. R., Edmunds, P. J., Wall, C. B., & Fan, T.-Y. (2013b). Brooded coral larvae differ in their response to high temperature and elevated pCO(2) depending on the day of release. *Marine Biology, 160*(11), 2903-2917. doi:10.1007/s00227-013-2280-y

Cumbo, V. R., Fan, T. Y., & Edmunds, P. J. (2013c). Effects of exposure duration on the response of Pocillopora damicornis larvae to elevated temperature and high pCO(2). *Journal of Experimental Marine Biology and Ecology, 439*, 100-107. doi:10.1016/j.jembe.2012.10.019

Cunning, R., Gillette, P., Capo, T., Galvez, K., & Baker, A. (2015). Growth tradeoffs associated with thermotolerant symbionts in the coral Pocillopora damicornis are lost in warmer oceans. *Coral reefs*, 1-6.

Doney, S. C., Fabry, V. J., Feely, R. A., & Kleypas, J. A. (2009). Ocean acidification: the other CO2 problem. *Marine Science, 1*.

Donner, S. D., Skirving, W. J., Little, C. M., Oppenheimer, M., & Hoegh-Guldberg, O. (2005). Global assessment of coral bleaching and required rates of adaptation under climate change. *Global Change Biology, 11*(12), 2251-2265.

Doropoulos, C., & Diaz-Pulido, G. (2013). High CO2 reduces the settlement of a spawning coral on three common species of crustose coralline algae. *Marine Ecology Progress Series, 475*, 93-99. doi:10.3354/meps10096

Doropoulos, C., Ward, S., Diaz-Pulido, G., Hoegh-Guldberg, O., & Mumby, P. J. (2012). Ocean acidification reduces coral recruitment by disrupting intimate larval-algal settlement interactions. *Ecology Letters, 15*(4), 338-346. doi:10.1111/j.1461-0248.2012.01743.x

Drenkard, E. J., Cohen, A. L., McCorkle, D. C., de Putron, S. J., Starczak, V. R., & Zicht, A. E. (2013). Calcification by juvenile corals under heterotrophy and elevated CO2. *Coral reefs, 32*(3), 727-735. doi:10.1007/s00338-013-1021-5

Dufault, A. M., Ninokawa, A., Bramanti, L., Cumbo, V. R., Fan, T. Y., & Edmunds, P. J. (2013). The role of light in mediating the effects of ocean acidification on coral calcification. *Journal of Experimental Biology, 216*(9), 1570-1577. doi:10.1242/jeb.080549

Dupont, S., Dorey, N., & Thorndyke, M. (2010). What meta-analysis can tell us about vulnerability of marine biodiversity to ocean acidification? *Estuarine, Coastal and Shelf Science, 89*(2), 182-185. doi:http://dx.doi.org/10.1016/j.ecss.2010.06.013

Economics, A. (2007). Measuring the economic and financial value of the Great Barrier Reef Marine Park 2005/06. *Report by Access Economics Pty Limited for Great Barrier Reef Marine Park Authority. Great Barrier Reef Marine Park Authority, Townsville*.

Edmunds, P., Gates, R., & Gleason, D. (2001). The biology of larvae from the reef coral Porites astreoides, and their response to temperature disturbances. *Marine Biology, 139*(5), 981-989.

Edmunds, P. J. (2005). The effect of sub-lethal increases in temperature on the growth and population trajectories of three scleractinian corals on the southern Great Barrier Reef. *Oecologia, 146*(3), 350-364. doi:10.1007/s00442-005-0210-5

Edmunds, P. J. (2011). Zooplanktivory ameliorates the effects of ocean acidification on the reef coral Porites spp. *Limnology and Oceanography, 56*(6), 2402-2410.

Edmunds, P. J., Brown, D., & Moriarty, V. (2012). Interactive effects of ocean acidification and temperature on two scleractinian corals from Moorea, French Polynesia. *Global Change Biology, 18*(7), 2173-2183.

Edmunds, P. J., Carpenter, R. C., & Comeau, S. (2013a). UNDERSTANDING THE THREATS OF OCEAN ACIDIFICATION TO CORAL REEFS. *Oceanography, 26*(3), 149-152.

Edmunds, P. J., Cumbo, V. R., & Fan, T.-Y. (2013b). Metabolic costs of larval settlement and metamorphosis in the coral Seriatopora caliendrum under ambient and elevated pCO 2. *Journal of Experimental Marine Biology and Ecology, 443*, 33-38.

Edmunds, P. J., Gates, R. D., Leggat, W., Hoegh-Guldberg, O., & Allen-Requa, L. (2005). The effect of temperature on the size and population density of dinoflagellates in larvae of the reef coral Porites astreoides. *Invertebrate Biology, 124*(3), 185-193. doi:10.1111/j.1744-7410.2005.00018.x

Evenhuis, C., Lenton, A., Cantin, N. E., & Lough, J. M. (2015). Modelling coral calcification accounting for the impacts of coral bleaching and ocean acidification. *Biogeosciences, 12*(9), 2607-2630. doi:10.5194/bg-12-2607-2015

Fabricius, K. E., Langdon, C., Uthicke, S., Humphrey, C., Noonan, S., De/'ath, G., . . . Lough, J. M. (2011). Losers and winners in coral reefs acclimatized to elevated carbon dioxide concentrations. *Nature Clim. Change, 1*(3), 165-169. doi:http://www.nature.com/nclimate/journal/v1/n3/abs/nclimate1122.html#supplementary-information

Fadlallah, Y. H. (1983). Sexual reproduction, development and larval biology in scleractinian corals. *Coral reefs, 2*(3), 129-150. doi:10.1007/bf00336720

Fassbender, A. J., Sabine, C. L., & Feifel, K. M. (2016). Consideration of coastal carbonate chemistry in understanding biological calcification. *Geophysical Research Letters, 43*(9), 4467-4476. doi:10.1002/2016GL068860

Feely, R. A., Doney, S. C., & Cooley, S. R. (2009). Ocean acidification: present conditions and future changes in a high-CO2 world.

Figueiredo, J., Baird, A. H., Harii, S., & Connolly, S. R. (2014). Increased local retention of reef coral larvae as a result of ocean warming. *Nature Climate Change, 4*(6), 498-502.

Form, A. U., & Riebesell, U. (2012). Acclimation to ocean acidification during long-term CO2 exposure in the cold-water coral Lophelia pertusa. *Global Change Biology, 18*(3), 843-853. doi:10.1111/j.1365-2486.2011.02583.x

Foster, T., Gilmour, J. P., Chua, C. M., Falter, J. L., & McCulloch, M. T. (2015). Effect of ocean warming and acidification on the early life stages of subtropical Acropora spicifera. *Coral reefs, 34*(4), 1217-1226. doi:10.1007/s00338-015-1342-7

Gates, R. D., & Edmunds, P. J. (1999). The Physiological Mechanisms of Acclimatization in Tropical Reef Corals. *American Zoologist, 39*(1), 30-43. doi:10.1093/icb/39.1.30

Gell, F. R., & Roberts, C. M. (2003). Benefits beyond boundaries: the fishery effects of marine reserves. *Trends in ecology & evolution, 18*(9), 448-455.

Gleason, M. (1993). Effects of disturbance on coral communities: bleaching in Moorea, French Polynesia. *Coral reefs, 12*(3-4), 193-201.

Golbuu, Y., Gouezo, M., Kurihara, H., Rehm, L., & Wolanski, E. (2016). Long-term isolation and local adaptation in Palau's Nikko Bay help corals thrive in acidic waters. *Coral reefs*, 1-10. doi:10.1007/s00338-016-1457-5

Goreau, T. F. (1963). Calcium carbonate deposition by coralline algae and corals in relation to their roles as reef-builders. *Annals of the New York Academy of Sciences, 109*, 127-167. doi:10.1111/j.1749-6632.1963.tb13465.x

Grottoli, A. G., Rodrigues, L. J., & Palardy, J. E. (2006). Heterotrophic plasticity and resilience in bleached corals. *Nature, 440*(7088), 1186-1189.

Gurevitch, J., & Hedges, L. V. (1999). Statistical issues in ecological meta-analyses. *Ecology, 80*(4), 1142-1149. doi:10.1890/0012-9658(1999)080[1142:siiema]2.0.co;2

Gurevitch, J., Morrison, J. A., Hedges, L. V., & Associate Editor: Peter, J. M. (2000). The Interaction between Competition and Predation: A Meta‐analysis of Field Experiments. *The American Naturalist, 155*(4), 435-453. doi:10.1086/303337

Harvell, C. D., Mitchell, C. E., Ward, J. R., Altizer, S., Dobson, A. P., Ostfeld, R. S., & Samuel, M. D. (2002). Climate warming and disease risks for terrestrial and marine biota. *Science, 296*(5576), 2158-2162.

Harvey, B. P., Gwynn-Jones, D., & Moore, P. J. (2013). Meta-analysis reveals complex marine biological responses to the interactive effects of ocean acidification and warming. *Ecology and evolution, 3*(4), 1016-1030.

Haryanti, D., Yasuda, N., Harii, S., & Hidaka, M. (2015). High tolerance of symbiotic larvae of Pocillopora damicornis to thermal stress. *Zoological Studies, 54*. doi:10.1186/s40555-015-0134-7

Hedges, L. V., Gurevitch, J., & Curtis, P. S. (1999). The meta-analysis of response ratios in experimental ecology. *Ecology, 80*(4), 1150-1156.

Hendriks, I. E., Duarte, C. M., & Álvarez, M. (2010). Vulnerability of marine biodiversity to ocean acidification: a meta-analysis. *Estuarine, Coastal and Shelf Science, 86*(2), 157-164.

Hoegh-Guldberg, O. (1999). Climate change, coral bleaching and the future of the world's coral reefs. *Marine and freshwater research, 50*(8), 839-866.

Hoegh-Guldberg, O., Mumby, P., Hooten, A., Steneck, R., Greenfield, P., Gomez, E., . . . Caldeira, K. (2007). Coral reefs under rapid climate change and ocean acidification. *Science, 318*(5857), 1737-1742.

Holcomb, M., McCorkle, D. C., & Cohen, A. L. (2010). Long-term effects of nutrient and CO2 enrichment on the temperate coral Astrangia poculata (Ellis and Solander, 1786). *Journal of Experimental Marine Biology and Ecology, 386*(1-2), 27-33. doi:10.1016/j.jembe.2010.02.007

Howells, E., Beltran, V., Larsen, N., Bay, L., Willis, B., & Van Oppen, M. (2012). Coral thermal tolerance shaped by local adaptation of photosymbionts. *Nature Climate Change, 2*(2), 116-120.

Hughes, T. P., Bellwood, D. R., Folke, C. S., McCook, L. J., & Pandolfi, J. M. (2007). No-take areas, herbivory and coral reef resilience. *Trends in ecology & evolution, 22*(1), 1-3.

IPCC. (2014). *Climate Change 2014: Synthesis Report. Contribution of Working Groups I, II and III to the Fifth Assessment Report of the Intergovernmental Panel on Climate Change [Core Writing Team, R.K. Pachauri and L.A. Meyer (eds.)]*. IPCC, Geneva, Switzerland.

Jiang, L., Huang, H., Yuan, X. C., Yuan, T., Zhang, Y. Y., Wen, C. K. C., . . . Zhou, G. W. (2015). Effects of elevated pCO(2) on the post-settlement development of Pocillopora damicornis. *Journal of Experimental Marine Biology and Ecology, 473*, 169-175. doi:10.1016/j.jembe.2015.09.004

Jokiel, P., & Coles, S. (1990). Response of Hawaiian and other Indo-Pacific reef corals to elevated temperature. *Coral reefs, 8*(4), 155-162.

Jokiel, P. L. (2011). The reef coral two compartment proton flux model: A new approach relating tissue-level physiological processes to gross corallum morphology. *Journal of Experimental Marine Biology and Ecology, 409*(1–2), 1-12. doi:http://dx.doi.org/10.1016/j.jembe.2011.10.008

Jokiel, P. L. (2016). Predicting the impact of ocean acidification on coral reefs: evaluating the assumptions involved. *Ices Journal of Marine Science, 73*(3), 550-557. doi:10.1093/icesjms/fsv091

Jones, A., & Berkelmans, R. (2010). Potential costs of acclimatization to a warmer climate: growth of a reef coral with heat tolerant vs. sensitive symbiont types. *PLoS One, 5*(5), e10437.

Jury, C. P., Whitehead, R. F., & Szmant, A. M. (2010). Effects of variations in carbonate chemistry on the calcification rates of Madracis auretenra (= Madracis mirabilis sensu Wells, 1973): bicarbonate concentrations best predict calcification rates. *Global Change Biology, 16*(5), 1632-1644. doi:10.1111/j.1365-2486.2009.02057.x

Kleypas, J. A., Buddemeier, R. W., Archer, D., Gattuso, J.-P., Langdon, C., & Opdyke, B. N. (1999). Geochemical consequences of increased atmospheric carbon dioxide on coral reefs. *Science, 284*(5411), 118-120.

Kleypas, J. A., & Langdon, C. (2006). Coral reefs and changing seawater carbonate chemistry. *Coral reefs and climate change: science and management*, 73-110.

Kleypas, J. A., & Yates, K. K. (2009). Coral reefs and ocean acidification. *Oceanography, 22*.

Koricheva, J., Gurevitch, J., & Mengersen, K. (2013). *Handbook of meta-analysis in ecology and evolution*: Princeton University Press.

Kroeker, K. J., Kordas, R. L., Crim, R., Hendriks, I. E., Ramajo, L., Singh, G. S., . . . Gattuso, J. P. (2013). Impacts of ocean acidification on marine organisms: quantifying sensitivities and interaction with warming. *Global Change Biology, 19*(6), 1884-1896.

Kump, L. R., Bralower, T. J., & Ridgwell, A. (2009). Ocean acidification in deep time. *Oceanography, 22*(4), 94.

Langdon, C., & Atkinson, M. J. (2005). Effect of elevated pCO 2 on photosynthesis and calcification of corals and interactions with seasonal change in temperature/irradiance and nutrient enrichment. *Journal of Geophsical Research-Part C-Oceans, 110*(C9), 16 pp.-16 pp. doi:10.1029/2004jc002576

Lee, K., Tong, L. T., Millero, F. J., Sabine, C. L., Dickson, A. G., Goyet, C., . . . Key, R. M. (2006). Global relationships of total alkalinity with salinity and temperature in surface waters of the world's oceans. *Geophysical Research Letters, 33*(19). doi:10.1029/2006gl027207

Lesser, M. P. (2006). Oxidative stress in marine environments: biochemistry and physiological ecology. *Annu. Rev. Physiol., 68*, 253-278.

Lippmann, F. (1973). Crystal Chemistry of Sedimentary Carbonate Minerals *Sedimentary Carbonate Minerals* (pp. 5-96). Berlin, Heidelberg: Springer Berlin Heidelberg.

Liu, G., Strong, A. E., & Skirving, W. (2003). Remote sensing of sea surface temperatures during 2002 Barrier Reef coral bleaching. *Eos, Transactions American Geophysical Union, 84*(15), 137-141.

Lough, J., & Barnes, D. (2000). Environmental controls on growth of the massive coral Porites. *Journal of Experimental Marine Biology and Ecology, 245*(2), 225-243.

Lough, J. M., & Cantin, N. E. (2014). Perspectives on Massive Coral Growth Rates in a Changing Ocean. *The Biological Bulletin, 226*(3), 187-202.

Loya, Y., Sakai, K., Yamazato, K., Nakano, Y., Sambali, H., & Van Woesik, R. (2001). Coral bleaching: the winners and the losers. *Ecology Letters, 4*(2), 122-131.

Marshall, D. J., Monro, K., Bode, M., Keough, M. J., & Swearer, S. (2010). Phenotype-environment mismatches reduce connectivity in the sea. *Ecology Letters, 13*(1), 128-140. doi:10.1111/j.1461-0248.2009.01408.x

McClanahan, T. R., & Maina, J. (2003). Response of coral assemblages to the interaction between natural temperature variation and rare warm-water events. *Ecosystems, 6*(6), 551-563. doi:10.1007/s10021-002-0104-x

McCulloch, M., Falter, J., Trotter, J., & Montagna, P. (2012). Coral resilience to ocean acidification and global warming through pH up-regulation. *Nature Climate Change, 2*(8), 623-633. doi:10.1038/nclimate1473

Middlebrook, R., Hoegh-Guldberg, O., & Leggat, W. (2008). The effect of thermal history on the susceptibility of reef-building corals to thermal stress. *Journal of Experimental Biology, 211*(7), 1050-1056. doi:10.1242/jeb.013284

Miller, K., & Mundy, C. (2003). Rapid settlement in broadcast spawning corals: implications for larval dispersal. *Coral reefs, 22*(2), 99-106. doi:10.1007/s00338-003-0290-9

Mitchell, J. F. (1989). The "greenhouse" effect and climate change. *Reviews of Geophysics, 27*(1), 115-139.

Moberg, F., & Folke, C. (1999). Ecological goods and services of coral reef ecosystems. *Ecological Economics, 29*(2), 215-233. doi:10.1016/s0921-8009(99)00009-9

Movilla, J., Calvo, E., Pelejero, C., Coma, R., Serrano, E., Fernandez-Vallejo, P., & Ribes, M. (2012). Calcification reduction and recovery in native and non-native Mediterranean corals in response to ocean acidification. *Journal of Experimental Marine Biology and Ecology, 438*, 144-153. doi:10.1016/j.jembe.2012.09.014

Munday, P. L. (2015). Evolutionary ecology: Survival of the fittest. *Nature Clim. Change, 5*(2), 102-103. doi:10.1038/nclimate2496

Munday, P. L., Leis, J. M., Lough, J. M., Paris, C. B., Kingsford, M. J., Berumen, M. L., & Lambrechts, J. (2009). Climate change and coral reef connectivity. *Coral reefs, 28*(2), 379-395. doi:10.1007/s00338-008-0461-9

Mydlarz, L. D., McGinty, E. S., & Harvell, C. D. (2010). What are the physiological and immunological responses of coral to climate warming and disease? *Journal of Experimental Biology, 213*(6), 934-945. doi:10.1242/jeb.037580

Nakamura, M., Ohki, S., Suzuki, A., & Sakai, K. (2011). Coral Larvae under Ocean Acidification: Survival, Metabolism, and Metamorphosis. *PLoS One, 6*(1). doi:10.1371/journal.pone.0014521

Negri, A. P., & Hoogenboom, M. O. (2011). Water Contamination Reduces the Tolerance of Coral Larvae to Thermal Stress. *PLoS One, 6*(5). doi:10.1371/journal.pone.0019703

Negri, A. P., Marshall, P. A., & Heyward, A. J. (2007). Differing effects of thermal stress on coral fertilization and early embryogenesis in four Indo Pacific species. *Coral reefs, 26*(4), 759-763. doi:10.1007/s00338-007-0258-2

Nesa, B., Baird, A. H., Harii, S., Yakovleva, I., & Hidaka, M. (2012). Algal Symbionts Increase DNA Damage in Coral Planulae Exposed to Sunlight. *Zoological Studies, 51*(1), 12-17.

Norstrom, A. V., Nystrom, M., Lokrantz, J., & Folke, C. (2009). Alternative states on coral reefs: beyond coral-macroalgal phase shifts. *Marine Ecology Progress Series, 376*, 295-306. doi:10.3354/meps07815

Nozawa, Y., & Harrison, P. L. (2007). Effects of elevated temperature on larval settlement and post-settlement survival in scleractinian corals, Acropora solitaryensis and Favites chinensis. *Marine Biology, 152*(5), 1181-1185. doi:10.1007/s00227-007-0765-2

Ohki, S., Irie, T., Inoue, M., Shinmen, K., Kawahata, H., Nakamura, T., . . . van Woesik, R. (2013). Calcification responses of symbiotic and aposymbiotic corals to near-future levels of ocean acidification. *Biogeosciences, 10*(11), 6807-6814. doi:10.5194/bg-10-6807-2013

Orr, J. C., Fabry, V. J., Aumont, O., Bopp, L., Doney, S. C., Feely, R. A., . . . Yool, A. (2005). Anthropogenic ocean acidification over the twenty-first century and its impact on calcifying organisms. *Nature, 437*(7059), 681-686. doi:10.1038/nature04095

Palumbi, S. R., Barshis, D. J., Traylor-Knowles, N., & Bay, R. A. (2014). Mechanisms of reef coral resistance to future climate change. *Science, 344*(6186), 895-898. doi:10.1126/science.1251336

Pandolfi, J. M., Connolly, S. R., Marshall, D. J., & Cohen, A. L. (2011). Projecting Coral Reef Futures Under Global Warming and Ocean Acidification. *Science, 333*(6041), 418-422. doi:10.1126/science.1204794

Patterson, M. R. (1992). A MASS-TRANSFER EXPLANATION OF METABOLIC SCALING RELATIONS IN SOME AQUATIC INVERTEBRATES AND ALGAE. *Science, 255*(5050), 1421-1423. doi:10.1126/science.255.5050.1421

Pearson, P. N., & Palmer, M. R. (2000). Atmospheric carbon dioxide concentrations over the past 60 million years. *Nature, 406*(6797), 695-699. doi:10.1038/35021000

Polidoro, B., & Carpenter, K. (2013). Dynamics of Coral Reef Recovery. *Science, 340*(6128), 34-35. doi:http://dx.doi.org/10.1126/science.1236833

Przeslawski, R., Byrne, M., & Mellin, C. (2015). A review and meta-analysis of the effects of multiple abiotic stressors on marine embryos and larvae. *Global Change Biology, 21*(6), 2122-2140. doi:10.1111/gcb.12833

Putnam, H. M., & Edmunds, P. J. (2011). The physiological response of reef corals to diel fluctuations in seawater temperature. *Journal of Experimental Marine Biology and Ecology, 396*(2), 216-223. doi:10.1016/j.jembe.2010.10.026

Putnam, H. M., Edmunds, P. J., & Fan, T.-Y. (2010). Effect of a fluctuating thermal regime on adult and larval reef corals. *Invertebrate Biology, 129*(3), 199-209. doi:10.1111/j.1744-7410.2010.00199.x

Putnam, H. M., Mayfield, A. B., Fan, T. Y., Chen, C. S., & Gates, R. D. (2013). The physiological and molecular responses of larvae from the reef-building coral Pocillopora damicornis exposed to near-future increases in temperature and pCO(2). *Marine Biology, 160*(8), 2157-2173. doi:10.1007/s00227-012-2129-9

Qin, D., Plattner, G. K., Tignor, M., Allen, S. K., Boschung, J., Nauels, A., . . . Midgley, P. M. (2014). Climate change 2013: The physical science basis. *Cambridge, UK, and New York: Cambridge University Press.*

R Development Core Team. (2010). R: A language and environment for statistical computing. Vienna, Austria: R Foundation for Statistical Computing. Retrieved from www.R-project.org

Randall, C. J., & Szmant, A. M. (2009a). Elevated Temperature Affects Development, Survivorship, and Settlement of the Elkhorn Coral, Acropora palmata (Lamarck 1816). *Biological Bulletin, 217*(3), 269-282.

Randall, C. J., & Szmant, A. M. (2009b). Elevated temperature reduces survivorship and settlement of the larvae of the Caribbean scleractinian coral, Favia fragum (Esper). *Coral reefs, 28*(2), 537-545. doi:10.1007/s00338-009-0482-z

Reynaud, S., Leclercq, N., Romaine-Lioud, S., Ferrier-Pages, C., Jaubert, J., & Gattuso, J. P. (2003). Interacting effects of CO2 partial pressure and temperature on photosynthesis and calcification in a scleractinian coral. *Global Change Biology, 9*(11), 1660-1668. doi:10.1046/j.1529-8817.2003.00678.x

Rodolfo-Metalpa, R., Martin, S., Ferrier-Pages, C., & Gattuso, J. P. (2010). Response of the temperate coral Cladocora caespitosa to mid- and long-term exposure to pCO(2) and temperature levels projected for the year 2100 AD. *Biogeosciences, 7*(1), 289-300.

Roleda, M. Y., Boyd, P. W., & Hurd, C. L. (2012). BEFORE OCEAN ACIDIFICATION: CALCIFIER CHEMISTRY LESSONS. *Journal of Phycology, 48*(4), 840-843. doi:10.1111/j.1529-8817.2012.01195.x

Rosenthal, R. (1979). The file drawer problem and tolerance for null results. *Psychological Bulletin, 86*(3), 638-641. doi:10.1037/0033-2909.86.3.638

Rosón, G., Guallart, E. F., Pérez, F. F., & Ríos, A. F. (2016). Calcium distribution in the subtropical Atlantic Ocean: Implications for calcium excess and saturation horizons. *Journal of Marine Systems, 158*, 45-51. doi:http://dx.doi.org/10.1016/j.jmarsys.2016.01.011

Ross, C., Ritson-Williams, R., Olsen, K., & Paul, V. J. (2013). Short-term and latent post-settlement effects associated with elevated temperature and oxidative stress on larvae from the coral Porites astreoides. *Coral reefs, 32*(1), 71-79. doi:10.1007/s00338-012-0956-2

Sabine, C. L., & Feely, R. A. (2003). The oceanic sink for carbon dioxide. Pp. 31–49 in Greenhouse Gas Sinks. D. Reay, N. Hewitt, J. Grace, and K. Smith, eds. *CABI Publishing, Oxfordshire, UK.*

Sabine, C. L., Feely, R. A., Gruber, N., Key, R. M., Lee, K., Bullister, J. L., . . . Rios, A. F. (2004). The oceanic sink for anthropogenic CO2. *Science, 305*(5682), 367-371. doi:10.1126/science.1097403

Scheibner, C., & Speijer, R. (2008). Late Paleocene–early Eocene Tethyan carbonate platform evolution—a response to long-and short-term paleoclimatic change. *Earth-Science Reviews, 90*(3), 71-102.

Schnitzler, C. E., Hollingsworth, L. L., Krupp, D. A., & Weis, V. M. (2012). Elevated temperature impairs onset of symbiosis and reduces survivorship in larvae of the Hawaiian coral, Fungia scutaria. *Marine Biology, 159*(3), 633-642. doi:10.1007/s00227-011-1842-0

Shamberger, K. E. F., Cohen, A. L., Golbuu, Y., McCorkle, D. C., Lentz, S. J., & Barkley, H. C. (2014). Diverse coral communities in naturally acidified waters of a Western Pacific reef. *Geophysical Research Letters, 41*(2), 499-504. doi:10.1002/2013gl058489

Sheppard, C., Dixon, D. J., Gourlay, M., Sheppard, A., & Payet, R. (2005). Coral mortality increases wave energy reaching shores protected by reef flats: Examples from the Seychelles. *Estuarine Coastal and Shelf Science, 64*(2-3), 223-234. doi:10.1016/j.ecss.2005.02.016

Suwa, R., Nakamura, M., Morita, M., Shimada, K., Iguchi, A., Sakai, K., & Suzuki, A. (2010). Effects of acidified seawater on early life stages of scleractinian corals (Genus Acropora). *Fisheries Science, 76*(1), 93-99. doi:10.1007/s12562-009-0189-7

Szmant, A. M., & Gassman, N. J. (1990). THE EFFECTS OF PROLONGED BLEACHING ON THE TISSUE BIOMASS AND REPRODUCTION OF THE REEF CORAL MONTASTREA-ANNULARIS. *Coral reefs, 8*(4), 217-224. doi:10.1007/bf00265014

Takahashi, S., Yoshioka-Nishimura, M., Nanba, D., & Badger, M. R. (2013). Thermal Acclimation of the Symbiotic Alga Symbiodinium spp. Alleviates Photobleaching under Heat Stress. *Plant Physiology, 161*(1), 477-485. doi:10.1104/pp.112.207480

Tay, Y. C., Guest, J. R., Chou, L. M., & Todd, P. A. (2011). Vertical distribution and settlement competencies in broadcast spawning coral larvae: Implications for dispersal models. *Journal of Experimental Marine Biology and Ecology, 409*(1-2), 324-330. doi:10.1016/j.jembe.2011.09.013

Usdowski, H. E. (1968). The Formation of Dolomite in Sediments. pp. 21–32 in Recent Developments in Carbonate Sedimentology in Central Europe. Müller G & Friedman G M, eds. *Springer-Verlag, Berlin*.

van Oppen, M. J. H., Oliver, J. K., Putnam, H. M., & Gates, R. D. (2015). Building coral reef resilience through assisted evolution. *Proceedings of the National Academy of Sciences of the United States of America, 112*(8), 2307-2313. doi:10.1073/pnas.1422301112

van Woesik, R., Sakai, K., Ganase, A., & Loya, Y. (2011). Revisiting the winners and the losers a decade after coral bleaching. *Marine Ecology Progress Series, 434*, 67-76. doi:10.3354/meps09203

Venn, A. A., Tambutte, E., Holcomb, M., Laurent, J., Allemand, D., & Tambutte, S. (2013). Impact of seawater acidification on pH at the tissue-skeleton interface and calcification in reef corals. *Proceedings of the National Academy of Sciences of the United States of America, 110*(5), 1634-1639. doi:10.1073/pnas.1216153110

Viyakarn, V., Lalitpattarakit, W., Chinfak, N., Jandang, S., Kuanui, P., Khokiattiwong, S., & Chavanich, S. (2015). Effect of lower pH on settlement and development of coral, Pocillopora damicornis (Linnaeus, 1758). *Ocean Science Journal, 50*(2), 475-480. doi:10.1007/s12601-015-0043-z

Wall, C. B., & Edmunds, P. J. (2013). In Situ Effects of Low pH and Elevated HCO3− on Juvenile Massive Porites spp. in Moorea, French Polynesia. *The Biological Bulletin, 225*(2), 92-101.

Wall, C. B., Fan, T. Y., & Edmunds, P. J. (2014). Ocean acidification has no effect on thermal bleaching in the coral Seriatopora caliendrum. *Coral reefs, 33*(1), 119-130. doi:10.1007/s00338-013-1085-2

Ward, S. (1992). EVIDENCE FOR BROADCAST SPAWNING AS WELL AS BROODING IN THE SCLERACTINIAN CORAL POCILLOPORA-DAMICORNIS. *Marine Biology, 112*(4), 641-646. doi:10.1007/bf00346182

Ward, S., Harrison, P., & Hoegh-Guldberg, O. (2002). *Coral bleaching reduces reproduction of scleractinian corals and increases susceptibility to future stress*.

Webster, N. S., Uthicke, S., Botte, E. S., Flores, F., & Negri, A. P. (2013). Ocean acidification reduces induction of coral settlement by crustose coralline algae. *Global Change Biology, 19*(1), 303-315. doi:10.1111/gcb.12008

Wernberg, T., Smale, D. A., & Thomsen, M. S. (2012). A decade of climate change experiments on marine organisms: procedures, patterns and problems. *Global Change Biology, 18*(5), 1491-1498. doi:10.1111/j.1365-2486.2012.02656.x

Winkler, N. S., Pandolfi, J. M., & Sampayo, E. M. (2015). Symbiodinium identity alters the temperature-dependent settlement behaviour of Acropora millepora coral larvae before the onset of symbiosis. *Proceedings of the Royal Society B-Biological Sciences, 282*(1801). doi:10.1098/rspb.2014.2260

Woolsey, E. S., Byrne, M., & Baird, A. H. (2013). The effects of temperature on embryonic development and larval survival in two scleractinian corals. *Marine Ecology Progress Series, 493*, 179-184. doi:10.3354/meps10499

Woolsey, E. S., Keith, S. A., Byrne, M., Schmidt-Roach, S., & Baird, A. H. (2015). Latitudinal variation in thermal tolerance thresholds of early life stages of corals. *Coral reefs, 34*(2), 471-478. doi:10.1007/s00338-014-1253-z

Yadav, S., Rathod, P., Alcoverro, T., & Arthur, R. (2016). "Choice" and destiny: the substrate composition and mechanical stability of settlement structures can mediate coral recruit fate in post-bleached reefs. *Coral reefs, 35*(1), 211-222. doi:10.1007/s00338-015-1358-z

Yakovleva, I. M., Baird, A. H., Yamamoto, H. H., Bhagooli, R., Nonaka, M., & Hidaka, M. (2009). Algal symbionts increase oxidative damage and death in coral larvae at high temperatures. *Marine Ecology Progress Series, 378*, 105-112. doi:10.3354/meps07857

Yeo, B. H. (2004). The recreational benefits of coral reefs: A case study of Pulau Payar Marine Park, Kedah, Malaysia. *Economic valuation and policy priorities for sustainable management of coral reefs*, 108-117. doi:10.5539/jsd.v2n2p95

Yost, D. M., Wang, L.-H., Fan, T.-Y., Chen, C.-S., Lee, R. W., Sogin, E., & Gates, R. D. (2013). Diversity in skeletal architecture influences biological heterogeneity and Symbiodinium habitat in corals. *Zoology, 116*(5), 262-269. doi:http://dx.doi.org/10.1016/j.zool.2013.06.001

Zeebe, R. E., & Wolf-Gladrow, D. A. (2001). CO2 in seawater: equilibrium, kinetics, isotopes (Vol. 65). Gulf Professional Publishing. *Gulf Professional Publishing, 65*.

Supplementary material

Table S1: Description of independent variables with statistical properties, brief explanation and group specific subsamples.

Variable	*Type*	*Description*	*Classes*
Family	Categorical	Coral family of study organism	*Acroporidae, Agariciidae, Astrocoeniidae, Caryophylliidae, Dendrophylliidae, Faviidae, Oculinidae, Pocilloporidae, Poritidae, Rhizangiidae, Siderastreidae*
Reproduction	Dichotomous	Reproductive mode	*Broadcast spawners, Brooders*
Sexuality	Categorical	Type of sexuality	*Gonochoric, Hermaphroditic, Mixed*
Skeleton	Dichotomous	Porosity of CaCO3 secreted	*Perforate, Imperforate*
Growth form	Categorical	Shape of coral growth	*Branching, Encrusting, Folacious, Massive, Solitary*
Growth rate	Dichotomous	Speed of coral growth	*Fast, Slow*
Symbionts	Dichotomous	Presence of symbionts	*Yes, No*
Shore distance	Dichotomous	Proximity to next populated shore	*Nearshore, Offshore*
Size	Ordinal	Size of individual coral fragments	*Small, Medium, Large (as described by author)*
Stage	Dichotomous	Life cycle stage of study organisms	*Adults, Juveniles*
Collection site	Categorical	Type of habitat at the collection site	*Back reef, Fore reef, Fringing reef, Patch reef, Reef flat, Lagoon, Open, Open bay, Deep, Aqaba*
Abiotic variability	Dichotomous	Describes the strength of natural pH/temperature variation at the collection site	*Stable, Variable*
Depth	Ordinal	Water depth at the collection site	*Very shallow (≤ 2 m), Shallow (2 – 15 m), Deep (16 – 100 m)*
Climate	Categorical	Climate at the collection site	*Tropical, Subtropical, Temperate*

Ocean	Categorical	Separation into common regions	*East Pacific, Indo-Pacific, Mediterranean, Red Sea,, East Atlantic, West Atlantic*
Duration	Ordinal	Duration of experiment	*Short (≤ 24 hours), Medium (25 – 168 hours), Long (169 – 720 hours), Very long (> 720 hours)*
Food	Dichotomous	Describes whether corals were fed during experiment	*Yes, No*
Filtration	Continuous	Describes whether seawater was filtered	*Yes, No*
Filter size I	Dichotomous	Describes whether seawater was filtered with 50 µm or less	*Yes, No*
Filter size II	Ordinal	Describes maximum size of plankton present in treatments	*Pico, Nano, Micro, Macro*
Measurement	Categorical	Type of measurement to quantify calcification	*Alkalinity anomaly, Buoyant weighing, Dry weight, Surface area*
Rate of increase	Ordinal	Speed of temperature increase experiences by study organisms	*Low (> 0.2˚C per day), Medium (0.2 - 2˚C per day), High (abrupt)*
Invasive collection	Dichotomous	Describes whether parent colonies were extracted from the field	*Yes, No*
Timing of larvae/ gamete release	Categorical	Describes when spawning occurred in relation to common peak time of the study organism	*Early, All, Late*
Substrate	Categorical	Type of substrate	*CCA, Well, Tile*
Tile conditioning	Categorical	Describes how tiles where conditioned	*Natural, Experimental, None*
Temperature	Dichotomous	Describes magnitude of temperature increase in experimental treatments	*Moderate (< 5˚C), Extreme (≥ 5˚C)*
pCO_2	Ordinal	Describes magnitude of pCO2 increase in experimental treatments	*Low (≤ 600 ppm), Medium (601 - 900 ppm), High (901 - 1350 ppm), Very high (> 1350 ppm)*

Table S2: Literature searches on ISI Web of Science 7 (Thomson Reuters) for articles published between 1965 and 2015 with number of articles returned for each set of keywords and total number of suitable articles.

Search	Keyword 1	Keyword 2	Keyword 3	No. of articles returned
1-1	Coral	Climate change	Larvae	175
1-2	Coral	Climate change	Reproduction	155
1-3	Coral	Climate change	Survival	278
1-4	Coral	Climate change	Settlement	171
1-5	Coral	Climate change	Metamorphosis	36
1-6	Coral	Climate change	Calcification	355
Combined				1170
2-1	Coral	Ocean acidification	Larvae	96
2-2	Coral	Ocean acidification	Reproduction	46
2-3	Coral	Ocean acidification	Survival	118
2-4	Coral	Ocean acidification	Settlement	74
2-5	Coral	Ocean acidification	Metamorphosis	27
2-6	Coral	Ocean acidification	Calcification	501
Combined				862
3-1	Coral	Ocean warming	Larvae	36
3-2	Coral	Ocean warming	Reproduction	37
3-3	Coral	Ocean warming	Survival	56
3-4	Coral	Ocean warming	Settlement	35
3-5	Coral	Ocean warming	Metamorphosis	8
3-6	Coral	Ocean warming	Calcification	124
Combined				296
Total number of articles returned (incl. duplicates)				2328
Articles with suitable measurements				100

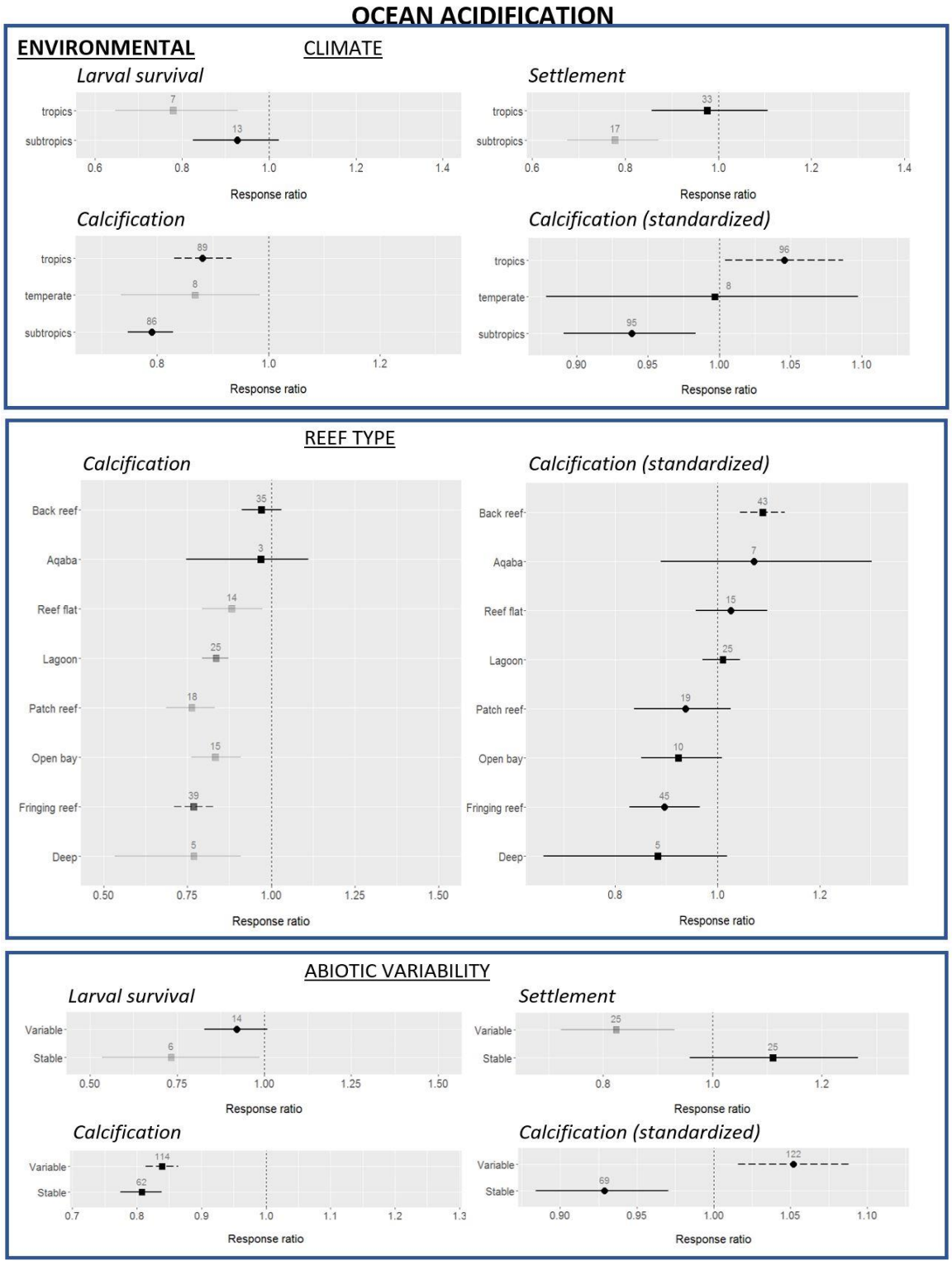

Figure S1: Effect sizes showing coral calcification response to ocean acidification, sorted by independent factorial variables. Data are weighted means ± 95% CI. Means were calculated using either *mixed effects* (circles) or *fixed effects* (squares) models. Confidence intervals were calculated using parametric methods (dashed lines) or bootstrapping (solid lines). Shown are percentage values using original data and deviation from expected mean responses using standardized data for calcification responses only (bottom right). Numbers are sample sizes and transparency represents sensitivity to publication bias.

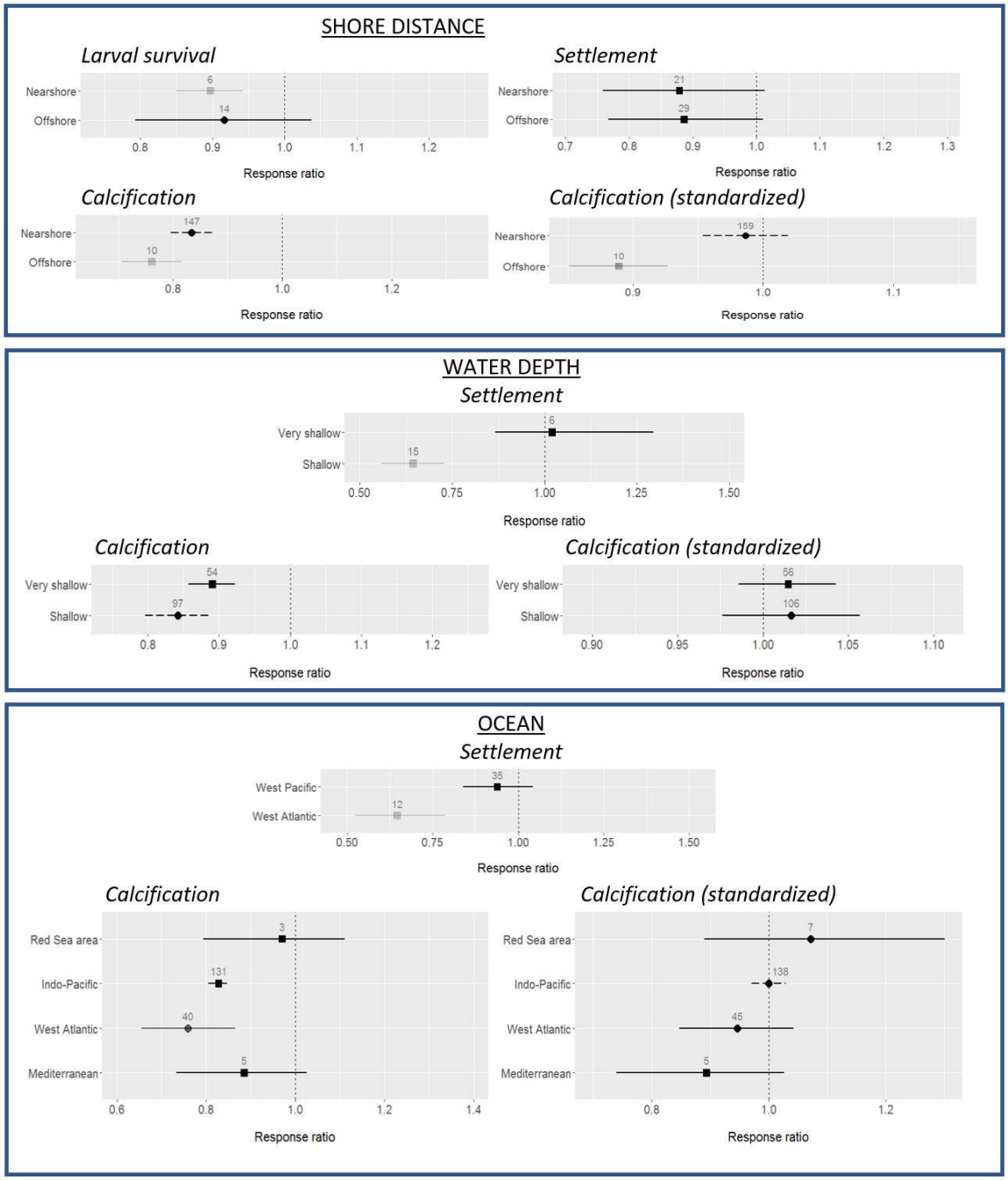

Figure S1 continued

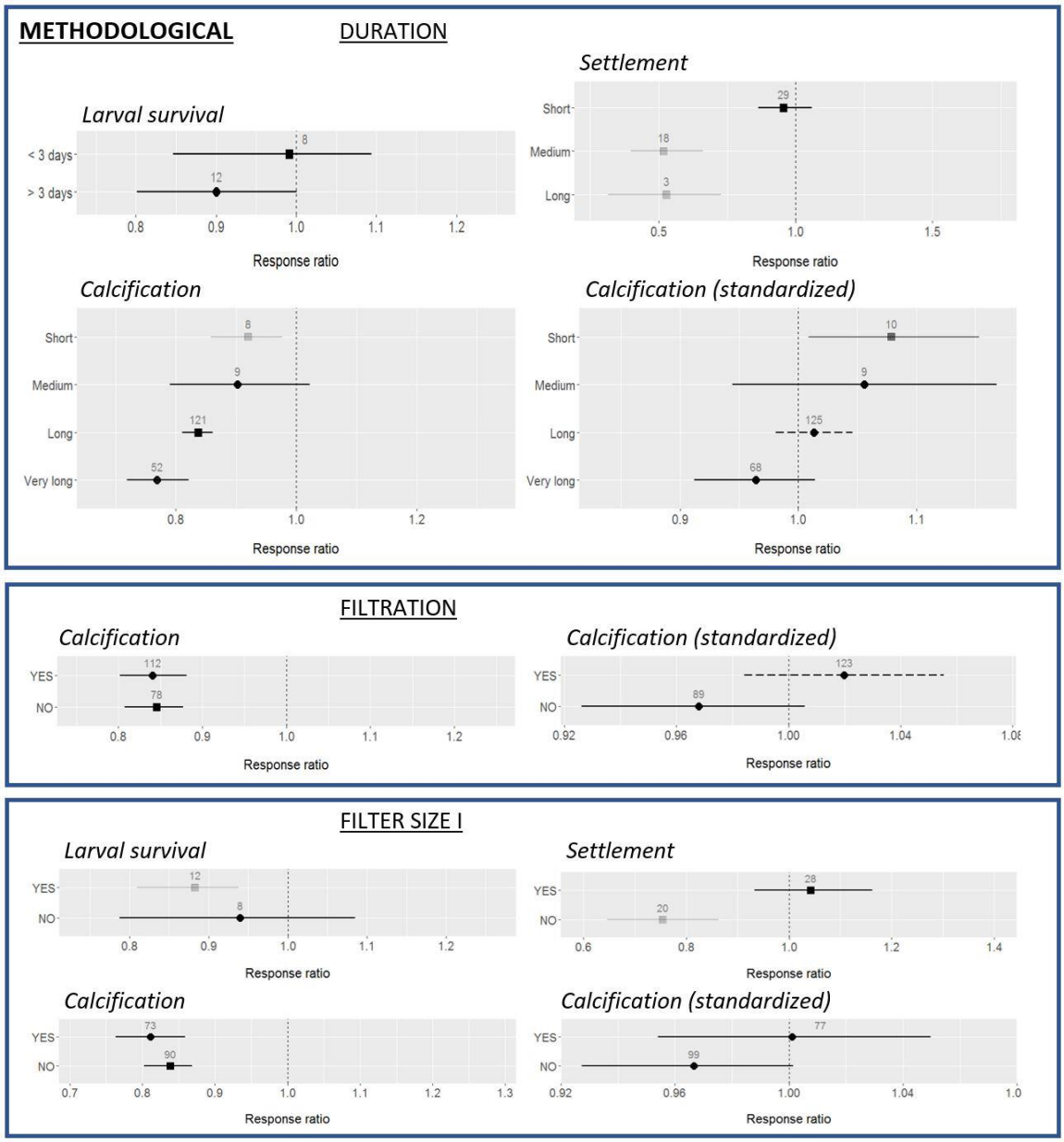

Figure S1 continued

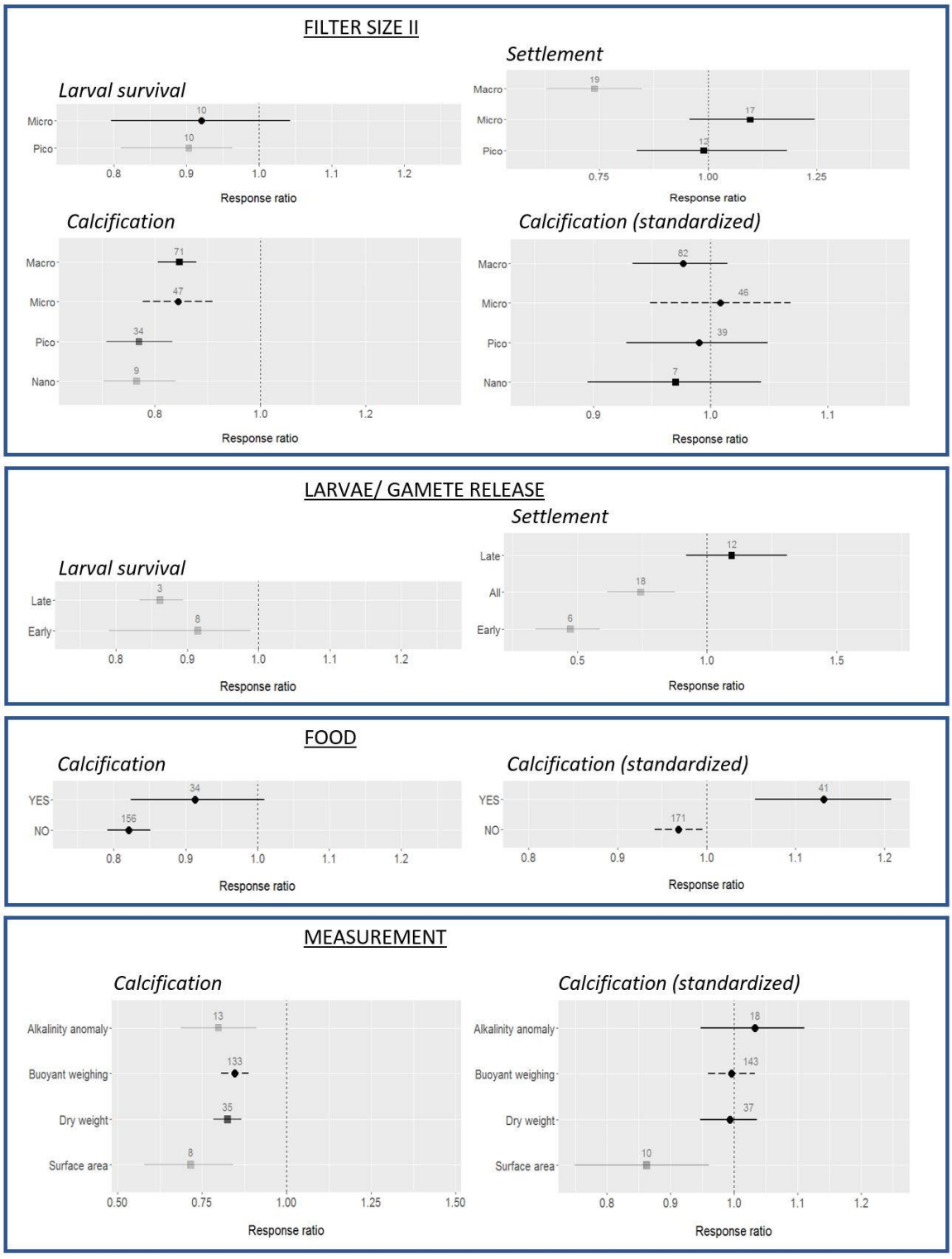

Figure S1 continued

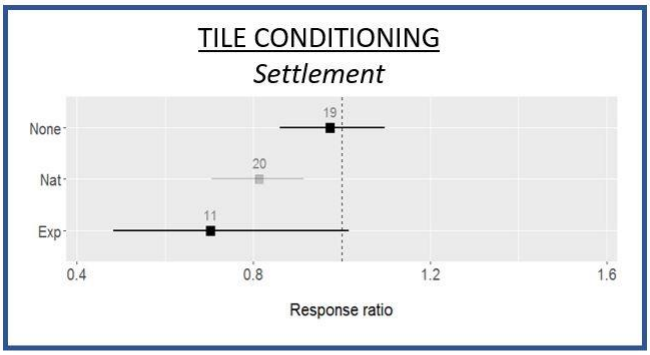

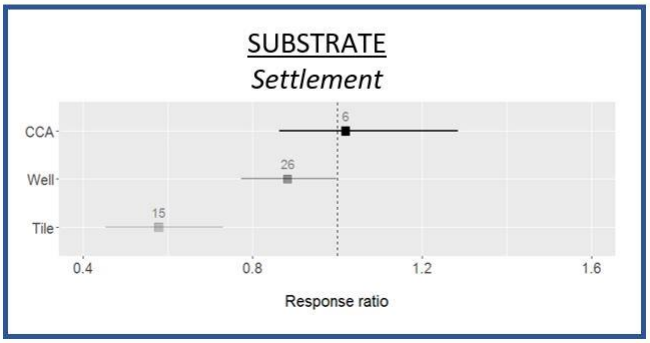

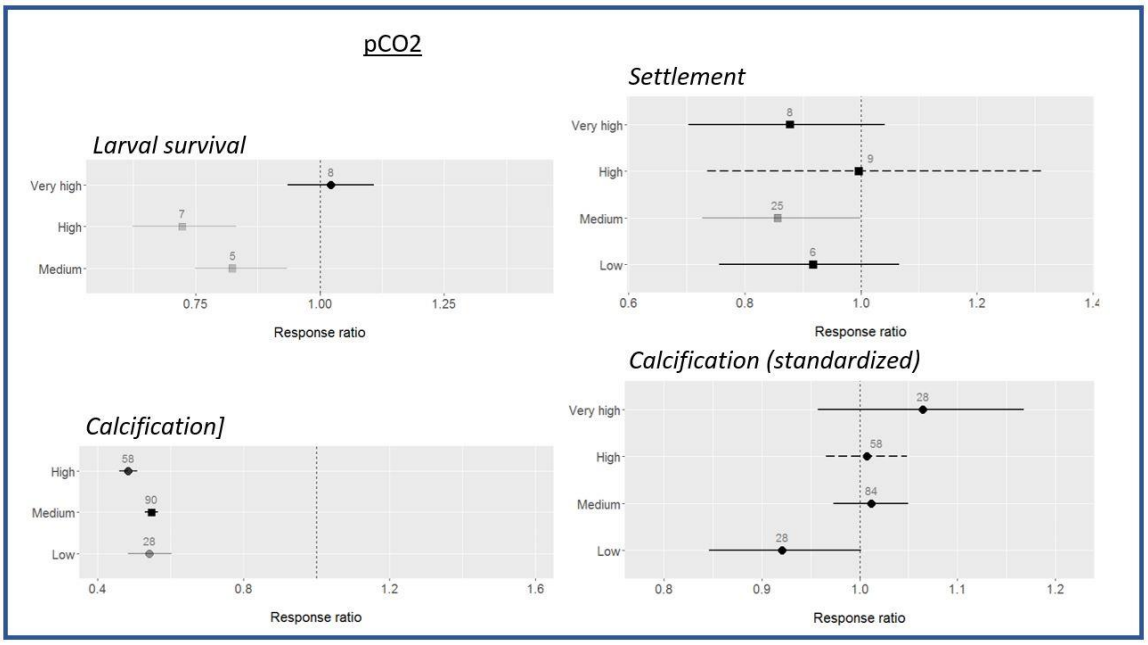

Figure S1 continued

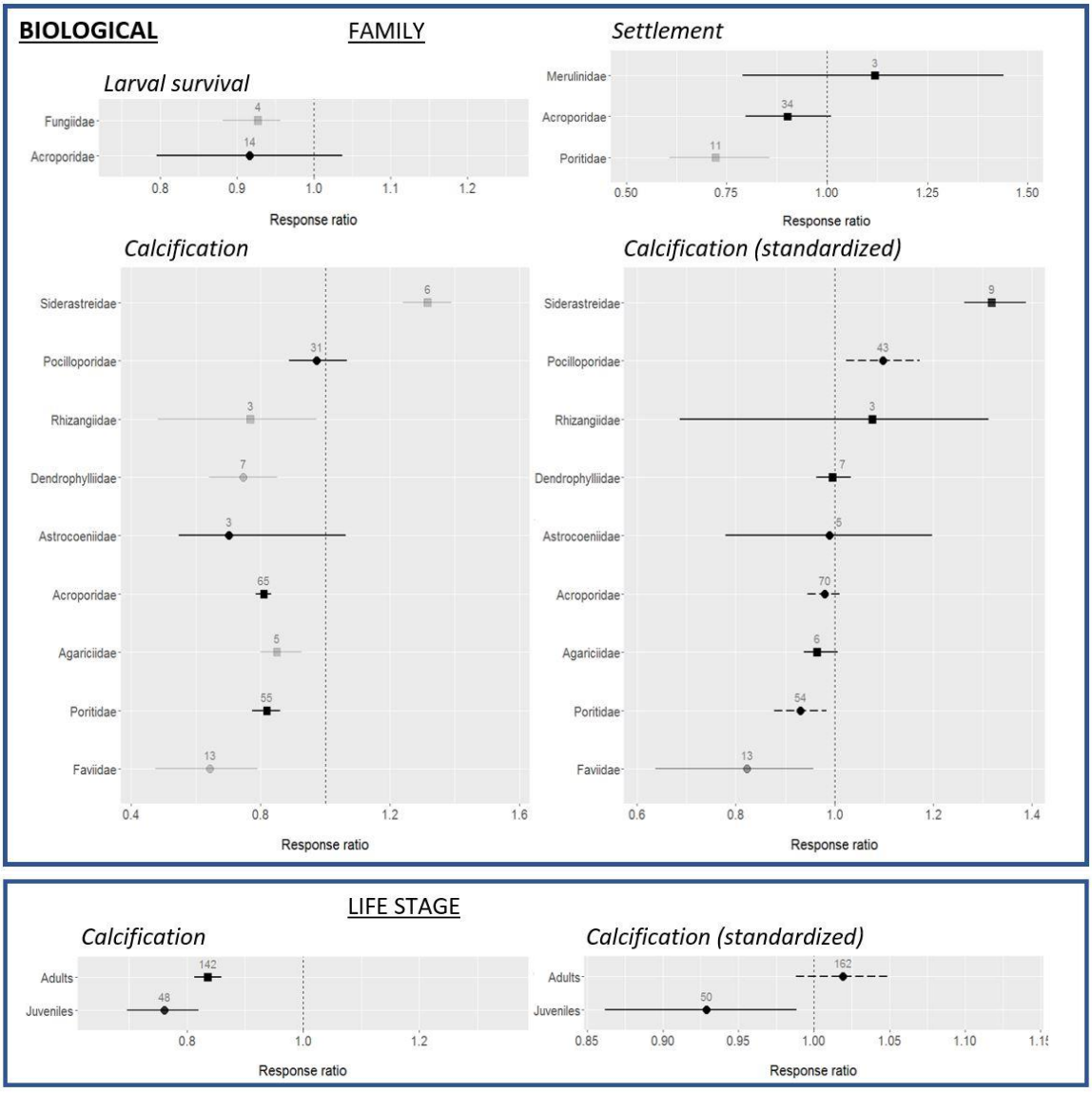

Figure S1 continued

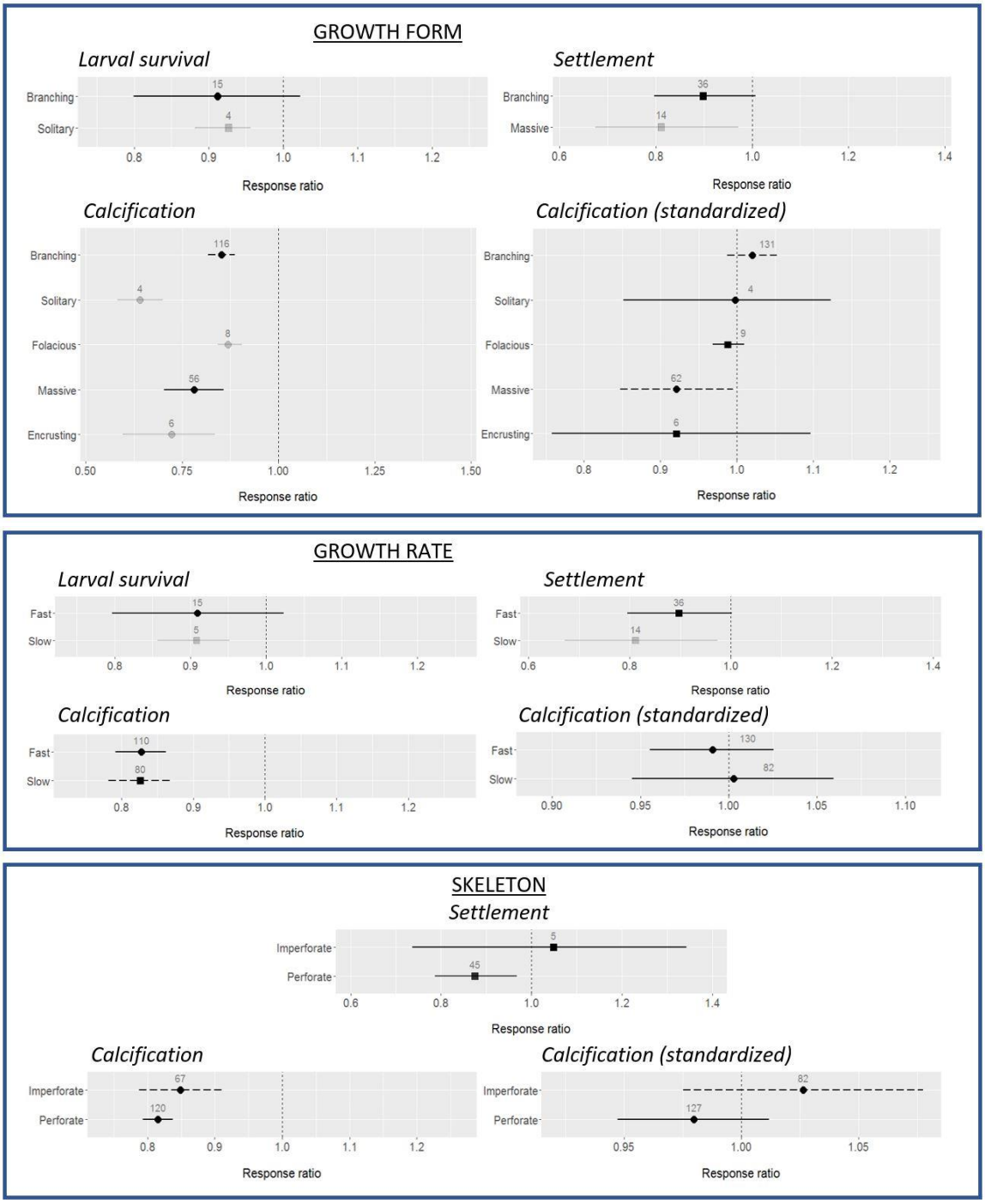

Figure S1 continued

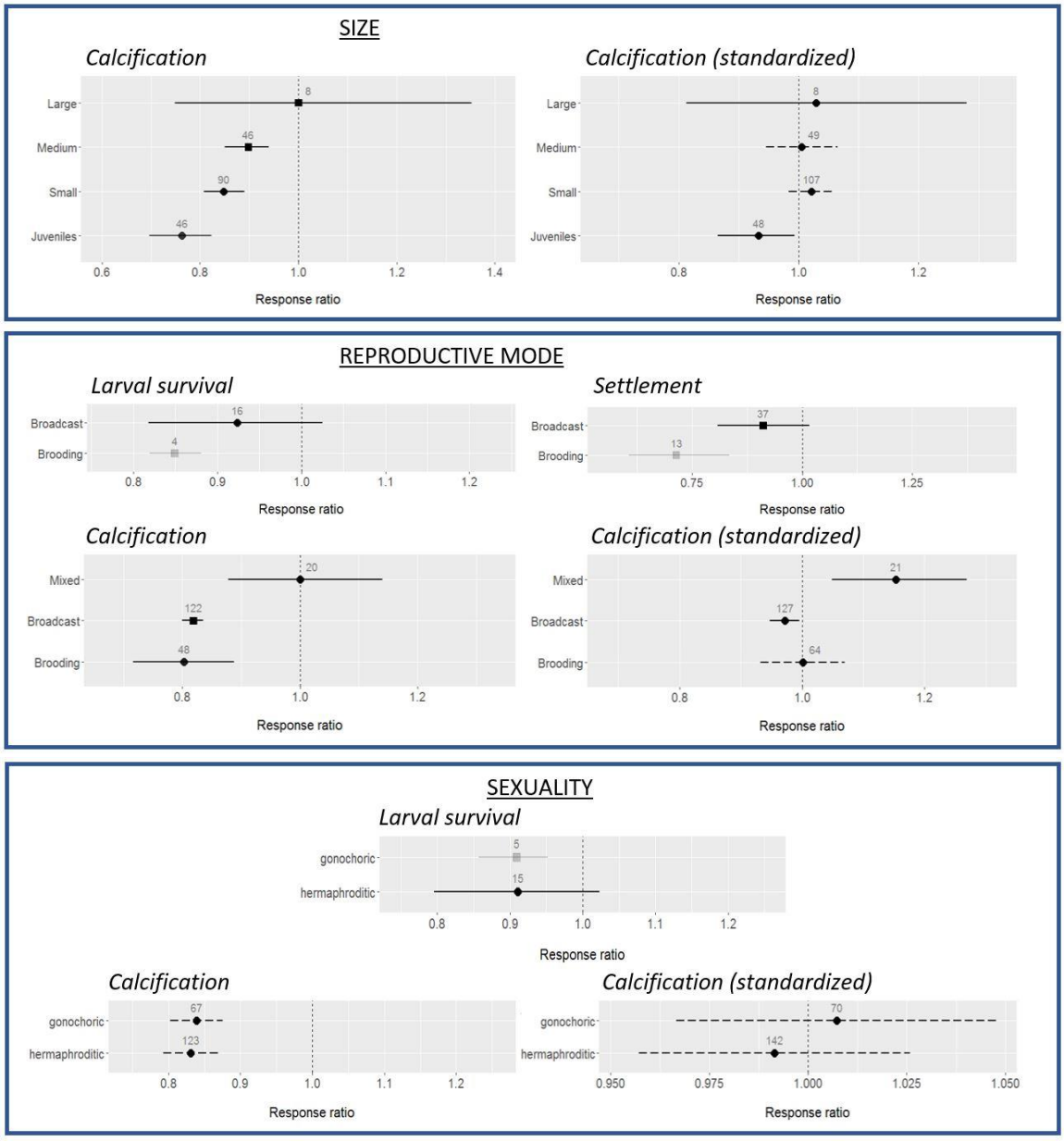

Figure S1 continued

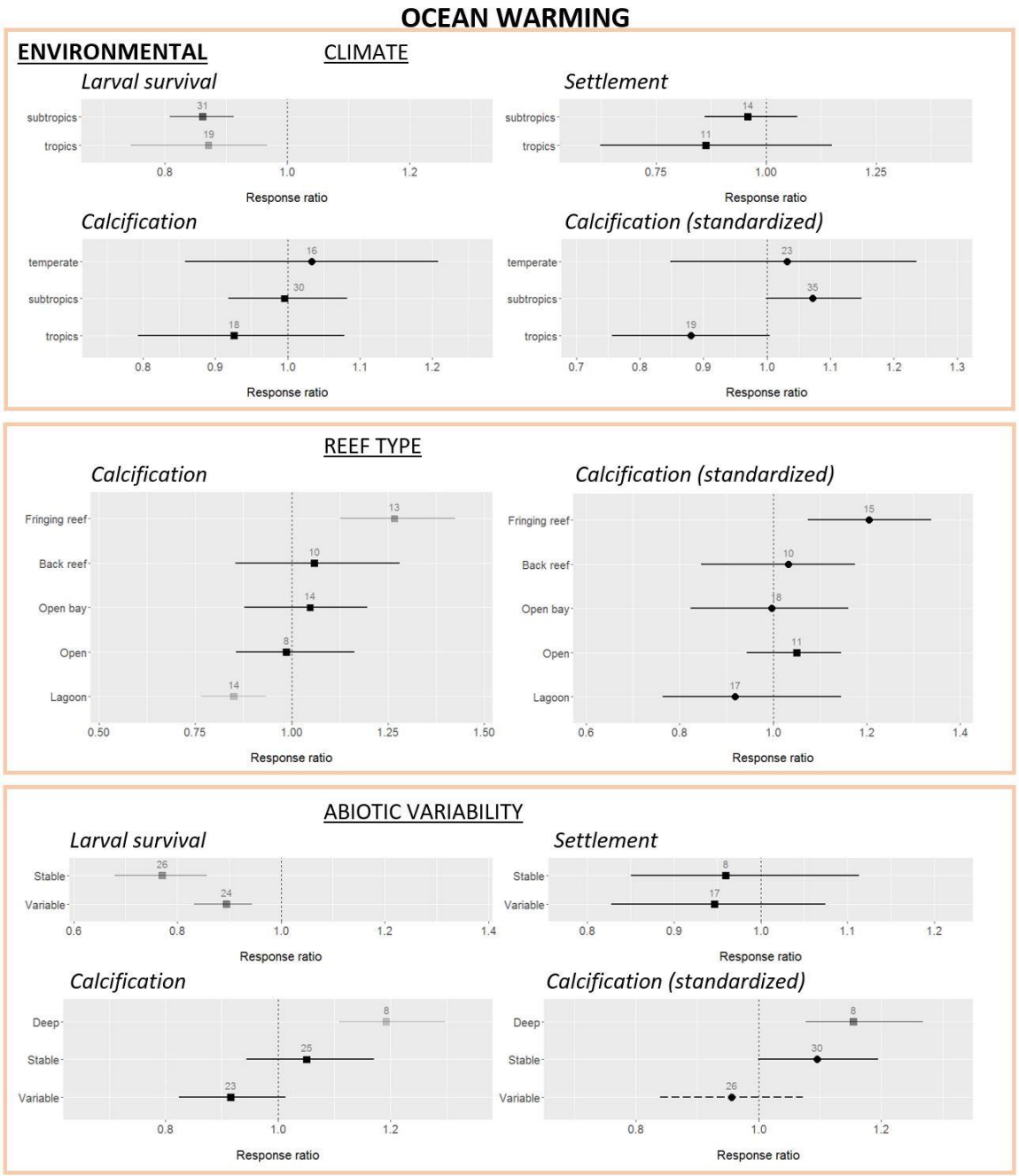

Figure S2: Effect sizes showing coral calcification response to ocean warming, sorted by independent factorial variables. Data are weighted means ± 95% CI. Means were calculated using either *mixed effects* (circles) or *fixed effects* (squares) models. Confidence intervals were calculated using parametric methods (dashed lines) or bootstrapping (solid lines). Shown are percentage values using original data and deviation from expected mean responses using standardized data for calcification responses only (bottom right). Numbers are sample sizes and transparency represents sensitivity to publication bias.

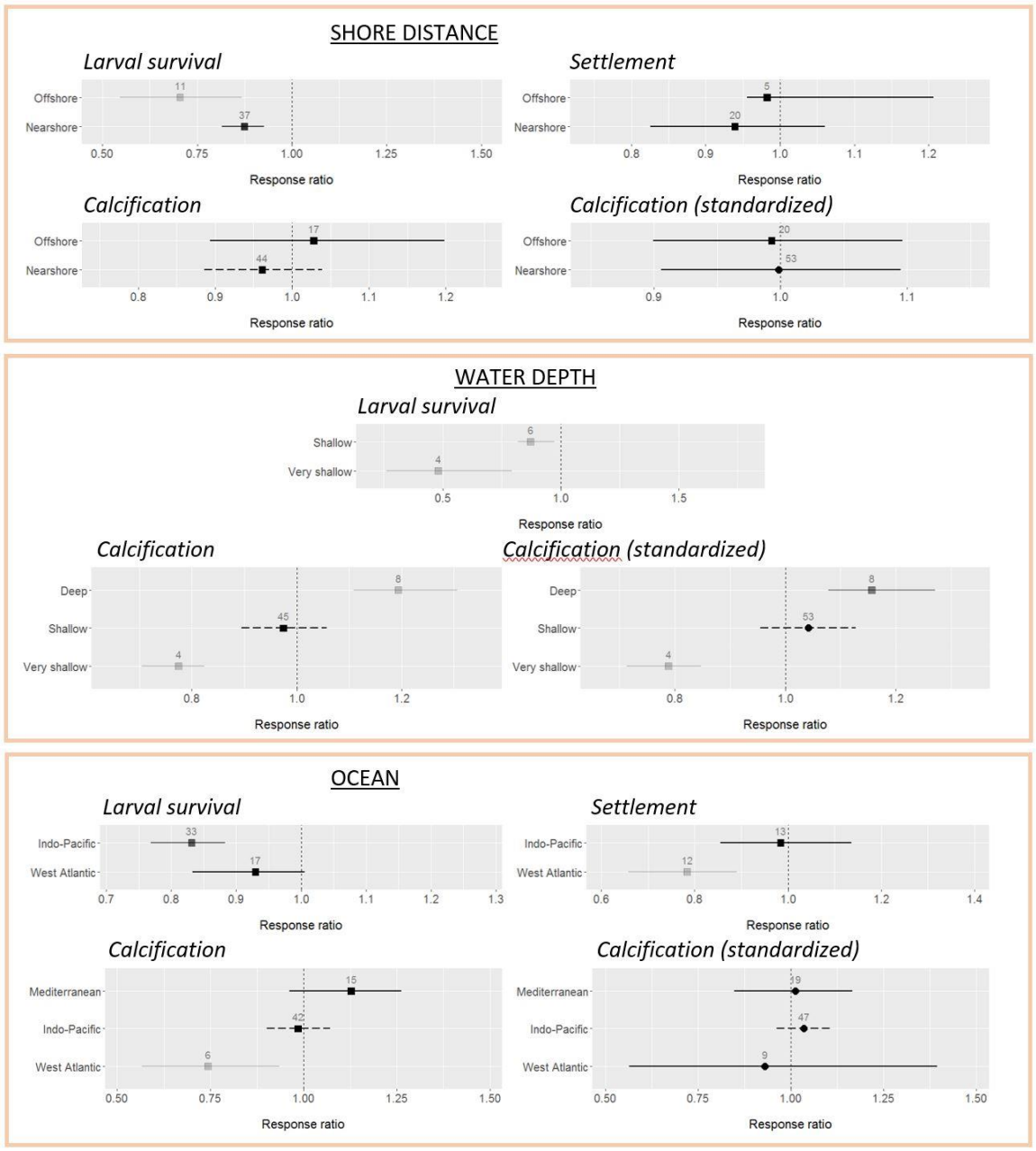

Figure S2 continued

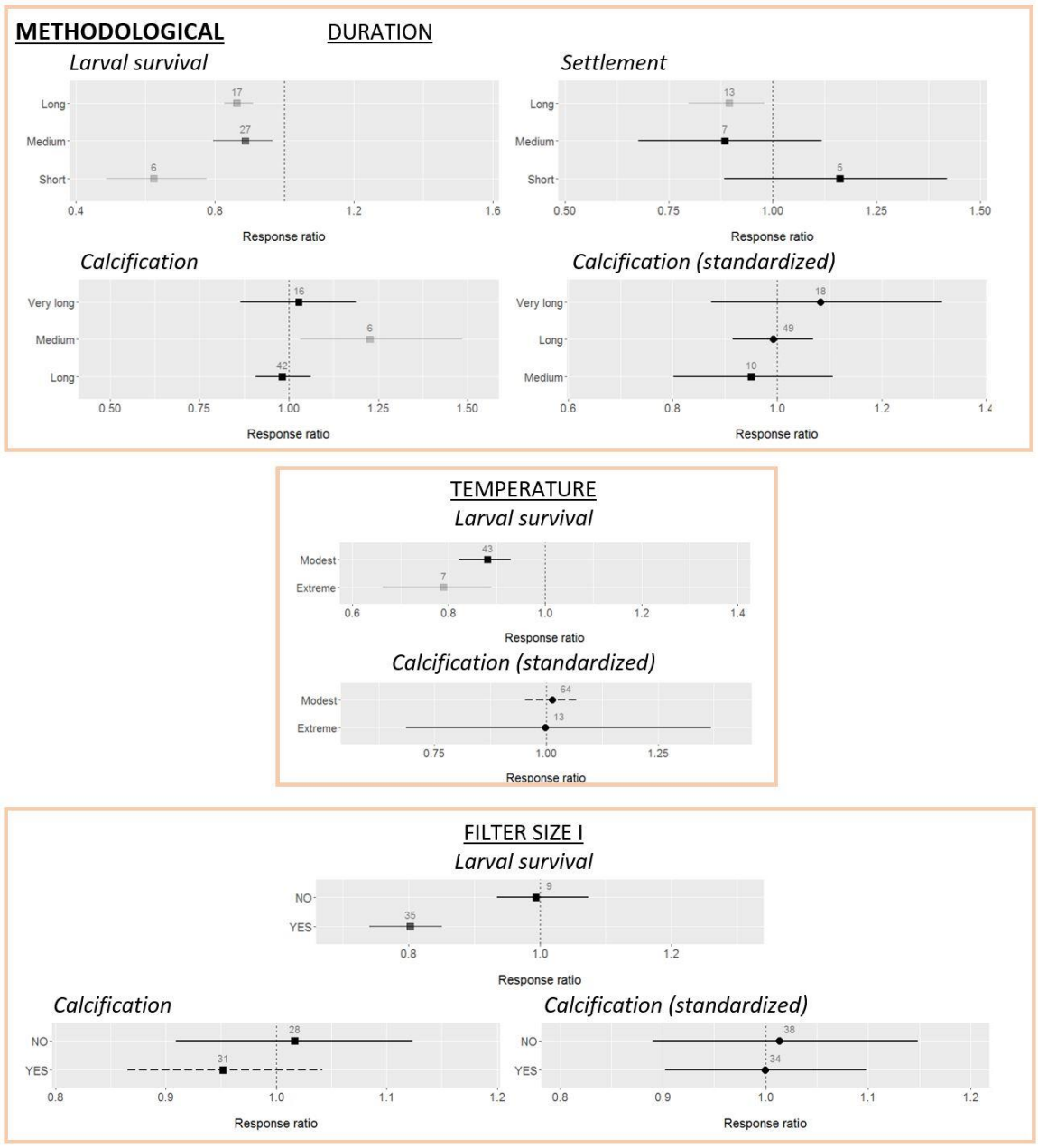

Figure S2 continued

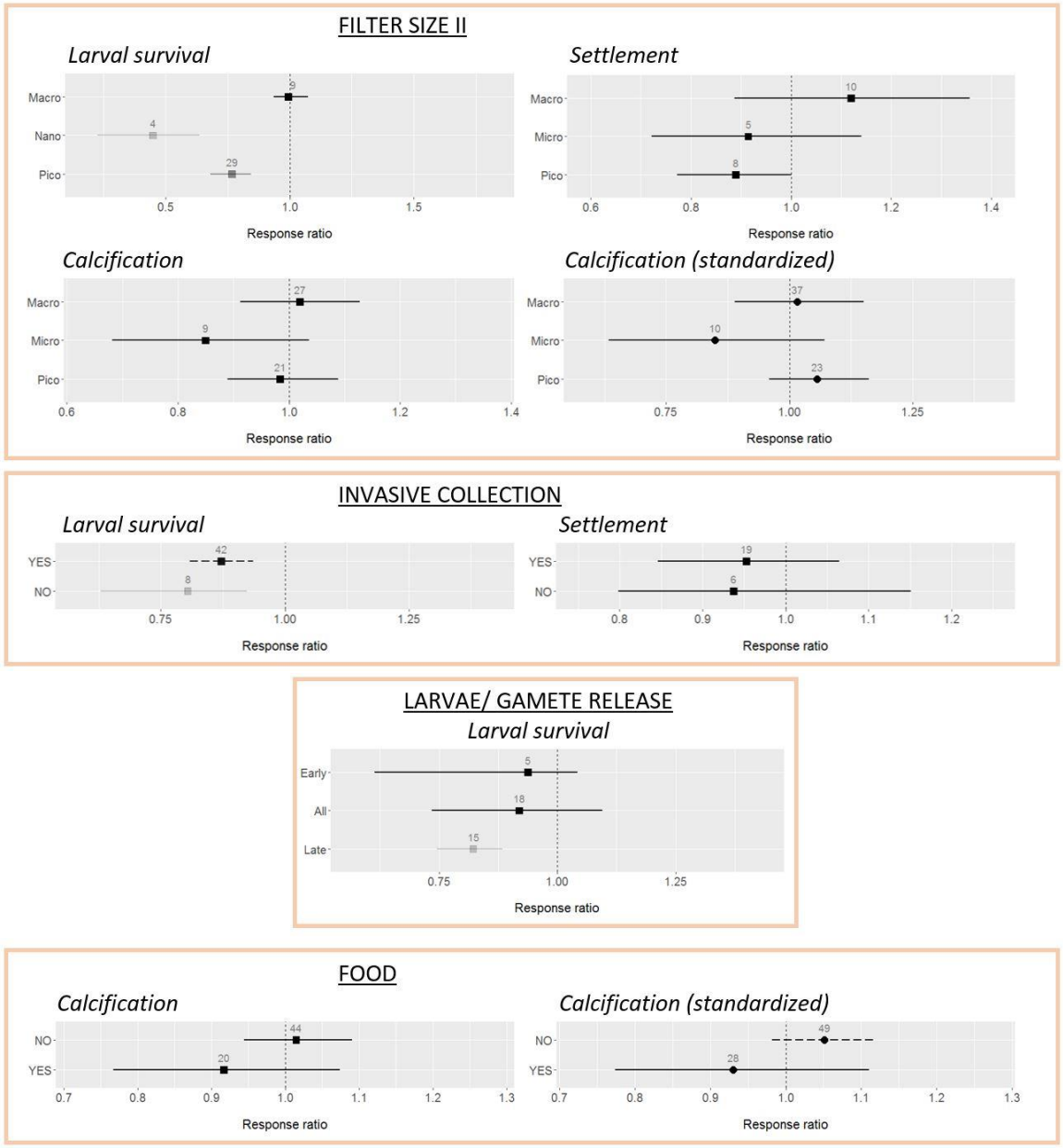

Figure S2 continued

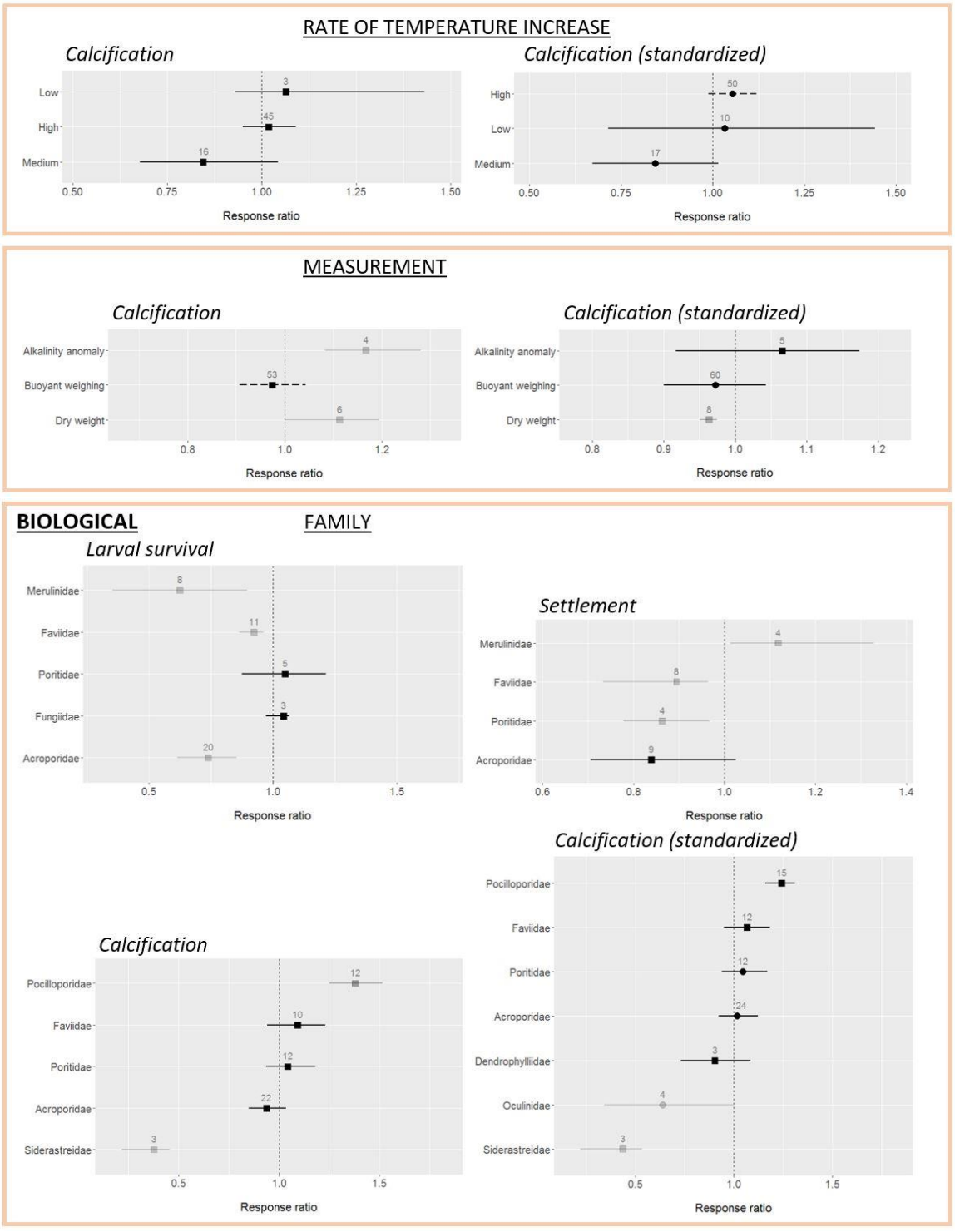

Figure S2 continued

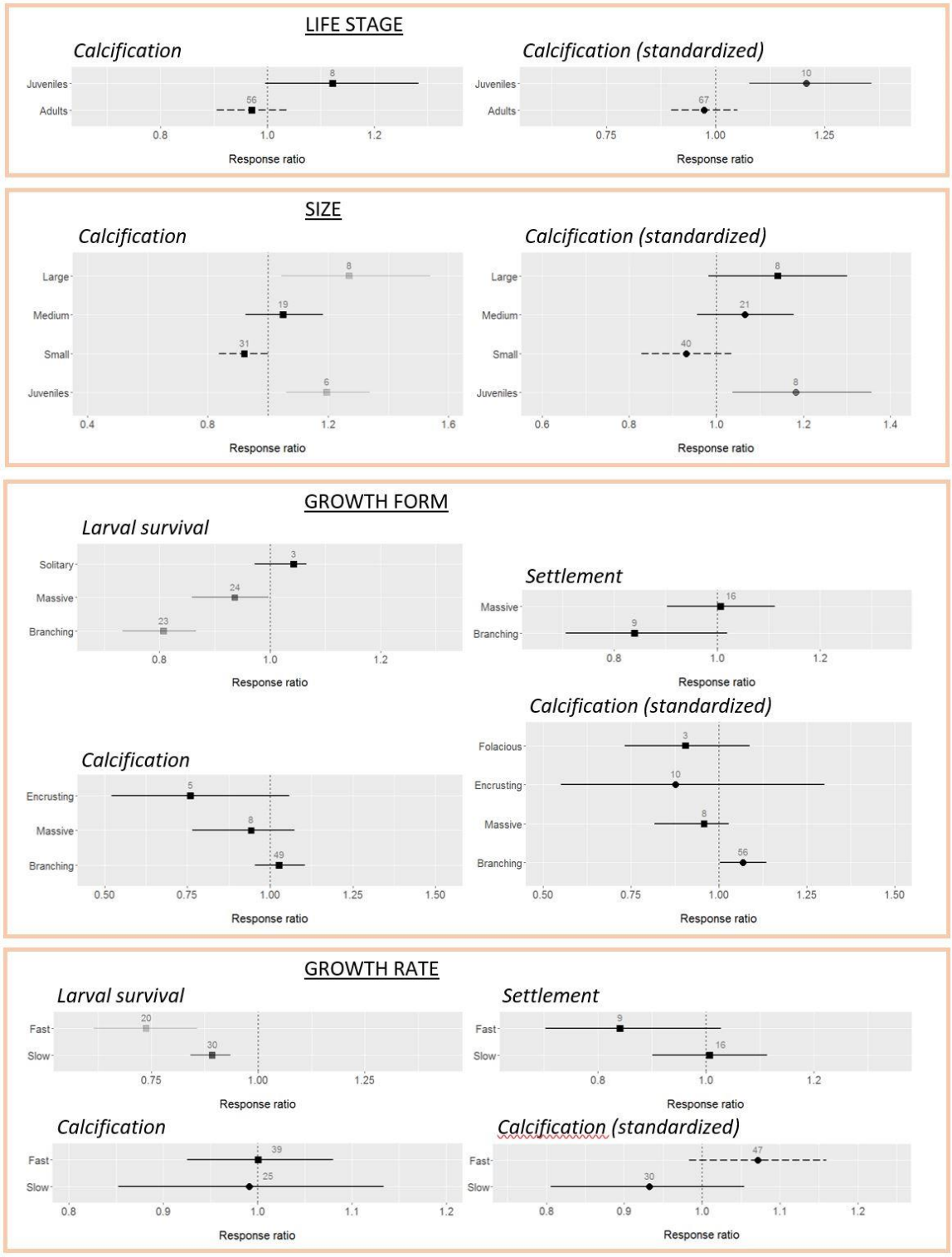

Figure S2 continued

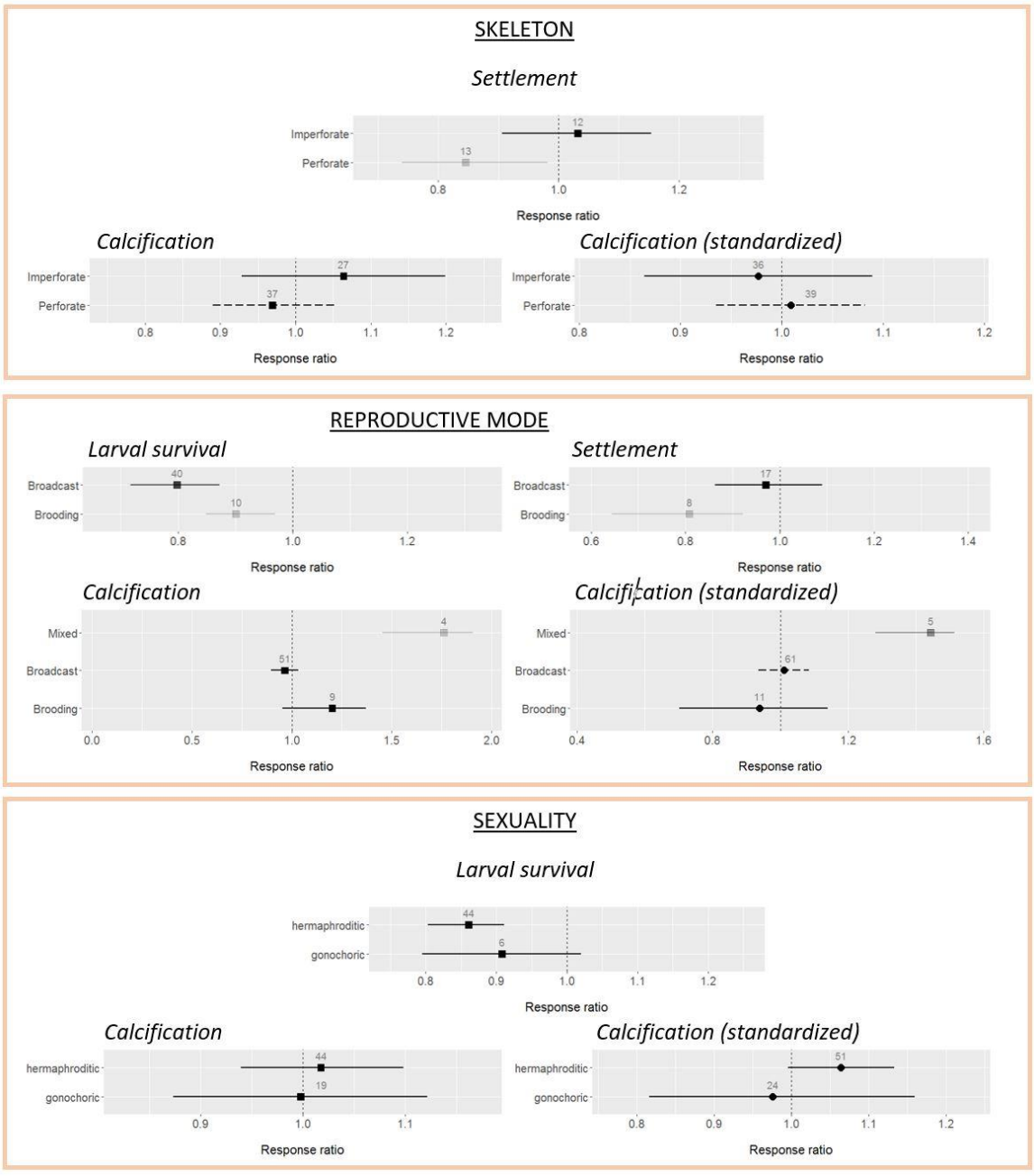

Figure S2 continued

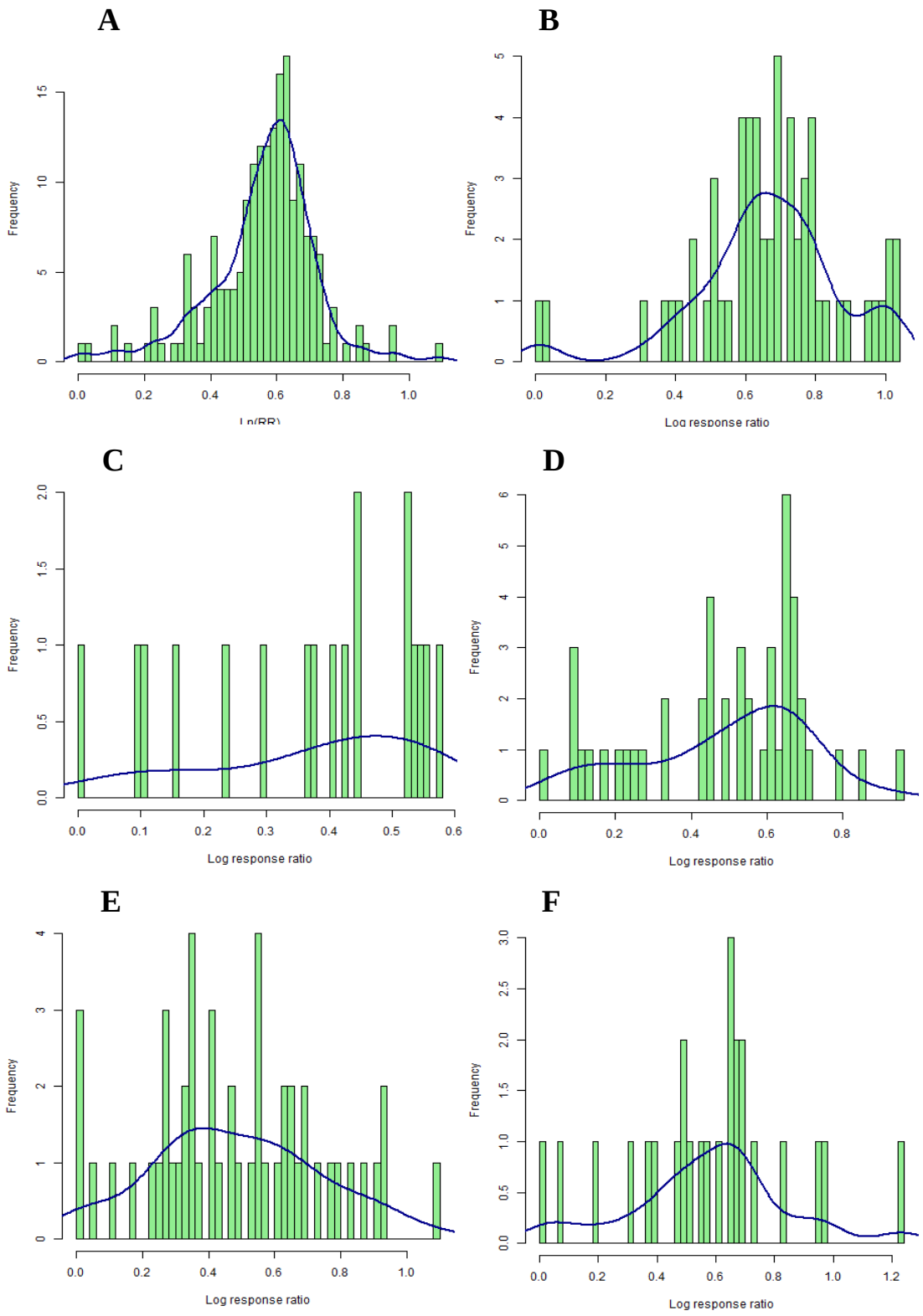

Figure S3: Frequency distributions of effect sizes for the different datasets. Shown are coral calcification responses to ocean acidification (A) and ocean warming (B), larval survival responses to ocean acidification (C) and ocean warming (D), and coral settlement responses to ocean acidification (E) and ocean warming (F).

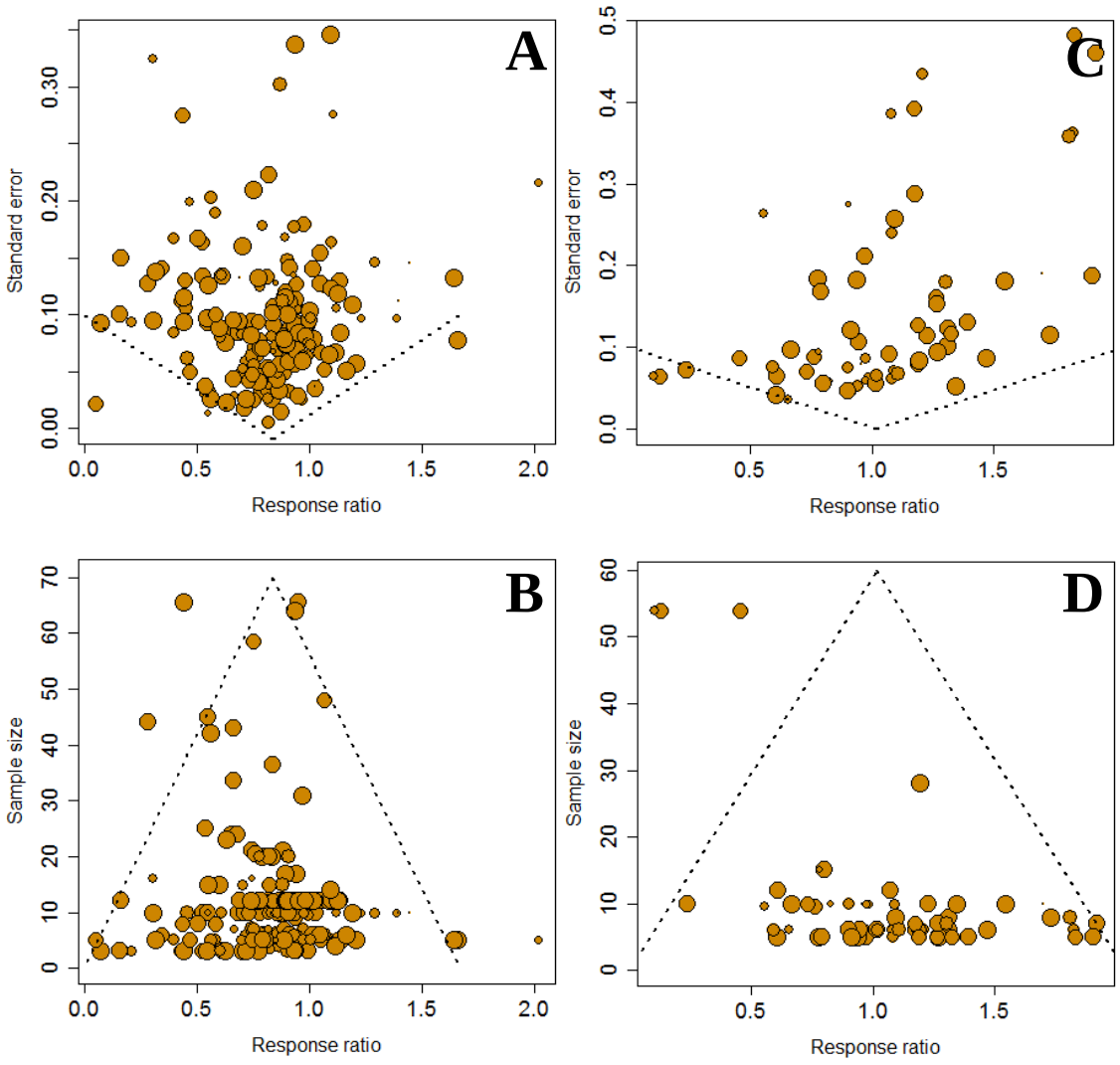

Figure S4: Funnel plots of effect sizes based on standard error (top) or sample size (bottom) for coral calcification responses to ocean acidification (A, B) and ocean warming (C, D). Point size represents precision of each estimate. Dashed lines were added to illustrate the expected 'funneling' towards the common mean with decreasing standard error and increasing sample size.

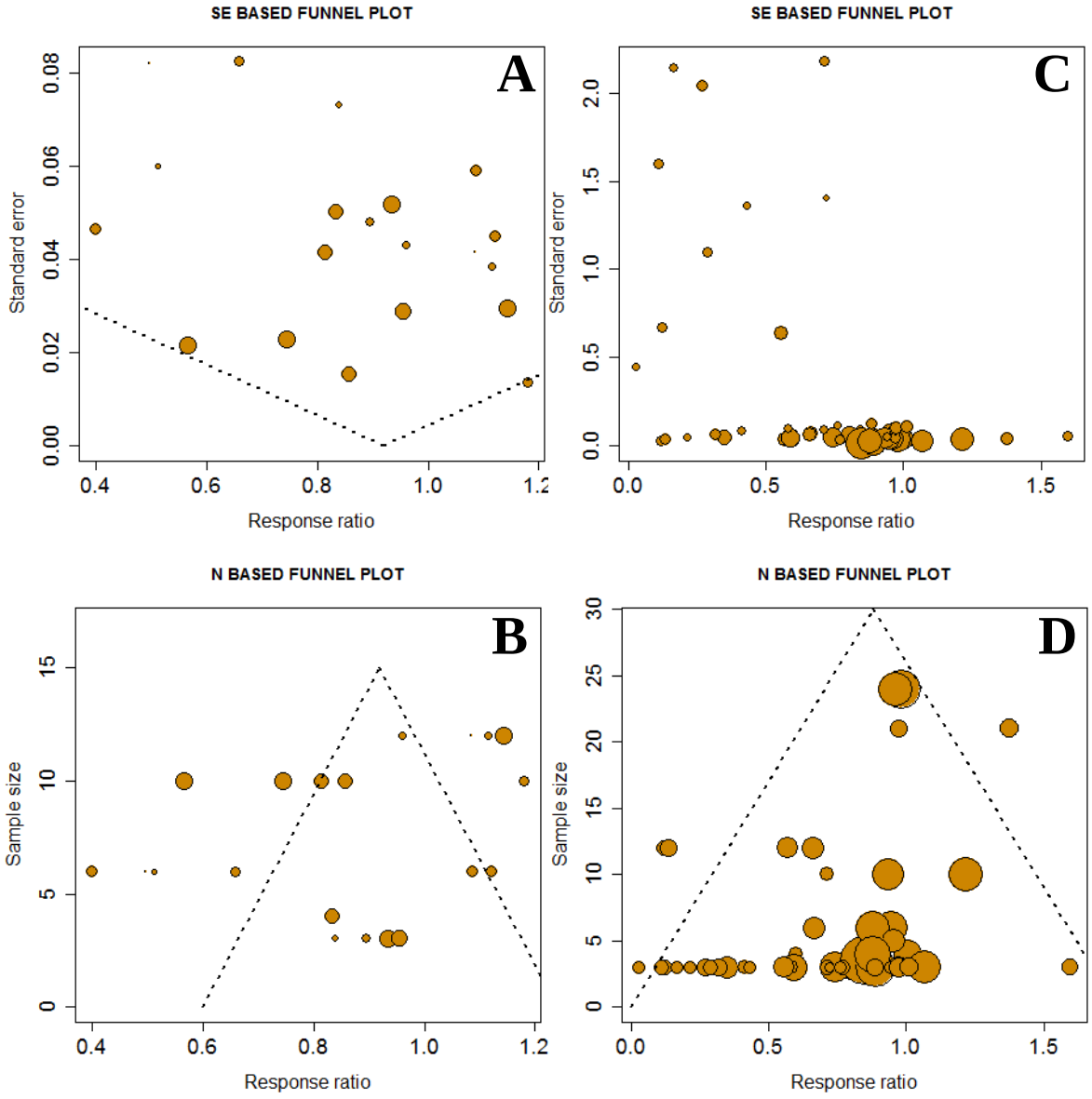

Figure S5: Funnel plots of effect sizes based on standard error (top) or sample size (bottom) for coral larval survival responses to ocean acidification (A, B) and ocean warming (C, D). Point size represents precision of each estimate. Dashed lines were added to illustrate the expected 'funneling' towards the common mean with decreasing standard error and increasing sample size.

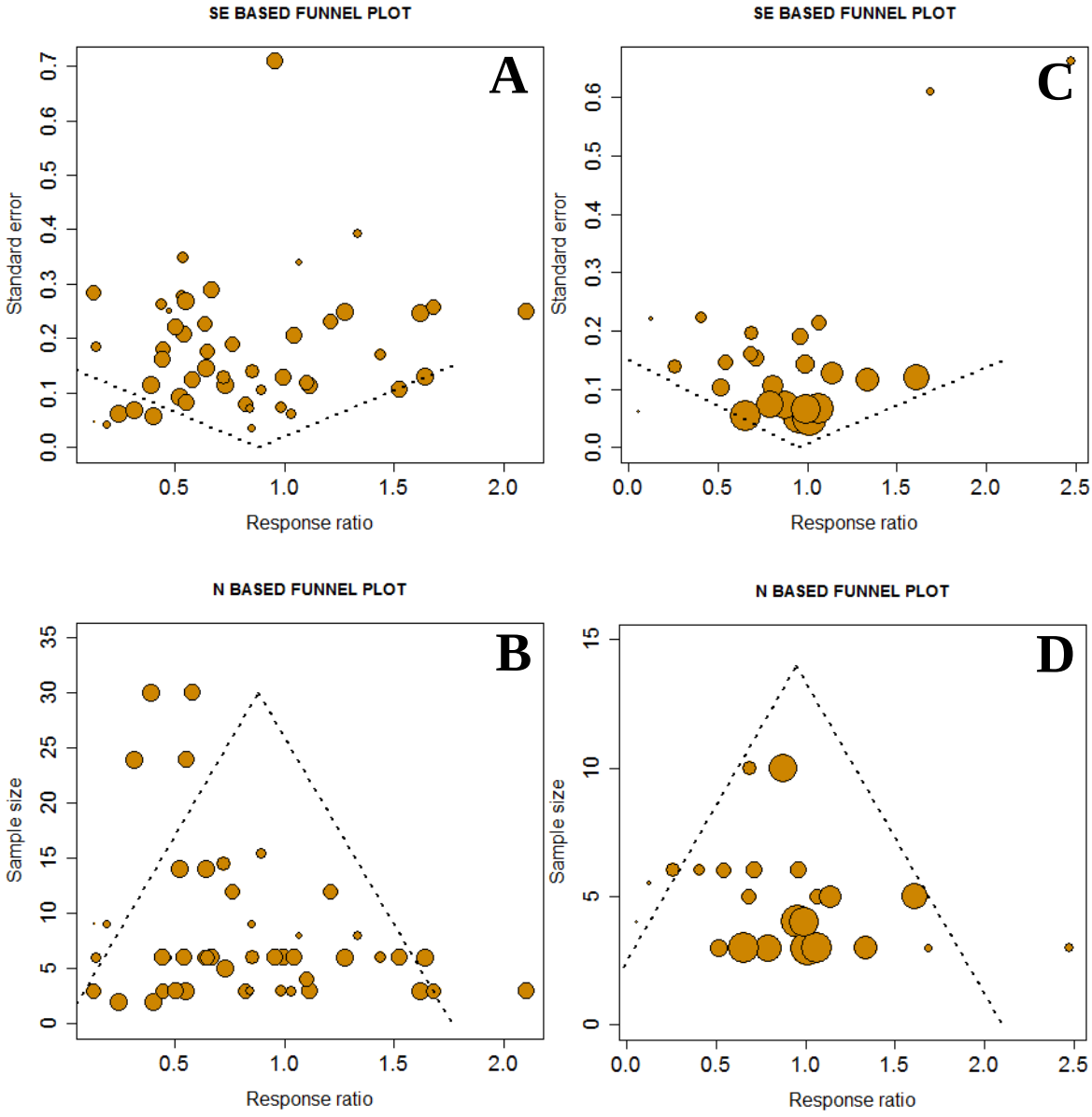

Figure S6: Funnel plots of effect sizes based on standard error (top) or sample size (bottom) for coral setlement responses to ocean acidification (A, B) and ocean warming (C, D). Point size represents precision of each estimate. Dashed lines were added to illustrate the expected 'funneling' towards the common mean with decreasing standard error and increasing sample size.

R Code

The code below provides an example of vector allocation to extract separate subsamples (here responses to ocean warming according to coral taxa). Only the first two taxa are shown. The code lines at the end are preset names, which the model uses to save outputs.

```
g1<-read.csv("T_Calcification_64.csv")

g2<-g1[!is.na(g1$Family),]
g2<-g2[-which(g2$Family=="Dendrophyllidae"),]
g2<-g2[-which(g2$Family=="insertae sedis"),]
g2<-g2[-which(g2$Family=="Oculinidae"),]
attach(g2)
X_con0<-g2$X_con
X_exp0<-g2$X_exp
SD_con0<-g2$SD_con
SD_exp0<-g2$SD_exp
N_con0<-g2$N_con
N_exp0<-g2$N_exp
RR0<-g2$RR
#group1
X_con1<-g2$X_con[g2$Family=="Acroporidae"]
X_exp1<-g2$X_exp[g2$Family=="Acroporidae"]
SD_con1<-g2$SD_con[g2$Family=="Acroporidae"]
SD_exp1<-g2$SD_exp[g2$Family=="Acroporidae"]
N_con1<-g2$N_con[g2$Family=="Acroporidae"]
N_exp1<-g2$N_exp[g2$Family=="Acroporidae"]
RR1<-g2$RR[g2$Family=="Acroporidae"]
#group2
X_con2<-g2$X_con[g2$Family=="Faviidae"]
X_exp2<-g2$X_exp[g2$Family=="Faviidae"]
SD_con2<-g2$SD_con[g2$Family=="Faviidae"]
SD_exp2<-g2$SD_exp[g2$Family=="Faviidae"]
N_con2<-g2$N_con[g2$Family=="Faviidae"]
N_exp2<-g2$N_exp[g2$Family=="Faviidae"]
RR2<-g2$RR[g2$Family=="Faviidae"]
Cat<-c()
Cat[1]<-paste("Total")
Cat[2]<-paste("Acroporidae")
Cat[3]<-paste("Faviidae")
Cat[4]<-paste("Pocilloporidae")
Cat[5]<-paste("Poritidae")
Cat[6]<-paste("Siderastreidae")
G<-length(Cat)#number of groups including total
n<-length(X_con0)
aa<-paste("ass_T_C_Family.xlsx")
Ana<-paste("T_Calcification_")
bb<-paste("T_C_Family_boot.xlsx")
cc<-paste("T_C_Family_para.xlsx")
dd<-paste("diff_T_C_Family_para.xlsx")
```

The code below transforms the data vectors of individual subsamples, creates frequency distributions and QQ-plots, and evaluates basic assumptions (normality, skewness, kurtosis, percentage of precise estimates). Output is generated as excel file named 'Assumptions'. Maximum number of subsamples per categorization was 11, so all computations are repeated 11 times, each time using a different vector that incorporates data of a specific subsample. If fewer than 11 subsamples are compared, the access code is not applied since R does not find the specific vectors.

```
install.packages("ggplot2")
install.packages("xlsx")
install.packages("R.basic")
install.packages("doBy")
install.packages("lme4")
install.packages("lmtest")
install.packages("lsmeans")
install.packages("bear")
library(R.basic)
library(xlsx)
library(ggplot2)
library(doBy)
library(lme4)
library(lattice)
library(lmtest)
library(lsmeans)
library(bear)

#obtain sample size and transformation parameter
n0<-length(X_con0)
n1<-length(X_con1)
n2<-length(X_con2)
n3<-length(X_con3)
n4<-length(X_con4)
n5<-length(X_con5)
n6<-length(X_con6)
n7<-length(X_con7)
n8<-length(X_con8)
n9<-length(X_con9)
n10<-length(X_con10)
n11<-length(X_con11)
ns<-c(n0, n1, n2)
ns<-c(n0, n1, n2, n3)
ns<-c(n0, n1, n2, n3, n4)
ns<-c(n0, n1, n2, n3, n4, n5)
ns<-c(n0, n1, n2, n3, n4, n5, n6)
ns<-c(n0, n1, n2, n3, n4, n5, n6, n7)
ns<-c(n0, n1, n2, n3, n4, n5, n6, n7, n8)
ns<-c(n0, n1, n2, n3, n4, n5, n6, n7, n8, n9)
ns<-c(n0, n1, n2, n3, n4, n5, n6, n7, n8, n9, n10)
ns<-c(n0, n1, n2, n3, n4, n5, n6, n7, n8, n9, n10, n11)

RR<-numeric(length(X_con0))
N<-length(X_con0)
```

```
for(i in 1:N){
  RR[i]<-X_exp[i]/X_con[i]
}
RRmin<-min(RR)
C<-1-RRmin

#data transformation
trans<-function(X_con, X_exp, SD_con, SD_exp, N_con, N_exp){
  RR<-c()
  LogRR<-c()
  N<-length(X_con)
  for(i in 1:N){
    RR[i]<-X_exp[i]/X_con[i]
  }
  for(i in 1:N){
    LogRR[i]<-log(RR[i]+C)
  }
  return(LogRR)
}

LogRR0<-trans(X_con0, X_exp0, SD_con0, SD_exp0, N_con0, N_exp0)
LogRR1<-trans(X_con1, X_exp1, SD_con1, SD_exp1, N_con1, N_exp1)
LogRR2<-trans(X_con2, X_exp2, SD_con2, SD_exp2, N_con2, N_exp2)
LogRR3<-trans(X_con3, X_exp3, SD_con3, SD_exp3, N_con3, N_exp3)
LogRR4<-trans(X_con4, X_exp4, SD_con4, SD_exp4, N_con4, N_exp4)
LogRR5<-trans(X_con5, X_exp5, SD_con5, SD_exp5, N_con5, N_exp5)
LogRR6<-trans(X_con6, X_exp6, SD_con6, SD_exp6, N_con6, N_exp6)
LogRR7<-trans(X_con7, X_exp7, SD_con7, SD_exp7, N_con7, N_exp7)
LogRR8<-trans(X_con8, X_exp8, SD_con8, SD_exp8, N_con8, N_exp8)
LogRR9<-trans(X_con9, X_exp9, SD_con9, SD_exp9, N_con9, N_exp9)
LogRR10<-trans(X_con10, X_exp10, SD_con10, SD_exp10, N_con10, N_exp10)
LogRR11<-trans(X_con11, X_exp11, SD_con11, SD_exp11, N_con11, N_exp11)

#normality
qqnorm(LogRR0, main=Cat[1], col="darkred")
qqline(LogRR0, col="darkblue", lwd=2)
dev.copy(png, paste0("QQ_", Ana, Cat[1], ".png"))
dev.off()
hist0 <- hist(LogRR0, breaks=50, plot=FALSE)
mult0 <- hist0$counts / hist0$density
dens0 <- density(LogRR0)
dens0$y <- dens0$y * mult0[1]
plot(hist0, main=Cat[1], xlab="Log response ratio", col="lightgreen")
lines(dens0, col="darkblue", lwd=2)
dev.copy(png, paste0("hist_", Ana, Cat[1], ".png"))
dev.off()
setEPS()
postscript(paste0("QQ_", Ana, Cat[1], ".eps"))
plot(hist0, main=Cat[1], xlab="Log response ratio", col="lightgreen")
lines(dens0, col="darkblue", lwd=2)
dev.off()
setEPS()
postscript(paste0("hist_", Ana, Cat[1], ".eps"))
hist0 <- hist(LogRR0, breaks=50, plot=FALSE)
mult0 <- hist0$counts / hist0$density
dens0 <- density(LogRR0)
dens0$y <- dens0$y * mult0[1]
```

```
plot(hist0, main=Cat[1], xlab="Log response ratio", col="lightgreen")
lines(dens0, col="darkblue", lwd=2)
dev.off()

if (length(LogRR1>0)){
qqnorm(LogRR1, main=Cat[2], col="darkred")
qqline(LogRR1, col="darkblue", lwd=2)
dev.copy(png, paste0("QQ_", Ana, Cat[2], ".png"))
dev.off()
hist1 <- hist(LogRR1, breaks=50, plot=FALSE)
mult1 <- hist1$counts / hist1$density
dens1 <- density(LogRR1)
dens1$y <- dens1$y * mult1[1]
plot(hist1, main=Cat[2], xlab="Log response ratio", col="lightgreen")
lines(dens1, col="darkblue", lwd=2)
dev.copy(png, paste0("hist_", Ana, Cat[2], ".png"))
dev.off()
setEPS()
postscript(paste0("QQ_", Ana, Cat[2], ".eps"))
plot(hist1, main=Cat[2], xlab="Log response ratio", col="lightgreen")
lines(dens1, col="darkblue", lwd=2)
dev.off()
setEPS()
postscript(paste0("hist_", Ana, Cat[2], ".eps"))
hist1 <- hist(LogRR1, breaks=50, plot=FALSE)
mult1 <- hist1$counts / hist1$density
dens1 <- density(LogRR1)
dens1$y <- dens1$y * mult1[1]
plot(hist1, main=Cat[2], xlab="Log response ratio", col="lightgreen")
lines(dens1, col="darkblue", lwd=2)
dev.off()
}else{}

if (length(LogRR2>0)){
qqnorm(LogRR2, main=Cat[3], col="darkred")
qqline(LogRR2, col="darkblue", lwd=2)
dev.copy(png, paste0("QQ_", Ana, Cat[3], ".png"))
dev.off()
hist2 <- hist(LogRR2, breaks=50, plot=FALSE)
mult2 <- hist2$counts / hist2$density
dens2 <- density(LogRR2)
dens2$y <- dens2$y * mult2[1]
plot(hist2, main=Cat[3], xlab="Log response ratio", col="lightgreen")
lines(dens2, col="darkblue", lwd=2)
dev.copy(png, paste0("hist_", Ana, Cat[3], ".png"))
dev.off()
setEPS()
postscript(paste0("QQ_", Ana, Cat[3], ".eps"))
plot(hist2, main=Cat[3], xlab="Log response ratio", col="lightgreen")
lines(dens2, col="darkblue", lwd=2)
dev.off()
setEPS()
postscript(paste0("hist_", Ana, Cat[3], ".eps"))
hist2 <- hist(LogRR2, breaks=50, plot=FALSE)
mult2 <- hist2$counts / hist2$density
dens2 <- density(LogRR2)
dens2$y <- dens2$y * mult2[1]
```

```
plot(hist2, main=Cat[3], xlab="Log response ratio", col="lightgreen")
lines(dens2, col="darkblue", lwd=2)
dev.off()
}else{}

if (G >= 4){
qqnorm(LogRR3, main=Cat[4], col="darkred")
qqline(LogRR3, col="darkblue", lwd=2)
dev.copy(png, paste0("QQ_", Ana, Cat[4], ".png"))
dev.off()
hist3 <- hist(LogRR3, breaks=50, plot=FALSE)
mult3 <- hist3$counts / hist3$density
dens3 <- density(LogRR3)
dens3$y <- dens3$y * mult3[1]
plot(hist3, main=Cat[4], xlab="Log response ratio", col="lightgreen")
lines(dens3, col="darkblue", lwd=2)
dev.copy(png, paste0("hist_", Ana, Cat[4], ".png"))
dev.off()
setEPS()
postscript(paste0("QQ_", Ana, Cat[4], ".eps"))
plot(hist3, main=Cat[4], xlab="Log response ratio", col="lightgreen")
lines(dens3, col="darkblue", lwd=2)
dev.off()
setEPS()
postscript(paste0("hist_", Ana, Cat[4], ".eps"))
hist3 <- hist(LogRR3, breaks=50, plot=FALSE)
mult3 <- hist3$counts / hist3$density
dens3 <- density(LogRR3)
dens3$y <- dens3$y * mult3[1]
plot(hist3, main=Cat[4], xlab="Log response ratio", col="lightgreen")
lines(dens3, col="darkblue", lwd=2)
dev.off()
}else{}
if (G >= 5){
qqnorm(LogRR4, main=Cat[5], col="darkred")
qqline(LogRR4, col="darkblue", lwd=2)
dev.copy(png, paste0("QQ_", Ana, Cat[5], ".png"))
dev.off()
hist4 <- hist(LogRR4, breaks=50, plot=FALSE)
mult4 <- hist4$counts / hist4$density
dens4 <- density(LogRR4)
dens4$y <- dens4$y * mult4[1]
plot(hist4, main=Cat[5], xlab="Log response ratio", col="lightgreen")
lines(dens4, col="darkblue", lwd=2)
dev.copy(png, paste0("hist_", Ana, Cat[5], ".png"))
dev.off()
setEPS()
postscript(paste0("QQ_", Ana, Cat[5], ".eps"))
plot(hist4, main=Cat[5], xlab="Log response ratio", col="lightgreen")
lines(dens4, col="darkblue", lwd=2)
dev.off()
setEPS()
postscript(paste0("hist_", Ana, Cat[5], ".eps"))
hist4 <- hist(LogRR4, breaks=50, plot=FALSE)
mult4 <- hist4$counts / hist4$density
dens4 <- density(LogRR4)
dens4$y <- dens4$y * mult4[1]
```

```
plot(hist4, main=Cat[5], xlab="Log response ratio", col="lightgreen")
lines(dens4, col="darkblue", lwd=2)
dev.off()
}else{}
if (G >= 6){
qqnorm(LogRR5, main=Cat[6], col="darkred")
qqline(LogRR5, col="darkblue", lwd=2)
dev.copy(png, paste0("QQ_", Ana, Cat[6], ".png"))
dev.off()
hist5 <- hist(LogRR5, breaks=50, plot=FALSE)
mult5 <- hist5$counts / hist5$density
dens5 <- density(LogRR5)
dens5$y <- dens5$y * mult5[1]
plot(hist5, main=Cat[6], xlab="Log response ratio", col="lightgreen")
lines(dens5, col="darkblue", lwd=2)
dev.copy(png, paste0("hist_", Ana, Cat[6], ".png"))
dev.off()
setEPS()
postscript(paste0("QQ_", Ana, Cat[6], ".eps"))
plot(hist5, main=Cat[6], xlab="Log response ratio", col="lightgreen")
lines(dens5, col="darkblue", lwd=2)
dev.off()
setEPS()
postscript(paste0("hist_", Ana, Cat[6], ".eps"))
hist5 <- hist(LogRR5, breaks=50, plot=FALSE)
mult5 <- hist5$counts / hist5$density
dens5 <- density(LogRR5)
dens5$y <- dens5$y * mult5[1]
plot(hist5, main=Cat[6], xlab="Log response ratio", col="lightgreen")
lines(dens5, col="darkblue", lwd=2)
dev.off()
}else{}
if (G >= 7){
qqnorm(LogRR6, main=Cat[7], col="darkred")
qqline(LogRR6, col="darkblue", lwd=2)
dev.copy(png, paste0("QQ_", Ana, Cat[7], ".png"))
dev.off()
hist6 <- hist(LogRR6, breaks=50, plot=FALSE)
mult6 <- hist6$counts / hist6$density
dens6 <- density(LogRR6)
dens6$y <- dens6$y * mult6[1]
plot(hist6, main=Cat[7], xlab="Log response ratio", col="lightgreen")
lines(dens6, col="darkblue", lwd=2)
dev.copy(png, paste0("hist_", Ana, Cat[7], ".png"))
dev.off()
setEPS()
postscript(paste0("QQ_", Ana, Cat[7], ".eps"))
plot(hist6, main=Cat[7], xlab="Log response ratio", col="lightgreen")
lines(dens6, col="darkblue", lwd=2)
dev.off()
setEPS()
postscript(paste0("hist_", Ana, Cat[7], ".eps"))
hist6 <- hist(LogRR6, breaks=50, plot=FALSE)
mult6 <- hist6$counts / hist6$density
dens6 <- density(LogRR6)
dens6$y <- dens6$y * mult6[1]
plot(hist6, main=Cat[7], xlab="Log response ratio", col="lightgreen")
```

```
lines(dens6, col="darkblue", lwd=2)
dev.off()
}else{}
if (G >= 8){
qqnorm(LogRR7, main=Cat[8], col="darkred")
qqline(LogRR7, col="darkblue", lwd=2)
dev.copy(png, paste0("QQ_", Ana, Cat[8], ".png"))
dev.off()
hist7 <- hist(LogRR7, breaks=50, plot=FALSE)
mult7 <- hist7$counts / hist7$density
dens7 <- density(LogRR7)
dens7$y <- dens7$y * mult7[1]
plot(hist7, main=Cat[8], xlab="Log response ratio", col="lightgreen")
lines(dens7, col="darkblue", lwd=2)
dev.copy(png, paste0("hist_", Ana, Cat[8], ".png"))
dev.off()
setEPS()
postscript(paste0("QQ_", Ana, Cat[8], ".eps"))
plot(hist7, main=Cat[8], xlab="Log response ratio", col="lightgreen")
lines(dens7, col="darkblue", lwd=2)
dev.off()
setEPS()
postscript(paste0("hist_", Ana, Cat[8], ".eps"))
hist7 <- hist(LogRR7, breaks=50, plot=FALSE)
mult7 <- hist7$counts / hist7$density
dens7 <- density(LogRR7)
dens7$y <- dens7$y * mult7[1]
plot(hist7, main=Cat[8], xlab="Log response ratio", col="lightgreen")
lines(dens7, col="darkblue", lwd=2)
dev.off()
}else{}
if (G >= 9){
qqnorm(LogRR8, main=Cat[9], col="darkred")
qqline(LogRR8, col="darkblue", lwd=2)
dev.copy(png, paste0("QQ_", Ana, Cat[9], ".png"))
dev.off()
hist8 <- hist(LogRR8, breaks=50, plot=FALSE)
mult8 <- hist8$counts / hist8$density
dens8 <- density(LogRR8)
dens8$y <- dens8$y * mult8[1]
plot(hist8, main=Cat[9], xlab="Log response ratio", col="lightgreen")
lines(dens8, col="darkblue", lwd=2)
dev.copy(png, paste0("hist_", Ana, Cat[9], ".png"))
dev.off()
setEPS()
postscript(paste0("QQ_", Ana, Cat[9], ".eps"))
plot(hist8, main=Cat[9], xlab="Log response ratio", col="lightgreen")
lines(dens8, col="darkblue", lwd=2)
dev.off()
setEPS()
postscript(paste0("hist_", Ana, Cat[9], ".eps"))
hist8 <- hist(LogRR8, breaks=50, plot=FALSE)
mult8 <- hist8$counts / hist8$density
dens8 <- density(LogRR8)
dens8$y <- dens8$y * mult8[1]
plot(hist8, main=Cat[9], xlab="Log response ratio", col="lightgreen")
lines(dens8, col="darkblue", lwd=2)
```

```
dev.off()
}else{}
if (G >= 10){
qqnorm(LogRR9, main=Cat[10], col="darkred")
qqline(LogRR9, col="darkblue", lwd=2)
dev.copy(png, paste0("QQ_", Ana, Cat[10], ".png"))
dev.off()
hist9 <- hist(LogRR9, breaks=50, plot=FALSE)
mult9 <- hist9$counts / hist9$density
dens9 <- density(LogRR9)
dens9$y <- dens9$y * mult9[1]
plot(hist9, main=Cat[10], xlab="Log response ratio", col="lightgreen")
lines(dens9, col="darkblue", lwd=2)
dev.copy(png, paste0("hist_", Ana, Cat[10], ".png"))
dev.off()
setEPS()
postscript(paste0("QQ_", Ana, Cat[10], ".eps"))
plot(hist9, main=Cat[10], xlab="Log response ratio", col="lightgreen")
lines(dens9, col="darkblue", lwd=2)
dev.off()
setEPS()
postscript(paste0("hist_", Ana, Cat[10], ".eps"))
hist9 <- hist(LogRR9, breaks=50, plot=FALSE)
mult9 <- hist9$counts / hist9$density
dens9 <- density(LogRR9)
dens9$y <- dens9$y * mult9[1]
plot(hist9, main=Cat[10], xlab="Log response ratio", col="lightgreen")
lines(dens9, col="darkblue", lwd=2)
dev.off()
}else{}
if (G >= 11){
qqnorm(LogRR10, main=Cat[11], col="darkred")
qqline(LogRR10, col="darkblue", lwd=2)
dev.copy(png, paste0("QQ_", Ana, Cat[11], ".png"))
dev.off()
hist10 <- hist(LogRR10, breaks=50, plot=FALSE)
mult10 <- hist10$counts / hist0$density
dens10 <- density(LogRR10)
dens10$y <- dens10$y * mult10[1]
plot(hist10, main=Cat[11], xlab="Log response ratio", col="lightgreen")
lines(dens10, col="darkblue", lwd=2)
dev.copy(png, paste0("hist_", Ana, Cat[11], ".png"))
dev.off()
setEPS()
postscript(paste0("QQ_", Ana, Cat[11], ".eps"))
plot(hist10, main=Cat[11], xlab="Log response ratio", col="lightgreen")
lines(dens10, col="darkblue", lwd=2)
dev.off()
setEPS()
postscript(paste0("hist_", Ana, Cat[11], ".eps"))
hist10 <- hist(LogRR10, breaks=50, plot=FALSE)
mult10 <- hist10$counts / hist10$density
dens10 <- density(LogRR10)
dens10$y <- dens10$y * mult10[1]
plot(hist10, main=Cat[11], xlab="Log response ratio", col="lightgreen")
lines(dens10, col="darkblue", lwd=2)
dev.off()
```

```
}else{}
if (G >= 12){
qqnorm(LogRR11, main=Cat[12], col="darkred")
qqline(LogRR11, col="darkblue", lwd=2)
dev.copy(png, paste0("QQ_", Ana, Cat[12], ".png"))
dev.off()
hist11 <- hist(LogRR11, breaks=50, plot=FALSE)
mult11 <- hist11$counts / hist11$density
dens11 <- density(LogRR11)
dens11$y <- dens11$y * mult11[1]
plot(hist11, main=Cat[12], xlab="Log response ratio", col="lightgreen")
lines(dens11, col="darkblue", lwd=2)
dev.copy(png, paste0("hist_", Ana, Cat[12], ".png"))
dev.off()
setEPS()
postscript(paste0("QQ_", Ana, Cat[12], ".eps"))
plot(hist11, main=Cat[12], xlab="Log response ratio", col="lightgreen")
lines(dens11, col="darkblue", lwd=2)
dev.off()
setEPS()
postscript(paste0("hist_", Ana, Cat[12], ".eps"))
hist11 <- hist(LogRR11, breaks=50, plot=FALSE)
mult11 <- hist11$counts / hist11$density
dens11 <- density(LogRR11)
dens11$y <- dens11$y * mult11[1]
plot(hist11, main=Cat[12], xlab="Log response ratio", col="lightgreen")
lines(dens11, col="darkblue", lwd=2)
dev.off()
}else{}
#suitability ratios
conSR0<-sqrt(N_con0)*(X_con0/SD_con0)
conSR1<-sqrt(N_con1)*(X_con1/SD_con1)
conSR2<-sqrt(N_con2)*(X_con2/SD_con2)
conSR3<-sqrt(N_con3)*(X_con3/SD_con3)
conSR4<-sqrt(N_con4)*(X_con4/SD_con4)
conSR5<-sqrt(N_con5)*(X_con5/SD_con5)
conSR6<-sqrt(N_con6)*(X_con6/SD_con6)
conSR7<-sqrt(N_con7)*(X_con7/SD_con7)
conSR8<-sqrt(N_con8)*(X_con8/SD_con8)
conSR9<-sqrt(N_con9)*(X_con9/SD_con9)
conSR10<-sqrt(N_con10)*(X_con10/SD_con10)
conSR11<-sqrt(N_con11)*(X_con11/SD_con11)

expSR0<-sqrt(N_exp0)*(X_exp0/SD_exp0)
expSR1<-sqrt(N_exp1)*(X_exp1/SD_exp1)
expSR2<-sqrt(N_exp2)*(X_exp2/SD_exp2)
expSR3<-sqrt(N_exp3)*(X_exp3/SD_exp3)
expSR4<-sqrt(N_exp4)*(X_exp4/SD_exp4)
expSR5<-sqrt(N_exp5)*(X_exp5/SD_exp5)
expSR6<-sqrt(N_exp6)*(X_exp6/SD_exp6)
expSR7<-sqrt(N_exp7)*(X_exp7/SD_exp7)
expSR8<-sqrt(N_exp8)*(X_exp8/SD_exp8)
expSR9<-sqrt(N_exp9)*(X_exp9/SD_exp9)
expSR10<-sqrt(N_exp10)*(X_exp10/SD_exp10)
expSR11<-sqrt(N_exp11)*(X_exp11/SD_exp11)

SR0<-numeric(length(conSR0))
```

```
SR1<-numeric(length(conSR1))
SR2<-numeric(length(conSR2))
SR3<-numeric(length(conSR3))
SR4<-numeric(length(conSR4))
SR5<-numeric(length(conSR5))
SR6<-numeric(length(conSR6))
SR7<-numeric(length(conSR7))
SR8<-numeric(length(conSR8))
SR9<-numeric(length(conSR9))
SR10<-numeric(length(conSR10))
SR11<-numeric(length(conSR11))
srs0<-numeric(length(conSR0))
srl0<-numeric(length(conSR0))
srs1<-numeric(length(conSR0))
srl1<-numeric(length(conSR0))
srs2<-numeric(length(conSR0))
srl2<-numeric(length(conSR0))
srs3<-numeric(length(conSR0))
srl3<-numeric(length(conSR0))
srs4<-numeric(length(conSR0))
srl4<-numeric(length(conSR0))
srs5<-numeric(length(conSR0))
srl5<-numeric(length(conSR0))
srs6<-numeric(length(conSR0))
srl6<-numeric(length(conSR0))
srs7<-numeric(length(conSR0))
srl7<-numeric(length(conSR0))
srs8<-numeric(length(conSR0))
srl8<-numeric(length(conSR0))
srs9<-numeric(length(conSR0))
srl9<-numeric(length(conSR0))
srs10<-numeric(length(conSR0))
srl10<-numeric(length(conSR0))
srs11<-numeric(length(conSR0))
srl11<-numeric(length(conSR0))

for (i in 1:length(conSR0)){
 SR0[i]<-min(conSR0[i], expSR0[i])
 if (SR0[i]<3){
   srs0[i]<-max(srs0)+1
 }else{
   srl0[i]<-max(srl0)+1
 }
}
for (i in 1:length(conSR1)){
  SR1[i]<-min(conSR1[i], expSR1[i])
  if (SR1[i]<3){
    srs1[i]<-max(srs1)+1
  }else{
    srl1[i]<-max(srl1)+1
  }
}
for (i in 1:length(conSR2)){
  SR2[i]<-min(conSR2[i], expSR2[i])
  if (SR2[i]<3){
    srs2[i]<-max(srs2)+1
  }else{
```

```
    srl2[i]<-max(srl2)+1
  }
}
for (i in 1:length(conSR3)){
  SR3[i]<-min(conSR3[i], expSR3[i])
  if (SR3[i]<3){
    srs3[i]<-max(srs3)+1
  }else{
    srl3[i]<-max(srl3)+1
  }
}
for (i in 1:length(conSR4)){
  SR4[i]<-min(conSR4[i], expSR4[i])
  if (SR4[i]<3){
    srs4[i]<-max(srs4)+1
  }else{
    srl4[i]<-max(srl4)+1
  }
}
for (i in 1:length(conSR5)){
  SR5[i]<-min(conSR5[i], expSR5[i])
  if (SR5[i]<3){
    srs5[i]<-max(srs5)+1
  }else{
    srl5[i]<-max(srl5)+1
  }
}
for (i in 1:length(conSR6)){
  SR6[i]<-min(conSR6[i], expSR6[i])
  if (SR6[i]<3){
    srs6[i]<-max(srs6)+1
  }else{
    srl6[i]<-max(srl6)+1
  }
}
for (i in 1:length(conSR7)){
  SR7[i]<-min(conSR7[i], expSR7[i])
  if (SR7[i]<3){
    srs7[i]<-max(srs7)+1
  }else{
    srl7[i]<-max(srl7)+1
  }
}
for (i in 1:length(conSR8)){
  SR8[i]<-min(conSR8[i], expSR8[i])
  if (SR8[i]<3){
    srs8[i]<-max(srs8)+1
  }else{
    srl8[i]<-max(srl8)+1
  }
}
for (i in 1:length(conSR9)){
  SR9[i]<-min(conSR9[i], expSR9[i])
  if (SR9[i]<3){
    srs9[i]<-max(srs9)+1
  }else{
    srl9[i]<-max(srl9)+1
```

```
  }
}
for (i in 1:length(conSR10)){
  SR10[i]<-min(conSR110[i], expSR10[i])
  if (SR10[i]<3){
    srs10[i]<-max(srs10)+1
  }else{
    srl10[i]<-max(srl10)+1
  }
}
for (i in 1:length(conSR11)){
  SR11[i]<-min(conSR11[i], expSR11[i])
  if (SR11[i]<3){
    srs11[i]<-max(srs11)+1
  }else{
    srl11[i]<-max(srl11)+1
  }
}
perc<-c()
perc0<-100*max(srs0)/(max(srs0)+max(srl0))
perc1<-100*max(srs1)/(max(srs1)+max(srl1))
perc2<-100*max(srs2)/(max(srs2)+max(srl2))
if (G>3){
perc3<-100*max(srs3)/(max(srs3)+max(srl3))}
if (G>4){
perc4<-100*max(srs4)/(max(srs4)+max(srl4))}
if (G>5){
perc5<-100*max(srs5)/(max(srs5)+max(srl5))}
if (G>6){
perc6<-100*max(srs6)/(max(srs6)+max(srl6))}
if (G>7){
perc7<-100*max(srs7)/(max(srs7)+max(srl7))}
if (G>8){
perc8<-100*max(srs8)/(max(srs8)+max(srl8))}
if (G>9){
perc9<-100*max(srs9)/(max(srs9)+max(srl9))}
if (G>10){
perc10<-100*max(srs10)/(max(srs10)+max(srl10))}
if (G>11){
perc11<-100*max(srs11)/(max(srs11)+max(srl11))}

SigRatio<-c(perc0, perc1, perc2)
SigRatio<-c(perc0, perc1, perc2, perc3)
SigRatio<-c(perc0, perc1, perc2, perc3, perc4)
SigRatio<-c(perc0, perc1, perc2, perc3, perc4, perc5)
SigRatio<-c(perc0, perc1, perc2, perc3, perc4, perc5, perc6)
SigRatio<-c(perc0, perc1, perc2, perc3, perc4, perc5, perc6, perc7)
SigRatio<-c(perc0,  perc1,  perc2,  perc3,  perc4,  perc5,  perc6,  perc7,
perc8)
SigRatio<-c(perc0,  perc1,  perc2,  perc3,  perc4,  perc5,  perc6,  perc7,
perc8, perc9)
SigRatio<-c(perc0,  perc1,  perc2,  perc3,  perc4,  perc5,  perc6,  perc7,
perc8, perc9, perc10)
SigRatio<-c(perc0,  perc1,  perc2,  perc3,  perc4,  perc5,  perc6,  perc7,
perc8, perc9, perc10, perc11)

#Shapiro-Wilk test
```

```
Norm<-numeric()
Norm[1]<-shapiro.test(LogRR0)$p.value
Norm[2]<-shapiro.test(LogRR1)$p.value
Norm[3]<-shapiro.test(LogRR2)$p.value
Norm[4]<-shapiro.test(LogRR3)$p.value
Norm[5]<-shapiro.test(LogRR4)$p.value
Norm[6]<-shapiro.test(LogRR5)$p.value
Norm[7]<-shapiro.test(LogRR6)$p.value
Norm[8]<-shapiro.test(LogRR7)$p.value
Norm[9]<-shapiro.test(LogRR8)$p.value
Norm[10]<-shapiro.test(LogRR9)$p.value
Norm[11]<-shapiro.test(LogRR10)$p.value
Norm[12]<-shapiro.test(LogRR11)$p.value

#Kurtosis test
kurtosis.test <- function (x) {
  m4 <- sum((x-mean(x))^4)/length(x)
  s4 <- var(x)^2
  kurt <- (m4/s4) - 3
  sek <- sqrt(24/length(x))
  totest <- kurt/sek
  pvalue <- pt(totest,(length(x)-1))
  pvalue
}

Kurt<-numeric()
Kurt[1]<-kurtosis.test(LogRR0)
Kurt[2]<-kurtosis.test(LogRR1)
Kurt[3]<-kurtosis.test(LogRR2)
Kurt[4]<-kurtosis.test(LogRR3)
Kurt[5]<-kurtosis.test(LogRR4)
Kurt[6]<-kurtosis.test(LogRR5)
Kurt[7]<-kurtosis.test(LogRR6)
Kurt[8]<-kurtosis.test(LogRR7)
Kurt[9]<-kurtosis.test(LogRR8)
Kurt[10]<-kurtosis.test(LogRR9)
Kurt[11]<-kurtosis.test(LogRR10)
Kurt[12]<-kurtosis.test(LogRR11)

#Analysis test
skew.test <- function (x) {
  m3 <- sum((x-mean(x))^3)/length(x)
  s3 <- sqrt(var(x))^3
  skew <- m3/s3
  ses <- sqrt(6/length(x))
  totest <- skew/ses
  pt(totest,(length(x)-1))
  pval <- pt(totest,(length(x)-1))
  pval
}

Skew<-numeric()
Skew[1]<-skew.test(LogRR0)
Skew[2]<-skew.test(LogRR1)
Skew[3]<-skew.test(LogRR2)
Skew[4]<-skew.test(LogRR3)
Skew[5]<-skew.test(LogRR4)
```

```
Skew[6]<-skew.test(LogRR5)
Skew[7]<-skew.test(LogRR6)
Skew[8]<-skew.test(LogRR7)
Skew[9]<-skew.test(LogRR8)
Skew[10]<-skew.test(LogRR9)
Skew[11]<-skew.test(LogRR10)
Skew[12]<-skew.test(LogRR11)


assumptions<-data.frame(Cat, Norm, Kurt, Skew, SigRatio, ns)
assumptions

write.xlsx(x = assumptions, file = paste(aa), row.names = FALSE)
```

The code below is the parametric part of the statistical model. First, the significance of random variance is tested, followed by computation of statistical weights, overall means, and confidence intervals. Subsequently, the data is back transformed and Q statistics are estimated. Then, *Z*-values and *p*-values are extracted from individual t-tests comparing the subsamples. Finally, Rosenthal's fail-safe number is computed for each subsample mean and the results are written out as excel file with the annotation 'para'.

```
randomsig<-function(X_con, X_exp, SD_con, SD_exp, N_con, N_exp)
{
  RR<-c()
  LogRR<-c()
  v<-c()
  w<-c()
  w2<-c()
  wLogRR<-c()
  wLogRR2<-c()
  N<-length(X_con)
  for(i in 1:N){
    RR[i]<-X_exp[i]/X_con[i]
  }
  for(i in 1:N){
    LogRR[i]<-log(RR[i]+C)
    v[i]<-
(SD_exp[i]^2/(N_exp[i]*X_exp[i]^2))+(SD_con[i]^2/(N_con[i]*X_con[i]^2))
    w[i]<-1/v[i]
    w2[i]<-w[i]^2
    wLogRR[i]<-w[i]*LogRR[i]
    wLogRR2[i]<-w[i]*LogRR[i]^2
  }
  Q1<-sum(w)
  W<-sum(w2)
  Q2<-sum(wLogRR)
  Q3<-sum(wLogRR2)
  Q<-Q3-(Q2^2/Q1)
  Chi.value<-qchisq(.95, df=N-1)
  if(Q>Chi.value){
    Var.sig<-as.factor("True")
  } else {
    Var.sig<-as.factor("False")
  }
  test<-as.character(Var.sig)
  return(test)
}

Rsig<-c()
Rsig[1]<-randomsig(X_con0, X_exp0, SD_con0, SD_exp0, N_con0, N_exp0)
Rsig[2]<-randomsig(X_con1, X_exp1, SD_con1, SD_exp1, N_con1, N_exp1)
Rsig[3]<-randomsig(X_con2, X_exp2, SD_con2, SD_exp2, N_con2, N_exp2)
Rsig[4]<-randomsig(X_con3, X_exp3, SD_con3, SD_exp3, N_con3, N_exp3)
Rsig[5]<-randomsig(X_con4, X_exp4, SD_con4, SD_exp4, N_con4, N_exp4)
Rsig[6]<-randomsig(X_con5, X_exp5, SD_con5, SD_exp5, N_con5, N_exp5)
Rsig[7]<-randomsig(X_con6, X_exp6, SD_con6, SD_exp6, N_con6, N_exp6)
Rsig[8]<-randomsig(X_con7, X_exp7, SD_con7, SD_exp7, N_con7, N_exp7)
```

```
Rsig[9]<-randomsig(X_con8, X_exp8, SD_con8, SD_exp8, N_con8, N_exp8)
Rsig[10]<-randomsig(X_con9, X_exp9, SD_con9, SD_exp9, N_con9, N_exp9)
Rsig[11]<-randomsig(X_con10,  X_exp10,  SD_con10,  SD_exp10,  N_con10,
N_exp10)
Rsig[12]<-randomsig(X_con11,  X_exp11,  SD_con11,  SD_exp11,  N_con11,
N_exp11)
#obtaining weight vector
weightmixed<-function(X_con, X_exp, SD_con, SD_exp, N_con, N_exp)
{
  RR<-c()
  LogRR<-c()
  v<-c()
  w<-c()
  w2<-c()
  wLogRR<-c()
  wLogRR2<-c()
  N<-length(X_con)
  for(i in 1:N){
    RR[i]<-X_exp[i]/X_con[i]
  }
  for(i in 1:N){
    LogRR[i]<-log(RR[i]+C)
    v[i]<-
(SD_exp[i]^2/(N_exp[i]*X_exp[i]^2))+(SD_con[i]^2/(N_con[i]*X_con[i]^2))
    w[i]<-1/v[i]
    w2[i]<-w[i]^2
    wLogRR[i]<-w[i]*LogRR[i]
    wLogRR2[i]<-w[i]*LogRR[i]^2
  }
  Q1<-sum(w)
  W<-sum(w2)
  Q2<-sum(wLogRR)
  Q3<-sum(wLogRR2)
  Q<-Q3-(Q2^2/Q1)
  qs<-(Q-(N-1))/(Q1-W/Q1)
  q<-sqrt(qs^2)
  weight<-c()
  for(i in 1:N){
    weight[i]<-1/(v[i]+q)
  }
  return(weight)
}
weightfixed<-function(X_con, X_exp, SD_con, SD_exp, N_con, N_exp)
{
  RR<-c()
  LogRR<-c()
  v<-c()
  w<-c()
  w2<-c()
  wLogRR<-c()
  wLogRR2<-c()
  N<-length(X_con)
  for(i in 1:N){
    RR[i]<-X_exp[i]/X_con[i]
  }
  for(i in 1:N){
    LogRR[i]<-log(RR[i]+C)
```

```
    v[i]<-
(SD_exp[i]^2/(N_exp[i]*X_exp[i]^2))+(SD_con[i]^2/(N_con[i]*X_con[i]^2))
  }
  weight<-c()
  for(i in 1:N){
    weight[i]<-1/(v[i])
  }
  return(weight)
}

if (Rsig[1]=="False"){
  weight0<-as.numeric(weightfixed(X_con0,   X_exp0,   SD_con0,   SD_exp0,
N_con0, N_exp0))
}else{
  weight0<-as.numeric(weightmixed(X_con0,   X_exp0,   SD_con0,   SD_exp0,
N_con0, N_exp0))
}
if (Rsig[2]=="False"){
  weight1<-as.numeric(weightfixed(X_con1,   X_exp1,   SD_con1,   SD_exp1,
N_con1, N_exp1))
}else{
  weight1<-as.numeric(weightmixed(X_con1,   X_exp1,   SD_con1,   SD_exp1,
N_con1, N_exp1))
}
if (Rsig[3]=="False"){
  weight2<-as.numeric(weightfixed(X_con2,   X_exp2,   SD_con2,   SD_exp2,
N_con2, N_exp2))
}else{
  weight2<-as.numeric(weightmixed(X_con2,   X_exp2,   SD_con2,   SD_exp2,
N_con2, N_exp2))
}
if (Rsig[4]=="False"){
  weight3<-as.numeric(weightfixed(X_con3,   X_exp3,   SD_con3,   SD_exp3,
N_con3, N_exp3))
}else{
  weight3<-as.numeric(weightmixed(X_con3,   X_exp3,   SD_con3,   SD_exp3,
N_con3, N_exp3))
}
if (Rsig[5]=="False"){
  weight4<-as.numeric(weightfixed(X_con4,   X_exp4,   SD_con4,   SD_exp4,
N_con4, N_exp4))
}else{
  weight4<-as.numeric(weightmixed(X_con4,   X_exp4,   SD_con4,   SD_exp4,
N_con4, N_exp4))
}
if (Rsig[6]=="False"){
  weight5<-as.numeric(weightfixed(X_con5,   X_exp5,   SD_con5,   SD_exp5,
N_con5, N_exp5))
}else{
  weight5<-as.numeric(weightmixed(X_con5,   X_exp5,   SD_con5,   SD_exp5,
N_con5, N_exp5))
}
if (Rsig[7]=="False"){
  weight6<-as.numeric(weightfixed(X_con6,   X_exp6,   SD_con6,   SD_exp6,
N_con6, N_exp6))
}else{
```

```
  weight6<-as.numeric(weightmixed(X_con6,   X_exp6,   SD_con6,   SD_exp6,
N_con6, N_exp6))
}
if (Rsig[8]=="False"){
  weight7<-as.numeric(weightfixed(X_con7,   X_exp7,   SD_con7,   SD_exp7,
N_con7, N_exp7))
}else{
  weight7<-as.numeric(weightmixed(X_con7,   X_exp7,   SD_con7,   SD_exp7,
N_con7, N_exp7))
}
if (Rsig[9]=="False"){
  weight8<-as.numeric(weightfixed(X_con8,   X_exp8,   SD_con8,   SD_exp8,
N_con8, N_exp8))
}else{
  weight8<-as.numeric(weightmixed(X_con8,   X_exp8,   SD_con8,   SD_exp8,
N_con8, N_exp8))
}
if (Rsig[10]=="False"){
  weight9<-as.numeric(weightfixed(X_con9,   X_exp9,   SD_con9,   SD_exp9,
N_con9, N_exp9))
}else{
  weight9<-as.numeric(weightmixed(X_con9,   X_exp9,   SD_con9,   SD_exp9,
N_con9, N_exp9))
}
if (Rsig[11]=="False"){
  weight10<-as.numeric(weightfixed(X_con10, X_exp10, SD_con10, SD_exp10,
N_con10, N_exp10))
}else{
  weight10<-as.numeric(weightmixed(X_con10, X_exp10, SD_con10, SD_exp10,
N_con10, N_exp10))
}
if (Rsig[12]=="False"){
  weight11<-as.numeric(weightfixed(X_con11, X_exp11, SD_con11, SD_exp11,
N_con11, N_exp11))
}else{
  weight11<-as.numeric(weightmixed(X_con11, X_exp11, SD_con11, SD_exp11,
N_con11, N_exp11))
}

#functions
fixed<-function(X_con, X_exp, SD_con, SD_exp, N_con, N_exp)
{
  RR<-c()
  LogRR<-c()
  df<-c()
  v<-c()
  w<-c()
  w2<-c()
  wLogRR<-c()
  wLogRR2<-c()
  N<-length(X_con)
  for(i in 1:N){
    RR[i]<-X_exp[i]/X_con[i]
  }
  for(i in 1:N){
    LogRR[i]<-log(RR[i]+C)
    df[i]<-(N_con[i]+N_exp[i]-2)
```

```
    v[i]<-
(SD_exp[i]^2/(N_exp[i]*X_exp[i]^2))+(SD_con[i]^2/(N_con[i]*X_con[i]^2))
    w[i]<-1/v[i]
    w2[i]<-w[i]^2
    wLogRR[i]<-w[i]*LogRR[i]
    wLogRR2[i]<-w[i]*LogRR[i]^2
  }
  Q1<-sum(w)
  W<-sum(w2)
  Q2<-sum(wLogRR)
  Q3<-sum(wLogRR2)
  Q<-Q3-(Q2^2/Q1)
  qs<-(Q-(N-1))/(Q1-W/Q1)
  q<-sqrt(qs^2)
  SD<-sqrt(q)
  weight<-c()
  weightLogRR<-c()
  for(i in 1:N){
    weight[i]<-1/(v[i])
    weightLogRR[i]<-weight[i]*LogRR[i]
  }
  L1<-sum(weight)
  L2<-sum(weightLogRR)
  MeanLogRR<-L2/L1
  Var<-1/L1
  #small sample error term
  ss<-c()
  for(i in 1:N){
    ss[i]<-(1/df[i])*(weight[i]/w[i])^2*(weight[i]*(L1-weight[i])/L1^2)
  }
  SS<-sum(ss)
  SE<-sqrt(1/L1)
  SEss<-sqrt((1/L1)*(1+(4*SS)))
  if(N > 19){
    Int<-95
  } else{
    Int<-91
  }
  if(N > 49){
    LogCIL<-MeanLogRR-1.96*SE
    LogCIU<-MeanLogRR+1.96*SE
    R<-data.frame(MeanLogRR=MeanLogRR,   LogCIL=LogCIL,   LogCIU=LogCIU,
Int=Int, SD=SD, Var=Var)
  } else {
    LogCIL<-MeanLogRR-1.96*SEss
    LogCIU<-MeanLogRR+1.96*SEss
    R<-data.frame(MeanLogRR=MeanLogRR,   LogCIL=LogCIL,   LogCIU=LogCIU,
Int=Int, SD=SD, Var=Var)
  }
  return(R)
}

mixed<-function(X_con, X_exp, SD_con, SD_exp, N_con, N_exp)
{
  RR<-c()
  LogRR<-c()
  df<-c()
```

```
  v<-c()
  w<-c()
  w2<-c()
  wLogRR<-c()
  wLogRR2<-c()
  N<-length(X_con)
  for(i in 1:N){
    RR[i]<-X_exp[i]/X_con[i]
  }
  for(i in 1:N){
    LogRR[i]<-log(RR[i]+C)
    df[i]<-(N_con[i]+N_exp[i]-2)
    v[i]<-
(SD_exp[i]^2/(N_exp[i]*X_exp[i]^2))+(SD_con[i]^2/(N_con[i]*X_con[i]^2))
    w[i]<-1/v[i]
    w2[i]<-w[i]^2
    wLogRR[i]<-w[i]*LogRR[i]
    wLogRR2[i]<-w[i]*LogRR[i]^2
  }
  Q1<-sum(w)
  W<-sum(w2)
  Q2<-sum(wLogRR)
  Q3<-sum(wLogRR2)
  Q<-Q3-(Q2^2/Q1)
  qs<-(Q-(N-1))/(Q1-W/Q1)
  q<-sqrt(qs^2)
  SD<-sqrt(q)
  weight<-c()
  weightLogRR<-c()
  for(i in 1:N){
    weight[i]<-1/(v[i]+q)
    weightLogRR[i]<-weight[i]*LogRR[i]
  }
  L1<-sum(weight)
  L2<-sum(weightLogRR)
  MeanLogRR<-L2/L1
  Var<-1/L1
  #small sample error term
  ss<-c()
  for(i in 1:N){
    ss[i]<-(1/df[i])*(weight[i]/w[i])^2*(weight[i]*(L1-weight[i])/L1^2)
  }
  SS<-sum(ss)
  SE<-sqrt(1/L1)
  SEss<-sqrt((1/L1)*(1+(4*SS)))
  if(N > 19){
    Int<-95
  } else{
    Int<-91
  }
  if(N > 49){
    LogCIL<-MeanLogRR-1.96*SE
    LogCIU<-MeanLogRR+1.96*SE
    R<-data.frame(MeanLogRR=MeanLogRR,   LogCIL=LogCIL,   LogCIU=LogCIU,
Int=Int, SD=SD, Var=Var)
  } else {
    LogCIL<-MeanLogRR-1.96*SEss
```

```
    LogCIU<-MeanLogRR+1.96*SEss
    R<-data.frame(MeanLogRR=MeanLogRR,   LogCIL=LogCIL,   LogCIU=LogCIU,
Int=Int, SD=SD, Var=Var)
  }
  return(R)
}

#run analyses
pRR<-c()
pCIL<-c()
pCIU<-c()
Int<-c()
SD<-c()
VAR<-c()

if (Rsig[1]=="False"){
  pRR[1]<-as.numeric(fixed(X_con0,  X_exp0,  SD_con0,  SD_exp0,  N_con0,
N_exp0)[1])
  pCIL[1]<-as.numeric(fixed(X_con0,  X_exp0,  SD_con0,  SD_exp0,  N_con0,
N_exp0)[2])
  pCIU[1]<-as.numeric(fixed(X_con0,  X_exp0,  SD_con0,  SD_exp0,  N_con0,
N_exp0)[3])
  Int[1]<-as.numeric(fixed(X_con0,  X_exp0,  SD_con0,  SD_exp0,  N_con0,
N_exp0)[4])
  SD[1]<-as.numeric(fixed(X_con0,  X_exp0,  SD_con0,  SD_exp0,  N_con0,
N_exp0)[5])
  VAR[1]<-as.numeric(fixed(X_con0,  X_exp0,  SD_con0,  SD_exp0,  N_con0,
N_exp0)[6])
}else{
  pRR[1]<-as.numeric(mixed(X_con0,  X_exp0,  SD_con0,  SD_exp0,  N_con0,
N_exp0)[1])
  pCIL[1]<-as.numeric(mixed(X_con0,  X_exp0,  SD_con0,  SD_exp0,  N_con0,
N_exp0)[2])
  pCIU[1]<-as.numeric(mixed(X_con0,  X_exp0,  SD_con0,  SD_exp0,  N_con0,
N_exp0)[3])
  Int[1]<-as.numeric(mixed(X_con0,  X_exp0,  SD_con0,  SD_exp0,  N_con0,
N_exp0)[4])
  SD[1]<-as.numeric(mixed(X_con0,  X_exp0,  SD_con0,  SD_exp0,  N_con0,
N_exp0)[5])
  VAR[1]<-as.numeric(mixed(X_con0,  X_exp0,  SD_con0,  SD_exp0,  N_con0,
N_exp0)[6])
}
if (Rsig[2]=="False"){
  pRR[2]<-as.numeric(fixed(X_con1,  X_exp1,  SD_con1,  SD_exp1,  N_con1,
N_exp1)[1])
  pCIL[2]<-as.numeric(fixed(X_con1,  X_exp1,  SD_con1,  SD_exp1,  N_con1,
N_exp1)[2])
  pCIU[2]<-as.numeric(fixed(X_con1,  X_exp1,  SD_con1,  SD_exp1,  N_con1,
N_exp1)[3])
  Int[2]<-as.numeric(fixed(X_con1,  X_exp1,  SD_con1,  SD_exp1,  N_con1,
N_exp1)[4])
  SD[2]<-as.numeric(fixed(X_con1,  X_exp1,  SD_con1,  SD_exp1,  N_con1,
N_exp1)[5])
  VAR[2]<-as.numeric(fixed(X_con1,  X_exp1,  SD_con1,  SD_exp1,  N_con1,
N_exp1)[6])
}else{
```

```
  pRR[2]<-as.numeric(mixed(X_con1,  X_exp1,  SD_con1,  SD_exp1,  N_con1,
N_exp1)[1])
  pCIL[2]<-as.numeric(mixed(X_con1,  X_exp1,  SD_con1,  SD_exp1,  N_con1,
N_exp1)[2])
  pCIU[2]<-as.numeric(mixed(X_con1,  X_exp1,  SD_con1,  SD_exp1,  N_con1,
N_exp1)[3])
  Int[2]<-as.numeric(mixed(X_con1,  X_exp1,  SD_con1,  SD_exp1,  N_con1,
N_exp1)[4])
  SD[2]<-as.numeric(mixed(X_con1,  X_exp1,  SD_con1,  SD_exp1,  N_con1,
N_exp1)[5])
  VAR[2]<-as.numeric(mixed(X_con1,  X_exp1,  SD_con1,  SD_exp1,  N_con1,
N_exp1)[6])
}
if (Rsig[3]=="False"){
  pRR[3]<-as.numeric(fixed(X_con2,  X_exp2,  SD_con2,  SD_exp2,  N_con2,
N_exp2)[1])
  pCIL[3]<-as.numeric(fixed(X_con2,  X_exp2,  SD_con2,  SD_exp2,  N_con2,
N_exp2)[2])
  pCIU[3]<-as.numeric(fixed(X_con2,  X_exp2,  SD_con2,  SD_exp2,  N_con2,
N_exp2)[3])
  Int[3]<-as.numeric(fixed(X_con2,  X_exp2,  SD_con2,  SD_exp2,  N_con2,
N_exp2)[4])
  SD[3]<-as.numeric(fixed(X_con2,  X_exp2,  SD_con2,  SD_exp2,  N_con2,
N_exp2)[5])
  VAR[3]<-as.numeric(fixed(X_con2,  X_exp2,  SD_con2,  SD_exp2,  N_con2,
N_exp2)[6])
}else{
  pRR[3]<-as.numeric(mixed(X_con2,  X_exp2,  SD_con2,  SD_exp2,  N_con2,
N_exp2)[1])
  pCIL[3]<-as.numeric(mixed(X_con2,  X_exp2,  SD_con2,  SD_exp2,  N_con2,
N_exp2)[2])
  pCIU[3]<-as.numeric(mixed(X_con2,  X_exp2,  SD_con2,  SD_exp2,  N_con2,
N_exp2)[3])
  Int[3]<-as.numeric(mixed(X_con2,  X_exp2,  SD_con2,  SD_exp2,  N_con2,
N_exp2)[4])
  SD[3]<-as.numeric(mixed(X_con2,  X_exp2,  SD_con2,  SD_exp2,  N_con2,
N_exp2)[5])
  VAR[3]<-as.numeric(mixed(X_con2,  X_exp2,  SD_con2,  SD_exp2,  N_con2,
N_exp2)[6])
}
if (Rsig[4]=="False"){
  pRR[4]<-as.numeric(fixed(X_con3,  X_exp3,  SD_con3,  SD_exp3,  N_con3,
N_exp3)[1])
  pCIL[4]<-as.numeric(fixed(X_con3,  X_exp3,  SD_con3,  SD_exp3,  N_con3,
N_exp3)[2])
  pCIU[4]<-as.numeric(fixed(X_con3,  X_exp3,  SD_con3,  SD_exp3,  N_con3,
N_exp3)[3])
  Int[4]<-as.numeric(fixed(X_con3,  X_exp3,  SD_con3,  SD_exp3,  N_con3,
N_exp3)[4])
  SD[4]<-as.numeric(fixed(X_con3,  X_exp3,  SD_con3,  SD_exp3,  N_con3,
N_exp3)[5])
  VAR[4]<-as.numeric(fixed(X_con3,  X_exp3,  SD_con3,  SD_exp3,  N_con3,
N_exp3)[6])
}else{
  pRR[4]<-as.numeric(mixed(X_con3,  X_exp3,  SD_con3,  SD_exp3,  N_con3,
N_exp3)[1])
```

```
  pCIL[4]<-as.numeric(mixed(X_con3,  X_exp3,  SD_con3,  SD_exp3,  N_con3,
N_exp3)[2])
  pCIU[4]<-as.numeric(mixed(X_con3,  X_exp3,  SD_con3,  SD_exp3,  N_con3,
N_exp3)[3])
  Int[4]<-as.numeric(mixed(X_con3,  X_exp3,  SD_con3,  SD_exp3,  N_con3,
N_exp3)[4])
  SD[4]<-as.numeric(mixed(X_con3,  X_exp3,  SD_con3,  SD_exp3,  N_con3,
N_exp3)[5])
  VAR[4]<-as.numeric(mixed(X_con3,  X_exp3,  SD_con3,  SD_exp3,  N_con3,
N_exp3)[6])
}
if (Rsig[5]=="False"){
  pRR[5]<-as.numeric(fixed(X_con4,  X_exp4,  SD_con4,  SD_exp4,  N_con4,
N_exp4)[1])
  pCIL[5]<-as.numeric(fixed(X_con4,  X_exp4,  SD_con4,  SD_exp4,  N_con4,
N_exp4)[2])
  pCIU[5]<-as.numeric(fixed(X_con4,  X_exp4,  SD_con4,  SD_exp4,  N_con4,
N_exp4)[3])
  Int[5]<-as.numeric(fixed(X_con4,  X_exp4,  SD_con4,  SD_exp4,  N_con4,
N_exp4)[4])
  SD[5]<-as.numeric(fixed(X_con4,  X_exp4,  SD_con4,  SD_exp4,  N_con4,
N_exp4)[5])
  VAR[5]<-as.numeric(fixed(X_con4,  X_exp4,  SD_con4,  SD_exp4,  N_con4,
N_exp4)[6])
}else{
  pRR[5]<-as.numeric(mixed(X_con4,  X_exp4,  SD_con4,  SD_exp4,  N_con4,
N_exp4)[1])
  pCIL[5]<-as.numeric(mixed(X_con4,  X_exp4,  SD_con4,  SD_exp4,  N_con4,
N_exp4)[2])
  pCIU[5]<-as.numeric(mixed(X_con4,  X_exp4,  SD_con4,  SD_exp4,  N_con4,
N_exp4)[3])
  Int[5]<-as.numeric(mixed(X_con4,  X_exp4,  SD_con4,  SD_exp4,  N_con4,
N_exp4)[4])
  SD[5]<-as.numeric(mixed(X_con4,  X_exp4,  SD_con4,  SD_exp4,  N_con4,
N_exp4)[5])
  VAR[5]<-as.numeric(mixed(X_con4,  X_exp4,  SD_con4,  SD_exp4,  N_con4,
N_exp4)[6])
}
if (Rsig[6]=="False"){
  pRR[6]<-as.numeric(fixed(X_con5,  X_exp5,  SD_con5,  SD_exp5,  N_con5,
N_exp5)[1])
  pCIL[6]<-as.numeric(fixed(X_con5,  X_exp5,  SD_con5,  SD_exp5,  N_con5,
N_exp5)[2])
  pCIU[6]<-as.numeric(fixed(X_con5,  X_exp5,  SD_con5,  SD_exp5,  N_con5,
N_exp5)[3])
  Int[6]<-as.numeric(fixed(X_con5,  X_exp5,  SD_con5,  SD_exp5,  N_con5,
N_exp5)[4])
  SD[6]<-as.numeric(fixed(X_con5,  X_exp5,  SD_con5,  SD_exp5,  N_con5,
N_exp5)[5])
  VAR[6]<-as.numeric(fixed(X_con5,  X_exp5,  SD_con5,  SD_exp5,  N_con5,
N_exp5)[6])
}else{
  pRR[6]<-as.numeric(mixed(X_con5,  X_exp5,  SD_con5,  SD_exp5,  N_con5,
N_exp5)[1])
  pCIL[6]<-as.numeric(mixed(X_con5,  X_exp5,  SD_con5,  SD_exp5,  N_con5,
N_exp5)[2])
```

```
  pCIU[6]<-as.numeric(mixed(X_con5,  X_exp5,  SD_con5,  SD_exp5,  N_con5,
N_exp5)[3])
  Int[6]<-as.numeric(mixed(X_con5,  X_exp5,  SD_con5,  SD_exp5,  N_con5,
N_exp5)[4])
  SD[6]<-as.numeric(mixed(X_con5,  X_exp5,  SD_con5,  SD_exp5,  N_con5,
N_exp5)[5])
  VAR[6]<-as.numeric(mixed(X_con5,  X_exp5,  SD_con5,  SD_exp5,  N_con5,
N_exp5)[6])
}
if (Rsig[7]=="False"){
  pRR[7]<-as.numeric(fixed(X_con6,  X_exp6,  SD_con6,  SD_exp6,  N_con6,
N_exp6)[1])
  pCIL[7]<-as.numeric(fixed(X_con6,  X_exp6,  SD_con6,  SD_exp6,  N_con6,
N_exp6)[2])
  pCIU[7]<-as.numeric(fixed(X_con6,  X_exp6,  SD_con6,  SD_exp6,  N_con6,
N_exp6)[3])
  Int[7]<-as.numeric(fixed(X_con6,  X_exp6,  SD_con6,  SD_exp6,  N_con6,
N_exp6)[4])
  SD[7]<-as.numeric(fixed(X_con6,  X_exp6,  SD_con6,  SD_exp6,  N_con6,
N_exp6)[5])
  VAR[7]<-as.numeric(fixed(X_con6,  X_exp6,  SD_con6,  SD_exp6,  N_con6,
N_exp6)[6])
}else{
  pRR[7]<-as.numeric(mixed(X_con6,  X_exp6,  SD_con6,  SD_exp6,  N_con6,
N_exp6)[1])
  pCIL[7]<-as.numeric(mixed(X_con6,  X_exp6,  SD_con6,  SD_exp6,  N_con6,
N_exp6)[2])
  pCIU[7]<-as.numeric(mixed(X_con6,  X_exp6,  SD_con6,  SD_exp6,  N_con6,
N_exp6)[3])
  Int[7]<-as.numeric(mixed(X_con6,  X_exp6,  SD_con6,  SD_exp6,  N_con6,
N_exp6)[4])
  SD[7]<-as.numeric(mixed(X_con6,  X_exp6,  SD_con6,  SD_exp6,  N_con6,
N_exp6)[5])
  VAR[7]<-as.numeric(mixed(X_con6,  X_exp6,  SD_con6,  SD_exp6,  N_con6,
N_exp6)[6])
}
if (Rsig[8]=="False"){
  pRR[8]<-as.numeric(fixed(X_con7,  X_exp7,  SD_con7,  SD_exp7,  N_con7,
N_exp7)[1])
  pCIL[8]<-as.numeric(fixed(X_con7,  X_exp7,  SD_con7,  SD_exp7,  N_con7,
N_exp7)[2])
  pCIU[8]<-as.numeric(fixed(X_con7,  X_exp7,  SD_con7,  SD_exp7,  N_con7,
N_exp7)[3])
  Int[8]<-as.numeric(fixed(X_con7,  X_exp7,  SD_con7,  SD_exp7,  N_con7,
N_exp7)[4])
  SD[8]<-as.numeric(fixed(X_con7,  X_exp7,  SD_con7,  SD_exp7,  N_con7,
N_exp7)[5])
  VAR[8]<-as.numeric(fixed(X_con7,  X_exp7,  SD_con7,  SD_exp7,  N_con7,
N_exp7)[6])
}else{
  pRR[8]<-as.numeric(mixed(X_con7,  X_exp7,  SD_con7,  SD_exp7,  N_con7,
N_exp7)[1])
  pCIL[8]<-as.numeric(mixed(X_con7,  X_exp7,  SD_con7,  SD_exp7,  N_con7,
N_exp7)[2])
  pCIU[8]<-as.numeric(mixed(X_con7,  X_exp7,  SD_con7,  SD_exp7,  N_con7,
N_exp7)[3])
```

```
  Int[8]<-as.numeric(mixed(X_con7,  X_exp7,  SD_con7,  SD_exp7,  N_con7,
N_exp7)[4])
  SD[8]<-as.numeric(mixed(X_con7,  X_exp7,  SD_con7,  SD_exp7,  N_con7,
N_exp7)[5])
  VAR[8]<-as.numeric(mixed(X_con7,  X_exp7,  SD_con7,  SD_exp7,  N_con7,
N_exp7)[6])
}
if (Rsig[9]=="False"){
  pRR[9]<-as.numeric(fixed(X_con8,  X_exp8,  SD_con8,  SD_exp8,  N_con8,
N_exp8)[1])
  pCIL[9]<-as.numeric(fixed(X_con8,  X_exp8,  SD_con8,  SD_exp8,  N_con8,
N_exp8)[2])
  pCIU[9]<-as.numeric(fixed(X_con8,  X_exp8,  SD_con8,  SD_exp8,  N_con8,
N_exp8)[3])
  Int[9]<-as.numeric(fixed(X_con8,  X_exp8,  SD_con8,  SD_exp8,  N_con8,
N_exp8)[4])
  SD[9]<-as.numeric(fixed(X_con8,  X_exp8,  SD_con8,  SD_exp8,  N_con8,
N_exp8)[5])
  VAR[9]<-as.numeric(fixed(X_con8,  X_exp8,  SD_con8,  SD_exp8,  N_con8,
N_exp8)[6])
}else{
  pRR[9]<-as.numeric(mixed(X_con8,  X_exp8,  SD_con8,  SD_exp8,  N_con8,
N_exp8)[1])
  pCIL[9]<-as.numeric(mixed(X_con8,  X_exp8,  SD_con8,  SD_exp8,  N_con8,
N_exp8)[2])
  pCIU[9]<-as.numeric(mixed(X_con8,  X_exp8,  SD_con8,  SD_exp8,  N_con8,
N_exp8)[3])
  Int[9]<-as.numeric(mixed(X_con8,  X_exp8,  SD_con8,  SD_exp8,  N_con8,
N_exp8)[4])
  SD[9]<-as.numeric(mixed(X_con8,  X_exp8,  SD_con8,  SD_exp8,  N_con8,
N_exp8)[5])
  VAR[9]<-as.numeric(mixed(X_con8,  X_exp8,  SD_con8,  SD_exp8,  N_con8,
N_exp8)[6])
}
if (Rsig[10]=="False"){
  pRR[10]<-as.numeric(fixed(X_con9,  X_exp9,  SD_con9,  SD_exp9,  N_con9,
N_exp9)[1])
  pCIL[10]<-as.numeric(fixed(X_con9,  X_exp9,  SD_con9,  SD_exp9,  N_con9,
N_exp9)[2])
  pCIU[10]<-as.numeric(fixed(X_con9,  X_exp9,  SD_con9,  SD_exp9,  N_con9,
N_exp9)[3])
  Int[10]<-as.numeric(fixed(X_con9,  X_exp9,  SD_con9,  SD_exp9,  N_con9,
N_exp9)[4])
  SD[10]<-as.numeric(fixed(X_con9,  X_exp9,  SD_con9,  SD_exp9,  N_con9,
N_exp9)[5])
  VAR[10]<-as.numeric(fixed(X_con9,  X_exp9,  SD_con9,  SD_exp9,  N_con9,
N_exp9)[6])
}else{
  pRR[10]<-as.numeric(mixed(X_con9,  X_exp9,  SD_con9,  SD_exp9,  N_con9,
N_exp9)[1])
  pCIL[10]<-as.numeric(mixed(X_con9,  X_exp9,  SD_con9,  SD_exp9,  N_con9,
N_exp9)[2])
  pCIU[10]<-as.numeric(mixed(X_con9,  X_exp9,  SD_con9,  SD_exp9,  N_con9,
N_exp9)[3])
  Int[10]<-as.numeric(mixed(X_con9,  X_exp9,  SD_con9,  SD_exp9,  N_con9,
N_exp9)[4])
```

```
  SD[10]<-as.numeric(mixed(X_con9,  X_exp9,  SD_con9,  SD_exp9,  N_con9,
N_exp9)[5])
  VAR[10]<-as.numeric(mixed(X_con9,  X_exp9,  SD_con9,  SD_exp9,  N_con9,
N_exp9)[6])
}
if (Rsig[11]=="False"){
  pRR[11]<-as.numeric(fixed(X_con10,   X_exp10,   SD_con10,   SD_exp10,
N_con10, N_exp10)[1])
  pCIL[11]<-as.numeric(fixed(X_con10,   X_exp10,   SD_con10,   SD_exp10,
N_con10, N_exp10)[2])
  pCIU[11]<-as.numeric(fixed(X_con10,   X_exp10,   SD_con10,   SD_exp10,
N_con10, N_exp10)[3])
  Int[11]<-as.numeric(fixed(X_con10,   X_exp10,   SD_con10,   SD_exp10,
N_con10, N_exp10)[4])
  SD[11]<-as.numeric(fixed(X_con10,   X_exp10,   SD_con10,   SD_exp10,
N_con10, N_exp10)[5])
  VAR[11]<-as.numeric(fixed(X_con10,   X_exp10,   SD_con10,   SD_exp10,
N_con10, N_exp10)[6])
}else{
  pRR[11]<-as.numeric(mixed(X_con10,   X_exp10,   SD_con10,   SD_exp10,
N_con10, N_exp10)[1])
  pCIL[11]<-as.numeric(mixed(X_con10,   X_exp10,   SD_con10,   SD_exp10,
N_con10, N_exp10)[2])
  pCIU[11]<-as.numeric(mixed(X_con10,   X_exp10,   SD_con10,   SD_exp10,
N_con10, N_exp10)[3])
  Int[11]<-as.numeric(mixed(X_con10,   X_exp10,   SD_con10,   SD_exp10,
N_con10, N_exp10)[4])
  SD[11]<-as.numeric(mixed(X_con10,   X_exp10,   SD_con10,   SD_exp10,
N_con10, N_exp10)[5])
  VAR[11]<-as.numeric(mixed(X_con10,   X_exp10,   SD_con10,   SD_exp10,
N_con10, N_exp10)[6])
}
if (Rsig[12]=="False"){
  pRR[12]<-as.numeric(fixed(X_con11,   X_exp11,   SD_con11,   SD_exp11,
N_con11, N_exp11)[1])
  pCIL[12]<-as.numeric(fixed(X_con11,   X_exp11,   SD_con11,   SD_exp11,
N_con11, N_exp11)[2])
  pCIU[12]<-as.numeric(fixed(X_con11,   X_exp11,   SD_con11,   SD_exp11,
N_con11, N_exp11)[3])
  Int[12]<-as.numeric(fixed(X_con11,   X_exp11,   SD_con11,   SD_exp11,
N_con11, N_exp11)[4])
  SD[12]<-as.numeric(fixed(X_con11,   X_exp11,   SD_con11,   SD_exp11,
N_con11, N_exp11)[5])
  VAR[12]<-as.numeric(fixed(X_con11,   X_exp11,   SD_con11,   SD_exp11,
N_con11, N_exp11)[6])
}else{
  pRR[12]<-as.numeric(mixed(X_con11,   X_exp11,   SD_con11,   SD_exp11,
N_con11, N_exp11)[1])
  pCIL[12]<-as.numeric(mixed(X_con11,   X_exp11,   SD_con11,   SD_exp11,
N_con11, N_exp11)[2])
  pCIU[12]<-as.numeric(mixed(X_con11,   X_exp11,   SD_con11,   SD_exp11,
N_con11, N_exp11)[3])
  Int[12]<-as.numeric(mixed(X_con11,   X_exp11,   SD_con11,   SD_exp11,
N_con11, N_exp11)[4])
  SD[12]<-as.numeric(mixed(X_con11,   X_exp11,   SD_con11,   SD_exp11,
N_con11, N_exp11)[5])
```

```
  VAR[12]<-as.numeric(mixed(X_con11,   X_exp11,   SD_con11,   SD_exp11,
N_con11, N_exp11)[6])
}

#back transformation
transpRR<-c()
transpCIL<-c()
transpCIU<-c()
for(i in 1:length(pRR)){
  transpRR[i]<-exp(pRR[i])-C
  transpCIL[i]<-exp(pCIL[i])-C
  transpCIU[i]<-exp(pCIU[i])-C
}

#Q values
SW<-numeric()
SW[1]<-sum(weight0)
SW[2]<-sum(weight1)
SW[3]<-sum(weight2)
SW[4]<-sum(weight3)
SW[5]<-sum(weight4)
SW[6]<-sum(weight5)
SW[7]<-sum(weight6)
SW[8]<-sum(weight7)
SW[9]<-sum(weight8)
SW[10]<-sum(weight9)
SW[11]<-sum(weight10)
SW[12]<-sum(weight11)
#Model heterogeneity
qm<-numeric()
for (i in 2:G){
  qm[i-1]<-SW[i]*(pRR[i]-pRR[1])^2
}
QM<-numeric(G)
QM[1]<-sum(qm)
#Total heterogeneity
qt<-numeric()
for (i in 1:length(LogRR0)){
    qt[i]<-weight0[i]*(LogRR0[i]-pRR[1])^2
}
QT<-numeric(G)
QT[1]<-sum(qt)
#Error heterogeneity
QE<-numeric(G)
QE[1]<-QT-QM
Qs<-data.frame(QT, QM, QE)

#z-scores tailed
Z<-numeric()
Z1<-numeric()
Z2<-numeric()
Z3<-numeric()
Z4<-numeric()
Z5<-numeric()
Z6<-numeric()
Z7<-numeric()
Z8<-numeric()
```

```
Z9<-numeric()
Z10<-numeric()
Z11<-numeric()
p<-numeric()
p1<-numeric()
p2<-numeric()
p3<-numeric()
p4<-numeric()
p5<-numeric()
p6<-numeric()
p7<-numeric()
p8<-numeric()
p9<-numeric()
p10<-numeric()
p11<-numeric()
for (i in 1:G){
 Z[i]<-(transpRR[i]-1)/((transpRR[i]-transpCIL[i])/1.96)
 if (transpRR[i]<=1){
 p[i]<-1-pnorm(sqrt(Z[i]^2))
 }else{
   p[i]<-1-pnorm(-sqrt(Z[i]^2))
 }
}
for (i in 2:G){
 Z1[i]<-(transpRR[i]-transpRR[2])/((transpRR[i]-transpCIL[i])/1.96)
 p1[i]<-2*(1-pnorm(sqrt(Z1[i]^2)))
 if (i==2){
   Z1[i]<-NA
   p1[i]<-NA
 }else{}
 Z2[i]<-(transpRR[i]-transpRR[3])/((transpRR[i]-transpCIL[i])/1.96)
 p2[i]<-2*(1-pnorm(sqrt(Z2[i]^2)))
 if (i==3){
   Z2[i]<-NA
   p2[i]<-NA
 }else{}
 Z3[i]<-(transpRR[i]-transpRR[4])/((transpRR[i]-transpCIL[i])/1.96)
 p3[i]<-2*(1-pnorm(sqrt(Z3[i]^2)))
 if (i==4){
   Z3[i]<-NA
   p3[i]<-NA
 }else{}
 Z4[i]<-(transpRR[i]-transpRR[5])/((transpRR[i]-transpCIL[i])/1.96)
 p4[i]<-2*(1-pnorm(sqrt(Z4[i]^2)))
 if (i==5){
   Z4[i]<-NA
   p4[i]<-NA
 }else{}
 Z5[i]<-(transpRR[i]-transpRR[6])/((transpRR[i]-transpCIL[i])/1.96)
 p5[i]<-2*(1-pnorm(sqrt(Z5[i]^2)))
 if (i==6){
   Z5[i]<-NA
   p5[i]<-NA
 }else{}
 Z6[i]<-(transpRR[i]-transpRR[7])/((transpRR[i]-transpCIL[i])/1.96)
 p6[i]<-2*(1-pnorm(sqrt(Z6[i]^2)))
 if (i==7){
```

```
  Z6[i]<-NA
  p6[i]<-NA
 }else{}
 Z7[i]<-(transpRR[i]-transpRR[8])/((transpRR[i]-transpCIL[i])/1.96)
 p7[i]<-2*(1-pnorm(sqrt(Z7[i]^2)))
 if (i==8){
  Z7[i]<-NA
  p7[i]<-NA
 }else{}
 Z8[i]<-(transpRR[i]-transpRR[9])/((transpRR[i]-transpCIL[i])/1.96)
 p8[i]<-2*(1-pnorm(sqrt(Z8[i]^2)))
 if (i==9){
  Z8[i]<-NA
  p8[i]<-NA
 }else{}
 Z9[i]<-(transpRR[i]-transpRR[10])/((transpRR[i]-transpCIL[i])/1.96)
 p9[i]<-2*(1-pnorm(sqrt(Z9[i]^2)))
 if (i==10){
  Z9[i]<-NA
  p9[i]<-NA
 }else{}
 Z10[i]<-(transpRR[i]-transpRR[11])/((transpRR[i]-transpCIL[i])/1.96)
 p10[i]<-2*(1-pnorm(sqrt(Z10[i]^2)))
 if (i==11){
  Z10[i]<-NA
  p10[i]<-NA
 }else{}
 Z11[i]<-(transpRR[i]-transpRR[12])/((transpRR[i]-transpCIL[i])/1.96)
 p11[i]<-2*(1-pnorm(sqrt(Z11[i]^2)))
 if (i==11){
  Z11[i]<-NA
  p11[i]<-NA
 }else{}
}
#Rosenthal's Fail safe analysis (I statistic)
thres<-numeric()
I<-numeric()
Rat<-numeric()
for (i in 1:G){
  if (p[i]<0.05){
    thres[i]<-5*ns[i]+10
    I[i]<-(ns[i]/2.706)*((ns[i]*pRR[i]^2)-2.706)
  }else{
    I[i]<-NA
    thres[i]<-5*ns[i]+10
  }
  Rat[i]<-I[i]/thres[i]
}
#write results
results<-data.frame(Cat, pRR, pCIL, pCIU, transpRR, transpCIL, transpCIU,
ns, SD, VAR, QT, QM, QE, Int, Rsig, I, thres, Rat)
write.xlsx(x = results, file = paste(cc), row.names = FALSE)
differences<-data.frame(Cat, Z, p, Z1, p1, Z2, p2, Z3, p3, Z4, p4, Z5,
p5, Z6, p6, Z7, p7, Z8, p8, Z9, p9, Z10, p10, Z11, p11)
write.xlsx(x = differences, file = paste(dd), row.names = FALSE)
```

The code below is the non-parametric part of the statistical model. First, the significance of random variance is tested, followed by computation of statistical weights. Weights are then transformed into probabilities. Overall means, and bootstrapped confidence intervals are computed in individual resampling commands. Subsequently, Q statistics are estimated. Finally, Rosenthal's fail-safe number is computed for each subsample mean and the results are written out as excel file with the annotation 'boot'.

```
randomsig<-function(X_con, X_exp, SD_con, SD_exp, N_con, N_exp)
{
  RR<-c()
  LogRR<-c()
  v<-c()
  w<-c()
  w2<-c()
  wLogRR<-c()
  wLogRR2<-c()
  N<-length(X_con)
  for(i in 1:N){
    RR[i]<-X_exp[i]/X_con[i]
  }
  for(i in 1:N){
    LogRR[i]<-log(RR[i]+C)
    v[i]<-
(SD_exp[i]^2/(N_exp[i]*X_exp[i]^2))+(SD_con[i]^2/(N_con[i]*X_con[i]^2))
    w[i]<-1/v[i]
    w2[i]<-w[i]^2
    wLogRR[i]<-w[i]*LogRR[i]
    wLogRR2[i]<-w[i]*LogRR[i]^2
  }
  Q1<-sum(w)
  W<-sum(w2)
  Q2<-sum(wLogRR)
  Q3<-sum(wLogRR2)
  Q<-Q3-(Q2^2/Q1)
  Chi.value<-qchisq(.95, df=N-1)
  if(Q>Chi.value){
    Var.sig<-as.factor("True")
  } else {
    Var.sig<-as.factor("False")
  }
  test<-as.character(Var.sig)
  return(test)
}

Rsig<-c()
Rsig[1]<-randomsig(X_con0, X_exp0, SD_con0, SD_exp0, N_con0, N_exp0)
Rsig[2]<-randomsig(X_con1, X_exp1, SD_con1, SD_exp1, N_con1, N_exp1)
Rsig[3]<-randomsig(X_con2, X_exp2, SD_con2, SD_exp2, N_con2, N_exp2)
Rsig[4]<-randomsig(X_con3, X_exp3, SD_con3, SD_exp3, N_con3, N_exp3)
Rsig[5]<-randomsig(X_con4, X_exp4, SD_con4, SD_exp4, N_con4, N_exp4)
Rsig[6]<-randomsig(X_con5, X_exp5, SD_con5, SD_exp5, N_con5, N_exp5)
```

```
Rsig[7]<-randomsig(X_con6, X_exp6, SD_con6, SD_exp6, N_con6, N_exp6)
Rsig[8]<-randomsig(X_con7, X_exp7, SD_con7, SD_exp7, N_con7, N_exp7)
Rsig[9]<-randomsig(X_con8, X_exp8, SD_con8, SD_exp8, N_con8, N_exp8)
Rsig[10]<-randomsig(X_con9, X_exp9, SD_con9, SD_exp9, N_con9, N_exp9)
Rsig[11]<-randomsig(X_con10,   X_exp10,   SD_con10,   SD_exp10,   N_con10,
N_exp10)
Rsig[12]<-randomsig(X_con11,   X_exp11,   SD_con11,   SD_exp11,   N_con11,
N_exp11)

#obtaining weight vector
weightmixed<-function(X_con, X_exp, SD_con, SD_exp, N_con, N_exp)
{
  RR<-c()
  LogRR<-c()
  v<-c()
  w<-c()
  w2<-c()
  wLogRR<-c()
  wLogRR2<-c()
  N<-length(X_con)
  for(i in 1:N){
    RR[i]<-X_exp[i]/X_con[i]
  }
  for(i in 1:N){
    LogRR[i]<-log(RR[i]+C)
    v[i]<-
(SD_exp[i]^2/(N_exp[i]*X_exp[i]^2))+(SD_con[i]^2/(N_con[i]*X_con[i]^2))
    w[i]<-1/v[i]
    w2[i]<-w[i]^2
    wLogRR[i]<-w[i]*LogRR[i]
    wLogRR2[i]<-w[i]*LogRR[i]^2
  }
  Q1<-sum(w)
  W<-sum(w2)
  Q2<-sum(wLogRR)
  Q3<-sum(wLogRR2)
  Q<-Q3-(Q2^2/Q1)
  qs<-(Q-(N-1))/(Q1-W/Q1)
  q<-sqrt(qs^2)
  weight<-c()
  for(i in 1:N){
    weight[i]<-1/(v[i]+q)
  }
  return(weight)
}
weightfixed<-function(X_con, X_exp, SD_con, SD_exp, N_con, N_exp)
{
  RR<-c()
  LogRR<-c()
  v<-c()
  w<-c()
  w2<-c()
  wLogRR<-c()
  wLogRR2<-c()
  N<-length(X_con)
  for(i in 1:N){
    RR[i]<-X_exp[i]/X_con[i]
```

```
  }
  for(i in 1:N){
    LogRR[i]<-log(RR[i]+C)
    v[i]<-
(SD_exp[i]^2/(N_exp[i]*X_exp[i]^2))+(SD_con[i]^2/(N_con[i]*X_con[i]^2))
  }
  weight<-c()
  for(i in 1:N){
    weight[i]<-1/(v[i])
  }
  return(weight)
}
if (Rsig[1]=="False"){
  weight0<-as.numeric(weightfixed(X_con0,   X_exp0,   SD_con0,   SD_exp0,
N_con0, N_exp0))
}else{
  weight0<-as.numeric(weightmixed(X_con0,   X_exp0,   SD_con0,   SD_exp0,
N_con0, N_exp0))
}
if (Rsig[2]=="False"){
  weight1<-as.numeric(weightfixed(X_con1,   X_exp1,   SD_con1,   SD_exp1,
N_con1, N_exp1))
}else{
  weight1<-as.numeric(weightmixed(X_con1,   X_exp1,   SD_con1,   SD_exp1,
N_con1, N_exp1))
}
if (Rsig[3]=="False"){
  weight2<-as.numeric(weightfixed(X_con2,   X_exp2,   SD_con2,   SD_exp2,
N_con2, N_exp2))
}else{
  weight2<-as.numeric(weightmixed(X_con2,   X_exp2,   SD_con2,   SD_exp2,
N_con2, N_exp2))
}
if (Rsig[4]=="False"){
  weight3<-as.numeric(weightfixed(X_con3,   X_exp3,   SD_con3,   SD_exp3,
N_con3, N_exp3))
}else{
  weight3<-as.numeric(weightmixed(X_con3,   X_exp3,   SD_con3,   SD_exp3,
N_con3, N_exp3))
}
if (Rsig[5]=="False"){
  weight4<-as.numeric(weightfixed(X_con4,   X_exp4,   SD_con4,   SD_exp4,
N_con4, N_exp4))
}else{
  weight4<-as.numeric(weightmixed(X_con4,   X_exp4,   SD_con4,   SD_exp4,
N_con4, N_exp4))
}
if (Rsig[6]=="False"){
  weight5<-as.numeric(weightfixed(X_con5,   X_exp5,   SD_con5,   SD_exp5,
N_con5, N_exp5))
}else{
  weight5<-as.numeric(weightmixed(X_con5,   X_exp5,   SD_con5,   SD_exp5,
N_con5, N_exp5))
}
if (Rsig[7]=="False"){
  weight6<-as.numeric(weightfixed(X_con6,   X_exp6,   SD_con6,   SD_exp6,
N_con6, N_exp6))
```

```
}else{
  weight6<-as.numeric(weightmixed(X_con6,   X_exp6,   SD_con6,   SD_exp6,
N_con6, N_exp6))
}
if (Rsig[8]=="False"){
  weight7<-as.numeric(weightfixed(X_con7,   X_exp7,   SD_con7,   SD_exp7,
N_con7, N_exp7))
}else{
  weight7<-as.numeric(weightmixed(X_con7,   X_exp7,   SD_con7,   SD_exp7,
N_con7, N_exp7))
}
if (Rsig[9]=="False"){
  weight8<-as.numeric(weightfixed(X_con8,   X_exp8,   SD_con8,   SD_exp8,
N_con8, N_exp8))
}else{
  weight8<-as.numeric(weightmixed(X_con8,   X_exp8,   SD_con8,   SD_exp8,
N_con8, N_exp8))
}
if (Rsig[10]=="False"){
  weight9<-as.numeric(weightfixed(X_con9,   X_exp9,   SD_con9,   SD_exp9,
N_con9, N_exp9))
}else{
  weight9<-as.numeric(weightmixed(X_con9,   X_exp9,   SD_con9,   SD_exp9,
N_con9, N_exp9))
}
if (Rsig[11]=="False"){
  weight10<-as.numeric(weightfixed(X_con10, X_exp10, SD_con10, SD_exp10,
N_con10, N_exp10))
}else{
  weight10<-as.numeric(weightmixed(X_con10, X_exp10, SD_con10, SD_exp10,
N_con10, N_exp10))
}
if (Rsig[12]=="False"){
  weight11<-as.numeric(weightfixed(X_con11, X_exp11, SD_con11, SD_exp11,
N_con11, N_exp11))
}else{
  weight11<-as.numeric(weightmixed(X_con11, X_exp11, SD_con11, SD_exp11,
N_con11, N_exp11))
}

WWW0<-sum(weight0)
weightprob0<-weight0/WWW0
WWW1<-sum(weight1)
weightprob1<-weight1/WWW1
WWW2<-sum(weight2)
weightprob2<-weight2/WWW2
WWW3<-sum(weight3)
weightprob3<-weight3/WWW3
WWW4<-sum(weight4)
weightprob4<-weight4/WWW4
WWW5<-sum(weight5)
weightprob5<-weight5/WWW5
WWW6<-sum(weight6)
weightprob6<-weight6/WWW6
WWW7<-sum(weight7)
weightprob7<-weight7/WWW7
WWW8<-sum(weight8)
```

```
weightprob8<-weight8/WWW8
WWW9<-sum(weight9)
weightprob9<-weight9/WWW9
WWW10<-sum(weight10)
weightprob10<-weight10/WWW10
WWW11<-sum(weight11)
weightprob11<-weight11/WWW11

#create bootstrap samples
bootmean<-c()
bootlow<-c()
boothigh<-c()
mittel0<-numeric(9999)
samp0<-matrix(nrow=length(LogRR0), ncol=9999)
for (i in 1:9999){
  samp0[,i]<- sample(LogRR0, length(LogRR0), rep=TRUE, prob=weightprob0)
  mittel0[i]<-mean(samp0[,i])
}
bootmean[1]<-mean(samp0)
bootlow[1]<-quantile(mittel0,probs=c(.025,.975))[1]
boothigh[1]<-quantile(mittel0,probs=c(.025,.975))[2]

mittel1<-numeric(9999)
samp1<-matrix(nrow=length(LogRR1), ncol=9999)
for (i in 1:9999){
  samp1[,i]<- sample(LogRR1, length(LogRR1), rep=TRUE, prob=weightprob1)
  mittel1[i]<-mean(samp1[,i])
}
bootmean[2]<-mean(samp1)
bootlow[2]<-quantile(mittel1,probs=c(.025,.975))[1]
boothigh[2]<-quantile(mittel1,probs=c(.025,.975))[2]

mittel2<-numeric(9999)
samp2<-matrix(nrow=length(LogRR2), ncol=9999)
for (i in 1:9999){
  samp2[,i]<- sample(LogRR2, length(LogRR2), rep=TRUE, prob=weightprob2)
  mittel2[i]<-mean(samp2[,i])
}
bootmean[3]<-mean(samp2)
bootlow[3]<-quantile(mittel2,probs=c(.025,.975))[1]
boothigh[3]<-quantile(mittel2,probs=c(.025,.975))[2]

mittel3<-numeric(9999)
samp3<-matrix(nrow=length(LogRR3), ncol=9999)
for (i in 1:9999){
  samp3[,i]<- sample(LogRR3, length(LogRR3), rep=TRUE, prob=weightprob3)
  mittel3[i]<-mean(samp3[,i])
}
bootmean[4]<-mean(samp3)
bootlow[4]<-quantile(mittel3,probs=c(.025,.975))[1]
boothigh[4]<-quantile(mittel3,probs=c(.025,.975))[2]

mittel4<-numeric(9999)
samp4<-matrix(nrow=length(LogRR4), ncol=9999)
for (i in 1:9999){
  samp4[,i]<- sample(LogRR4, length(LogRR4), rep=TRUE, prob=weightprob4)
  mittel4[i]<-mean(samp4[,i])
```

```
}
bootmean[5]<-mean(samp4)
bootlow[5]<-quantile(mittel4,probs=c(.025,.975))[1]
boothigh[5]<-quantile(mittel4,probs=c(.025,.975))[2]

mittel5<-numeric(9999)
samp5<-matrix(nrow=length(LogRR5), ncol=9999)
for (i in 1:9999){
  samp5[,i]<- sample(LogRR5, length(LogRR5), rep=TRUE, prob=weightprob5)
  mittel5[i]<-mean(samp5[,i])
}
bootmean[6]<-mean(samp5)
bootlow[6]<-quantile(mittel5,probs=c(.025,.975))[1]
boothigh[6]<-quantile(mittel5,probs=c(.025,.975))[2]

mittel6<-numeric(9999)
samp6<-matrix(nrow=length(LogRR6), ncol=9999)
for (i in 1:9999){
  samp6[,i]<- sample(LogRR6, length(LogRR6), rep=TRUE, prob=weightprob6)
  mittel6[i]<-mean(samp6[,i])
}
bootmean[7]<-mean(samp6)
bootlow[7]<-quantile(mittel6,probs=c(.025,.975))[1]
boothigh[7]<-quantile(mittel6,probs=c(.025,.975))[2]

mittel7<-numeric(9999)
samp7<-matrix(nrow=length(LogRR7), ncol=9999)
for (i in 1:9999){
  samp7[,i]<- sample(LogRR7, length(LogRR7), rep=TRUE, prob=weightprob7)
  mittel7[i]<-mean(samp7[,i])
}
bootmean[8]<-mean(samp7)
bootlow[8]<-quantile(mittel7,probs=c(.025,.975))[1]
boothigh[8]<-quantile(mittel7,probs=c(.025,.975))[2]

mittel8<-numeric(9999)
samp8<-matrix(nrow=length(LogRR8), ncol=9999)
for (i in 1:9999){
  samp8[,i]<- sample(LogRR8, length(LogRR8), rep=TRUE, prob=weightprob8)
  mittel8[i]<-mean(samp8[,i])
}
bootmean[9]<-mean(samp8)
bootlow[9]<-quantile(mittel8,probs=c(.025,.975))[1]
boothigh[9]<-quantile(mittel8,probs=c(.025,.975))[2]

mittel9<-numeric(9999)
samp9<-matrix(nrow=length(LogRR9), ncol=9999)
for (i in 1:9999){
  samp9[,i]<- sample(LogRR9, length(LogRR9), rep=TRUE, prob=weightprob9)
  mittel9[i]<-mean(samp9[,i])
}
bootmean[10]<-mean(samp9)
bootlow[10]<-quantile(mittel9,probs=c(.025,.975))[1]
boothigh[10]<-quantile(mittel9,probs=c(.025,.975))[2]


mittel10<-numeric(9999)
```

```
samp10<-matrix(nrow=length(LogRR10), ncol=9999)
for (i in 1:9999){
  samp10[,i]<-      sample(LogRR10,      length(LogRR10),      rep=TRUE,
prob=weightprob10)
  mittel10[i]<-mean(samp10[,i])
}
bootmean[11]<-mean(samp10)
bootlow[11]<-quantile(mittel10,probs=c(.025,.975))[1]
boothigh[11]<-quantile(mittel10,probs=c(.025,.975))[2]


mittel11<-numeric(9999)
samp11<-matrix(nrow=length(LogRR11), ncol=9999)
for (i in 1:9999){
  samp11[,i]<-      sample(LogRR11,      length(LogRR11),      rep=TRUE,
prob=weightprob11)
  mittel11[i]<-mean(samp11[,i])
}
bootmean[12]<-mean(samp11)
bootlow[12]<-quantile(mittel11,probs=c(.025,.975))[1]
boothigh[12]<-quantile(mittel11,probs=c(.025,.975))[2]

bootlow<-bootlow[1:G]
boothigh<-boothigh[1:G]
#back gtransformation
transmean<-c()
translow<-c()
transhigh<-c()
for(i in 1:length(bootmean)){
    transmean[i]<-exp(bootmean[i])-C
    translow[i]<-exp(bootlow[i])-C
    transhigh[i]<-exp(boothigh[i])-C
}

#Q values
SW<-numeric()
SW[1]<-sum(weight0)
SW[2]<-sum(weight1)
SW[3]<-sum(weight2)
SW[4]<-sum(weight3)
SW[5]<-sum(weight4)
SW[6]<-sum(weight5)
SW[7]<-sum(weight6)
SW[8]<-sum(weight7)
SW[9]<-sum(weight8)
SW[10]<-sum(weight9)
SW[11]<-sum(weight10)
SW[12]<-sum(weight11)
#Model heterogeneity
qm<-numeric()
for (i in 2:G){
  qm[i-1]<-SW[i]*(bootmean[i]-bootmean[1])^2
}
QM<-numeric(G)
QM[1]<-sum(qm)
#Total heterogeneity
qt<-numeric()
```

```
for (i in 1:length(LogRR0)){
  qt[i]<-weight0[i]*(LogRR0[i]-bootmean[1])^2
}
QT<-numeric(G)
QT[1]<-sum(qt)
#Error heterogeneity
QE<-numeric(G)
QE[1]<-QT-QM

#Standard deviation and variance
SE<-numeric(G)
SD<-numeric(G)
VAR<-numeric(G)
for (i in 1:G){
  SE[i]<-(boothigh[i]-bootmean[i])/1.96
  SD[i]<-SE[i]*sqrt(ns[i])
  VAR[i]<-SD[i]^2
}

#Rosenthal's Fail safe analysis (I statistic)
thres<-numeric()
I<-numeric()
Rat<-numeric()
for (i in 1:G){
    thres[i]<-5*ns[i]+10
    I[i]<-(ns[i]/2.706)*((ns[i]*bootmean[i]^2)-2.706)
    Rat[i]<-I[i]/thres[i]
}

#create and write results file
results<-data.frame(Cat,   bootmean,   bootlow,   boothigh,   transmean,
translow, transhigh, ns, SD, VAR, QT, QM, QE, Rsig, I, thres, Rat)
write.xlsx(x = results, file = paste(bb), row.names = FALSE)
```

The code below is part of the sensitivity analysis. First, funnel plots are generated for the entire dataset. After general computation of subsample means and confidence intervals, the procedure is repeaded 5 times under individual omission of the 5 most significant estimates.

```
Kr<-paste("boot")
dd<-paste("Kroeker_para_T_LS.xlsx")
ee<-paste("Kroeker_boot_T_LS.xlsx")

g1<-read.csv("T_Settlement_25.csv")
attach(g1)

X_con0<-g1$X_con
X_exp0<-g1$X_exp
SD_con0<-g1$SD_con
SD_exp0<-g1$SD_exp
N_con0<-g1$N_con
N_exp0<-g1$N_exp
RR0<-g1$RR

n0<-length(X_con0)

RR<-numeric(length(X_con0))
N<-length(X_con0)
for(i in 1:N){
  RR[i]<-X_exp[i]/X_con[i]
}
RRmin<-min(RR)
C<-1-RRmin

#data transformation
trans<-function(X_con, X_exp, SD_con, SD_exp, N_con, N_exp){
  RR<-c()
  LogRR<-c()
  N<-length(X_con)
  for(i in 1:N){
    RR[i]<-X_exp[i]/X_con[i]
  }
  for(i in 1:N){
    LogRR[i]<-log(RR[i]+C)
  }
  return(LogRR)
}

randomsig<-function(X_con, X_exp, SD_con, SD_exp, N_con, N_exp)
{
  RR<-c()
  LogRR<-c()
  v<-c()
  w<-c()
  w2<-c()
  wLogRR<-c()
  wLogRR2<-c()
```

```
  N<-length(X_con)
  for(i in 1:N){
    RR[i]<-X_exp[i]/X_con[i]
  }
  for(i in 1:N){
    LogRR[i]<-log(RR[i]+C)
    v[i]<-
(SD_exp[i]^2/(N_exp[i]*X_exp[i]^2))+(SD_con[i]^2/(N_con[i]*X_con[i]^2))
    w[i]<-1/v[i]
    w2[i]<-w[i]^2
    wLogRR[i]<-w[i]*LogRR[i]
    wLogRR2[i]<-w[i]*LogRR[i]^2
  }
  Q1<-sum(w)
  W<-sum(w2)
  Q2<-sum(wLogRR)
  Q3<-sum(wLogRR2)
  Q<-Q3-(Q2^2/Q1)
  Chi.value<-qchisq(.95, df=N-1)
  if(Q>Chi.value){
    Var.sig<-as.factor("True")
  } else {
    Var.sig<-as.factor("False")
  }
  test<-as.character(Var.sig)
  return(test)
}
Rsig<-randomsig(X_con0, X_exp0, SD_con0, SD_exp0, N_con0, N_exp0)
if (Rsig[1]=="False"){
  weight0<-as.numeric(weightfixed(X_con0,   X_exp0,   SD_con0,   SD_exp0,
N_con0, N_exp0))
}else{
  weight0<-as.numeric(weightmixed(X_con0,   X_exp0,   SD_con0,   SD_exp0,
N_con0, N_exp0))
}

LogRR0<-trans(X_con0, X_exp0, SD_con0, SD_exp0, N_con0, N_exp0)
WWW0<-sum(weight0)
weightprob0<-weight0/WWW0




plot(1, xlim=c(2004, 2016), ylim=c(0, max(Difference)),
     xlab="Year of Experimentation", ylab="delta T",
     cex.lab=1.3, cex.axis=1.5, type = "n")
points(Expyear,  Difference,  pch=21,  cex=log(weight0+1),  col="black",
bg="orange3")
dev.copy(png, paste0("Temperature_over_expyear.png"))
dev.off()

#set up Kroeker comparison, parametric or bootstrapping
Kr<-paste("boot")
dd<-paste("Kroeker_para_pH_C.xlsx")
ee<-paste("Kroeker_boot_pH_C.xlsx")
```

```
library(metafor)
#Funnel plot
Npool<-(N_con0 + N_exp0)/2
SEpool<-(SD_con0/sqrt(N_con0)+SD_exp0/sqrt(N_exp0))/2
plot(1,  main="SE  BASED  FUNNEL  PLOT",  xlim=c(min(RR0),  max(RR0)),
ylim=c(0, max(SEpool)),
     xlab="Response ratio", ylab="Standard error",
     cex.lab=1.3, cex.axis=1.5, type = "n")
points(RR0,    SEpool,    pch=21,    cex=log(weight0+1),    col="black",
bg="orange3")

dev.copy(png, paste0("funnelSE.png"))
dev.off()

plot(1, main="N BASED FUNNEL PLOT", xlim=c(min(RR0), max(RR0)), ylim=c(0,
max(Npool)+5),
     xlab="Response ratio", ylab="Sample size",
     cex.lab=1.3, cex.axis=1.5, type = "n")
points(RR0, Npool, pch=21, cex=log(weight0+1), col="black", bg="orange3")
lx1<-c(0, 0.949194163)
ly1<-c(0.15, 0)
lx2<-c(0.949194163, 2.098388)
ly2<-c(0, 0.15)
lines(lx1, ly1, lty=3, lwd=2, col="black")
lines(lx2, ly2, lty=3, lwd=2, col="black")
dev.copy(png, paste0("funnelN.png"))
dev.off()
```

```
#Kroeker's exclusion
mixed<-function(X_con, X_exp, SD_con, SD_exp, N_con, N_exp)
{
  RR<-c()
  LogRR<-c()
  df<-c()
  v<-c()
  w<-c()
  w2<-c()
  wLogRR<-c()
  wLogRR2<-c()
  N<-length(X_con)
  for(i in 1:N){
    RR[i]<-X_exp[i]/X_con[i]
  }
  for(i in 1:N){
    LogRR[i]<-log(RR[i]+C)
    df[i]<-(N_con[i]+N_exp[i]-2)
    v[i]<-
(SD_exp[i]^2/(N_exp[i]*X_exp[i]^2))+(SD_con[i]^2/(N_con[i]*X_con[i]^2))
    w[i]<-1/v[i]
```

```
    w2[i]<-w[i]^2
    wLogRR[i]<-w[i]*LogRR[i]
    wLogRR2[i]<-w[i]*LogRR[i]^2
  }
  Q1<-sum(w)
  W<-sum(w2)
  Q2<-sum(wLogRR)
  Q3<-sum(wLogRR2)
  Q<-Q3-(Q2^2/Q1)
  qs<-(Q-(N-1))/(Q1-W/Q1)
  q<-sqrt(qs^2)
  SD<-sqrt(q)
  weight<-c()
  weightLogRR<-c()
  for(i in 1:N){
    weight[i]<-1/(v[i]+q)
    weightLogRR[i]<-weight[i]*LogRR[i]
  }
  L1<-sum(weight)
  L2<-sum(weightLogRR)
  MeanLogRR<-L2/L1
  Var<-1/L1
  #small sample error term
  ss<-c()
  for(i in 1:N){
    ss[i]<-(1/df[i])*(weight[i]/w[i])^2*(weight[i]*(L1-weight[i])/L1^2)
  }
  SS<-sum(ss)
  SE<-sqrt(1/L1)
  SEss<-sqrt((1/L1)*(1+(4*SS)))
  if(N > 19){
    Int<-95
  } else{
    Int<-91
  }
  if(N > 49){
    LogCIL<-MeanLogRR-1.96*SE
    LogCIU<-MeanLogRR+1.96*SE
    R<-data.frame(MeanLogRR=MeanLogRR,   LogCIL=LogCIL,   LogCIU=LogCIU,
Int=Int, SD=SD, Var=Var)
  } else {
    LogCIL<-MeanLogRR-1.96*SEss
    LogCIU<-MeanLogRR+1.96*SEss
    R<-data.frame(MeanLogRR=MeanLogRR,   LogCIL=LogCIL,   LogCIU=LogCIU,
Int=Int, SD=SD, Var=Var)
  }
  return(R)
}
fixed<-function(X_con, X_exp, SD_con, SD_exp, N_con, N_exp)
{
  RR<-c()
  LogRR<-c()
  df<-c()
  v<-c()
  w<-c()
  w2<-c()
  wLogRR<-c()
```

```
  wLogRR2<-c()
  N<-length(X_con)
  for(i in 1:N){
    RR[i]<-X_exp[i]/X_con[i]
  }
  for(i in 1:N){
    LogRR[i]<-log(RR[i]+C)
    df[i]<-(N_con[i]+N_exp[i]-2)
    v[i]<-
(SD_exp[i]^2/(N_exp[i]*X_exp[i]^2))+(SD_con[i]^2/(N_con[i]*X_con[i]^2))
    w[i]<-1/v[i]
    w2[i]<-w[i]^2
    wLogRR[i]<-w[i]*LogRR[i]
    wLogRR2[i]<-w[i]*LogRR[i]^2
  }
  Q1<-sum(w)
  W<-sum(w2)
  Q2<-sum(wLogRR)
  Q3<-sum(wLogRR2)
  Q<-Q3-(Q2^2/Q1)
  qs<-(Q-(N-1))/(Q1-W/Q1)
  q<-sqrt(qs^2)
  SD<-sqrt(q)
  weight<-c()
  weightLogRR<-c()
  for(i in 1:N){
    weight[i]<-1/(v[i])
    weightLogRR[i]<-weight[i]*LogRR[i]
  }
  L1<-sum(weight)
  L2<-sum(weightLogRR)
  MeanLogRR<-L2/L1
  Var<-1/L1
  #small sample error term
  ss<-c()
  for(i in 1:N){
    ss[i]<-(1/df[i])*(weight[i]/w[i])^2*(weight[i]*(L1-weight[i])/L1^2)
  }
  SS<-sum(ss)
  SE<-sqrt(1/L1)
  SEss<-sqrt((1/L1)*(1+(4*SS)))
  if(N > 19){
    Int<-95
  } else{
    Int<-91
  }
  if(N > 49){
    LogCIL<-MeanLogRR-1.96*SE
    LogCIU<-MeanLogRR+1.96*SE
    R<-data.frame(MeanLogRR=MeanLogRR,   LogCIL=LogCIL,   LogCIU=LogCIU,
Int=Int, SD=SD, Var=Var)
  } else {
    LogCIL<-MeanLogRR-1.96*SEss
    LogCIU<-MeanLogRR+1.96*SEss
    R<-data.frame(MeanLogRR=MeanLogRR,   LogCIL=LogCIL,   LogCIU=LogCIU,
Int=Int, SD=SD, Var=Var)
  }
```

```
  return(R)
}

#parameters
X<-LogRR0#set up group being evaluated
mins<-c()
ID<-c()
IDs<-c()
n<-length(X)
mins[1]<-sort(X, TRUE)[n]
ID[1]<-match(c(mins[1]), X)
IDs[1]<-ID[1]

#finding minima
for (i in 2:5){
  X<-X[-ID[i-1]]
  n<-length(X)
  mins[i]<-sort(X, TRUE)[n]
  ID[i]<-match(c(mins[i]), X)
  if (ID[i]<ID[i-1]){
    IDs[i]<-ID[i]
  } else{
    IDs[i]<-ID[i]+1
  }
  if (IDs[i]==IDs[i-1]){
    IDs[i]<-IDs[i]+1
  } else{
    IDs[i]<-IDs[i]
  }
}

if (Kr=="para"){
  KRR<-numeric()
  KCIL<-numeric()
  KCIU<-numeric()
  #reruning analysis
  #original
  fail0<-mixed(X_con, X_exp, SD_con, SD_exp, N_con, N_exp)
  KRR[1]<-exp(fail0[,1])-C
  KCIL[1]<-exp(fail0[,2])-C
  KCIU[1]<-exp(fail0[,3])-C
  #First
  X_con<-g1$X_con[-IDs[1]]
  SD_con<-g1$SD_con[-IDs[1]]
  N_con<-g1$N_con[-IDs[1]]
  X_exp<-g1$X_exp[-IDs[1]]
  SD_exp<-g1$SD_exp[-IDs[1]]
  N_exp<-g1$N_exp[-IDs[1]]
  fail1<-mixed(X_con, X_exp, SD_con, SD_exp, N_con, N_exp)
  KRR[2]<-exp(fail1[,1])-C
  KCIL[2]<-exp(fail1[,2])-C
  KCIU[2]<-exp(fail1[,3])-C
  #Second
  X_con<-na.omit(g1$X_con)
  SD_con<-na.omit(g1$SD_con)
  N_con<-na.omit(g1$N_con)
  X_exp<-na.omit(g1$X_exp)
```

```
SD_exp<-na.omit(g1$SD_exp)
N_exp<-na.omit(g1$N_exp)
X_con<-g1$X_con[-IDs[2]]
SD_con<-g1$SD_con[-IDs[2]]
N_con<-g1$N_con[-IDs[2]]
X_exp<-g1$X_exp[-IDs[2]]
SD_exp<-g1$SD_exp[-IDs[2]]
N_exp<-g1$N_exp[-IDs[2]]
fail2<-mixed(X_con, X_exp, SD_con, SD_exp, N_con, N_exp)
KRR[3]<-exp(fail2[,1])-C
KCIL[3]<-exp(fail2[,2])-C
KCIU[3]<-exp(fail2[,3])-C
#Third
X_con<-na.omit(g1$X_con)
SD_con<-na.omit(g1$SD_con)
N_con<-na.omit(g1$N_con)
X_exp<-na.omit(g1$X_exp)
SD_exp<-na.omit(g1$SD_exp)
N_exp<-na.omit(g1$N_exp)
X_con<-g1$X_con[-IDs[3]]
SD_con<-g1$SD_con[-IDs[3]]
N_con<-g1$N_con[-IDs[3]]
X_exp<-g1$X_exp[-IDs[3]]
SD_exp<-g1$SD_exp[-IDs[3]]
N_exp<-g1$N_exp[-IDs[3]]
fail3<-mixed(X_con, X_exp, SD_con, SD_exp, N_con, N_exp)
KRR[4]<-exp(fail3[,1])-C
KCIL[4]<-exp(fail3[,2])-C
KCIU[4]<-exp(fail3[,3])-C
#Fourth
X_con<-na.omit(g1$X_con)
SD_con<-na.omit(g1$SD_con)
N_con<-na.omit(g1$N_con)
X_exp<-na.omit(g1$X_exp)
SD_exp<-na.omit(g1$SD_exp)
N_exp<-na.omit(g1$N_exp)
X_con<-g1$X_con[-IDs[4]]
SD_con<-g1$SD_con[-IDs[4]]
N_con<-g1$N_con[-IDs[4]]
X_exp<-g1$X_exp[-IDs[4]]
SD_exp<-g1$SD_exp[-IDs[4]]
N_exp<-g1$N_exp[-IDs[4]]
fail4<-mixed(X_con, X_exp, SD_con, SD_exp, N_con, N_exp)
KRR[5]<-exp(fail4[,1])-C
KCIL[5]<-exp(fail4[,2])-C
KCIU[5]<-exp(fail4[,3])-C
#Fifth
X_con<-na.omit(g1$X_con)
SD_con<-na.omit(g1$SD_con)
N_con<-na.omit(g1$N_con)
X_exp<-na.omit(g1$X_exp)
SD_exp<-na.omit(g1$SD_exp)
N_exp<-na.omit(g1$N_exp)
X_con<-g1$X_con[-IDs[5]]
SD_con<-g1$SD_con[-IDs[5]]
N_con<-g1$N_con[-IDs[5]]
X_exp<-g1$X_exp[-IDs[5]]
```

```
  SD_exp<-g1$SD_exp[-IDs[5]]
  N_exp<-g1$N_exp[-IDs[5]]
  fail5<-mixed(X_con, X_exp, SD_con, SD_exp, N_con, N_exp)
  KRR[6]<-exp(fail5[,1])-C
  KCIL[6]<-exp(fail5[,2])-C
  KCIU[6]<-exp(fail5[,3])-C
  Kroek<-data.frame(KRR, KCIL, KCIU)
  ff<-dd
}else{
  BRR<-c()
  BCIL<-c()
  BCIU<-c()
  #original
  LogRR0<-trans(X_con0, X_exp0, SD_con0, SD_exp0, N_con0, N_exp0)
  mittel0<-numeric(9999)
  samp0<-matrix(nrow=length(LogRR0), ncol=9999)
  for (i in 1:9999){
    samp0[,i]<-      sample(LogRR0,      length(LogRR0),      rep=TRUE,
prob=weightprob0)
    mittel0[i]<-mean(samp0[,i])
  }
  BRR[1]<-exp(mean(samp0))-C
  BCIL[1]<-exp(quantile(mittel0,probs=c(.025,.975))[1])-C
  BCIU[1]<-exp(quantile(mittel0,probs=c(.025,.975))[2])-C
  #First
  X_con<-g1$X_con[-IDs[1]]
  SD_con<-g1$SD_con[-IDs[1]]
  N_con<-g1$N_con[-IDs[1]]
  X_exp<-g1$X_exp[-IDs[1]]
  SD_exp<-g1$SD_exp[-IDs[1]]
  N_exp<-g1$N_exp[-IDs[1]]
  LogRR0<-trans(X_con0, X_exp0, SD_con0, SD_exp0, N_con0, N_exp0)
  mittel0<-numeric(9999)
  samp0<-matrix(nrow=length(LogRR0), ncol=9999)
  for (i in 1:9999){
    samp0[,i]<-      sample(LogRR0,      length(LogRR0),      rep=TRUE,
prob=weightprob0)
    mittel0[i]<-mean(samp0[,i])
  }
  BRR[2]<-exp(mean(samp0))-C
  BCIL[2]<-exp(quantile(mittel0,probs=c(.025,.975))[1])-C
  BCIU[2]<-exp(quantile(mittel0,probs=c(.025,.975))[2])-C
  #Second
  X_con<-na.omit(g1$X_con)
  SD_con<-na.omit(g1$SD_con)
  N_con<-na.omit(g1$N_con)
  X_exp<-na.omit(g1$X_exp)
  SD_exp<-na.omit(g1$SD_exp)
  N_exp<-na.omit(g1$N_exp)
  X_con<-g1$X_con[-IDs[2]]
  SD_con<-g1$SD_con[-IDs[2]]
  N_con<-g1$N_con[-IDs[2]]
  X_exp<-g1$X_exp[-IDs[2]]
  SD_exp<-g1$SD_exp[-IDs[2]]
  N_exp<-g1$N_exp[-IDs[2]]
  LogRR0<-trans(X_con0, X_exp0, SD_con0, SD_exp0, N_con0, N_exp0)
  mittel0<-numeric(9999)
```

```
  samp0<-matrix(nrow=length(LogRR0), ncol=9999)
  for (i in 1:9999){
    samp0[,i]<-      sample(LogRR0,      length(LogRR0),      rep=TRUE,
prob=weightprob0)
    mittel0[i]<-mean(samp0[,i])
  }
  BRR[3]<-exp(mean(samp0))-C
  BCIL[3]<-exp(quantile(mittel0,probs=c(.025,.975))[1])-C
  BCIU[3]<-exp(quantile(mittel0,probs=c(.025,.975))[2])-C
  #Third
  X_con<-na.omit(g1$X_con)
  SD_con<-na.omit(g1$SD_con)
  N_con<-na.omit(g1$N_con)
  X_exp<-na.omit(g1$X_exp)
  SD_exp<-na.omit(g1$SD_exp)
  N_exp<-na.omit(g1$N_exp)
  X_con<-g1$X_con[-IDs[3]]
  SD_con<-g1$SD_con[-IDs[3]]
  N_con<-g1$N_con[-IDs[3]]
  X_exp<-g1$X_exp[-IDs[3]]
  SD_exp<-g1$SD_exp[-IDs[3]]
  N_exp<-g1$N_exp[-IDs[3]]
  LogRR0<-trans(X_con0, X_exp0, SD_con0, SD_exp0, N_con0, N_exp0)
  mittel0<-numeric(9999)
  samp0<-matrix(nrow=length(LogRR0), ncol=9999)
  for (i in 1:9999){
    samp0[,i]<-      sample(LogRR0,      length(LogRR0),      rep=TRUE,
prob=weightprob0)
    mittel0[i]<-mean(samp0[,i])
  }
  BRR[4]<-exp(mean(samp0))-C
  BCIL[4]<-exp(quantile(mittel0,probs=c(.025,.975))[1])-C
  BCIU[4]<-exp(quantile(mittel0,probs=c(.025,.975))[2])-C
  #Fourth
  X_con<-na.omit(g1$X_con)
  SD_con<-na.omit(g1$SD_con)
  N_con<-na.omit(g1$N_con)
  X_exp<-na.omit(g1$X_exp)
  SD_exp<-na.omit(g1$SD_exp)
  N_exp<-na.omit(g1$N_exp)
  X_con<-g1$X_con[-IDs[4]]
  SD_con<-g1$SD_con[-IDs[4]]
  N_con<-g1$N_con[-IDs[4]]
  X_exp<-g1$X_exp[-IDs[4]]
  SD_exp<-g1$SD_exp[-IDs[4]]
  N_exp<-g1$N_exp[-IDs[4]]
  LogRR0<-trans(X_con0, X_exp0, SD_con0, SD_exp0, N_con0, N_exp0)
  mittel0<-numeric(9999)
  samp0<-matrix(nrow=length(LogRR0), ncol=9999)
  for (i in 1:9999){
    samp0[,i]<-      sample(LogRR0,      length(LogRR0),      rep=TRUE,
prob=weightprob0)
    mittel0[i]<-mean(samp0[,i])
  }
  BRR[5]<-exp(mean(samp0))-C
  BCIL[5]<-exp(quantile(mittel0,probs=c(.025,.975))[1])-C
  BCIU[5]<-exp(quantile(mittel0,probs=c(.025,.975))[2])-C
```

```
  #Fifth
  X_con<-na.omit(g1$X_con)
  SD_con<-na.omit(g1$SD_con)
  N_con<-na.omit(g1$N_con)
  X_exp<-na.omit(g1$X_exp)
  SD_exp<-na.omit(g1$SD_exp)
  N_exp<-na.omit(g1$N_exp)
  X_con<-g1$X_con[-IDs[5]]
  SD_con<-g1$SD_con[-IDs[5]]
  N_con<-g1$N_con[-IDs[5]]
  X_exp<-g1$X_exp[-IDs[5]]
  SD_exp<-g1$SD_exp[-IDs[5]]
  N_exp<-g1$N_exp[-IDs[5]]
  LogRR0<-trans(X_con0, X_exp0, SD_con0, SD_exp0, N_con0, N_exp0)
  mittel0<-numeric(9999)
  samp0<-matrix(nrow=length(LogRR0), ncol=9999)
  for (i in 1:9999){
    samp0[,i]<-      sample(LogRR0,      length(LogRR0),      rep=TRUE,
prob=weightprob0)
    mittel0[i]<-mean(samp0[,i])
  }
  BRR[6]<-exp(mean(samp0))-C
  BCIL[6]<-exp(quantile(mittel0,probs=c(.025,.975))[1])-C
  BCIU[6]<-exp(quantile(mittel0,probs=c(.025,.975))[2])-C
  Kroek<-data.frame(BRR, BCIL, BCIU)
  ff<-ee
}
write.xlsx(x = Kroek, file = paste(ff), row.names = FALSE)
```

The code below is part of the sensitivity analysis and randomly generates two subsamples with random sample size. The minimum distance between upper and lower confidence limits is then computed and used to evaluate significance of the result. This procedure is repeaded in an iteration command to generate a distribution of significance values. Finally, *p*-values are extracted from the distribution and represent the likelihood to obtain a significant diference based on chance.

```
library(xlsx)
g2<-read.csv("T_Settlement_25.csv")
tit<-paste("TS")
g3<-data.frame(X_con=g2$X_con,     X_exp=g2$X_exp,     SD_con=g2$SD_con,
SD_exp=g2$SD_exp, N_con=g2$N_con, N_exp=g2$N_exp)

RR<-c()
N<-length(g3$X_con)
for(i in 1:N){
  RR[i]<-g3$X_exp[i]/g3$X_con[i]
}
RRmin<-min(RR)
C<-1-RRmin

randomsig<-function(X_con, X_exp, SD_con, SD_exp, N_con, N_exp)
{
  RR<-c()
  LogRR<-c()
  v<-c()
  w<-c()
  w2<-c()
  wLogRR<-c()
  wLogRR2<-c()
  N<-length(X_con)
  for(i in 1:N){
    RR[i]<-X_exp[i]/X_con[i]
  }
  for(i in 1:N){
    LogRR[i]<-log(RR[i]+C)
    v[i]<-
(SD_exp[i]^2/(N_exp[i]*X_exp[i]^2))+(SD_con[i]^2/(N_con[i]*X_con[i]^2))
    w[i]<-1/v[i]
    w2[i]<-w[i]^2
    wLogRR[i]<-w[i]*LogRR[i]
    wLogRR2[i]<-w[i]*LogRR[i]^2
  }
  Q1<-sum(w)
  W<-sum(w2)
  Q2<-sum(wLogRR)
  Q3<-sum(wLogRR2)
  Q<-Q3-(Q2^2/Q1)
  Chi.value<-qchisq(.95, df=N-1)
  if(Q>Chi.value){
    Var.sig<-as.factor("True")
```

```
  } else {
    Var.sig<-as.factor("False")
  }
  test<-as.character(Var.sig)
  return(test)
}
weightmixed<-function(X_con, X_exp, SD_con, SD_exp, N_con, N_exp)
{
  RR<-c()
  LogRR<-c()
  v<-c()
  w<-c()
  w2<-c()
  wLogRR<-c()
  wLogRR2<-c()
  N<-length(X_con)
  for(i in 1:N){
    RR[i]<-X_exp[i]/X_con[i]
  }
  for(i in 1:N){
    LogRR[i]<-log(RR[i]+C)
    v[i]<-
(SD_exp[i]^2/(N_exp[i]*X_exp[i]^2))+(SD_con[i]^2/(N_con[i]*X_con[i]^2))
    w[i]<-1/v[i]
    w2[i]<-w[i]^2
    wLogRR[i]<-w[i]*LogRR[i]
    wLogRR2[i]<-w[i]*LogRR[i]^2
  }
  Q1<-sum(w)
  W<-sum(w2)
  Q2<-sum(wLogRR)
  Q3<-sum(wLogRR2)
  Q<-Q3-(Q2^2/Q1)
  qs<-(Q-(N-1))/(Q1-W/Q1)
  q<-sqrt(qs^2)
  weight<-c()
  for(i in 1:N){
    weight[i]<-1/(v[i]+q)
  }
  return(weight)
}
weightfixed<-function(X_con, X_exp, SD_con, SD_exp, N_con, N_exp)
{
  RR<-c()
  LogRR<-c()
  v<-c()
  w<-c()
  w2<-c()
  wLogRR<-c()
  wLogRR2<-c()
  N<-length(X_con)
  for(i in 1:N){
    RR[i]<-X_exp[i]/X_con[i]
  }
  for(i in 1:N){
    LogRR[i]<-log(RR[i]+C)
```

```
    v[i]<-
(SD_exp[i]^2/(N_exp[i]*X_exp[i]^2))+(SD_con[i]^2/(N_con[i]*X_con[i]^2))
  }
  weight<-c()
  for(i in 1:N){
    weight[i]<-1/(v[i])
  }
  return(weight)
}

dissigdist<-function(g3){
  dissig<-numeric()
  nsamp<-sample(3:(length(g3$X_con)-3), 1)
  samp1<- sample(g3$X_exp, nsamp, rep=FALSE)
  ind<-match(c(samp1),g3$X_exp)
  group1<-g3[ind,]
  group2<-g3[-ind,]

  X_con<-g3$X_con
  X_exp<-g3$X_exp
  SD_con<-g3$SD_con
  SD_exp<-g3$SD_exp
  N_con<-g3$N_con
  N_exp<-g3$N_exp
  mLogRR<-g3$mLogRR

  X_con0<-group1$X_con
  X_exp0<-group1$X_exp
  SD_con0<-group1$SD_con
  SD_exp0<-group1$SD_exp
  N_con0<-group1$N_con
  N_exp0<-group1$N_exp
  mLogRR0<-group1$mLogRR

  X_con1<-group2$X_con
  X_exp1<-group2$X_exp
  SD_con1<-group2$SD_con
  SD_exp1<-group2$SD_exp
  N_con1<-group2$N_con
  N_exp1<-group2$N_exp
  mLogRR1<-group2$mLogRR

  #data transformation
  trans<-function(X_con, X_exp, SD_con, SD_exp, N_con, N_exp){
    RR<-c()
    LogRR<-c()
    N<-length(X_con)
    for(i in 1:N){
      RR[i]<-X_exp[i]/X_con[i]
    }
    for(i in 1:N){
      LogRR[i]<-log(RR[i]+C)
    }
    return(LogRR)
  }

  LogRR<-trans(X_con, X_exp, SD_con, SD_exp, N_con, N_exp)
```

```
  LogRR0<-trans(X_con0, X_exp0, SD_con0, SD_exp0, N_con0, N_exp0)
  LogRR1<-trans(X_con1, X_exp1, SD_con1, SD_exp1, N_con1, N_exp1)


  Rsig<-c()
  Rsig[1]<-randomsig(X_con0, X_exp0, SD_con0, SD_exp0, N_con0, N_exp0)
  Rsig[2]<-randomsig(X_con1, X_exp1, SD_con1, SD_exp1, N_con1, N_exp1)
  if (Rsig[1]=="False"){
    weight0<-as.numeric(weightfixed(X_con0,  X_exp0,  SD_con0,  SD_exp0,
N_con0, N_exp0))
  }else{
    weight0<-as.numeric(weightmixed(X_con0,  X_exp0,  SD_con0,  SD_exp0,
N_con0, N_exp0))
  }
  if (Rsig[2]=="False"){
    weight1<-as.numeric(weightfixed(X_con1,  X_exp1,  SD_con1,  SD_exp1,
N_con1, N_exp1))
  }else{
    weight1<-as.numeric(weightmixed(X_con1,  X_exp1,  SD_con1,  SD_exp1,
N_con1, N_exp1))
  }

  WWW0<-sum(weight0)
  weightprob0<-weight0/WWW0
  WWW1<-sum(weight1)
  weightprob1<-weight1/WWW1

  bootmean<-c()
  bootlow<-c()
  boothigh<-c()
  mittel0<-numeric(2999)
  subsamp<-matrix(nrow=length(LogRR0), ncol=2999)
  for (i in 1:2999){
    subsamp[,i]<-     sample(LogRR0,     length(LogRR0),     rep=TRUE,
prob=weightprob0)
    mittel0[i]<-mean(subsamp[,i])
  }
  bootmean[1]<-mean(subsamp)
  bootlow[1]<-quantile(mittel0,probs=c(.025,.975))[1]
  boothigh[1]<-quantile(mittel0,probs=c(.025,.975))[2]

  mittel1<-numeric(2999)
  subsamp1<-matrix(nrow=length(LogRR1), ncol=2999)
  for (i in 1:2999){
    subsamp1[,i]<-     sample(LogRR1,     length(LogRR1),     rep=TRUE,
prob=weightprob1)
    mittel1[i]<-mean(subsamp1[,i])
  }
  bootmean[2]<-mean(subsamp1)
  bootlow[2]<-quantile(mittel1,probs=c(.025,.975))[1]
  boothigh[2]<-quantile(mittel1,probs=c(.025,.975))[2]

  #back gtransformation
  transmean<-c()
  translow<-c()
  transhigh<-c()
  for(i in 1:length(bootmean)){
```

```
    transmean[i]<-exp(bootmean[i])-C
    translow[i]<-exp(bootlow[i])-C
    transhigh[i]<-exp(boothigh[i])-C
  }

  results<-data.frame(bootmean, bootlow, boothigh, transmean, translow,
transhigh)

  mini<-numeric()
  mini[1]<-sqrt((transhigh[1]-translow[2])^2)
  mini[2]<-sqrt((transhigh[2]-translow[1])^2)
  if (mini[1]<=mini[2]){
    dissig<-transhigh[1]-translow[2]
  }else{
    dissig<-transhigh[2]-translow[1]
  }
  return(dissig)
}

dissigs<-numeric(2999)
for (i in 1:2999){
  dissigs[i]<-dissigdist(g3)
}
top<-numeric(2999)
for (i in 1:2999){
  if (dissigs[i]>0){
    top[i]<-0
  }else{
    top[i]<-1
  }
}
p<-(sum(top)+1)/3000
p<-data.frame(p)
p

hist0 <- hist(dissigs, breaks=100, plot=FALSE)
mult0 <- hist0$counts / hist0$density
dens0 <- density(dissigs)
dens0$y <- dens0$y * mult0[1]
plot(hist0,   main="Permutated   distribution",   xlab="Distance   from
Significance", col="lightgreen")
lines(dens0, col="darkblue", lwd=2)
dev.copy(png, paste0("hist_", tit, ".png"))
dev.off()
write.xlsx(x = p, file = "type_I_p.value.xlsx", row.names = FALSE)
```

The code below generates a meta-regression and respective plots. Q statistics are also computed.

```
fit1<- lm(LogRR ~ Cont, weights=weight)
fit2<- lm(LogRR ~ poly(Cont, 2, raw=FALSE), weights=weight)
fit3<- lm(LogRR ~ poly(Cont, 3, raw=FALSE), weights=weight)

#getting overall p value
obtp <- function (fit) {
  f <- summary(fit)$fstatistic
  p <- pf(f[1],f[2],f[3],lower.tail=F)
  attributes(p) <- NULL
  return(p)
}
pvs<-c(obtp(fit1), obtp(fit2), obtp(fit3))
num<-which.min(pvs)
if (num==1){
  export<-tidy(fit1)
  export$residualSE<-summary(fit1)$sigma
  export$df.residual<-fit1$df.residual
  export$R<-summary(fit1)$r.squared
  export$R.adj<-summary(fit1)$adj.r.squared
  export$p.model<-obtp(fit1)
  export$n<-length(X_con)
}else if (num==2){
  export<-tidy(fit2)
  export$residualSE<-summary(fit2)$sigma
  export$df.residual<-fit1$df.residual
  export$R<-summary(fit2)$r.squared
  export$R.adj<-summary(fit2)$adj.r.squared
  export$p.model<-obtp(fit2)
  export$n<-length(X_con)
}else if (num==3){
  export<-tidy(fit3)
  export$residualSE<-summary(fit3)$sigma
  export$df.residual<-fit1$df.residual
  export$R<-summary(fit3)$r.squared
  export$R.adj<-summary(fit3)$adj.r.squared
  export$p.model<-obtp(fit3)
  export$n<-length(X_con)
}

prd <- data.frame(Cont = seq(from = range(Cont)[1], to = range(Cont)[2],
length.out = length(Cont)))
if (num==1){
  err <- predict(fit1, newdata = prd, se.fit = TRUE)
}else if (num==2){
  err <- predict(fit2, newdata = prd, se.fit = TRUE)
}else if (num==3){
  err <- predict(fit3, newdata = prd, se.fit = TRUE)
}else if (num==4){
  err <- predict(fit4, newdata = prd, se.fit = TRUE)
}
prd$lci <- (err$fit - 1.96 * err$se.fit)
prd$fit <- (err$fit)
```

```
prd$uci <- (err$fit + 1.96 * err$se.fit)

#In case of too large dots use Sizes
sequ<-seq(1.2, by=0.05, length.out=length(Cont))
seq<-numeric(length(Cont))
Siz<-data.frame(weight=weight, seq=seq)
Siz<-Siz[order(Siz$weight),]
Siz[,2]<-sequ
target<-numeric(length(Cont))
for (i in 1:length(Cont)){
  target[i]<-as.character(weight[i])
}
Siz<-Siz[match(target, Siz$weight),]
Sizes<-Siz[,2]

#plotting model
ggplot(prd, aes(x = Cont, y = fit)) +
  xlim(min(Cont), max(Cont)) +
  ylim(0, 1.05) +
  theme_bw() +
  geom_line(size=1.2) +
  geom_smooth(aes(ymin = prd$lci, ymax = prd$uci), stat = "identity") +
  geom_point(x  =  Cont,  y  =  LogRR,  size=log(weight+1),  shape=21,
fill="dimgrey") +
  labs(x = xname, y = yname) +
  geom_hline(yintercept=0.6695512) +
  theme(axis.title.y = element_text(size = rel(1.8), angle = 90)) +
  theme(axis.title.x = element_text(size = rel(1.8), angle = 00)) +
  theme(axis.text.y     =   element_text(size=18),   axis.text.x     =
element_text(size=18))

dev.copy(png, paste0("reg_", ee, ".png"))
dev.off()

#Q Model
if (num==1){
  QM<-export$estimate[2]^2/export$std.error[2]^2
}else if (num==2){
  QM<-((export$estimate[2]^2/export$std.error[2]^2)
}else if (num==3){
  QM<-
((export$estimate[2]^2/export$std.error[2]^2)+(export$estimate[3]^2/exp
ort$std.error[3]^2)+(export$estimate[4]^2/export$std.error[4]^2))/3
}else if (num==4){
  QM<-
((export$estimate[2]^2/export$std.error[2]^2)+(export$estimate[3]^2/exp
ort$std.error[3]^2)+(export$estimate[4]^2/export$std.error[4]^2)+(expor
t$estimate[5]^2/export$std.error[5]^3))/4
}
#Q Total
qt<-numeric()
for (i in 1:length(LogRR)){
  qt[i]<-weight[i]*(LogRR[i]-MeanLogRR)^2
}
QT<-sum(qt)
#Q Error
QE<-QT-QM
```

```
export$Rsig<-Rsig
export$QT<-QT
export$QE<-QE
export$QM<-QM

#Resampling test for significance of QM
sampfile<-data.frame(LogRR=LogRR, weight=weight)
randomSample = function(df,n) {
  return (df[sample(nrow(df), n, replace = TRUE),])
}
Lsa<-numeric(length(LogRR))
Wsa<-numeric(length(LogRR))
Lsamp<-matrix(nrow=length(LogRR), ncol=4999)
Wsamp<-matrix(nrow=length(LogRR), ncol=4999)
Csamp<-matrix(nrow=length(LogRR), ncol=4999)
fits<-numeric()
tits<-numeric()
Qs<-numeric(4999)
Q<-numeric(4999)

for (i in 1:4999){
  sam<-randomSample(sampfile, nrow(sampfile))
  Lsa<-sam$LogRR
  Wsa<-sam$weight
  Lsamp[,i]<- Lsa
  Wsamp[,i]<- Wsa
  Csamp[,i]<- sample(Cont, length(LogRR), rep=TRUE)
  fits<- lm(Lsamp[,i] ~ poly(Csamp[,i], 2, raw=TRUE), weights=Wsamp[,i])
  tits<- tidy(fits)
  Qs[i]<-
((tits$estimate[2]^2/tits$std.error[2]^2)+(tits$estimate[3]^2/tits$std.
error[3]^2))/2
  if (Qs[i]>=QM){
    Q[i]<-1
  }else{
    Q[i]<-0
  }
}
Qp<-(sum(Q)+1)/5000

export$QMp.value<-Qp

write.xlsx(x = export, file = paste(ee), row.names = TRUE)
```

The code below generates forest plots from output excel files that are generates previously.

```
#forest plot
forestplot <- function(a2, xlab="\nEffect size", ylab=paste(ff)){
  require(ggplot2)
  p <- ggplot(a2, aes(x=Cat, y=transpRR, ymin=transpCIL, ymax=transpCIU))
+
    ylim(0.7, 1.3) +
    geom_pointrange(stat    =    "identity",    size=1,    color="black",
fill="black", shape=shapes, lty=lin, alpha=Tr) +
    coord_flip() +
    geom_hline(aes(yintercept=1), lty=2) +
    geom_text(aes(y   =   posn,label   =   ns),   size=6.3,   vjust=-0.5,
col="gray50") +
    ylab(xlab) +
    xlab(ylab) +
    theme(axis.title.y  =  element_text(size  =  rel(1.8),  angle  =  90),
panel.grid.major.y = element_blank()) +
    theme(axis.title.x  =  element_text(size  =  rel(1.8),  angle  =  00),
panel.grid.major.y = element_blank()) +
    theme(axis.text.y       =    element_text(size=18,    face="italic"),
axis.text.x  = element_text(size=18))
  return(p)
}
forestplot(a2)

a1<-read.csv("T_C_Growth.rate_comb.csv")
ff<-paste("Significant drivers\n")
attach(a1)


#forest plot (transpRR)
a1$Tr<-numeric(length(a1$Rat))
a1$shapes<-numeric(length(a1$Rat))
a1$lin<-numeric(length(a1$Rat))
a1$posn<-numeric(length(a1$Rat))
for (i in 1:length(a1$Rat)){
  a1$lin[i]<-1
  if (a1$Rat[i]>=1){
    a1$Rat[i]<-1
    }else{}
  if (a1$Rat[i]<0.2){
    a1$Tr[i]<-0.2
  }else{
    a1$Tr[i]<-a1$Rat[i]
  }
  if
(a1$Cat[i]=="1"||a1$Cat[i]=="2"||a1$Cat[i]=="3"||a1$Cat[i]=="4"||a1$Cat
[i]=="5"||a1$Cat[i]=="6"||a1$Cat[i]=="7"||a1$Cat[i]=="8"){
    a1$Tr[i]<-0
  }else{}
  if (a1$transpCIL[i]<1&a1$transpCIU[i]>1){
    a1$Tr[i]<-1
  }else{}
  if (a1$Rsig[i]=="FALSE"||a1$Rsig[i]=="False"){
    a1$shapes[i]<-22
  }else{
```

```
    a1$shapes[i]<-21
  }
  if (a1$transpRR[i]<=1.01&a1$transpRR[i]>=0.99){
    a1$posn[i]<-a1$transpRR[i]+0.02
  }else{
    a1$posn[i]<-a1$transpRR[i]
  }
}
G<-length(a1$Cat)
a2<-data.frame(Cat=a1$Cat, transpRR=a1$transpRR, transpCIL=a1$transpCIL,
transpCIU=a1$transpCIU,    Tr=a1$Tr,    shapes=a1$shapes,    lin=a1$lin,
ns=a1$ns, posn=a1$posn)
a2$Cat <- factor(a2$Cat, levels = a2$Cat)
a2<-a2[nrow(a2):1,]
a2$Cat <- as.factor(a2$Cat)
attach(a2)
fills<-numeric(G-1)
for (i in 1:(G-1)){
  if (a2$transpCIU[i]<1){
    fills[i]<-paste("red")
  }else if (a2$transpCIL[i]>1){
    fills[i]<-paste("yellow")
  }else{
    fills[i]<-paste("black")
  }
}
a2$val<-c(1:length(a2$Cat))
a2$Cat <- factor(a2$Cat, levels = a2$Cat[order(a2$val)])
forestplot(a2)
```